

Differentiated CTX human neural stem cells adopt a glial phenotype in RAFT-stabilised collagen hydrogels suitable for nerve tissue engineering

C Murray-Dunning¹, L Thanabalasundaram², AGE Day¹, N Vysokov², J Sinden², L Stevenato²,

JB Phillips¹

¹*Biomaterials & Tissue Engineering, UCL Eastman Dental Institute, University College London, UK.*

²*ReNeuron Ltd, Guildford, Surrey, UK.*

INTRODUCTION: Cellular collagen constructs have been used to support peripheral nerve regeneration, using Schwann cells and more recently using stem cells that have been differentiated to resemble Schwann cells [1-3]. In order to progress this technology towards clinical translation, the use of CTX human neural stem cells (ReNeuron, UK), as a potential allogeneic source of therapeutic cells was investigated. The ability of CTX cells to differentiate towards a Schwann cell-like phenotype was investigated in standard monolayer culture, and in a 3D collagen environment similar to that used in engineered neural tissue [1].

METHODS: CTX human neural stem cells were assessed for the presence of markers for neuronal (β III-tubulin, TUBB3) and glial (glial fibrillary acidic protein GFAP, S100B) phenotype before and after 2 weeks differentiation in flasks, using fluorescence immunostaining and quantitative PCR. Differentiated CTX (dCTX) cells were seeded within 2 mg/ml bovine collagen hydrogels (Koken Co Ltd, Japan) and stabilized using RAFT™ (TAP Biosystems, UK), then maintained in culture for 7 days. Control dCTX cells were maintained in monolayer for 7 days. Phenotype of the dCTX cells was then assessed as before, using 2-week monolayer dCTX cells as a baseline comparator.

RESULTS: Following 2 weeks differentiation in monolayer culture, upregulation in expression of all 3 markers was observed (Fig. 1).

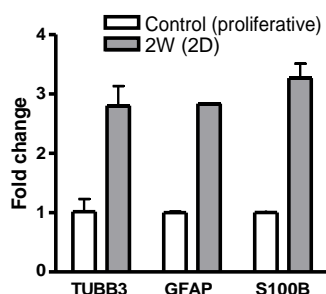


Fig. 1: Relative quantification (RQ) of gene expression in dCTX cells (grey bars) compared with undifferentiated control CTX cells (white bars; RQ=1).

After a subsequent 7 days culture in stabilised collagen gels, the dCTX cells exhibited a marked upregulation in the glial markers GFAP and S100, while TUBB3 expression remained similar to control and monolayer conditions (Fig. 2).

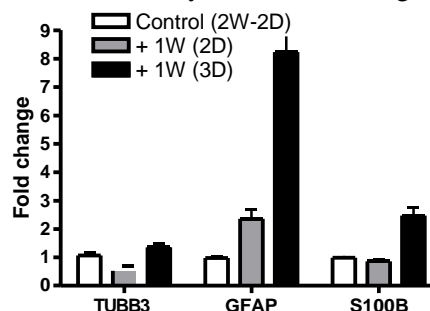


Fig. 2: Relative quantification (RQ) of gene expression in dCTX cells cultured in monolayer or within fully stabilised collagen gels after 7 days. 2 week monolayer dCTX cells constitute the calibrator (RQ=1).

DISCUSSION & CONCLUSIONS: After 2 weeks differentiation in flasks, CTX cells increased expression of markers for both neuronal and glial differentiation. Transferring these cells to stabilised collagen gels for a further 7 days culture resulted in a shift towards a more glial-like phenotype. These results suggest that CTX human neural stem cells can adopt some of the characteristics of Schwann cells when maintained within stabilised collagen gels, indicating their potential usefulness as an allogeneic source of therapeutic cells in peripheral nerve tissue engineering.

ACKNOWLEDGEMENTS: This work was supported by funding from the UK Technology Strategy Board (101599).

Developing an *in vitro* model of smooth muscle contraction

JC Bridge¹, GE Morris¹, JW Aylott², MP Lewis³, FRAJ Rose¹

¹ Division of drug delivery and tissue engineering, School of Pharmacy, University of Nottingham, England ² Laboratory of Biophysics and Surface Analysis, School of Pharmacy, University of Nottingham, England ³ School of Sport, Exercise and Health Sciences, Loughborough University, England

INTRODUCTION: Smooth muscle (SM) tissue is found in many parts of the body, primarily in sheets or bundles surrounding hollow organs. Its main function is to regulate organ tone *via* its contractile state. Dysfunction of SM in diseases such as asthma and atherosclerosis affect millions worldwide.

Current methods for studying SM primarily rely on *ex vivo* animal tissues or 2D *in vitro* models. These 2D models are cultured on stiff surfaces lacking the elastic properties and 3D morphology found in natural extracellular matrix *in vivo*.

The aim of this work was to develop an *in vitro* model of SM that possesses the ability to contract using both hydrogels and electrospun scaffolds. In addition, a method to measure the force generated by the models has also been developed. This will provide a platform to assess SM contraction/relaxation in response to new drug candidates and also the ability to develop disease SM models.

METHODS: Primary rat aortic SM cells were seeded into 2ml collagen gel constructs at a density of 5×10^4 cells ml^{-1} . Gels were cast in rectangular glass baths containing plastic floatation bars anchored at each end of the bath. Once seeded, constructs were incubated for 3 days to allow cell attachment and alignment. Constructs were then attached to a force transducer and stimulated with a contractile agonist (UTP). The contractile force generated by the construct was measured for 60 minutes. This method of force measurement was also used to measure the contractile force generated by primary rat aortic SM cells cultured upon aligned electrospun gelatin scaffolds

RESULTS: Smooth muscle collagen constructs produced a slow sustained contraction when stimulated with UTP which was measured using the force transducer. Peak forces measured were in the region of 200-250 μN and were reached after approx. 50 minutes of stimulation. In contrast, controls showed very little force measurement (20-25 μN) during the same period.

A range of electrospun gelatin based scaffolds were produced and cross-linked. Primary rat aortic SM cells were cultured on them for 10 days. During that time the cells remained viable and proliferated to form a confluent aligned layer of SM cells. The degree of nuclear alignment along the scaffolds was dependant on the scaffold fibre diameter.

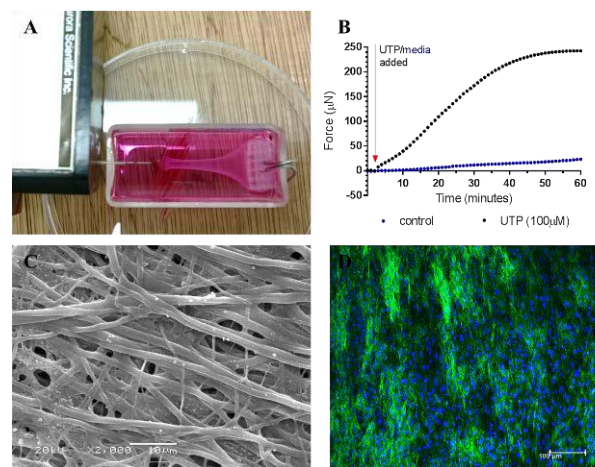


Fig. 1: A photograph of a contracting SM collagen gel attached to the force transducer (A) with a representative trace of force generated (B). An SEM image of a cross-linked electrospun gelatin scaffold (C) and a confocal image of fluorescently stained SM cells cultured on a similar scaffold.

DISCUSSION & CONCLUSIONS: A method has been developed to measure the contractile force generated by SM cells in response to an agonist in tissue engineered collagen constructs. This technique will be adapted to measure the contractile force generated by SM cells cultured on aligned electrospun gelatin scaffolds.

ACKNOWLEDGEMENTS: The authors would like to thank the EPSRC DTC in Regenerative medicine for funding this project.

Design and development of novel electrospun small diameter vascular prosthesis

[V. Parikh](#)¹, [M. MirafTAB](#)¹, [A. Hidalgo](#)², [M. Azzawi](#)²

¹[University of Bolton, Bolton, UK](#), ²[Manchester Metropolitan University, Manchester, UK](#),

INTRODUCTION: There is an acute clinical need for small-calibre (<6 mm) vascular grafts for surgery, however, these often fail primarily due to the early formation of thrombosis and intimal hyperplasia. Dynamics of blood flow and their effects on endothelial cell proliferation have been identified as one of the major deciding factors for the efficiency of grafts. Research has demonstrated that intimal hyperplasia develops preferentially in regions where there is a disturbed blood flow hemodynamics which leads to uneven shear stress, turbulent flow and resultant flow stagnancy in the periphery of the graft. Given the established advantages of swirling physiological blood flow^{1,2}, we have developed a new graft design with a swirling flow inducer on the inner surface of the graft throughout its longitudinal axis. This unique design is aimed at enhancing wall shear stress profile within the graft to prevent the occlusion and thus failure of the graft in long term use.

METHODS: Final elemental analysis was used to simulate blood flow profiles when subjected to different internal structures along with helix angle and number of rotations. Electrospinning was used to fabricate the proposed design and prototype samples were produced using polyvinyl alcohol (PVA) and gelatine. After cross-linking, prototype grafts were subjected to tests such as uniaxial tensile tests, bursting strength tests and suture retention test and results were evaluated and compared with standard grafts produced with no spiral features (Fig 1 (a) and 1(b)). Human coronary artery endothelial cells (HCAEC) were seeded on the helical graft using a surface seeding technique. At various time intervals cell proliferation, viability and morphology were assessed in the presence of static and circulating media and results were compared with their conventional counterpart kept under the same conditions. Pressure retention of seeded grafts was assessed using pressure myography at pressure ranges from 60 to 200 mmHg.

RESULTS: Initially, different swirling profiles were analysed using final elemental analysis and compared with conventional or plain grafts. The numerical analysis has revealed that the proposed design could indeed produce the swirling blood flow with improved hemodynamics. Compared to plain graft, in swirling graft, blood flow velocity near the vessel walls was significantly enhanced with uniform distribution of shear stress and thus could theoretically enhance performance of the grafts by providing the "wash away" effects and prevent plaque formation. A significant difference ($p < 0.05$) in cell spreading and cell viability in the helical graft compared to conventional graft were observed. Also, in the case of helical graft more uniformly arranged HCAEC were observed with the elongated morphology (Fig 1(c), 1(d) and 1(e)). Pressure myography studies demonstrated that endothelialized helical grafts were better able to withstand pressure compared to their conventional counterpart.

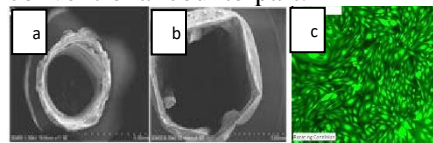


Fig 1: SEM images of the conventional and helical grafts (a, b), EC seeded helical graft (c),

DISCUSSION AND CONCLUSION: Our findings demonstrate that electrospun helical grafts can be an attractive candidate for use as a potential small diameter vascular graft for implantation based on its ability to enhance hemodynamics of blood flow in localised area and its resemblance to the native artery, providing a better environment for the endothelialisation of the grafts.

The capacity of growth factor releasing hydrogels to regenerate bone in an ex vivo chick femur defect model

JM Kanczler¹, D Gothard¹, EL Smith¹, LJ White², O Qutachi², KM Shakesheff², ROC Oreffo¹

¹*Bone and Joint Research Group, Centre for Human Development, Stem Cells and Regeneration, Institute of Developmental Sciences, University of Southampton.*

²*Wolfson Centre for Stem Cells, Tissue Engineering and Modelling, Centre for Biomolecular Sciences, University of Nottingham.*

INTRODUCTION: The need for alternative novel reparative approaches for bone repair and regeneration resulting from disease and trauma is increasing with the onset of an ever rising aged population. Classically *in vivo* models have been employed to study the efficacy of new bone regenerative strategies. However, with the onset of numerous tissue engineering therapies alternative strategies are required to assess these new techniques. Complex skeletal interactions can be studied by *ex vivo* model systems allowing for the extrapolation of therapeutic strategies between simple *in vitro* cell systems and intricate *in vivo* models. Using a 3D *ex vivo* segmental bone defect model system and *in ovo* chorioallantoic membrane (CAM) culture model (Figure 1A,B) we investigated novel cell/biomaterial constructs loaded with appropriate growth factors to assess their ability to repair bone defects.

METHODS: Alginate/bECM hydrogels¹ combined with poly(D,L-lactic-co-glycolic acid) (P_{D,L}LGA)/ Triblock (10-30 % P_{D,L}LGA-PEG-P_{D,L}LGA copolymer) microparticles² releasing single vascular endothelial growth factor (VEGF), transforming growth factor- β 3 (TGF- β 3) or bone morphogenic protein-2 (BMP-2) or dual combination growth factors (VEGF/TGF- β 3, VEGF/BMP-2, TGF- β 3/BMP-2) in human serum albumin (HSA) carrier protein, and seeded with or without Stro-1+ adult human bone marrow stromal cells (HBMSC), were positioned into segmental defects (2mm) in embryonic day 18 (D18) chick femurs and assessed for bone repair in the *in vitro* organotypic culture model and the CAM vascular model. Femurs were analysed by micro-computed tomography (μ CT), and histologically for proteoglycan (Alcian blue) and collagen production (Sirius red) as well as for Goldner's trichrome and tartrate resistant acid phosphatase (TRAP)

RESULTS: Extensive significant new bone formation was observed in the CAM vascular bone defect model following implantation with HSA/BMP-2 (Figure 1C), HSA/VEGF/TGF- β 3 and HSA/TGF- β 3/BMP-2 (+cells). Negligible new bone tissue formation or defect site regeneration

was observed following hydrogel construct implantation within organotypic cultured chick femurs over 10 days. μ CT and histological analysis revealed minimal to no changes both within and outside the defect site, indicating that a lack of a vascular supply impeded tissue repair.

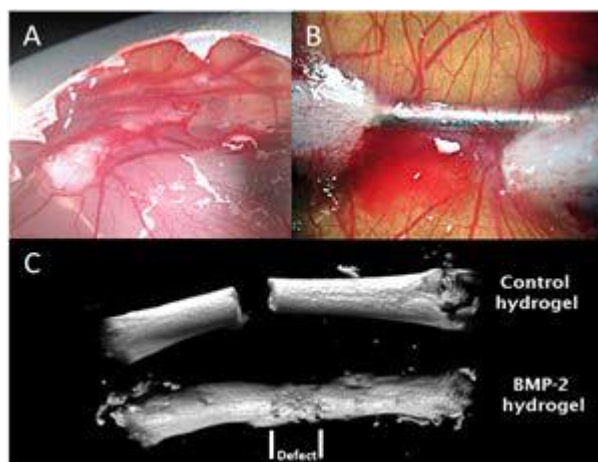


Fig. 1A: Implanted E18 chick femur in the vascularised bed of the CAM. Fig. 1B: E18 femur segmental defect cultured in the CAM (8 days). Fig. 1C: Bone regeneration of the chick femur defect (E18) with alginate/bECM hydrogel/BMP-2 after 8 days culture in the CAM.

DISCUSSION & CONCLUSIONS: This study demonstrates the importance of active vascularisation combined with delivery of bioactive growth factors from a novel alginate/bECM hydrogel to augment skeletal tissue formation. Furthermore, this study demonstrates the efficacy and successful use of an organotypic chick femur defect culture system as a high-throughput test model for scaffold/cell/growth factor therapies for regenerative medicine.

ACKNOWLEDGEMENTS: This work was supported by the strategic longer and larger grant (LOLA) from the BBSRC, UK-grant number BB/G010579/1.

Effects of GDF6, hypoxia and load on mesenchymal stem cell discogenic differentiation and tissue engineered construct composition and micromechanics.

LE Clarke¹, JC McConnell^{1,2}, MJ Sherratt¹, SM Richardson¹, JA Hoyland¹

1. Centre for Tissue Injury and Repair, The University of Manchester, UK. 2. Wellcome Trust Centre for Cell-Matrix Research, Faculty of Life Sciences, The University of Manchester, UK

INTRODUCTION: The combination of adipose-derived mesenchymal stem cells (AD-MSCs) and growth differentiation factor 6 (GDF6) results in differentiation of cells to a more discogenic phenotype compared to current differentiation protocols¹. Previous studies² have demonstrated that whilst addition of growth factors may induce a phenotypic change, a hypoxic environment enhances differentiation. The niche of the intervertebral disc (IVD) can be described as a harsh microenvironment being hypoxic and subjected to mechanical load, hence investigating these two environmental factors is important in assessing the potential efficacy of cell based IVD regenerative therapies. The aim of this study was to investigate whether exposing AD-MSCs supplemented with GDF6 to hypoxia (2%) or load (0.04MPa, 1Hz, 1hour) or a combination of the two enhances differentiation and also whether the factors act synergistically.

METHODS: Human AD-MSCs (n=3) were seeded in type I collagen hydrogels on Bioflex[®] culture plates and separated into four groups: 1). Normoxia (20%); 2). Normoxia + Load; 3). Hypoxia (2%); 4). Hypoxia + Load. Hydrogels were cultured in a differentiating media consisting of high glucose DMEM supplemented with 1% FCS, ITS, 10⁻⁷ M dexamethasone and GDF6 (100ng/ml) with media changed every 48 hours¹ and loaded groups exposed to a compressive load of 0.04MPa at a frequency of 1Hz for 1 hour everyday³. After 14 days QPCR analysis of discogenic differentiation markers was undertaken, along with analysis of sGAG content (DMMB). AFM micro-indentation was performed using a spherically tipped cantilever. The local reduced modulus was determined for each of 100 points in a 20x20µm region, indented at a frequency of 1 Hz. For each, 3 areas were assessed and a total of 1200 force curves collected and analysed using a Herzian (spherical) model and a maximum force fit of 70%.

RESULTS: AD-MSCs treated with GDF6 exposed to all groups resulted in enhanced discogenic differentiation compared to normoxia. Hypoxia + Load increased PG content, shown by

the greatest sGAG synthesis and upregulation of ACAN. However, the combination of treatments upregulated COL2A1, resulting in the lowest ACAN:COL2A1 ratio. Micromechanical analysis showed that constructs treated in Hypoxia + Load had a stiffer matrix composition than constructs cultured in Normoxia.

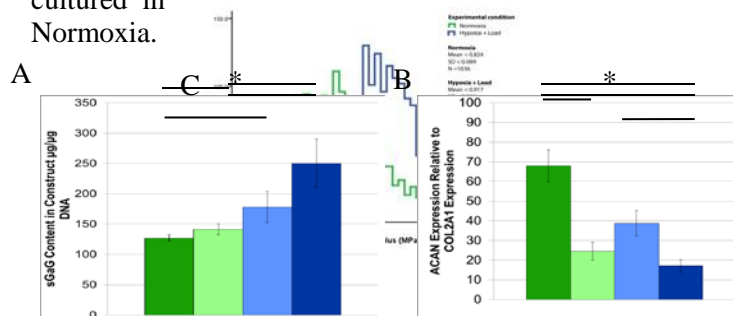


Fig. 1: A. sGAG content of constructs. B. ACAN:COL2A1 ratio. C. Micromechanical analysis of constructs.

DISCUSSION & CONCLUSIONS: Whilst hypoxia and load enhance discogenic differentiation, the matrix composition and micromechanics are stiffer compared to constructs in normoxia. Therefore in addition to gene expression, these characteristics must be analysed to ensure that there is synthesis of an appropriate functional matrix.

ACKNOWLEDGEMENTS: Rosetrees Trust for funding. The atomic force microscopy was conducted in the BioAFM Facility at UoM.

Assessing early skeletal stem cell differentiation into adipocytes using coherent anti-Stokes Raman scattering microscopy

CC Moura^{1,2,3}, JP Smus^{1,2}, RS Tare³, ROC Oreffo³, S Mahajan^{1,2}

¹ Institute for Life Sciences, ² Department of Chemistry, Faculty of Natural Environmental Sciences,

³ Bone and Joint Research Group, Centre for Human Development, Stem Cells and Regeneration, Institute of Developmental Sciences

University of Southampton, UK

INTRODUCTION: Skeletal stem cells (SSCs) from human bone marrow offer new possibilities for tissue repair and disease treatment.¹ Currently, SSCs differentiation into the stromal lineages of bone, cartilage and fat, is assessed using different approaches that require cell fixation or lysis, which are invasive, or even destructive. Imaging techniques based on Raman spectroscopy, such as coherent anti-Stokes Raman scattering (CARS), present an exciting alternative for studying biological systems in their natural state. We examined whether CARS could provide a label-free imaging tool to evaluate SSCs differentiation.

METHODS: Human SSCs differentiation into adipocytes, from adult human bone marrow samples was evaluated using quantitative real-time polymerase chain reaction (qPCR) analysis. Raman spectra of the samples were obtained at day 14, to confirm the characteristic peaks of SSCs cultured in basal and adipogenic media. Additionally, image analysis of the formation of lipid droplets using CARS microscopy was undertaken, since lipids display a strong C-H stretching vibration signal at 2845 cm^{-1} .² The label-free images were compared to Oil Red O photomicrographs.

RESULTS: CARS imaging demonstrated the presence of large cytoplasmic lipid droplets in the absence of any exogenous label. Critically, CARS microscopy proved extremely sensitive in contrast to conventional imaging with Oil Red O staining, detecting adipogenic differentiation at significantly earlier time points (day 3). Adipogenesis progression was also verified by gene expression profiling.

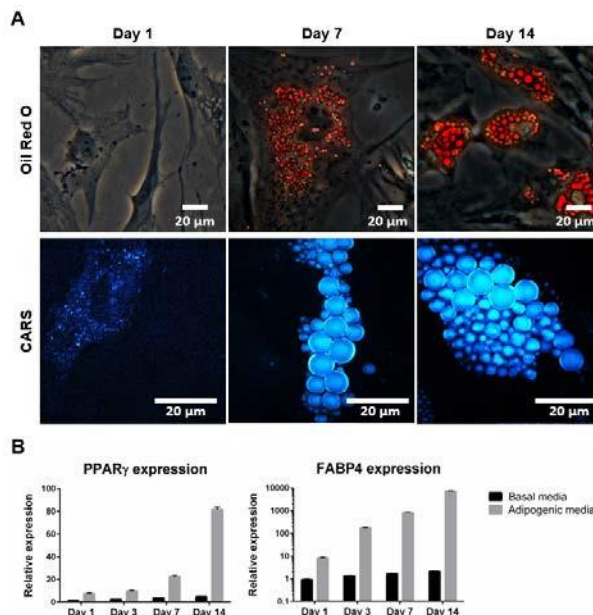


Fig. 1: (A) Comparison of label (Oil red O staining) and label-free (CARS) imaging to assay adipogenesis; (B) Expression of PPAR γ and FABP4 during adipogenic differentiation.

DISCUSSION & CONCLUSIONS: The current studies demonstrate a non-invasive and non-destructive approach for monitoring SSCs differentiation into adipocytes. The results confirm the potential value of using CARS as a label-free imaging tool for skeletal stem cell biology and regenerative medicine.

ACKNOWLEDGEMENTS: Funding from the University of Southampton, Institute for Life Sciences and BBSRC is gratefully acknowledged.

GET: Glycosaminoglycan (GAG)-binding Enhanced Transduction of Functional Proteins

JE Dixon^{1*}, G Osman¹, G Morris¹, C Denning³, KM Shakesheff¹

Wolfson Centre for Stem Cells, Tissue Engineering, and Modelling (STEM), Centre of Biomolecular Sciences,

¹School of Pharmacy, ³School of Medicine; ²Flow Cytometry Facility, School of Medicine; University of Nottingham, Nottingham, NG7 2RD, UK; University of Nottingham, Nottingham, NG7 2RD, UK.

james.dixon@nottingham.ac.uk

INTRODUCTION:

Protein transduction domains (PTDs) are powerful non-genetic tools that allow intracellular delivery of conjugated cargoes to modify cell behaviour. Their use in biomedicine has been hampered by inefficient delivery to nuclear and cytoplasmic targets.

METHODS:

mRFP1, Cre Recombinase, transcription factors, antibiotic resistance proteins and PTDs were cloned, fused and expressed in/purified from *E.coli* using GST affinity chromatography. Cells were as described¹. Flow cytometry used a MoFlo™ DP (DAKO) using a 488nm green laser. Cre assays used NIH3t3: LSL-eGFP cells created in-house.

RESULTS:

Here we overcame PTD deficiencies by developing a novel fusion protein that couples a membrane docking peptide to heparan sulfate glycosaminoglycans (GAGs) with a PTD. We showed this GET (GAG-binding Enhanced Transduction) system could deliver fluorescent reporters (mRFP1), functional enzymes (Cre, neomycin phosphotransferase) and transcription factors (NANOG, MYOD) at efficiencies of up to two-orders of magnitude higher than previously reported in cell types considered hard to transduce, such as mouse embryonic stem cells (mESCs), human ESCs (hESCs) and induced pluripotent stem cells (hiPSCs).

DISCUSSION & CONCLUSIONS:

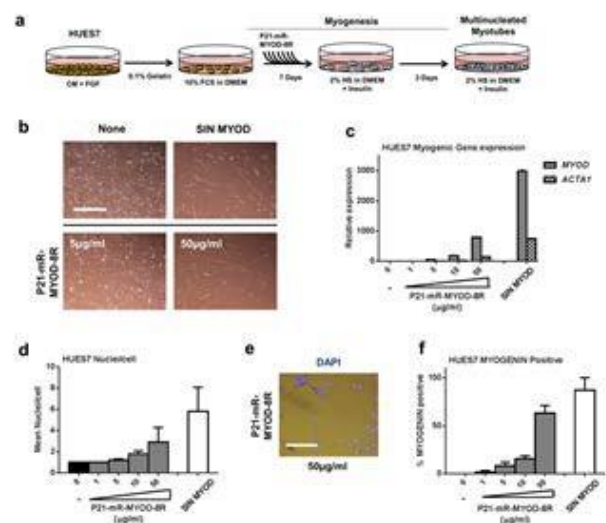
This technology represents an efficient strategy for controlling cell behaviour and directing cell fate that has broad applicability for basic research, disease modelling and clinical application.

Figure 1. GET of MYOD promotes Myogenic differentiation of human embryonic stem cells. (a) Scheme of testing the differentiation activity of transduced MYOD in HUES7 cells. (b-f) P21-mR-MYOD-8R drives myogenic differentiation of HUES7 cells to multinucleated Myotubes. (b) Light microscopy of HUES7 cells cultured under the myogenic regime. bar, 100µm. (c) Relative gene expression analyses of HUES7 cultures using quantitative PCR (QPCR). Error bars indicate s.e. (d-f) P21-mR-MYOD-8R differentiated cells are multinucleated and MYOGENIN positive. Error bars indicate s.d.

ACKNOWLEDGMENTS:

We would like to thank Dr. Andrew D. Johnson (University of Nottingham) and Dr. Catherine Merry (University of Manchester) for helpful discussions. We thank the European Research Council under the European Community's Seventh Framework Programme (FP7/2007-2013)/ERC grant agreement 227845 for funding. KMS acknowledges the support of the UK Regenerative Medicine Platform.

www.ecmconferences.org



Developing a layer-by-layer biomaterials coating approach with heparin and patient's blood to induce angiogenesis

G Gigliobianco¹, L Dew¹, S MacNeil¹

¹ *Department of Materials Science and Engineering, University of Sheffield, UK*

INTRODUCTION: Slow angiogenesis is a limiting factor for initial integration of 3D tissue constructs after their implantation¹. There are existing materials and new materials that could all benefit from being surface modified to promote angiogenesis. **AIM:** The aim of this study is to assess a heparin coating technology which we previously developed² to see whether it can be used with the patient's blood to improve the angiogenic response to biomaterials.

METHODS: Electrospun PLLA was plasma polymerized with PolyAcrylic Acid (PAC) and coated with alternate layers of PolyEthyleneImine and PAC for a total of seven layers. Coated scaffolds were then dipped in heparin and then in freshly isolated human plasma. Surface chemistry of coated scaffolds was verified by X-Ray Photon Electron Spectroscopy. The ability of the heparin functionalised scaffolds to attract VEGF from plasma was detected by measuring VEGF levels in plasma pre and post incubation with scaffolds by ELISA and also by imaging the VEGF bound to scaffolds using immunostaining for VEGF on scaffolds. The chick Chorionic Allantoic Membrane (CAM) assay was used to assess the *in-vivo* angiogenic potential of the scaffolds coated with and without plasma.

RESULTS: XPS showed that PAA was plasma polymerised on the PLLA surface and that heparin was bound to these scaffolds. The ability of the heparin functionalised scaffolds to bind VEGF from normal plasma was detected by measuring VEGF levels in plasma pre and post incubation with scaffolds. This showed that scaffolds bound about 2 ng of VEGF per 1 cm² when immersed for 2 hours in either a solution of VEGF (10 ng/ml) or human plasma. Figure 1 shows immunostaining for VEGF on scaffolds after their incubation in a solution of VEGF or human plasma compared to uncoated scaffolds. Figure 2 shows that the functionalized scaffolds induced blood vessel growth into the scaffolds when placed in the CAM assay. This did not occur in non-functionalised scaffolds (2a).

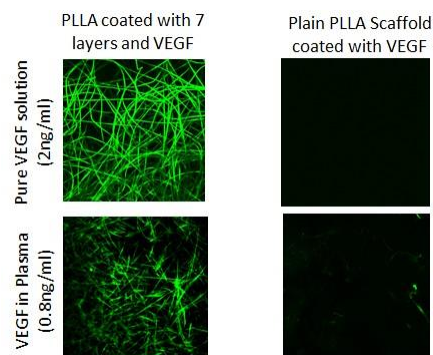


Fig. 1: VEGF binding to scaffolds. Scaffolds were stained with anti-human VEGF and FITC conjugated secondary antibody.

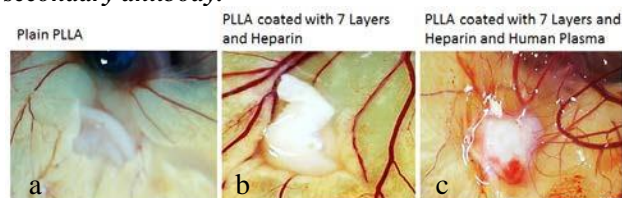


Fig. 2: Directional growth of new blood vessels using CAM assay comparing control and functionalised scaffolds.

DISCUSSION & CONCLUSIONS: This study tested the ability of our layer-by-layer coating with heparin to bind VEGF present in human plasma. We demonstrate that this functionalization approach (which can be applied to a range of scaffolds)² allows one to use patient's blood as the source of pro-angiogenic mitogens. The results confirm the feasibility of this approach. We suggest this versatile coating technology will enhance the tissue integration of a range of biomaterials

ACKNOWLEDGEMENTS: X-ray photoelectron spectra were obtained at the National EPSRC XPS User's Service (NEXUS) at Newcastle University, an EPSRC Mid-Range Facility.

Design and Validation of Multiwell Acoustofluidic Bioreactor Platform for Tissue Engineering

US Jonnalagadda¹, P Glynn-Jones², ROC Oreffo³, M Hill², RS Tare^{1,3}

¹Bioengineering Science, Faculty of Engineering and the Environment, University of Southampton, UK

²ElectroMechanical Engineering, Faculty of Engineering and the Environment, University of Southampton, UK

³Center for Human Development, Stem Cells & Regeneration, Faculty of Medicine, University of Southampton, UK

INTRODUCTION: A variety of modalities have been harnessed for cartilage tissue engineering [1]; we have demonstrated the first application of ultrasonic cell traps to generate cartilage *in vitro* [2]. The initial system was a closed fluidic system consisting of a glass capillary attached to a piezoelectric transducer (PZT). At a characteristic (resonant) frequency, the PZT transmits a pressure wave, which is reflected back to establish an ultrasonic standing wave field. Cells within the field are directed towards the minimal pressure potential planes (pressure nodes), where they aggregate, and are cultured for 21 days with continuous perfusion of chondrogenic medium at a low-shear flow-rate to generate cartilage tissue.

Due to the close-circuit nature of the initial system, microbubble formation, perfusion and capture in the trap limited the reliability of the bioreactor. The aim of the current research is to improve the initial bioreactor system to enhance throughput, consistency and reliability. This enhanced system can then be used to generate thicker, more robust cartilage constructs.

METHODS: Layered resonators were designed to be a removable component of the bioreactor system. Acoustic devices were machined from ceramic and hand assembled. Assembled devices either had a fluid layer thickness of 300 μm (Figure 1A, thin device) or 1.25 mm (Figure 1B, thick device). Acoustic driving parameters were experimentally optimized to maximize the acoustic pressure, while minimizing streaming potential and heat transfer.

A custom-built manifold was used to house each device into a 38mm diameter well during culture. The manifold, peristaltic tubing, and medium reservoir were autoclaved prior to use and the devices were UV sterilized overnight. Devices were magnetically fixed into the wells and immersed in 3 mL of media prior to activation of the acoustic trap (Figure 1C). 1.5×10^6 chondrocytes were inserted into each device (n=4) and the bioreactor setup was maintained in a humidified atmosphere at 37°C and 5% CO₂.

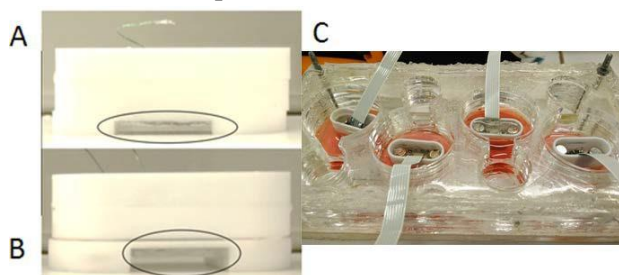


Figure 1: Two types of devices have been used within the bioreactor. (A) A thin device has an active region thickness of 0.3 mm (circled), while (B) a thick device has a thickness of 1.25 mm (circled). (C) Acoustic devices are fitted into 38mm diameter wells. The glass bottom of the manifold

functions as a reflector to generate the acoustic trap.

RESULTS MATLAB modeling demonstrated the generation of a single node in the thin device (Figure 2A), whereas the thick device was able to generate a wave fields with multiple nodes at different resonant frequencies (Figure 2B). Additionally, finite element modeling of the fluid layer was accomplished to characterize the kinetic energy distribution at the pressure nodes (Figure 2C, D).

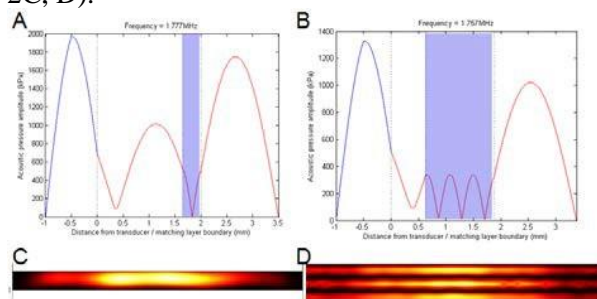


Figure 2: MATLAB model of acoustic pressure emitted through the devices for a thin device (A) and (B) thick device. Minimum peaks within the blue region (fluid layer) are given to be the pressure nodes. The kinetic energy distribution within the fluid layer is given for the (C) thin device and (D) thick device at the acoustic resonance.

Chondrocytic cells introduced into the thick devices at acoustic resonance and 9 Vpp aggregated at multiple pressure nodes. A large aggregate was observed within the thin devices driven at their respective acoustic resonance and 10 Vpp. Furthermore, microbubble formation was not prevalent throughout the culture period in the active region of the devices.

DISCUSSION AND CONCLUSION: In the current study, we have developed a multi-well acoustofluidic platform with an open fluid circuit to minimize the effects of microbubble perfusion into the acoustic trap, while increasing the throughput to have multiple acoustic devices in tandem. The thicker devices allow for the trapping of cells within multiple pressure nodes along the z axis, facilitating the generation of multicellular constructs at the pressure nodes. As the tissue develops, eventually, the constructs within the different nodes will coalesce and generate a thicker cartilage tissue, compared to tissue development within the thin devices. The current bioreactor therefore provides enhancements for bioengineering scaffold-free cartilage constructs.

Polymer surface mobility – a means to drive cellular behaviour through manipulating extracellular matrix organisation

M Bennett¹, F Bathawab¹, M Cantini¹, J Reboud¹, M Salmerón-Sánchez¹

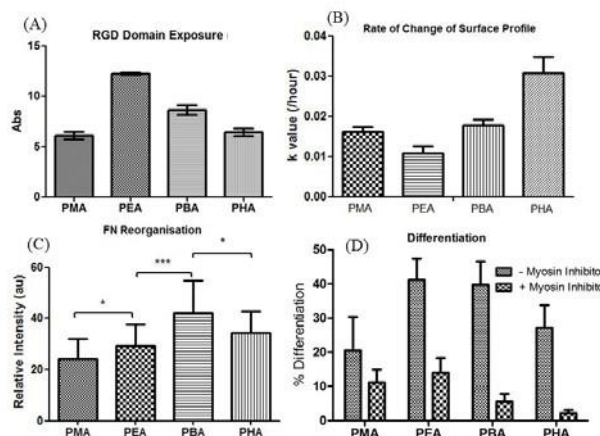
¹ Division of Biomedical Engineering, School of Engineering University of Glasgow, Glasgow, UK.

INTRODUCTION: Polymer surface mobility, like other surface properties, has the potential to direct stem cell fate⁽¹⁾. This is dependent on their glass transition temperature (T_g); the point at which a polymer transitions from an amorphous glass to a more liquid-like state⁽²⁾. This translates to interfacial mobility of extracellular matrix proteins adsorbed on the material surface. We have therefore utilised a series of polymers with similar chemistry, but different surface mobility in conjunction with fluorescent fibronectin to determine the mobility of this interfacial layer. We have also determined both how this affects fibronectin conformation and cell-mediated reorganisation, to understand the role of mobility in cell differentiation.

METHODS: FITC was conjugated to fibronectin, which was then coated on various polyalkyl acrylate surfaces with increasing length of the side chain (Methyl, Ethyl, Butyl and Hexyl acrylates) at a concentration of 20 $\mu\text{g/ml}$. The physical properties of the adsorbed protein were observed and compared to unlabelled protein via AFM and water contact angle measurements. The fluorescence return was measured by the rate of change of the surface profile as observed over N days. The availability of the integrin binding, FNIII₉₋₁₀ domain was determined via ELISA. Cell-mediated reorganisation was determined by the relative fluorescent difference within the cell area. Differentiation was quantified over four days using C2C12 cells and staining for sarcomeric myosin.

RESULTS: We observed that the physical properties of the fluorescent fibronectin were similar to those of unlabelled protein. We have found the protein mobility is non-monotonically dependent on the mobility of the underlying polymer. Interestingly, FNIII₉₋₁₀ domain availability shows a mirror image of this trend. Cell studies have determined that reorganisation of fibronectin adsorbed on the material surface increases to, what we hypothesise to be, an ideal polymer mobility, decreasing as FN mobility increases further, with a similar trend seen in C2C12 differentiation.

Fig. 1: (A) The availability of RGD domain, (B) the rate of change of the surface profile (C), the relative difference in fluorescent intensity and (D)



the amount of differentiation on C2C12 cells with and without myosin inhibitor.

DISCUSSION & CONCLUSIONS: We attribute the non-monotonic dependence of protein mobility on the polymer structure to the change from globular fibronectin on PMA to network-like organisation on PEA. This reduced motion of the network is then compensated for with higher surface mobility on PBA and PHA. We surmise that domain availability in these networks is greater on less mobile surfaces as adsorbed fibronectin cannot compensate for the exposure of energetically unfavourable residues. More mobile surfaces alleviate this strain allowing these domains to be hidden. We conclude that cell-mediated reorganisation and differentiation are determined by interplay between protein interfacial mobility and domain availability, defined by the polymer surface.

ACKNOWLEDGEMENTS: The support from ERC through HealInSynergy 306990 is acknowledged.

Does scaffold fibre alignment guide differentiation and matrix production by osteogenic progenitors?

RM Delaine-Smith¹, GC Reilly²

¹ Institute of Bioengineering, School of Engineering and Materials Science, Queen Mary University, UK. ² INSIGNEO Institute, Materials Science and Engineering, Sheffield University, UK.

INTRODUCTION: Physical cues from the local micro-environment, including matrix fibre orientation, may influence the differentiation of osteogenic progenitor cells [1] while the ability to replicate the structural anisotropy of musculoskeletal tissues is important to restore proper tissue function. The present study investigates how scaffold fibre orientation affects the behaviour of osteogenic progenitor cells and mature osteoblasts, and influences mineralised-collagen matrix organisation and the resulting construct mechanical properties.

METHODS: Human embryonic stem cell derived mesenchymal progenitors (hES-MP) and late stage osteoblasts (MLO-A5) were cultured in α -MEM (+ 10% FCS + 50 μ g/ml AA₂P + 5mM β GP) on scaffolds of electrospun poly(ϵ -caprolactone) (PCL) (Mn 80 kDa) fibres (~8 μ m), fabricated with either a high (aligned) or low (random) degree of alignment. Osteogenic differentiation was induced in hES-MPs by addition of 100nM Dex to medium. All cells were analysed for morphology, viability, migration, total DNA, ALP activity, collagen and calcium deposition. SEM and second harmonic generation (SHG) imaging was used to visualise matrix deposition and organisation in constructs over 2-4 weeks. Tensile properties were determined for osteo-induced hES-MP seeded constructs over the culture period.

RESULTS: HES-MPs preferred to spread and migrate along scaffold fibre direction but viability was unaffected. While both fibre geometries supported osteogenic differentiation, ALP activity, collagen and calcium deposition was highest on random scaffolds for hES-MPs, while the opposite was true for MLO-A5s. Both cell types showed a high degree of mineralised-matrix alignment on aligned scaffolds, while it was less organised on random fibres. SHG showed that collagen fibres were orientated between 0-30 degrees relative to scaffold fibres. All constructs showed increasing elastic modulus over time but aligned constructs (tested parallel) were 10-fold and 200-fold stiffer than random and aligned (tested perpendicular) respectively, after 21 days of matrix deposition.

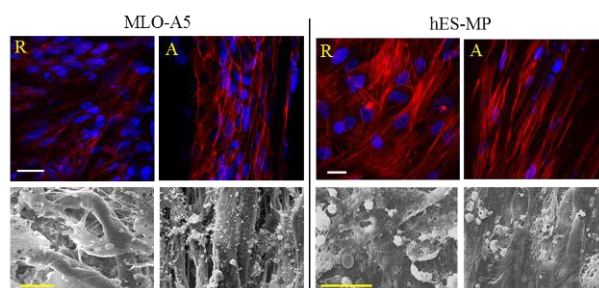


Fig. 1: Cell nuclei (blue) and F-actin (red) at day 7 (top row). SEM at days 12 (MLO-A5) and 28 (hES-MP). R = random, A = aligned. Scale bars; white = 25 μ m, yellow = 10 μ m.

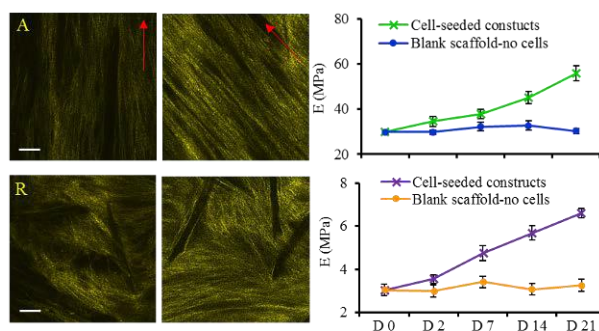


Fig. 2: SHG at days 14 (left) and 21 (right) for hES-MPs on aligned or random fibres. Construct tensile modulus at days 0-21. Scale bar is 25 μ m. Red arrow indicates scaffold fibre direction.

DISCUSSION & CONCLUSIONS: Scaffold fibre orientation can influence osteogenesis of progenitor cells and the organisation of deposited matrix. Early stages of osteogenesis may not benefit from culture on orientated scaffolds but mineralised matrix deposition can be controlled by fibre alignment. It may be that the most suitable scaffold for osteogenesis of MSCs is a scaffold combining both random and orientated elements to enhance differentiation and control matrix organisation.

ACKNOWLEDGEMENTS: Lynda Bonewald for kindly donated MLO-A5 cells; Kroto Research Institute imaging facility; EPSRC for funding.

Bioprinting of personalised tissue engineered cell constructs for nasal reconstruction.

[LA Ruiz Cantu](#)¹, [A Gleadall](#)², [C Faris](#)³, [J Segal](#)², [J Yang](#)¹, [K Shakesheff](#)¹

¹Tissue engineering, School of Pharmacy, [The University of Nottingham](#), United Kingdom.

²Department of Mechanical, Materials and Manufacturing Engineering, School of Engineering, The University of Nottingham, United Kingdom. ³Ear, nose and throat department, Nottingham University Hospitals, United Kingdom.

INTRODUCTION: Carcinoma of the nose has 2000 new cases diagnosed each year in the US and 400 in the UK. One of the severe social and functional side effects of this condition is nasal deformity following a lifesaving resection of the tumour. Current surgical approaches involve autologous cartilage grafts, alloplastic materials and titanium meshes which result in poor functional and aesthetic results¹. Our approach involves a personalised bioprinted composite for nasal reconstruction. The composite consists of polycaprolactone providing structural support, and a cell-laden thermoresponsive and UV crosslinkable hydrogel. With this composite we aim to mimic the mechanical properties and architecture of nasal cartilage.

METHODS:

Design of personalised 3D nose model. The 3D model was designed with MIMICS software using the CT scan of a patient.

3D printing of thermoplastic 3D nose model. The 3D model was printed using a RegenHU Bioprinter. Briefly, polycaprolactone was melted at 74°C and then extruded through a 23G needle at a deposition speed of 16mm/s.

Preparation of UV crosslinkable hydrogel. GelMA was prepared by the reaction of porcine gelatine type A with methacrylic anhydride at 50°C for 1hr. Dialysed, freeze-dried and stored at -20°C.

Chondrocytes isolation and cultivation. Ovine chondrocytes were isolated from articular cartilage.

Bioprinting Chondrocytes were encapsulated in three different concentrations of GelMA and bioprinted using a 27G needle at a deposition speed of 10mm/s. Scaffolds were UV cross-linked for 60 seconds.

RESULTS: Polycaprolactone 3D printed nose models represented with accuracy the shape and size of the 3D model of the patient's nose.

Porosity was measured with microCT and a porosity of 32% was obtained.

Bioprinted chondrocytes showed an average of 80% viability. Secretion of ECM and increase in the strength of the hydrogels were observed after 14 days of culture.

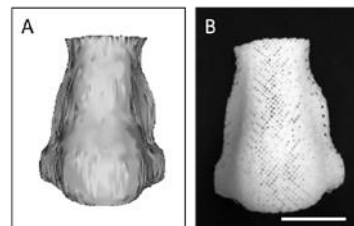


Figure 1 Personalised 3D printed nose model. A) 3D model design B) Polycaprolactone 3D printed porous nose. Scale bar represents 2cm.

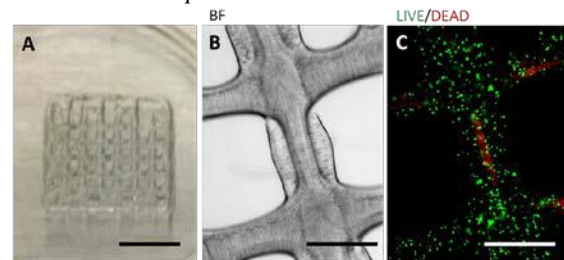


Figure 2 A bioprinted GelMA/chondrocytes construct. A) Macroscopic image of the construct. Scale bar represents 5mm. B and C) Representative images showing live and dead chondrocytes within the hydrogel. Scale bar represents 500µm

DISCUSSION & CONCLUSIONS:

We have demonstrated the feasibility of fabricating personalised nasal scaffolds using 3D printing. In addition, cell-laden GelMA was printed with high cell viability. In the future, printing of mechanically strong scaffolds and cell-laden hydrogel will be combined to produce composite scaffolds.

ACKNOWLEDGEMENTS: Financial support was received from EPSRC centre and CONACYT Mexico.

3D printing and plasma functionalisation of peripheral nerve guides

J Clarke¹, A Harding², F Boissonade², JW Haycock¹, F Claeysens¹

¹ Kroto Research Institute, The University of Sheffield, UK. ² School of Clinical Dentistry, The University of Sheffield, UK

INTRODUCTION: Nerve Guidance Conduits (NGC) are increasingly used in surgical peripheral nerve repair. Improving NGC performance is challenging as existing FDA approved materials are bio-inert. Microtopographical features and plasma surface functionalisation have been proposed to overcome this [1-2].

METHODS: 3D polycaprolactone (PCL) structures were manufactured by microstereolithography (μ SL) for *in vitro* & *in vivo* testing. PCL triol (Mn \approx 900 g/mol) was methacrylated by dissolving in dichloromethane and reacting with methacrylic anhydride to produce a photocurable prepolymer.

The μ SL setup consisted of a 405 nm diode laser and digital micromirror device (DMD). The required image was loaded onto the DMD and the laser light reflected from this, then focused onto the surface of the liquid prepolymer causing it to crosslink. 3D shapes were produced by lowering a stage within the prepolymer (fig 1).

Plasma chambers were used to air etch and coat substrates with either acrylic acid (AAc), allylamine (AAm) or maleic anhydride (MA).

in vitro - NG108-15 neuronal cells and RN22 Schwann cells were cultured on surfaces. MTT assay was used to confirm cell viability. After 72 hours, cells were fixed and labelled with phalloidin-TRITC (actin filaments) and DAPI (nuclei). Cells were imaged by confocal microscopy and neurite growth analysed using ImageJ software.

in vivo - Grooved and smooth NGCs were implanted in *thy-1-YFP-H* mouse common fibular nerve and compared with nerve graft. Regeneration was assessed by confocal-like microscopy. n = 5 for each condition, results are shown as average \pm SEM (fig 2).

RESULTS: Guidance features $<100 \mu\text{m}$ were created on the inner surfaces of the NGC (fig 1). Plasma coating was achieved evenly on the inner surfaces of NGCs $<1 \text{ mm}$ internal diameter with a length of 5 mm. Preliminary results show increased cell viability and neurite growth on AAc coated surfaces. Cells adhered well to other coated surfaces but neurite growth was less extensive.

Micro geometries showed significantly improved regeneration comparable to autograft.

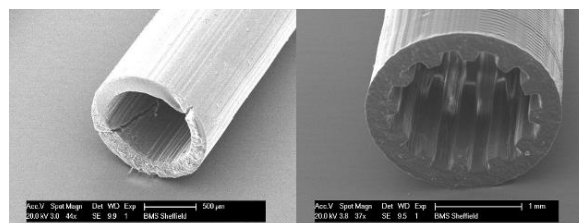


Fig. 1: Micrographs of NGC produced by μ SL.

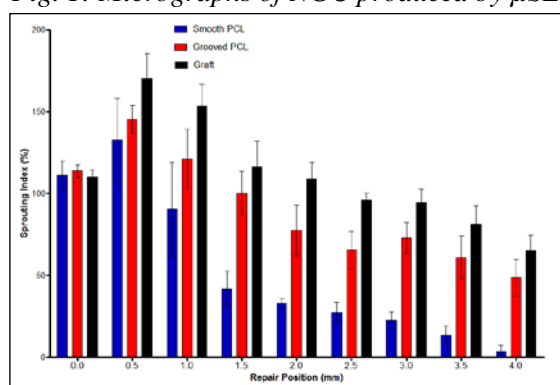


Fig. 2: Sprouting index of *thy-1-YFP-H* mouse common fibular nerve repair

DISCUSSION & CONCLUSIONS: We have produced NGC with user-defined topography and surface chemistry. Plasma treatment may be used to enhance neuronal and Schwann cell responses to otherwise bio-inert materials. Topographical features enhance peripheral nerve regeneration in an animal model.

ACKNOWLEDGEMENTS: We thank EPSRC for DTA funding and NEXUS XPS at Newcastle University. Confocal Imaging was performed at the Kroto Research Institute.

Role of miR-146b-5p in chondrogenesis

E Budd¹, T Sanchez-Elsner², ROC Oreffo¹

¹*Bone and Joint Research Group, Institute for Developmental and Regenerative Medicine, Faculty of Medicine, University of Southampton.* ²*Junk RNA group, Clinical and Experimental Sciences, Faculty of Medicine, University of Southampton.*

INTRODUCTION: Loss of chondrocytes accompanied by diminishment of specialised extracellular matrix is often the outcome of articular cartilage injury and can progress to the onset of osteoarthritis. Endogenous regeneration does not sufficiently replace articular cartilage and therefore stem cells provide a favourable option for the regeneration of articular cartilage. A class of non-coding RNA; microRNAs which regulate gene expression post transcriptionally have been shown to be important in the processes of stem cell proliferation and differentiation. Stem cells which are found to be regulated in part by microRNAs offer novel approaches for the application of microRNAs *in vitro* and *in vivo* for the regeneration of cartilaginous tissue and could also have compelling implications in cartilage associated disorders such as osteoarthritis.

METHODS: Human skeletal stem cells were isolated from six individual patients and cultured an *in vitro* high density micromass culture system using TGF- β 3 across 21 days to induce chondrogenesis. Chondrogenic gene analysis and microRNA analysis using qPCR and TaqMan qPCR was carried out on cells lysed at 7 day intervals. The bioinformatics programme TargetScan was used to identify a potential target of a microRNA observed to be down-regulated during the process. Transient transfection with the microRNA mimic into human skeletal stem cells followed by western blotting and densitometry analysis was used to analyse protein expression of the microRNA target. Human articular chondrocytes were also isolated from the cartilage of osteoarthritic patients and patients with an osteoporotic fracture (NOF), chondrocytes were analysed by qPCR for the expression of the novel identified microRNA.

RESULTS: We have identified for the first time that miR-146b-5p is significantly down-regulated in human skeletal stem cells during the process of chondrogenesis (Figure 1). TargetScan identified that the 3'UTR of *SOX5* contains a potential binding site of miR-146b-5p, making it a likely target of miR-146b-5p. Overexpression of miR-146b-5p through transient transfection of miR-146b-5p mimic into human skeletal stem cells

induced a ~50% reduction in SOX5 protein expression. Additionally, miR-146b-5p was found to have a ~200 fold increase in expression in human articular chondrocytes isolated from osteoarthritic patients (Figure 2).

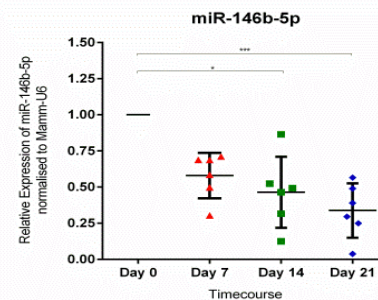


Fig. 1: Expression of miR-146b-5p in human skeletal stem cells cultured across 21 days in TGF- β 3 in a high density micromass system analysed by TaqMan qPCR ($n=6$, * $P<0.05$, *** $P<0.001$).

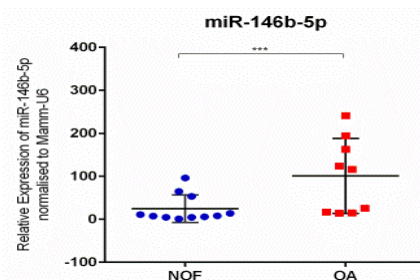


Fig. 2: Expression of miR-146b-5p in human articular chondrocytes isolated from cartilage of either patients with a NOF or with osteoarthritis analysed by TaqMan qPCR ($n=6$, *** $P<0.001$).

DISCUSSION & CONCLUSIONS: miR-146b-5p was identified as significantly down-regulated during chondrogenesis of human skeletal stem cells, likely due to targeting a positive regulator of early chondrogenesis; *SOX5*. MiR-146b-5p was also identified as significantly up-regulated in human articular chondrocytes from osteoarthritic patients. Application of miR-146b-5p along with other identified microRNAs in combination with stem cells therapy could potentially aid in the enhancement of cartilaginous tissue regeneration. Furthermore, miR-146b-5p may serve as a potential innovative target in the treatment of osteoarthritis.

Differential signalling through natriuretic peptide receptors mediates the chondrogenic effects of C-type natriuretic peptide

N Peake¹, S Thorpe¹, B Pinguuan-Murphy³, DA Lee¹, AJ Hobbs², TT Chowdhury¹

¹ Institute of Bioengineering, School of Engineering and Materials Science, ² William Harvey Research Institute, Barts and the London School of Medicine and Dentistry, Queen Mary University of London. ³ Department of Biomedical Engineering, Faculty of Engineering, University of Malaya, Kuala Lumpur, Malaysia.

INTRODUCTION: C-type natriuretic peptide (CNP) has critical roles in cartilage homeostasis and endochondral bone formation [1]. In mesenchymal stem cells (MSCs), treatment with CNP mediates differentiation to chondrocytes in the presence of TGF- β . The mechanism involves signalling through natriuretic peptide receptor 2 (Npr2) and subsequent production of cGMP leading to matrix synthesis. Targeting CNP signalling may therefore be a useful approach for cartilage repair by tissue engineering. In a previous study, treatment of chondrocytes with low CNP concentrations increased proliferation, whereas higher concentrations promoted matrix synthesis without influencing proliferation [2]. These contrasting responses are mediated by the differential effects of Npr2 and Npr3 [3]. In this study we examined Npr expression and investigated the effects of pharmacological agents that target both Npr pathways on hMSC differentiation.

METHODS: hMSCs were obtained from Stem Cell Technologies (Cambridge, UK), and cultured in defined chondrogenic medium in the presence or absence of TGF- β (10 ng/mL) and CNP (100nM). Experiments were performed for MSCs in monolayer culture, and seeded at 10×10^4 cells/mL in 2% agarose constructs. Functional effects of Nprs were assessed by treating with the Npr2 antagonist P19 (0.5 μ M), and the Npr3 agonist cANF (1 μ M). RT-qPCR was performed as previously described [3]. Cell proliferation was assessed using Alamar Blue assay, and sulphated glycosaminoglycan (sGAG) synthesis by DMB assay as described [3]. Statistical significance was determined using the Mann-Whitney U test, * = $p < 0.05$, ** = $p < 0.01$, *** = $p < 0.001$.

RESULTS: Our data demonstrated active Npr signalling in hMSCs. Both CNP and the Npr2 antagonist P19 potently inhibited proliferation in monolayer cultures (Fig 1), implicating Npr2 in this process. The Npr3 agonist cANF had no effect, and these effects were inhibited by the addition of TGF- β . 3D culture of hMSCs in agarose resulted in a significant down-regulation of both Nprs,

which was enhanced by TGF- β (Fig 2), indicating growth factor and biomechanical regulation of Npr expression. Finally, we observed that sGAG synthesis after 21 days of agarose culture is enhanced by both the Npr2 antagonist P19, and the Npr3 agonist cANF (Fig 3), suggesting a role for Npr3 in matrix synthesis. In the presence of TGF- β , sGAG synthesis was enhanced only by P19, indicating changes to Npr activation induced by the growth factor. Adding exogenous CNP had no impact on sGAG synthesis, indicating sufficient activation of Npr signalling by endogenous CNP.

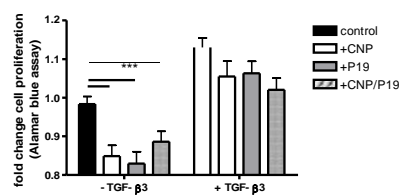


Fig. 1: Proliferation of hMSCs (day 3).

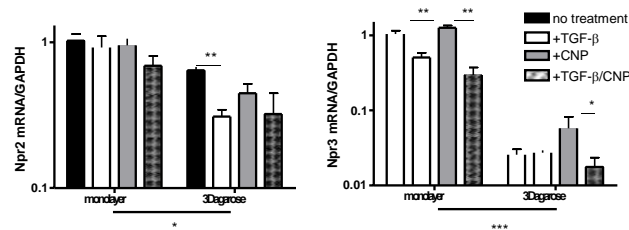


Fig. 2: mRNA expression of Nprs (day 3).

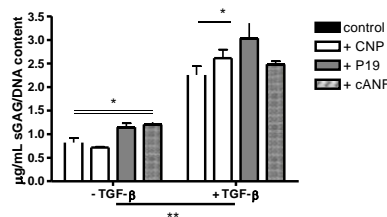


Fig. 3: hMSC sGAG synthesis in agarose (day 21).

DISCUSSION & CONCLUSIONS: Chondrogenic differentiation induced by 3D culture and TGF- β leads to a shift in the expression profile of Nprs, which has functional effects on differentiating hMSC proliferation and sGAG synthesis.

Human endothelial and foetal femur-derived stem cell co-cultures modulate osteogenesis and angiogenesis

[S Inglis](#)¹, [D Christensen](#)², [DI Wilson](#)², [JM Kanczler](#)¹, [ROC Oreffo](#)¹

¹Bone and Joint Research Group, Centre for Human Development, Stem Cells and Regeneration, University of Southampton, UK. ²Human Development and Health, Centre for Human Development, Stem Cells and Regeneration, University of Southampton, UK

INTRODUCTION: A functional vasculature is a prerequisite for bone formation. The interaction of bone cells and endothelial cells underpins the processes necessary to develop and regenerate bone. Previous studies have shown that adult human bone marrow stem cells in contact co-cultures with endothelial cells can drive osteogenesis¹⁻². In this study we investigated the intricate interactions of human foetal femur derived stem cells (FFDC) stemming from the diaphysis (FD) and epiphysis (FE) in contact co-culture with human umbilical cord endothelial cells (HUVEC), to investigate their osteogenic and angiogenic potential for bone regeneration.

METHODS: Human foetal femur epiphyseal and diaphyseal cells populations were isolated and cultured. HUVECs were isolated from full term umbilical cords. Co-cultures of FD/HUVEC and FE/HUVEC were setup in a 1:1 ratio and cultured in basal and VEGF-165 (100ng/ml) supplemented media for 7 days. Early osteogenic activity was assessed by alkaline phosphatase (ALP) stain and biochemical activity. Relative gene expression of osteogenic and angiogenic markers was measured using quantitative polymerase chain reaction. Additionally, E11 embryonic chick femurs were cultured over 10 days using an ex-vivo organotypic model to determine osteogenic effects of VEGF. Femurs were assessed using micro-computed tomography (μ CT). Femurs were also histologically assessed using Alcian blue/Sirius red staining and immunohistochemistry for CD31 expression.

RESULTS: ALP activity and gene expression of ALP and Type-1 collagen was enhanced in FFDC/HUVEC co-cultures. Conversely, the addition of VEGF significantly reduced levels of ALP gene expression in FD/HUVEC cocultures. ALP gene expression was significantly elevated in FE/HUVEC basal and VEGF-supplemented co-cultures. Changes in VEGF gene expression were negligible; however VEGF receptor 1 and 2 gene expression was significantly elevated in FFDC/HUVEC co-cultures with FD/HUVEC co-cultures demonstrating the greatest increase.

Finally, in cultures of E11 chick femurs, VEGF supplementation stimulated collagen formation and CD31 expression within the diaphyseal regions of the bone.

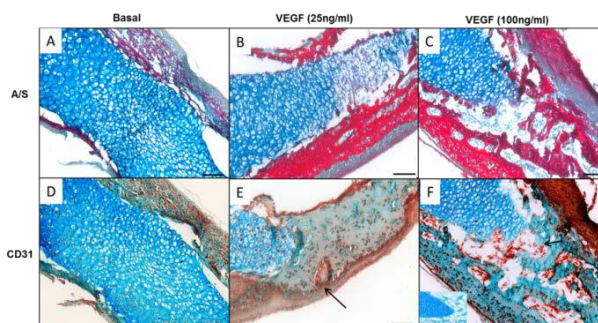


Fig. 1: Images of Alcian blue/Sirius red staining (A-C) and CD31 immunostaining (D-F) on E11 embryonic chick femurs at D10 of organotypic culture.

DISCUSSION & CONCLUSIONS: Human foetal femur derived stem cells in contact co-culture with endothelial cells enhance osteogenesis and modulate angiogenic markers. Differences in modulation of osteogenic markers by cells from the distinct regions of the foetal femur were observed. This study reveals a differential response of early skeletal stem cells cultured in vitro and ex vivo and emphasises the importance of the intricate temporal coordination of osteogenic and angiogenic processes during bone formation and implications this may have for effective approaches to bone regenerative therapies.

ACKNOWLEDGEMENTS: This research was supported by the BBSRC (LOLA grant BB/G010579/1). The authors would like to thank PAH for providing umbilical cords and the Bone and Joint Research Group for useful discussion.

Remote cell activation for bone regeneration - a preclinical animal study.

H Markides¹, J McLaren², JR Henstock¹, N Telling¹, B Scammell², K Shakesheff², AJ El Haj¹.

¹Institute for Science and Technology in Medicine, Keele University, Stoke-on-Trent, UK

²The University of Nottingham, Nottingham, UK

INTRODUCTION: We aim to develop a cell-based injectable solution for treatment of non-union bone fractures. Our approach is based on the use of functionalised magnetic particles (MNPs) targeted to the TREK-1 mechano-sensitive receptor on the mesenchymal stem cell (MSC) membrane. Attached MNPs respond to the application of an oscillating external magnetic field resulting in remote receptor activation and enhanced osteogenic differentiation. In this way, we can deliver functional mechanical stimuli to therapeutic cell populations *in vivo* following injection either systemically or to the repair site. This concept has been validated through a series of *in vitro*, *ex vivo* and small animal studies and is currently being tested in a pre-clinical sheep model for bone repair.

METHODS: A key element in the remote activation of MNP-labelled cells is the application of an oscillating magnetic field applied externally. Here, we describe the design of a magnetic array used to stimulate cell populations *in vivo* in a large animal model. The optimal magnet arrangement was chosen by investigating magnet shape, orientation and grade by 2D FEMM magnetic simulation software. The top 6 designs were fabricated and prototypes validated in 3D. An *ex vivo* sheep model was established to compare the tissue penetration depth of the 6 prototype and the final design incorporated into a sheep harness.

To evaluate the effect of remote magnetic activation on bone repair, 5×10^6 autologous MNP-labelled STRO-4 positive MSCs were encapsulated within a naturally derived bone extracellular matrix gel and implanted within a critical sized defect (0.8x1.5cm) in the medial femoral condyle of a sheep. Implanted cell populations were stimulated over 13 weeks by custom built magnetic array housed within a standard sheep harness. Bone fill was assessed by μ CT and validated histologically.

Variability in donor response to magnetic stimulation was further evaluated *in vitro* in a 3D hydrogel systems by encapsulating MNP-labelled MSCs from 17 donors within a 2.5mg/ml collagen hydrogel, magnetically stimulating (MICATM

bioreactor) for 1hr/day over 28 days and mineralisation levels analysed by μ CT

RESULTS: Results of the 2D FEMM magnetic simulation concluded that two 4x2cm N42 magnets arranged in opposing orientation were required to achieve greatest magnetic field strength with a tissue penetration depth of 3cm. Preliminary bone fill data suggests enhanced targeted bone fill in MNP-magnet stimulated cell groups over non-stimulated cell groups. Variation in donor response to magnetic stimulation *in vitro* was observed across all donor cells. In most cases, magnetic stimulation resulted in enhanced mineralisation within the collagen gel system.

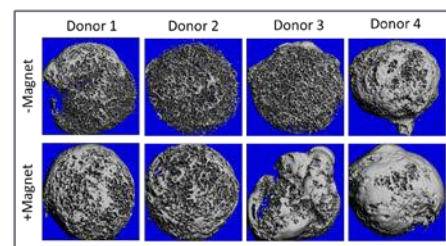


Fig. 1: MicroCT images comparing mineralisation levels of MSCs from 4 sheep donors encapsulated within a collagen hydrogel and their response to magnetic stimulation.

DISCUSSION & CONCLUSIONS: This project demonstrates the translational challenges faced when moving from bench to bench-side and our approach to overcoming such challenges. Our novel results further demonstrate the feasibility of a remote magnetic nanoparticle approach for cell therapy applications.

ACKNOWLEDGEMENTS: We acknowledge the financial support of the UKRMP acellular technologies hub.

Stem cell-derived exosomes: a new tool to treat nerve injuries?

RC Ching^{1,2}, M Wiberg^{1,2}, PJ Kingham¹

¹ Department of Integrative Medical Biology, Umeå University, Umeå, Sweden. ² Department of Perioperative & Surgical Sciences, Umeå University, Umeå, Sweden.

INTRODUCTION: Despite modern microsurgical techniques of peripheral nerve injury (PNI) repair, functional restoration is always incomplete. Approximately 2 in 10 PNI patients have a 'nerve gap' where direct repair of the two nerve stumps is not possible. Clinically these are treated with autologous nerve grafts and experimentally synthetic conduits impregnated with Schwann cells (SC) or stem cells have been developed¹. Both of these techniques have their drawbacks; with nerve grafting and SC use requiring the sacrifice of a healthy functioning nerve, and the risk of malignant transformation when using transplanted stem cells, along with many regulatory hurdles to overcome. We propose that exosomes (small intercellular messaging vesicles) isolated from adipose-derived stem cells (ASC) can contribute to the development of new strategies for treating these injuries.

METHODS: ASC were differentiated into a Schwann cell-like phenotype (dASC) using a defined mixture of growth factors². Exosomes were isolated from the media of the dASC and primary SC cultures. They were then applied to NG108-15 neurons *in vitro* for 24 hours, with computerised image analysis used to assess resultant neurite outgrowth for comparison against the control group. Exosomal cargo was also investigated using RT-PCR techniques to identify mRNA and microRNA involved in nerve regeneration.

RESULTS: Neurons extended neurites in the presence of dASC derived exosomes (Figure 1).

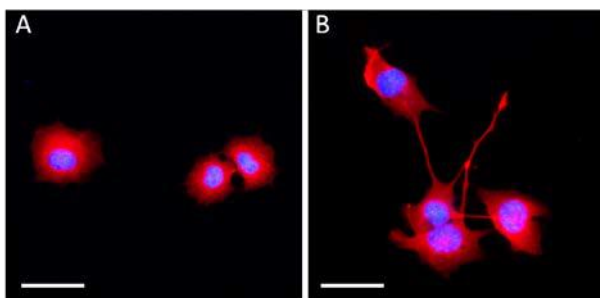


Fig. 1: Cultured neurons stained for β III-tubulin (red) with DAPI (blue); incubated in control media (A) or incubated with dASC exosomes (B). Scale bar = 50 μ m.

Quantification showed that both SC and dASC exosomes significantly ($p < 0.05$, one-way

ANOVA) enhanced the neurite length compared with the media only control group (Figure 2).

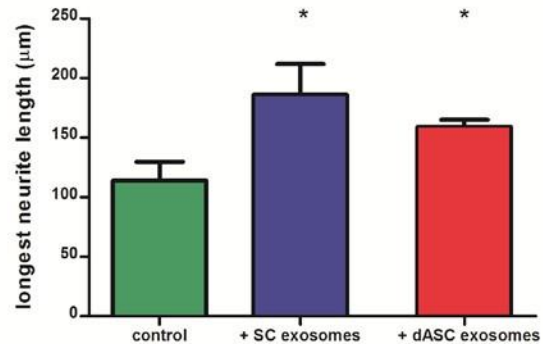


Fig. 2: Neurons incubated with either SC or dASC exosomes produced longer neurites compared to control ($p < 0.05$).

RNA shown to participate in nerve regeneration was identified in both cell type exosomes including mRNA for GAP43, NF200 and peripherin and microRNAs miR-1, miR-133a and let7d.

DISCUSSION & CONCLUSIONS: These results indicate dASC exosomes increase neurite outgrowth *in vitro*, mirroring the already proven success of their SC counterparts³. The mRNA and microRNA identified within these exosomes are likely to be instrumental in this increase. Future uses of exosomes in treatment for peripheral nerve injuries could include direct injections in primary repairs of simple injuries, or in combination with synthetic conduits for nerve gaps.

ACKNOWLEDGEMENTS: This study was supported by EU Regional Development funds, Västerbottens County Council (ALF) and Umeå University (Insamlingsstiftelsen).

Cell line creation using hTERT immortalisation impacts on sulphated glycosaminoglycan secretion and chondrogenic potential

[TP Dale](#)¹, [A DeCastro](#)², [EK Parkinson](#)², [NJ Kuiper](#)¹, [NR Forsyth](#)¹

¹ *Institute for Science and Technology in Medicine, Keele University, Staffordshire, UK*

² *Institute of Dentistry QMUL, London, UK*

INTRODUCTION: Limited therapeutic options for the treatment of cartilage damage or degeneration have driven the development of cell therapy alternatives. However, chondrogenesis in the relevant cell types is difficult to study due to the rapid onset of replicative senescence and culture induced de-differentiation. Replicative senescence may be ameliorated without loss of phenotype by re-expression of telomerase reverse transcriptase (hTERT).

We therefore sought to explore the effect of hTERT immortalisation on the chondrogenic differentiation of primary human bone-marrow mesenchymal stem cells (BMA13), chondrocytes (OK3) and embryonic stem cell derived mesenchymal-like cells (1C6), and their hTERT transduced counterparts (BMA13H, OK3H, 1C6H).

METHODS: In all cases pellets of ~250000 cells were maintained in a 2% O₂ incubator for 20 days in maintenance media (MM) or pro-chondrogenic media (PChM) supplemented with TGF- β 3. Subsequently pellets were proteinase K digested and the sGAG content of both pellets and spent culture media at day 0 and day 20 determined using the dimethyl-methylene blue assay and DNA content by PicoGreen assay. Quantitative gene expression analysis was performed for COL1A2, COL2A1, COL3A1, COL6A3 and COL10A1, ACAN, COMP and SOX9. Pellets were fixed in 4% paraformaldehyde and firstly scanned using micro computed tomography (μ CT) followed by paraffin embedding and sectioning. Sections were stained with toluidine blue for sGAG, picosirius red for collagen and immunostained for collagen types I, II, VI and X, and aggrecan.

RESULTS: Cell pellets were larger in PChM than in MM after 20 days and μ CT scanning revealed a relatively uniform density throughout (Fig. 1). Staining for collagen and sGAG was heterogenous, particularly in 1C6 and BMA13 and stronger at the periphery of pellets, transduced cell pellets stained more weakly.

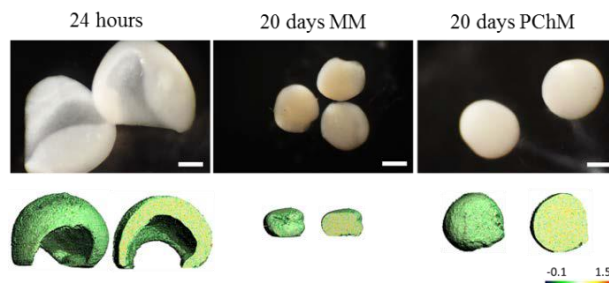


Fig. 1: BMA13H pellets after 24 hours and 20 days in MM or PChM. Upper panel:

Photomicrographs of pellets, scale 0.5mm. Lower panel μ CT scans of pellets, colour range indicates relative density.

In PChM absolute (μ g sGAG) and normalized (μ g sGAG/ μ g DNA), pellet associated, sGAG levels increased in all three primary cell types compared to day 0 levels (OK3 > BMA13 > 1C6). By day 20 all pellets except BMA13H had significantly more sGAG when cultured in PChM rather than MM ($p \leq 0.01$). Transduced cell pellets in PChM had reduced levels of sGAG in comparison to their non-transduced counterparts. In addition to pellet associated sGAG, spent culture media contained sGAG accounting for 8.4%, 46.2% and 92.8% of total sGAG in BMA13, 1C6, and OK3 with levels generally higher in transduced cells at 62.4%, 77.4% and 92.5% in BMA13H, 1C6H and OK3H when cultured in MM. Culture in PChM reduced sGAG secreted to the media to 2.4%, 34.8% and 70.8% in BMA13, 1C6, and OK3 and 27.9% 41.8% and 65.5% BMA13H, 1C6H and OK3H.

DISCUSSION & CONCLUSIONS: All three primary cell types displayed the anticipated response to pro-chondrogenic conditions however hTERT introduction led to variable outcomes with an overall reduction in chondrogenic response. Our results demonstrate that the introduction of telomerase to extend proliferative capacity may impact negatively on chondrogenic potential and require additional interventions to circumvent this

ACKNOWLEDGEMENTS: This work was funded by the EPSRC.

Examination of human bone tissue regeneration using the chorioallantoic membrane (CAM): an *ex vivo* replacement model for animal research

I Moreno¹, G Hulsart-Billström¹, S Lanham¹, ND Evans¹, ROC Oreffo¹

¹Centre of Human Development, Stem Cells and Regeneration, Faculty of Medicine, University of Southampton. England, UK.

INTRODUCTION: Loss of bone mass requires the use of bone material substitutes and their success is critically affected by the presence of stable blood vessel supply (angiogenesis) during the healing process¹. The efficacy and safety of bone tissue engineering novel constructs need to be tested *in vivo* before reaching the clinic. However, the use of animals in research is complex and raises ethical concerns². Here we propose the use of the chick chorioallantoic membrane (CAM) as an *ex vivo* vascular bed to culture freshly isolated human bone. In addition, the potential of a clay hydrogel (Laponite) to deliver Vascular Endothelial Growth Factor (VEGF) will be examined using this human *ex vivo* model.

METHODS: To investigate this, bone grafts were extracted from fresh human femoral heads and engineered as hollow cylinders to resemble a bone injury model (Fig. 1 A-B). Bone cylinders were perfused with Laponite, Laponite VEGF or Blank and cultured *in vitro* (organotypic), *ex vivo* (CAM) or left in buffered solution for 7 days (control). High resolution computed tomography (μ CT) was conducted before and after culture of the bone cylinders to quantify the relative change of bone volume, followed by histological examination.

RESULTS: Viability staining and explant culture showed that the bone tissue remained viable following CAM culture with intimate contact between the CAM and the bone cylinder. The invasion of the chick vasculature into the human tissue was noticed by the presence of avian capillaries (Fig. 1 C-D). In addition, Cathepsin K expression and collagenous-like structures were evidenced by histological analysis.

Multilevel μ CT analysis showed a significant increase in low dense bone (bone deposition) in parallel to a modest decrease in high dense bone (bone resorption) in all treatments. Laponite treatment showed significant bone formation ($p < 0.05$). *Ex vivo* culture of the bone cylinders on the CAM demonstrated significant bone volume change compared to the *in vitro* group ($p < 0.005$).

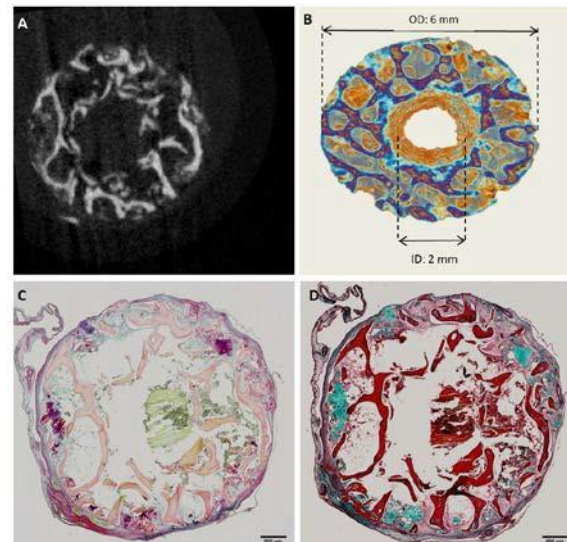


Fig. 1: Human bone engineered cylinder before (A-B) and after (C-D) CAM implantation. μ CT scan cross section of the bone graft (A) and top view of the 3D image. Histology image of the same cross section as (A) following CAM implantation, stained for Alcian blue and Sirius Red (C) and Goldner's Trichrome (D).

DISCUSSION & CONCLUSIONS: Overall, the CAM is a successful bioreactor for this human injury model, providing an active remodeling process of both deposition and resorption, as shown by the μ CT. Laponite delivery displayed the ability to modulate bone formation. Finally, this experimental set up provides a successful alternative model for animal research while using clinically relevant samples.

ACKNOWLEDGEMENTS: This project is kindly funded by the NC3Rs.

***In vitro* recreation of the 3-dimensional bone marrow niche for platelets production**

G Bouet¹, M Colzani¹, M Arumugam¹, D Howard¹, T Moreau¹, W Afshar-Saber¹, S Best², R Cameron², C Ghevaert¹

¹ *Department of Haematology, University of Cambridge and NHS Blood and Transplant, Cambridge, UK.* ² *Materials Science and Metallurgy, Cambridge Centre for Medical Materials, Cambridge, UK.*

INTRODUCTION: Platelets are produced in the bone marrow by megakaryocytes (MKs) and play a key role in homeostasis and clotting. Donor-derived platelet transfusions are therefore used to prevent bleeding in patients with low platelet counts. Donated platelets have limited shelf-life, which makes stocks dependent on regular donations. The need to provide HLA-matched platelets for alloimmunized patients can put additional strain on blood providers. An alternative would be to produce platelets *in vitro*, derived from cultured MKs. The advantage is that these cells would be free of blood-borne diseases and could be optimally matched to recipients. However, currently, we are hampered by the inability to obtain functional platelets *in vitro* in large amounts from cultured MKs. Thus, our aim is to recreate the bone marrow environment and the essential chemico-mechanical cues it provides for MK maturation, proplatelet formation and release using a GMP-compatible tissue engineering approach.

METHODS: The first step of this work aimed to develop a 3-dimensional support for MKs that mimics the vascular endothelium (extravascular side). We have developed, via a freeze-drying process, an inert collagen-based scaffold that functions as a “back-bone” 3D structure for *in vitro* culture of MK. This scaffold is subsequently specifically functionalized using chemical cross-linking methods with recombinant proteins in order to reproduce the cell surface landscape of the bone marrow sinusoids to give a direct contact signal to megakaryocytes to produce proplatelets.

The second step of this 3D culture system was aimed at recreating the shear stress of sinusoid lumen by introducing the functionalized scaffolds into a custom-made parallel flow bioreactor.

To produce functional platelets in our system, we have used MKs differentiated from either primary hematopoietic stem cells (cord blood) or human induced pluripotent stem cells (iPSC) obtained under GMP conditions using a forward programming protocol based on ectopic expression

of transcription factors (Moreau et al, in preparation).

RESULTS: We show that we boost platelet production of megakaryocytes seeded on 3D collagen scaffolds up to 6 times compared to the 2D classical system.

Out of a library of 50 ectodomain recombinant proteins derived from surface expressed protein of vascular cells, we identified two which positively regulate platelet formation. Platelet production is further enhanced when these two proteins are immobilized on the collagen scaffolds.

Finally the functionalized scaffolds will be incorporated into custom-made two chamber bioreactors to recreate the shear stress found in the bone marrow sinusoid lumen to facilitate platelet release and harvest into storage solutions compatible for human use.

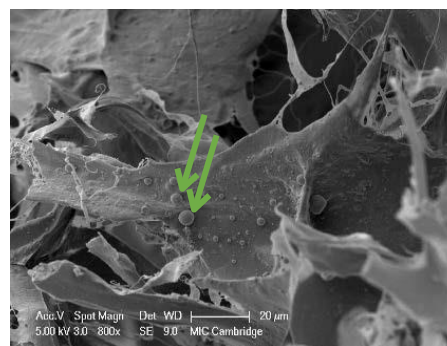


Fig. 1: Scanning electron microscopy image of platelets on scaffold after 3 days in culture

DISCUSSION & CONCLUSIONS: We have used a bespoke tissue engineering approach to recreate the bone marrow environment in order to harvest functional platelets from the cultured MKs to allow small-scale proof of principle human studies.

ACKNOWLEDGEMENTS: This work was supported by the National Institute for Health Research and by the Medical Research Council Centre Grant (UK).

Dynamic hydrostatic pressure – an osteogenic stimulus for mesenchymal stem cells in 3D hydrogel culture

JR Henstock¹, JCFA Price¹, AJ El Haj²

¹[Institute for Science and Technology in Medicine, University of Keele, UK](#)

INTRODUCTION: Hydrogel scaffolds provide an ideal culture environment for many cell types, being able to approximate some of the biochemical and structural elements of tissues. However, it can be challenging to provide an appropriate mechanical stimulus to cells in such a soft matrix – although physiological forces are known to be crucial in mediating critical aspects of tissue formation, function, growth and repair [1].

Dynamic hydrostatic pressure has been shown to be an important mechanical stimulus for cells in the body, transducing the compressive loading of bone and cartilage into a change in pressure in the interstitial fluid which can then be detected by cells. In this study, a range of hydrostatic pressure regimes were applied to human mesenchymal stem cells in tissue engineered hydrogels to study the effect of dynamic culture on osteogenesis.

METHODS: Human mesenchymal stem cells were seeded into 3D hydrogel scaffolds and cultured for 28 days in an osteogenic media. Hydrostatic pressure regimes of 0-280 kPa at 0.005 - 1Hz were applied to for 1 hour per day using a custom designed bioreactor (*fig. 1*) to simulate different types of physiological loading. Bone formation was assessed by weekly X-ray microtomography (μ CT) and histology.

RESULTS: Stimulation of the cells with 280kPa cyclic hydrostatic pressure at 1Hz (matched to normal physiological exercise) resulted in up to 75% mineralisation in the hydrogel, whilst static culture, constant high pressure or either low-frequency or low-magnitude stimulation had no effect (<2% mineralisation), *fig. 2*.

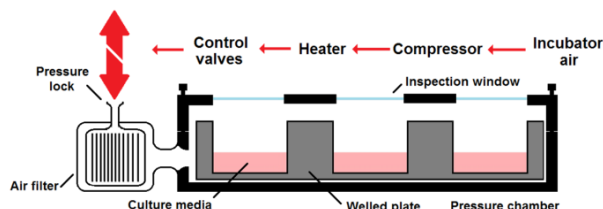


Fig. 1: Incubator air is compressed and directed into a chamber containing the cell-seeded hydrogels in a standard well culture plate. Dynamic (cyclic) pressures are applied for one hour per day over 28 days.

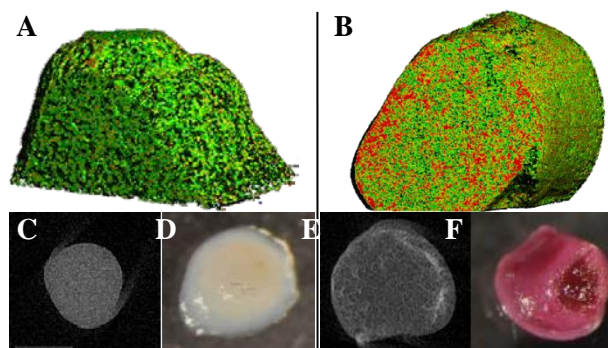


Fig. 2: Comparison of cell-seeded hydrogels after 28 days in either static culture (left) or stimulated (right). μ CT reconstructions (A&B) show bone formation in red within the low-density green hydrogel. Mineralisation is also visible in 2D X-ray (C&E) and alizarin red staining (D&F).

DISCUSSION & CONCLUSIONS: These results suggest that dynamic hydrostatic pressure is a potent stimulus in stimulating MSC differentiation into actively secreting osteoblasts, and cells may be primed to respond to loading forces within a specific physiological range [2].

As tissue engineering strategies are now entering clinical translation, understanding how physiological loading forces interact with, drive and direct tissue growth will be fundamental to optimising treatments. Appropriate mechanical signals are an essential component in recreating tissue environments and translating *in vitro* regenerative medicine into clinical treatments.

ACKNOWLEDGEMENTS: This work was supported by the BBSRC (sLoLa grant). We would like to thank our collaborators in groups led by Prof. Richard Oreffo, Prof. Kevin Shakesheff and Prof. Molly Stevens for their contributions to this project.

3D Bioprinting of soft-tissue substitutes from cell-seeded stimuli responsive hydrogels

A Aied, P Mistry, K Shakesheff, J Yang

Centre for Biomolecular Sciences, School of Pharmacy, University of Nottingham, UK. NG7 2RD

INTRODUCTION: Three dimensional bioprinting is being applied to tissue engineering and regenerative medicine as a manufacturing tool to produce 3D tissues and organs suitable for transplantation. In the present study, we use micro-extrusion based 3D bioprinting to generate complex hydrogel architecture that resembles human tissue. The hydrogels used for printing have unique thermoresponsive, photocrosslinkable, biodegradable and cell proliferation aiding properties that provide a biomimetic environment for tissue development.

METHODS: Non-viral transfection vectors were used to generate collagen type VII expressing RDEB keratinocytes that were previously incapable of producing the protein¹. The cells are then seeded into a printable thermoresponsive hybrid polymeric hydrogel from methacrylate monomers and collagen that support drug delivery, cell survival, attachment and proliferation. In addition, we have modified gelatin to make it photocrosslinkable and added liver cell binding carbohydrate to increase cellular attachment and proliferation.

Polymer synthesis and characterisation: Thermoresponsive and biodegradable methacrylate based polymers were synthesised from DE-ATRP² under nitrogen gas and using copper chloride as catalyst and ethyl-bromoisobutyrate as initiator. Throughout the experiment, samples are taken and the molecular weight is measured using proton NMR.

Photocrosslinkable gelatin modification: The photocrosslinkable gelatin was modified with HepG2 liver cell binding carbohydrate by primary amine substitution using EDC-NHS chemistry. The final product was purified and dialysed against water for five days before use.

RESULTS: The thermoresponsive polymer/collagen hybrid hydrogel provides viscous solution which can be printed into porous skin equivalent that house the genetically corrected keratinocytes (Figure 1). The modified gelatin with the added property of UV photocrosslinking (figure 2) was used to house HepG2 after modification with the HepG2 peptide (TP). Cell

viability was not compromised and proliferation studies are currently ongoing.

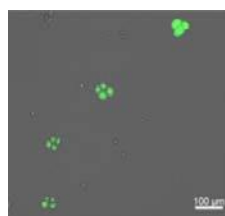


Fig. 1: GFP expressing keratinocytes stably transfected with polymer based transfection agent.

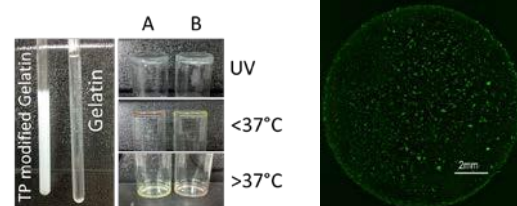


Fig. 2: Left: Gelatin modified with targeting HepG2 moiety (TP). A. photocrosslinkable gelatin and B. Photocrosslinking not affected by peptide conjugation to the gelatin. Right: Cell viability not affected by making gelatin photocrosslinkable or conjugation of the TP.

DISCUSSION & CONCLUSIONS: We have synthesised two unique hybrid hydrogels for the purpose of 3D bioprinting of skin and liver tissue. We modified collagen to make it printable and made gelatin multi-stimuli responsive. The results of proliferation, mechanical properties and vascular formation after 3D printing will be presented at the conference.

ACKNOWLEDGEMENTS: The research leading to these results has received funding from the People Programme (Marie Curie Actions) of the European Union's Seventh Framework Programme (FP7/2007-2013) under REA grant agreement No PCOFUND-GA-2012-600181.

Creating thermo-responsive co-electrospun fibres for 3D cell growth

AM Aladdad, LJ White, C Alexander, FRAJ Rose

Division of Drug Delivery and Tissue Engineering, Centre for Biomolecular Sciences, School of Pharmacy, University of Nottingham, UK

INTRODUCTION: The cell supply chain for regenerative medicine requires the development of new in vitro culture systems. Current methods to generate large quantities of cells destined for clinical use commonly use enzymatic digestion. However, using enzymatic digestion to extract cells from in vitro culture is not desirable for subsequent transfer to the body due to the destruction of important cell surface proteins and risk of contamination [1]. Research has led to the development of thermo-responsive surfaces for the continued culture of mammalian cells with passaging achieved with just a slight drop in culture temperature. Recognising that the 3D culture environment influences cell phenotype, our aim was to generate a thermo-responsive 3D fibre based scaffold using electrospinning.

METHODS: Thermo-responsive Poly (PEGMA₁₈₈) polymer, was prepared by free radical polymerization, then co-electrospun with PLGA or PET polymers to form thermo-responsive fibres. Inclusion of the thermo-responsive polymer was characterized by ¹H-NMR, XPS and WCA measurements. 3T3 mouse fibroblast cells, immortalized human mesenchymal stem cells and human cancer colon epithelial cells were seeded on these fibres. Subsequent cell viability assay (Alamar Blue) was performed to measure the difference in cell number while changing the culture temperature. Also, fluorescence microscopy was used to visualize the attachment and detachment of the cells.

RESULTS: This study has demonstrated that co-electrospinning is a promising way to create fibres with thermo-responsive surfaces, able to support cell adhesion and proliferation at 37 °C. Also, it was possible to detach the cells from the scaffolds by decreasing the temperature to 17 °C (Fig.1 and Fig.2). Importantly, cells were viable and proliferated in a similar manner to those cultured on control surfaces (PLGA or PET scaffolds).

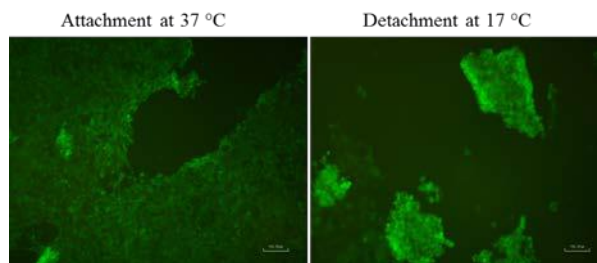


Fig. 1: Representative fluorescence microscopy images showing ihMsc cells attachment to thermo-responsive scaffolds at 37 °C and detachment after decreasing the environment temperature to 17 °C.

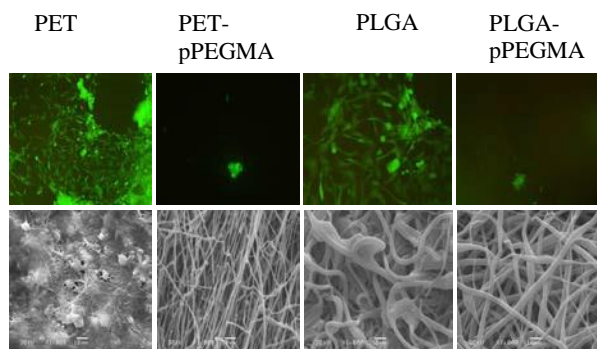


Fig. 2: Representative fluorescence microscopy and SEM images showing ihMsc cells detachment from scaffolds contacting poly (PEGMA₁₈₈) and cell remaining on PET and PLGA scaffolds alone at 17 °C.

DISCUSSION & CONCLUSIONS: These scaffolds were found to be suitable substitute for conventional cell culture methods with a number of different cell types by supporting cell attachment, growth and detachment inappropriate numbers without any negative effect on the viability, proliferation and adhesion potential of the cultured cells.

ACKNOWLEDGEMENTS: Funded by government of Saudi Arabia.

Stem cell product-based blockage of cytokine-induced apoptosis: implications for diabetes

B Al-Azzawi¹, C Kelly², NR Forsyth¹

¹Guy Hilton Research Center, Institution of Science and Technology in Medicine, Keele University

²Northern Ireland Centre for Stratified Medicine, Ulster University

INTRODUCTION: A feature of Type 1 diabetes mellitus (T1DM) is the cytokine-induced apoptosis of insulin-secreting Beta cells (β -cells). The cytokines are secreted from macrophages after infiltration into the pancreatic islets of Langerhans. Daily insulin supplementation is the only widely available treatment option for this disease, but this can lead to serious complications including diabetic ketoacidosis or cardiovascular disease. The utility of mesenchymal stem cells as a therapeutic and novel drug discovery tool is being widely explored. The aim of this study was to explore the therapeutic effectiveness of mesenchymal stem cells (MSC) on cytokine-induced apoptosis in β -cells.

METHODS BRIN BD11, an insulin-secreting β -cell line was exposed to pro-inflammatory cytokines and endotoxin (IFN- γ , TNF- α , IL-1 β and LPS) to induce β -cells apoptosis. This was performed with and without MSC serum-free conditioned media (SF-CM). SF-CM was conditioned for 24 hours on 70% confluent MSC monolayers. Cellular viability and apoptosis were determined with MTT and TUNEL assays respectively.

RESULTS: IFN- γ (1 μ g/ml), TNF- α (100ng/ml), IL-1 β (100ng/ml) AND LPS (500 μ g/ml) all reduced BRIN BD11 viability to approximately 50% at the concentrations indicated (Figure 1A). This effect was noted with and without serum where the latter resulted in decreased sensitivity to TNF- α and LPS. The TUNEL assay confirmed that this reduction in cellular viability resulted from programmed cell death (apoptosis) in all instances (Figure 1C). However, the addition of SF-CM significantly decreased the sensitivity of BRIN BD11 cells to all cytokines ($P \leq 0.05$) and endotoxin ($P \leq 0.05$) in the presence and absence of serum.

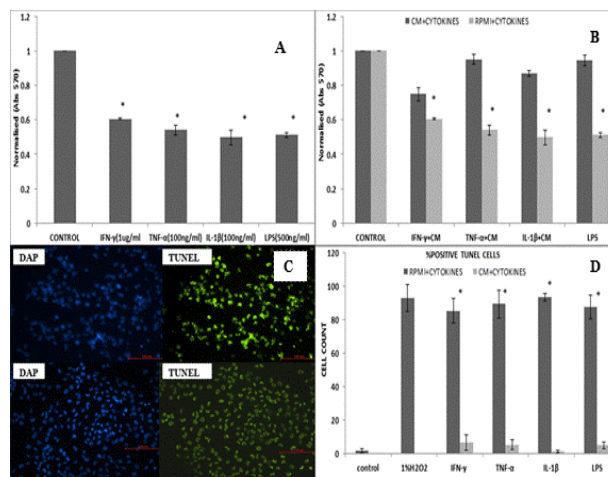


Fig. 1: -(A) Stimulating BRIN BD11 cells with different IFN- γ concentration. (B) comparison between cells treated with cytokines in ordinary media and those treated with cytokines in conditioned media. (C) tunel assay images. (D) %positive tunel cells.

DISCUSSION & CONCLUSIONS: Pro-inflammatory cytokines and endotoxin (IFN- γ , TNF- α , IL-1 β and LPS) induced β -cell apoptosis was blocked by the addition of MSC SF-CM. Characterization of MSC SF-CM has revealed promising candidate molecules for novel targeted diabetes therapies.

ACKNOWLEDGEMENTS: Funding for this project was provided by the Iraqi Ministry Of Higher Education and Scientific Research.

Hydrogel scaffold derived from decellularized bone matrix with osteogenesis-inducing activity and protein carrier ability for bone regeneration

N Alom, KM Shakesheff, LJ White

Drug Delivery and Tissue Engineering Division, Centre of Biomedical Science, University of Nottingham, UK

INTRODUCTION: Hydrogel scaffolds derived from the extracellular matrix (ECM) of mammalian tissues have been used to promote constructive remodelling *in vivo*. Such scaffolds have the advantage of being delivered in a minimally invasive manner, have the bioinductive properties of the native matrix, and may be used to fill an irregular shaped space. The objectives of this study were: (1) to determine the biological composition and osteoinductive properties of ECM hydrogels prepared from demineralized and decellularized bovine bone; (2) determine the ability of bECM as a carrier for local delivery of proteins.

METHODS: Bovine bone was demineralized and decellularized as previously described [1]; the resultant bone granules were digested and solubilized with pepsin and gelation was induced by neutralizing the pH and salt concentration. Mouse primary calvarial cells (mPCs) and C2C12 mouse myoblast cells were cultured on the surface of hydrogels and osteogenic differentiation was analysed by qPCR, immunohistochemistry, alkaline phosphatase (ALP) activity, and alkaline phosphatase staining in both basal and osteogenic media. The release of fluorescently labelled HSA from bECM gels of different concentrations was measured over 2 weeks.

RESULTS: Culture of C2C12 and mPCs on bECM and bDBM gels resulted in significant increases in expression of osteogenic markers ALP, osteopontin (OPN) and osteocalcin (OCN) compared to cells cultured on collagen type I for both basal and osteogenic media (Fig.1). bECM hydrogels demonstrated stable release of protein; the release kinetics of proteins from hydrogels was dependent on the bECM hydrogel concentration.

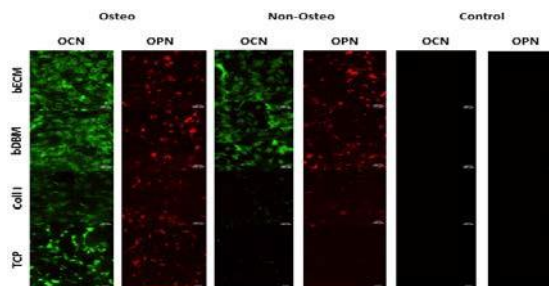


Fig. 1: Expression of osteocalcin and osteopontin in mouse primary calvarial cells cultured on collagen type I, tissue culture plate (TCP), decellularized bone matrix (bECM), and demineralized bovine bone (bDBM) with osteogenic and non-osteogenic media. Osteocalcin and osteopontin expression was assessed by immunocytochemistry on day 28. Control samples were only treated with secondary antibody.

DISCUSSION & CONCLUSIONS: Exposure to bDBM and bECM hydrogels promoted C2C12 and mPCs osteogenic differentiation *in vitro* compared to cells cultured on collagen type I. bECM hydrogels demonstrated stable release of protein with release kinetics controlled by changing the bECM hydrogel concentration.

Determination of headspace volatile levels: potential roles in mesenchymal stem cell biology

MA Al-Zubaidi¹, MR Siddique¹, J Sulé-Suso^{1,2}, NR Forsyth¹

¹ *Institute for Science and Technology in Medicine, Keele University, Stoke-On-Trent, United Kingdom.* ² *Cancer Center, University Hospital of North Staffordshire, Stoke-on-Trent, United Kingdom*

INTRODUCTION: Mesenchymal stem cells (MSCs) are multipotent stem cells that can be isolated from multiple sites including bone marrow. MSC biology is controlled by intrinsic genetic networks driven by extrinsic signals provided by the niche. MSCs are multipotent and can give rise to cells of different lineages, including chondrocyte, osteoblast and adipocyte. The specialized local extracellular microenvironment, or stem cell niche, provides essential cues that regulate stem cell fate decisions. Analysis of volatile organic compounds (VOCs) in the headspace of whole bone marrow aspirate and bone marrow-derived mesenchymal stem cells can be used as an approach to study preferred metabolic pathway choices to help further define the in vitro niche model.

METHODS: We have determined the catabolism and anabolism of VOCs by bone marrow aspirate (BMA) and MSCs using Selected Ion Flow Tube-Mass Spectrometry (SIFT-MS). Three independent bone marrow samples were examined and SIFT-MS performed on marrow and subsequently isolated MSC. MSCs were isolated according to a previously published adherence-based protocol¹. MSCs were isolated in either normoxic (21% O₂) or hypoxic, niche-like, conditions (2% O₂).

For marrow VOC analysis, samples were incubated for 24 hours and supernatant transferred into sealed glass bottles and incubated for a further 18 hours to allow headspace VOCs to concentrate. For MSCs, the cells were detached, resuspended in fresh media and transferred into sealed glass bottles and incubated for 18 hours. The headspace of the bottles was then analysed for the presence of volatile compounds. All samples were normalized to cell-free media incubated in identical conditions.

RESULTS: From a full scan of 180 mass peaks, eleven known compounds were evaluated. Differences in levels of acetone, acetaldehyde, pentanol, pentene and putrescine were noted between BMA and MSCs in both normoxic and hypoxic conditions (p<0.05). Differences in hexanal, butyric acid and xylene levels were noted

between BMA and MSC in normoxia and DMS/ethanethiol in hypoxic.

In normoxia, BMA and MSCs displayed evidence of catabolism of acetaldehyde, pentanol, DMS/ethanethiol, butyric acid, putrescine, terpenes and xylene, with acetone, ethanol and pentene for BMA only. In stark contrast MSCs displayed anabolism of acetone, ethanol and pentene while BMA and MSCs both anabolised hexanal.

In hypoxia, BMA and MSC catabolized acetaldehyde, pentanol, DMS/ethanethiol, butyric acid, terpenes and xylene while acetone, ethanol and pentene were unique to BMA and hexanal to MSCs. Anabolism of hexanal was noted to be unique to BMA and acetone, ethanol pentene and putrescine to MSCs.

Significant differences in levels of acetone, acetaldehyde, pentanol, hexanal, butyric acid, pentene and xylene were noted between BMA samples in hypoxia and normoxia (p<0.05). Interestingly MSCs in hypoxia catabolized hexanal and anabolized putrescine while MSC in normoxia did the reverse.

DISCUSSION & CONCLUSIONS: Our findings demonstrate that specific VOCs can be either derived from or consumed by MSCs in a culture condition-dependent manner. This may provide clues in the search for optimised culture conditions to support expansion and monitoring of MSCs for therapeutic application.

Quantifying the impact of delivery of mesenchymal stem cells using narrow-bore needles for cell therapy applications

MH Amer, LJ White, FRAJ Rose, KM Shakesheff

Wolfson Centre for Stem Cells, Tissue Engineering and Modelling (STEM), School of Pharmacy, University of Nottingham, Nottingham, NG7 2RD, UK

INTRODUCTION: Mesenchymal stem cells (MSCs) hold significant promise in regenerative medicine. Many injection-based cell therapy procedures are currently being undertaken for a variety of clinical indications, including stroke and retinal regeneration. The efficacy of these therapies relies on maintaining cell vitality and functionality post-injection. Therefore, following on our earlier work [1], we used a comprehensive toolset to evaluate MSC delivery post-ejection. This study investigates the effects of injectable administration on a range of cell characteristics, and investigates potential reasons for failure to deliver sufficient numbers of viable cells. This will assist clinicians to decide on the most suitable administration requirements for future cell therapy clinical trials.

METHODS: Primary human mesenchymal stem cell (hMSC) suspensions were ejected at controlled rates, ranging from 10 μ L/min to 300 μ L/min, using Hamilton 30G needles. Effects of the different ejection rates were then thoroughly assessed (Fig. 1) in terms of viability, apoptosis, differentiation capacity and other characteristics of human mesenchymal stem cells. A multiplex assay was used for ratiometric measurements of cell cytotoxicity and apoptosis independent of cell number. In addition, some parameters were compared with cells ejected using 34G needles.

RESULTS: Ejections at slower flow rates under investigation resulted in a significantly lower percentage of dose being delivered as viable cells among the ejection rates tested (Fig. 2). Normalised caspase-3/7 activity measurements of cells injected through 30G needles at 10 μ L/min were significantly higher than the control, with the differences in proportions of apoptotic cells being more apparent using the smaller needle bore size. A higher number of cells were demonstrated to be retained in the delivery device when ejected at lower rates. Adipogenic and osteogenic differentiation capacities of hMSCs were also affected by the ejection rate employed.

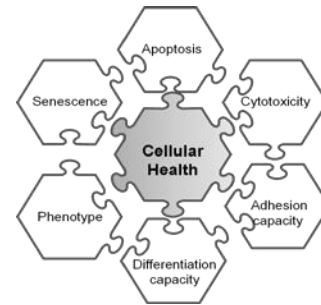


Fig. 1: Overview of the cellular health indicators quantified in order to evaluate the various aspects of cell functionality post-injection.

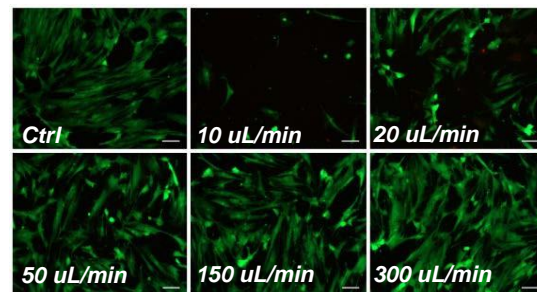


Fig. 2: Images showing LIVE/DEAD[®]-stained cells at 24hrs of incubation (Scale bar: 100 μ m)

DISCUSSION & CONCLUSIONS: Lower cell numbers delivered at slower ejection rates were mainly attributed to the retention of cells within the syringe, in addition to the significantly higher apoptotic cell proportions arising at these rates. Therefore, this study emphasises the importance of optimised cell delivery approaches to enhance the efficacy of cell therapy procedures.

ACKNOWLEDGEMENTS: We gratefully acknowledge support by MRC, EPSRC and BBSRC UK Regenerative Medicine Platform Hub "Acellular Approaches for Therapeutic Delivery", University of Nottingham International Office, Schlumberger Foundation and Misr EIKheir Foundation.

Enzyme responsive technology for mesenchymal stem cell control

HJ Anderson^{1,2}, JN Roberts¹, J Sahoo², CC Berry¹, ROC Oreffo³, R Uljin², MJ Dalby¹

¹ [Centre for Cell Engineering](#), Institute of Molecular, Cell, and Systems Biology, University of Glasgow, UK ² Department of Pure and Applied Chemistry, University of Strathclyde/WestCHEM, UK ³ Bone and Joint Research Group, Institute of Developmental Sciences, University of Southampton, UK

INTRODUCTION: Currently there are limitations to the *in vitro* expansion of MSCs. Traditional methods of culture fail to direct stem cell behaviour and thus generate a heterogeneous population of cells. The increasing synthesis of biomaterials i.e. biocompatible and bioresponsive materials provides novel methods to culture MSCs. Here we aim to provide an enabling technology using such a material that can not only direct MSC osteogenesis but also maintain stemness prior to differentiation. Using solid phase peptide synthesis (SPPS) we are able to design a material that is fully bioresponsive, which includes an enzyme responsive peptide sequence and the adhesive tripeptide arginine-glycine-aspartic acid (RGD). The enzyme responsive peptide can be altered depending on the enzyme that is to be applied. For example, a dialanine can be cleaved by elastase added into the cell suspension that can digest the PEG blocking group that caps the peptides and reveals RGD^[1].

METHODS: Glass coverslips were solvent cleaned and acid cleaned prior to treatment with glycidylxypropyl trimethoxysilane then polyethylene glycol (PEG₂₆). Selected Fmoc protected amino acids were added to the coverslip individually in 20mM solution with ethyl (hydroxyamino) cyanoacetate (EHICA) and 86.75µl N,N'-Diisopropyl carbodiimide (DIC) in 30ml DMF and left for 24 hours. After washing, and deprotection of Fmoc by piperidine the next amino acid was added under the same conditions. This is repeated until the final amino acid is added. Peptide chains are capped with PEG Mr=2000. Side chain protected amines are deprotected using trifluoroacetic acid (TFA). Glass coverslips were compared to undigested (PEG-D) and digested (DIGE-D) and stained for vinculin and stro-1 after 5 days and 21 days respectively (antibodies used at 1/50 in PBS/BSA). Digestion was achieved by adding 0.01mg/ml of elastase on day 3. Quantification was calculated based on results from 50 nuclei.

RESULTS: The DIGE-D surface promotes mature focal adhesions, which suggest the cell is binding to RGD (Fig 1A). The PEG-D surface shows a

large amount of Stro-1 staining which was quantified (Fig 1B) to show that the PEG-D material had a significantly more stro-1 expression than the DIGE-D and glass control.

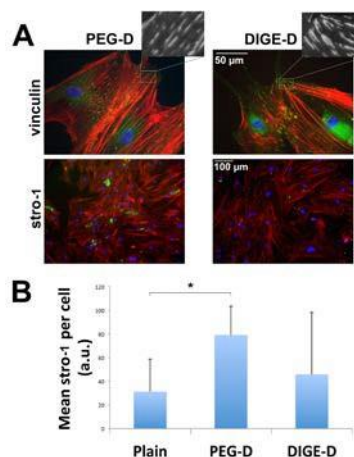


Fig. 1: Cell morphology and stro-1 expression on PEG-D and DIGE-D. A) Vinculin and stro-1 staining (green) on DIGE-D and PEG-D surfaces actin (red), nucleus (blue). B) Quantification of stro-1 expression. (results show mean \pm SD, statistics by ANOVA* = $p < 0.05$).

DISCUSSION & CONCLUSIONS: Initial experiments show that PEG-RGD can promote stemness of MSCs. More experiments are needed to confirm if the DIGE-D surface, when fully exposed to the cells, is promoting osteogenesis. It is also possible to alter the enzyme responsive peptide to allow surface digestion for another enzyme. For example we are starting to utilise the matrix metalloproteinases (MMP) enzymes that the cells naturally secrete.

ACKNOWLEDGEMENTS: Julia Wells (Bone and Joint Research Group, University of Southampton, UK) kindly provided MSCs. Funding for HA is through EBSRC DTC in Cell and Proteomic Technologies. The work is supported through BBSRC grant BB/K006908/1.

Focal mechanical injury induces astrogliosis in a 3D tissue engineered culture model

R Angus¹, CO'Rouke², A Michael-Titus¹, JB Phillips²

¹Blizard Institute, Barts and The London, School of Medicine and Dentistry, Queen Mary University of London. ²Biomaterials & Tissue Engineering, UCL Eastman Dental Institute, University College London, UK.

INTRODUCTION: Traumatic brain injury (TBI) is the largest cause of death and disability in young adults in the Western world [1]. The pathophysiology that follows a TBI leads to expansion of the initial lesion and symptoms such as cognitive and motor dysfunction. Astrogliosis has a main role in this pathophysiology. In vivo studies show that mechanically induced TBI triggers astrogliosis, with the astrocytes closest to the lesion site displaying a highly ramified morphology and expressing high levels of glial fibrillary acidic protein (GFAP) [2]. Studies have shown that the absence of the astrocytes worsens the outcome of TBI in mice [3]. We have established a novel model to investigate the astrocyte response to a focal mechanical injury in vitro.

METHODS: Primary astrocyte cultures were prepared from P2 GFP⁺ rat cortices. Astrocytes were dissociated and expanded for 2 weeks before being placed in 3D collagen gels [4]. Gels were impacted using the Hatteras PinPoint Precision Cortical ImpactorTM and then fixed at 24 hours, 5 days and 10 days post impact. The volume of GFAP immunoreactivity was measured in defined positions adjacent and distal to the lesion site using confocal microscopy and 3D image analysis.

RESULTS: Astrocytes in the impacted gels proliferated and exhibited a more ramified morphology in the regions of interest adjacent to the lesion site compared with equivalent regions in control gels (Fig. 1). There was a corresponding increase in GFAP volume per cell, which was maintained in peri-lesional regions of interest up to 10 days post impact. There was also an increase in the GFAP expression of astrocytes in the regions of interest away from the lesion in impacted gels.

DISCUSSION & CONCLUSIONS: The upregulation of GFAP by astrocytes both adjacent and distal to the lesion site, mirrors the behavior of the reactive astrocytes seen in the brains of mice following TBI. This novel in vitro model of astrogliosis induced by a focal mechanical injury, allows for the isolation of the astrocytic response

from the complex pathophysiology that follows TBI.

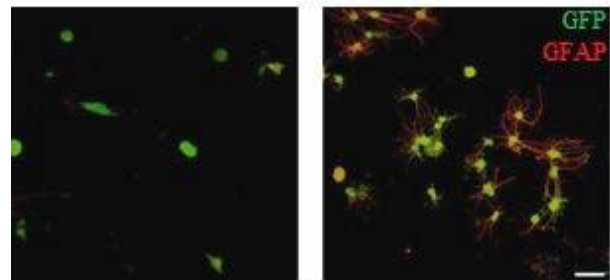


Fig. 1: Astrocytes in the ROI adjacent to the lesion site at 5 days in the un-impacted control gels (left) and the impacted gels (right). Scale bar 80 μ m.

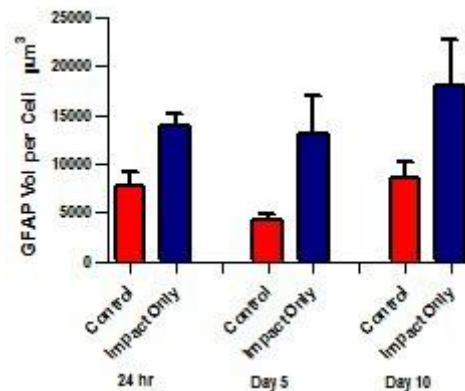


Fig 2: GFAP volume per cell in impacted gels versus control gels at 24 hours, 5 days and 10 days post impact in the region of interest adjacent to the lesion site. Mean \pm SEM of 4 gels.

Advanced scaffolds for adipose tissue reconstruction

J Appelt^{1,2}, AD Metcalfe^{1,2}, G Phillips², Y H. Martin^{1,2}

¹ *Blond McIndoe Research Foundation, East Grinstead, UK* ² *The Brighton Centre for Regenerative Medicine, University of Brighton, Brighton, UK*

INTRODUCTION: The loss of subcutaneous adipose tissue due to the removal of tumours, congenital malformations, deep burns or trauma can have a severe disfiguring impact on the normal body contour. This can leave patients distressed both physically and emotionally. Current clinical treatment methods applied to replace lost adipose tissue often fail to restore the natural body contour. We present a gelatin scaffold combined with an extracellular matrix environment, which supports adipogenesis.

METHODS: Gelatin scaffolds were created using particulate leaching of alginate beads as templates for the macroporous structure¹. The microporous structure within the gelatin walls was altered through the application of -80°C temperatures and freeze drying. The viability and distribution of human adipose-derived stem cells (ADSCs) within the scaffolds was assessed. Collagen I and laminin were combined to create an extracellular matrix environment within the scaffold. After culture, adipogenesis was investigated by assessing gene expression.

RESULTS: The scaffolds supported ADSC viability and cell distribution within the porous scaffold was different between frozen and freeze dried scaffolds. Thus, the freezing techniques can be used to control the scaffold architecture and therefore cell distribution.

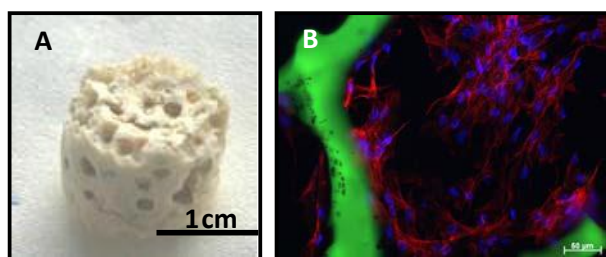


Fig. 1: Microporous macroporous (MM) scaffold supports cell infiltration and proliferation. (A) Freeze dried MM scaffold. (B) The macroporous structure supports cell infiltration and proliferation. Scale bars as indicated. Red = actin, blue = DAPI, Green = scaffold.

ADSCs delivered in the scaffold with a collagen I/laminin hydrogel showed increased adipogenic gene expression after culture for 10 days.

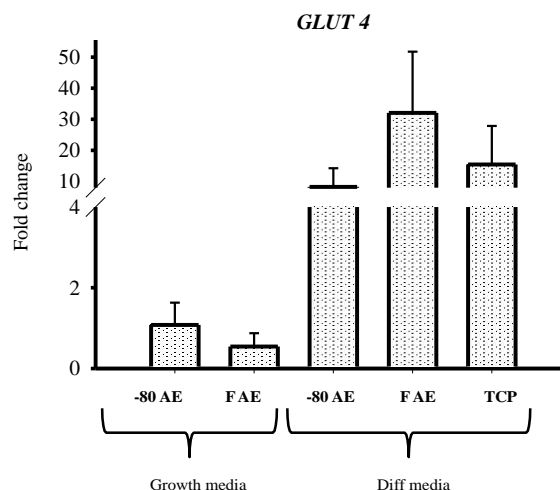


Fig. 2: Composite scaffolds support adipogenic gene expression. GLUT 4 is expressed by ADSCs cultured in the scaffolds and further upregulated in adipogenic differentiation (Diff) media. -80 AE = -80°C frozen, FAE = freeze dried. Fold change was calculated against ADSCs in growth medium on TCP. Error bars = SD. n = 3.

DISCUSSION & CONCLUSIONS: The integration of a natural adipose environment (AE) within the scaffold resulted in a composite scaffold with features that can support adipose tissue reconstruction.

ACKNOWLEDGEMENTS: This work was supported by charitable donations to the Blond McIndoe Research Foundation.

Surface tunable injectable microspheres for cell delivery applications

A Baki¹, C Rahman¹, O Qutachi¹, KM Shakesheff¹

¹ *Division of Tissue Engineering and Drug Delivery, Centre for Biomolecular Sciences, School of Pharmacy, University of Nottingham, UK*

INTRODUCTION:

Injectable Poly Lactic-Co-Glycolic Acid (PLGA) microspheres offer a minimally invasive cell delivery system for tissue repair applications⁽¹⁾. Gelatin methacrylate (GMA) has been shown to form hydrogels with controllable elasticity⁽²⁾. As substrate elasticity has been shown to direct stem cell differentiation⁽³⁾, this study propose a novel approach to modify the surface of PLGA microspheres with GMA hydrogels to help control the mechanical properties of the stem cell microenvironment. To achieve this, GMA molecules were immobilised onto PLGA microsphere surface using oxygen plasma and surface entrapment approaches⁽⁴⁾. Further GMA molecules were photo-cross-linked on microsphere surfaces to form elasticity controlled hydrogel coated microspheres.

METHODS:

Surface modification of PLGA microspheres: GMA was prepared by methacrylating bovine (type B) gelatin. PLGA microspheres (55±15 µm) were surface modified using a modifying mixture of TFE/GMA (entrapment) or O₂ plasma /GMA solution. Further GMA was photo-cross-linked to the surface to form hydrogel coated microspheres.

Surface Analysis: Modified PLGA microspheres were visualized using fluorescent and scanning electron microscopy (SEM). Surface chemistry was analyzed using X-ray photoelectron spectroscopy (XPS) and time of flight secondary ion mass spectroscopy (ToF SIMS). Hydrogel elasticity was measured with Atomic Force Microscopy (AFM).

RESULTS:

Surface immobilised Fit-C labelled GMA was visualized with fluorescent microscopy and SEM where morphological changes to the surface can be observed before and after coating (**Fig. 1**).

ToF SIMS mapping of PLGA microspheres have shown homogenous distribution of GMA specific ions on modified microspheres. Quantification of GMA specific XPS N1s peaks has shown more GMA concentration on the surface of plasma modified microspheres compared to adsorption or

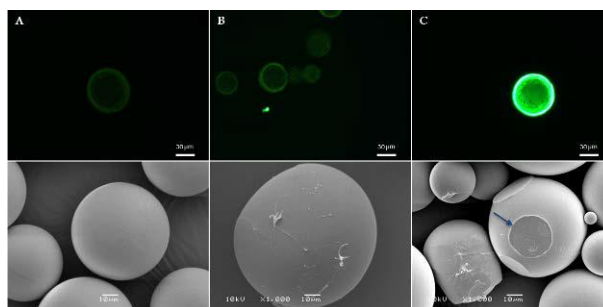


Fig. 1: Fluorescent and SEM Images of PLGA microspheres before (A) and after surface modification with Fit-C labelled GMA molecules (B) and hydrogels (C). Arrow points to a mark from a microscope slide left on the hydrogel layer of GMA coated microspheres.

entrapment modified microspheres. AFM measurements have shown a significant change in GMA hydrogel elasticity (Fig. 2).

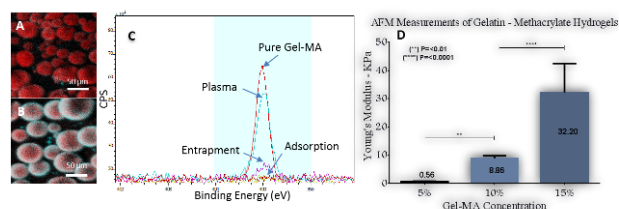


Fig. 2 TOF SMS ion mapping images of PLGA microspheres before (A) and after surface modification with GMA (B). XPS quantification of N1s peaks following different surface modification approaches (C). AFM measurements of GMA hydrogels with various ratios and exposure time (D).

DISCUSSION & CONCLUSIONS:

A novel method has been introduced to produce hydrogel coated PLGA microspheres with controllable surface elasticity. The proposed system can be tuned to control the mechanical properties of cell microenvironment to influence cell fate for regenerative medicine applications.

Effect of hypoxia on the expression of miR-21, miR-205 and miR-210 in primary keratinocytes

L Balakrishnan^{1,2}, FV Lali^{1,3}, AD Metcalfe^{1,3}, YH Martin^{1,3}

¹Blond McIndoe Research Foundation, Queen Victoria Hospital, East Grinstead, UK ²Brighton and Sussex Medical School, Brighton, UK ³The Brighton Centre for Regenerative Medicine, University of Brighton, Brighton, UK

INTRODUCTION: Physiological response to local wound hypoxia plays a critical role in successful wound healing. In this study, the effect of hypoxia on the expression of microRNA-21 (miR-21), microRNA-205 (miR-205) and microRNA 210 (miR-210) in primary keratinocytes was investigated. Intraellular as well as extracellular levels of miR-21, miR-205 and miR-210 in supernatants were analysed.

METHODS: Primary human keratinocytes, isolated from discarded skin from consented patients undergoing surgery, were expanded and exposed to hypoxia for 36 hours. Total RNA was extracted from cells and cellular supernatants. Expression of miR-21, miR-205 and miR-201 was quantified using Taqman qRT-PCR.

RESULTS: There were no significant differences in the intracellular expression levels of miR-21 and miR-205 after exposure to hypoxia, but miR-210 was upregulated by approximately six-fold compared to cells grown in normoxia (Fig. 1). Extracellular miR-205 could be detected in the supernatant in normoxia and was significantly reduced when cells were exposed to hypoxic conditions (Fig. 2).

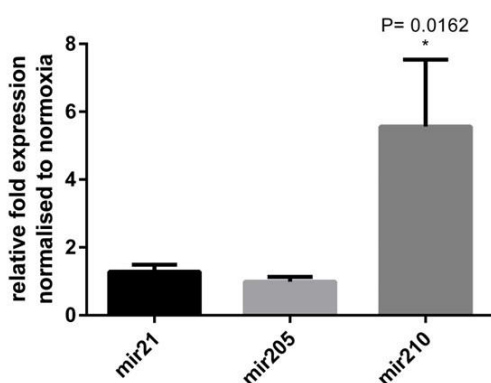


Fig. 1: Relative intracellular expression of miR-21, miR-205 and miR-210 in keratinocytes under hypoxic conditions normalized to cells cultured in normoxia. n=3; error bar=SD.

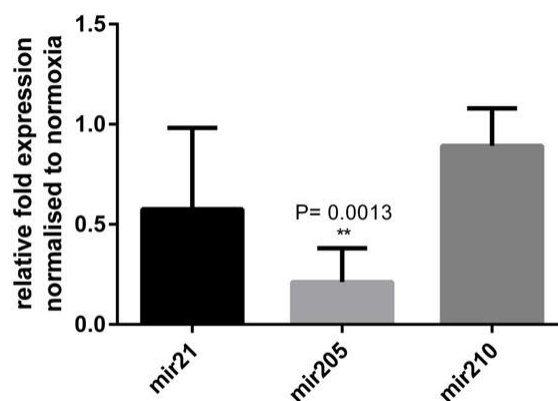


Fig. 2: Relative extracellular expression of miR-205 in supernatants from keratinocytes under hypoxic conditions normalized to supernatants from cells cultured in normoxia. n=3; error bar=SD.

DISCUSSION & CONCLUSIONS: Results from the current study show that miR-210 expression in primary keratinocytes is upregulated in hypoxia. Although miR-21 and miR-205 have been reported to be regulated by hypoxia in other cell types¹, this does not seem to be the case in primary keratinocytes. Extracellular miR-205 could be detected in the supernatant, which is reduced by hypoxia. The role of miRNAs in wound healing is complex and multifaceted, but hypoxia looks to be a driver of microRNA expression in keratinocytes and potentially in wound healing.

ACKNOWLEDGEMENTS: This study was funded by Brighton and Sussex Medical School and charitable donations to the Blond McIndoe Research Foundation.

Fluorescently monitoring poly(lactic-co-glycolic Acid) degradation and its effect on cellular osteogenic potential

K Bardsley¹, Y Yang¹, AJ El Haj¹

¹*Institute for Science and Technology in Medicine, Guy Hilton Research Centre, Keele University, Thornburrow Drive, Stoke-on-Trent, Staffordshire.*

INTRODUCTION: Novel fluorescent tagging of inert polymers is an advantageous tool for monitoring biomaterial degradation. Here we present a protocol for the fluorescent tagging of poly(lactic-co-glycolic acid) (PLGA) therefore allowing for accurate, non-destructive monitoring of degradation. This was applied to PLGA with various lactic/glycolic acid ratios and subsequently differing rates of degradation. The cellular response to the degradation rates of the biomaterial was then determined.

METHODS: PLGA with varying lactic/glycolic ratios (50/50, 65/35 and 80/20) was solvent cast in to a thin film (2% in chloroform) before undergoing ammonia plasma treatment. After this treatment amine bonds formed on the surface of the PLGA and were subsequently reacted with rhodamine b isothiocyanate in order to fluorescently label the polymer. The surface chemistry of the polymer was assessed using X-ray spectrophotometry (XPS) and high performance liquid chromatography (HPLC) to ensure that the fluorescence was bound to the polymer.

The films were then re-cast using salt leaching to produce a homogeneous fluorescent 3D porous scaffold (pore size 100-150µm). Degradation of the various PLGA was calculated using fluorescent by-product release and fluorescent retention within the scaffolds and this was correlated to changes in physical weight.

MG63, stably transfected with an osteocalcin luciferase reporter, were seeded on the scaffold (1.2×10^5 cells/ 6 mm x 1mm cylindrical scaffold) and cultured under osteogenic conditions for 14 days. Proliferation and the osteogenic potential of the cells on the scaffolds was assessed throughout the culture.

RESULTS: The ammonia plasma treatment of the PLGA films allowed for the binding of amine groups to the surface of the polymer and consequently the binding of the fluorescent molecule, rhodamine b isothiocyanate. Analysis through both XPS and HPLC showed that the fluorescence was bound to the surface and not merely entrapped during swelling.

Recasting of the PLGA via salt leaching produced a homogeneously fluorescently tagged, 3D, porous scaffold. Degradation experiments in PBS showed a correlation between changes in fluorescence, both through the release of soluble fluorescent by-products and the retention of solid phase fluorescence within the bulk of the scaffold, and the changes in wet weight across all three PLGA compositions.

When cultured with MG63 the varying degradation rates of the PLGA was shown to have a significant impact on the cellular response to the biomaterials. It was shown that the faster degrading PLGA (50/50) enhanced the osteogenic potential, through the up-regulation of both osteocalcin and osteopontin, while proliferation was decreased. Conversely the slower degrading PLGA exhibited increased proliferation and a decreased osteogenic potential.

DISCUSSION & CONCLUSIONS: This research has highlighted the ability to fluorescently label an inert PLGA polymer and track its degradation in a non-destructive manner. This is advantageous both *in vitro* and for potential *in vivo* studies as it enables biomaterials to be tracked throughout an experiment and decreases the reliance on destructive end-point analyses.

Interestingly there is a correlation between the rate of biomaterial degradation and the osteogenic and proliferative potential of cells. Increased degradation led to a higher osteogenic potential and a decrease in proliferation. This ability to modify cellular behaviour in response to biomaterial degradation may well enable the tailoring of biomaterials for required applications.

ACKNOWLEDGEMENTS: The authors would like to thank the EU-FP7 BioDesign 'Rational Bioactive Materials Design for Tissue Regeneration' Project for funding (#262948). We would like to thank Deniz Oeztuerk for contributing the transfected MG63 cell line.

Examining the effect of culture expansion on mesenchymal stem cells isolated from rat femoral compact bone

P Battersby¹, A Sloan¹, R Waddington¹

¹Mineralised Tissue Group, Department of Tissue Engineering and Reporative Dentistry, Dental Hospital, Cardiff University, Wales

INTRODUCTION: The study of mesenchymal stem cells (MSC) is widespread due to their potential for therapeutic tissue repair throughout the body derived from their multipotency, a defining characteristic of the population¹. Fresh MSC explants exhibit intra-population heterogeneity but whether this is maintained after long term expansion, and the affect this has on multipotency, is poorly understood. The aim of this work is to examine the effect of MSC culture expansion in vitro on markers unique to the population and age-related senescence and ultimately the effect on early osteogenic differentiation..

METHODS: Cells were isolated from femoral compact bone of 28 day old male Wistar rats and culture expanded to PD15, PD50, PD100 and PD200 and growth plotted alongside MSC marker expression. Cell morphology, colony forming efficiency, telomere length, expression of telomerase and expression of cell cycle proteins were used as markers of age-related senescence. Cells were cultured in osteogenic media up to 28 days during which cell expansion, by MTT, and expression of osteogenic markers by qPCR were assessed.

RESULTS: Population doubling (PD) was linear between PD5 and PD200 after a brief lag phase with no observable senescence and classical stem cell markers were expressed by all cells with an absence of non-stem cell markers; the expression of Osterix, an early regulator of osteogenic differentiation, by all cells is noted.

No change in either the average telomere length or telomerase expression were observed as PD increased. p16 was expressed in PD15 cells but declined by PD50 with constitutive expression of other p-proteins throughout. However, as PD increased cell surface area decreased (*Fig. 1*) with changes also found in colony forming efficiency, with few colonies formed by either PD15 and 200 cells but increased formation in 50 and 100.

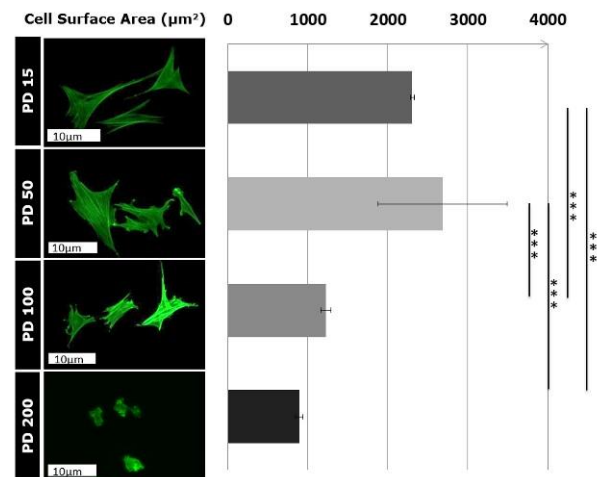


Fig. 1: Cell size (μm^2) as PD increases. After PD50 cell size decreases.

Cell expansion of PD15 and PD50 in osteogenic media slowed between days 2 and 6 relative to the control while no difference was observed in either PD100 and PD200. This effect was mirrored in early osteogenic markers where PD15 and 50 showed a decrease in cell cycle marker Ki-67 and increase of osteoid matrix deposition marker Colla1 relative to the control while no observable difference existed in either PD100 or 200.

DISCUSSION & CONCLUSIONS: Early explant cultures are heterogeneous transient amplifying (TA) cells with two populations: high proliferation, high potency and low proliferation, low potency. Though MSC characteristics are maintained the latter is lost by PD50 leaving a homogenous group of the former which is capable of undergoing osteogenic differentiation. As cells are further expanded this group transitions to the low proliferation, low potency TAs and lose this ability. Our work has shown that though culture expanded cells have an altered response to osteogenic media this is due to the expansion process and not increased aging of these cells.

Development of a novel culture system to investigate cellular interactions at engineered tissue interfaces

D Bellamy, H Alsaykhan, JZ Paxton

School of Biomedical Sciences, University of Edinburgh, Edinburgh, EH8 9XD

INTRODUCTION: The attachment point of tendon to bone possesses a complex anatomical arrangement¹. The soft tendon attaches to the hard bone via a highly organised tissue interface region known as the enthesis. Following tendon injury and detachment, this specialised region fails to be replicated during healing, and a weak scar tissue is formed that is prone to further injury¹. Little is known about how these tissue interfaces form during development and repair following injury. Therefore, this study aims to design and produce a novel culture system to allow investigation into the interaction of the cell types found at these tissue regions in 3-Dimensions (3D).

METHODS:

Cell labelling: Osteoblasts (MC3T3 cells) were labelled with CellTracker™ Red CMTPX Dye as per the manufacturer's instructions (Life Technologies, UK). Tendon fibroblasts were isolated from GFP-tagged chick embryos on day 13.5. These processes enabled the culture of bone cells in red and tendon cells in green. Both cell types were cultured in Dulbecco's Modified Eagles Medium (DMEM) containing 10% Fetal Bovine Serum and 1% Penicillin/Streptomycin. (Sigma, UK) Cell cultures were maintained at 37°C, 5% CO₂ for the duration of the experiment. **3D culture setup:** PDMS (polydimethylsiloxane) wells were created using 3D-printed blocks manufactured from ABS (Acrylonitrile butadiene styrene). Several different designs were tested to find the optimal shape for the 3D system. The ABS blocks were placed into the wells of a 12-well plate and pre-cured PDMS solution was poured around them. Once cured, the printed blocks were removed to leave a void suitable for 3D cell encapsulation in polymer gels. Following sterilisation with 70% ethanol, one half of the ABS block was replaced into the void. One labelled cell type was encapsulated in 1% agarose solution (One part cells, four parts polymer solution) and 250µl of this solution was added to the exposed void in the well. Once the gel set, the remaining ABS block was removed and the process was repeated with the remaining cell type.

RESULTS: Several materials and designs were tested before the optimal system described here was produced. The final design comprises two

different-shaped halves to enable quick and easy identification of each cell region in culture and for post-culture analysis (Figure 1A). Furthermore, this system allows for two cell populations to be cultured in 3D in close apposition, providing a more "tissue-like" environment to investigate cellular interactions at artificial interfaces (Figure 1B). This study is therefore a proof of concept that 3D co-cultures can be set up to allow investigation at artificial interfaces.

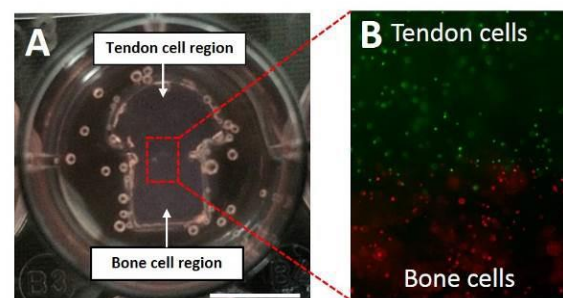


Fig. 1: Tendon-Bone Co-Culture. A) 2 cell populations are encapsulated within agarose hydrogels. B) Tendon cells (green) and bone cells (red) are in close apposition forming an artificial interface. Scale bar in A = 10mm.

DISCUSSION & CONCLUSIONS: The culture system developed during this study is an important step in the future investigation of tissue interfaces, as it allows co-cultures of cells from apposing tissue types to be investigated in 3D. Here, the bone-tendon interface can be investigated using bone and tendon cells, but other musculoskeletal interfaces such as bone-cartilage and tendon-muscle are also a possibility. Future work is now aimed at using this system to study cellular interactions at artificial interfaces to give insight into developmental and repair mechanisms.

ACKNOWLEDGEMENTS: We would like to thank Tenovus Scotland for funding this work.

Low density sub-culturing is essential for maintaining the self-renewal and differentiation potential of MSCs

R Balint¹, S Richardson², SH Cartmell¹

¹*School of Materials, The University of Manchester, UK.* ²*Institute of Inflammation and Repair, The University of Manchester, UK*

INTRODUCTION: Human Mesenchymal Stem Cells (hMSCs) enjoy widespread use in tissue engineering and regenerative medicine. However, reliable expansion of hMSCs, without compromising their stem cell capabilities, remains a challenging task. We hypothesise that high confluence (above 50%) is detrimental to MSC quality.

METHODS: hMSCs were expanded to passage 5 using two methods: Protocol A (40% to 70% confluence) or Protocol B (10% to 50% confluence). Other culture parameters were kept the same between the two treatment groups. The effect of the two methods was measured on the proliferation rate (PicoGreen); cellular size (CellMask staining and CellProfiler image analysis); MSC surface antigen expression (flow cytometry); and senescence (β -Galactosidase staining) of the generated MSC cultures. Following tri-lineage differentiation using conventional methods, passage 5 cells were assayed for the gene expression of osteogenic (alkaline phosphatase, collagen type I, osterix, osteopontin, osteocalcin), adipogenic (adiponectin, leptin) and chondrogenic (aggrecan, collagen type II) markers through qRT-PCR. Alkaline phosphatase activity; lipid formation (Oil Red O); glycosaminoglycan (DMMB, Alcian Blue) and proteoglycan (Safranin O) content were also investigated.

RESULTS: Protocol B produced MSCs with significantly higher (+10-15%) proliferation rate. Furthermore, after 14 days Protocol B cultures contained 23% more cells in growth, 12% more in cells in osteogenic and 78% more cells in adipogenic medium. In chondrogenic pellet cultures however, after 21 days Protocol A samples contained 27% more cells.

Comparison of the cell sizes from the two regimes using Student's T-test showed no significant difference. Furthermore, the Kolmogorov-Smirnov test has showed that the size of the cells with the two treatments follow the same probability distribution function.

Flow cytometry has shown that Protocol A cells display reduced purity, expressing CD105 in only

76%, compared to the 96.7% in Protocol B populations.

Furthermore, Protocol A cultures contained significantly more (+4.2%) senescent cells.

Differentiation marker gene expression was comparable between the two protocols. However, alkaline phosphatase activity was three times higher, glycosaminoglycan production 16% greater, while lipid levels were significantly lower, with Protocol B.

DISCUSSION & CONCLUSIONS: Expanding MSCs at only low confluence levels resulted in cells with better self-renewal capability, as Protocol B provided a higher proliferation rate, and greater cell numbers in almost all culture conditions. Furthermore, our findings show that the traditional (high confluence) culture technique results in a loss of immunophenotype and causes MSCs to enter senescence sooner. Although there was no clear difference between the protocols in the expression of various differentiation marker genes, at the secretional level Protocol B cells showed faster ECM deposition under osteogenic and chondrogenic conditions. This suggests that Protocol B generated cells with superior differentiation capabilities. The results of our quantitative cell size comparison shows that the loss of MSC characteristics in Protocol A cultures may not be due to the RS to SR sub-phenotype transition that has been previously suggested in the literature.

Our findings demonstrate that low density sub-culturing is essential for the maintenance of MSC quality.

ACKNOWLEDGEMENTS: We would like to thank Orthopaedic Research UK and the EPSRC Doctoral Prize account for providing funding for this study. The flow cytometer was purchased through an equipment grant (20442) funded by Arthritis Research UK and Mr Andrew Fotheringham is acknowledged for his technical assistance.

Comparison of manufacture and sterilisation techniques on in vivo biological response: a six-week study using electrospun yarns grafted into mouse tendons

LA Bosworth¹, P Bhaskar¹, MA O'Brien¹, H Kriel², E Smit^{2,3}, SH Cartmell¹

¹School of Materials, The University of Manchester, Oxford Road, Manchester, M13 9PL, UK. ²The Stellenbosch Nanofiber Company (Pty) Ltd, 7 Marconi Road, Montague Gardens, Cape Town 7441, South Africa. ³Department of Chemistry and Polymer Science, Stellenbosch University, Private Bag X1, Matieland, 7602, South Africa

INTRODUCTION: Medical devices intended for implantation into humans require sterilisation using regulatory approved methods. Within a research lab setting however, this sterilisation process often incorporates non-approved techniques because they are considerably cheaper and have a quick turnaround. This study compared the in vivo biological response of electrospun poly(ϵ -caprolactone) fibre yarns fabricated by two different manufacturers and subsequently sterilised by irradiation (approved) or ethanol submersion (non-approved). The efficacy of the implant was further compared to autograft - the current gold standard treatment for tendons requiring reconstruction.

METHODS: Electrospun poly(ϵ -caprolactone) (PCL) yarns were manufactured at two separate sites – in-house (UOM) and The Stellenbosch Nanofiber Company (SNC). Yarns were sterilised by either gamma irradiation (25 kGy, Synergy Health) or submersed in increasing concentrations of ethanol (70-100 % w/v) and washed in phosphate buffered saline solution. Individual yarns were implanted into purpose-made defects within the flexor digitorum longus tendon of mice and held in place by single-knot sutures at either end (Fig.1A). Yarns were compared to autograft at 3, 21 and 42 days (n=4). Cell infiltration (migration into and along the graft), cell proliferation (cell coverage within implant area) and immunohistochemistry staining for 4 key processes was performed: (1) inflammation (CD45, F4/80, Ly6G); (2) collagen production (Hsp47); (3) cell turnover (BrdU, TUNEL); and (4) blood vessel formation (CD31, SMA). Staining was semi-quantified from serial tissue sections (5 μ m thick) using a maximum +++ or --- score system to indicate the level of positive staining compared to the control.

RESULTS: Cells were observed to have infiltrated all electrospun yarns at 3 days and continued to migrate through to the centre of the implant with time, >90% at 42 days (Fig.1B).

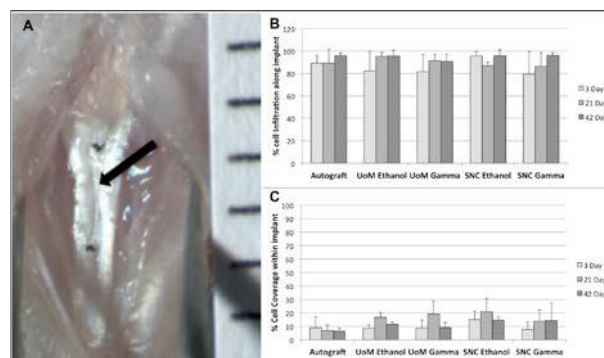


Fig. 1: (A) Arrow indicates position of electrospun yarn in situ. Black dots represent suture knots. (B) % cell infiltration along the implant and (C) % cell coverage within the implant for all electrospun yarns compared to autograft.

Cells colonised a low percentage of the total implant area for all yarns implanted, though cell coverage was comparable to the autograft tissue (Fig.1C). Collagen production was similar to the autograft control for all yarns over time (Table 1).

Table 1. Level of immunostaining for Hsp47 (collagen production) for implant area compared to autograft (0 = no observed difference).

Hsp47	3 day	21 day	42 day
UOM EtOH	0	0	0
UOM Gamma	0	+	0
SNC EtOH	0	0	0
SNC Gamma	0	0	0

DISCUSSION & CONCLUSIONS: Irrespective of manufacturer and sterilisation technique, the biological response of the electrospun yarns in vivo was similar to the current gold standard, autograft. This would suggest ethanol submersion, as a sterilisation technique is acceptable when undertaking short-term in vivo animal studies.

ACKNOWLEDGEMENTS: This study was supported by the MRC-DPFS (Grant no: G1000788-98812 and MR/M007642/1).

The impact of prolonged 3D growth on cytoskeletal re-organisation, adhesion signaling and cell metabolism

A Chhatwal^{1,2}, S Przyborski^{1,2}

¹ School of Biological and Biomedical Sciences, Durham University, Durham UK ² ReproCELL Reinnervate, NETPark Incubator, Sedgfield, TS21, 3FD, UK

INTRODUCTION: Mammalian cells respond to changes in the chemical composition and dimensionality of their micro-environment through complex signalling events at adhesion sites along their membrane. Changes in the micro-environment can result in the up/down regulation of integrins, and changes in signalling downstream of adhesion. Using commercially available porous polystyrene scaffolds, a methodology was developed to propagate cells continually in 3D. This has been used to analyse how long-term growth in 3D affects cytoskeletal organisation and whether adhesion signalling differs between 2D and 3D maintained cells.

METHODS: HepG2 cells were seeded onto 6 well Alvetex® Strata inserts at a density of 5×10^5 and grown for 5 days. Cells were scraped off, counted, re-suspended and plated onto fresh inserts every 5 days. This process was conducted in parallel with HepG2 cells maintained in 2D. 2D and 3D passaged cells were stained for cytoskeletal markers and antibodies specific to key signalling molecules. The structural phenotype and signalling patterns of these cells were analysed using super resolution microscopy and quantified using ImageJ software. Cells were also assessed for functionality using commercially-available metabolic assays. Statistical significance presented as mean \pm SEM.

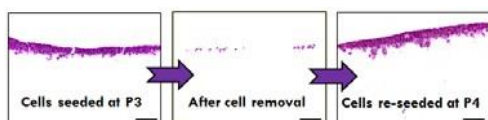


Fig1: H&E stained sections of Strata showing the scaffold before and after cell removal. These cells can then be re-seeded onto fresh scaffolds as shown. Scale bars 100µm.

RESULTS: Cells maintained in 3D show a general decrease in intracellular stress fibres. This cytoskeletal re-organisation corresponds with specific changes in cell morphology, with cells maintained in 3D showing a quantifiably rounder phenotype. 3D cells show a significant decrease in the phosphorylation of Focal Adhesion Kinase (FAK), as well as an increased adhesion to fibronectin-coated surfaces when compared to 2D counterparts. In addition, cells maintained in 2D show higher expression of the $\alpha\beta3$ integrin than those maintained in 3D; in contrast, cells maintained in 3D show higher levels of $\alpha5\beta1$. Antibody blocking studies revealed that blockage of

$\alpha5\beta1$ led to partial recovery of FAK phosphorylation. This change in mechanotransduction is followed through to the nucleoskeleton through changes in lamin expression at nuclear pores. These phenotypic and signalling changes correlate to changes in metabolism, with cells in 3D consuming significantly more glucose, and producing more albumin and urea.

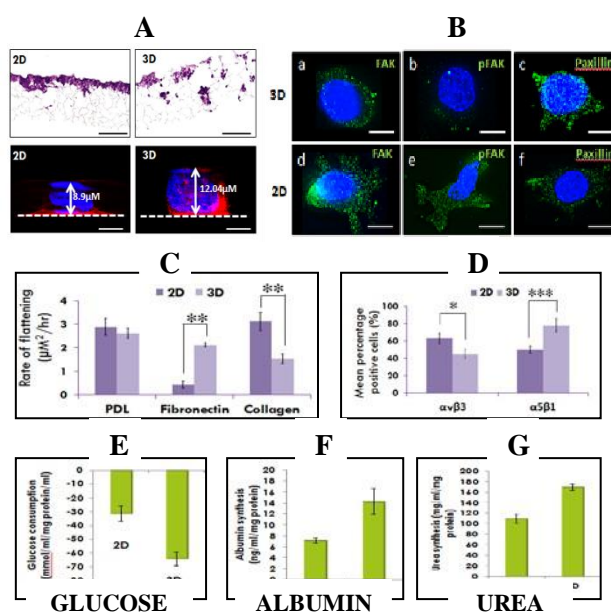


Fig2: 3D cells show a rounder, more circular phenotype and less flattening [A]. They also demonstrate different adhesion signaling patterns to 2D cells, namely an absence of pFAK³⁹⁷ and an increase in Paxillin [B]. This results in altered adhesion to fibronectin and collagen substrates [C] as underlined by differential integrin expression [D]. These changes also result in 3D cells being more metabolically active [E-G]. Scale bars 10µm (100µm in H&E images in [A].)

DISCUSSION & CONCLUSIONS: Altering the dimensionality in which cells are grown leads to changes in signalling and cytoskeletal organisation. Several key changes are observed both at the cell membrane, in terms of integrin expression, and further downstream in the FAK mechanotransduction pathway. These findings are important when considering how changes in cell shape brought about by 3D cell culture impact the observable cell function.

ACKNOWLEDGEMENTS: BBSRC and ReproCELL Reinnervate for funding.

Membrane emulsification : a platform to fabricate injectable porous PLGA microparticles

SS Chowdhury, O Qutachi, FRAJ Rose, KM Shakesheff

Division of Drug Delivery and Tissue Engineering, School of Pharmacy, University of Nottingham, Nottingham, UK

INTRODUCTION: Injectable porous microparticles (porMPs) have been used in the field of tissue engineering (TE) due to their practical advantages of providing better diffusion of nutrients and oxygen as well as removal of metabolic waste¹⁻². Emulsification is the most widely used MPs fabrication technique but conventional emulsification (CE) technique such as high shear homogenizer needs high energy input and it cannot ensure uniformity of MPs size³. Membrane emulsification (ME) is a robust technique in terms of fabricating monodisperse microparticles of a wide range of sizes by low energy input but only solid MPs fabrication have been reported³⁻⁴. Uniform size porMPs fabrication using this technique can be valuable in TE applications in terms of evaluating how cellular behaviour is affected due to variation in MPs size distribution. This study aimed at preparing larger size (around 50 μm) monodisperse porous PLGA microparticles to assess the efficiency of the particles for injectable cell delivery applications.

METHODS: In ME technique, disperse phase or pre-emulsion is injected through a porous glass membrane of certain porosity under low nitrogen gas pressure into circulating continuous phase. The emulsion droplets are formed in the continuous phase. Subsequent solvent evaporation and freeze drying yield MPs. For making porMPs, we have prepared a series of PLGA 85:15 (Mw 50 kDa) solutions in DCM to get a solution of certain viscosity that will be suitable for making uniform size porMPs. The other process parameters (working pressure, viscosity of polymer solution, surfactant concentration) were previously optimised for polycaprolactone (PCL) solid MPs. The PLGA solution was homogenized with 30 v/v% of phosphate buffer saline (PBS) using conventional homogenization technique. This primary emulsion was then injected through the membrane under N_2 pressure into circulating 0.3% PVA solution to get uniform porous PLGA microparticles of around 50 μm size. Span factor was measured to assess the uniformity of size distribution. In general, the closer the span factor

to zero, the more uniform the MPs size distribution is.

RESULTS: In comparison to CE method, ME method provided uniform porMPs (ME: Mean 50 $\mu\text{m}\pm 0.04$; CE: 48 $\mu\text{m}\pm 0.29$) as evident from the microscopic images of the emulsion droplets (Fig. 1a-b) and MPs (Fig. 1c). Span factor (ME: 0.40 ± 0.001 , CE: 0.98 ± 0.014) also indicated better uniformity of porMPs prepared by ME method.

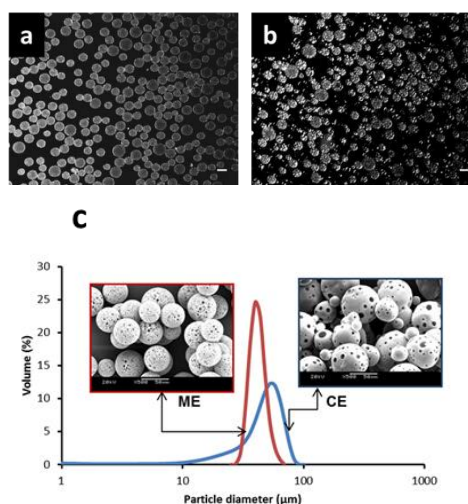


Fig.1:a) monodisperse emulsion droplets prepared by ME; b) polydisperse emulsion droplets prepared by CE; c) relatively uniform 50 μm size porous PLGA MPs prepared by ME in comparison to that of CE method. Scale bar 50 μm .

DISCUSSION & CONCLUSIONS: Using ME technique, we have managed to prepare uniform size porous PLGA in comparison to that of CE method and further study will be done to assess the efficiency of the particles for injectable delivery application

ACKNOWLEDGEMENT: The authors would like to thank Islamic Development Bank for funding to this project.

Modification of electrospun nanofibrous scaffolds for improved cellular adhesion and biocompatibility

BDM Coverdale¹, JE Gough¹, JA Hoyland²

¹*Biomaterials and Tissue Engineering Group, University of Manchester, UK.* ²*Centre for Tissue Injury and Repair, University of Manchester, UK*

INTRODUCTION: Electrospinning produces nanofibrous scaffolds which can be used for the repair and regeneration of damaged or non-functional tissues. The process however, is poorly regulated meaning scaffolds are often irregular and hydrophobic leading to poor biocompatibility and cellular attachment. This study aims to elucidate the effects of incorporating surfactants into electrospun poly (ϵ -caprolactone) (PCL) scaffolds on cellular adherence and consistency of fibre diameters and pore sizes.

METHODS: Solutions of PCL containing various concentrations of lecithin were electrospun to create 0%, 1%, 2%, 5% and 20% lecithin PCL scaffolds. Hydrophobicity of scaffolds was determined with water contact angle analysis. Fibre diameters and pore sizes of scaffolds were analysed using an SEM fibremetric analysis package and ImageJ. Relationships between fibre diameter and pore size were established using mathematical modelling. Cellular adherence was investigated using Saos-2 osteoblasts through metabolic comparisons of scaffold versus media activity over 1, 3 and 24 hours post seeding. Additionally, proliferation of cells was evaluated at 1, 3, 7 and 14 days using similar metabolic analysis and SEM imaging.

RESULTS: Lecithin significantly reduced the hydrophobicity of PCL scaffolds in a dose dependent manner. Higher metabolic activity levels of Saos-2 osteoblasts were detected on scaffolds containing lecithin rather than PCL alone, indicating increased cellular adherence (fig 1). Cells showed significant increases in proliferation on all scaffolds over 14 days of culture showing no cytotoxic effects. The addition of lecithin reduced mean fibre diameter of scaffolds from 1.33 μ m (PCL) to 1.02 μ m (20%) as well as reducing overall width distribution of fibres by 0.5 μ m (fig 2). Mathematical modelling confirmed a relationship between fibre diameter and pore size, indicating that lecithin also acts to reduce the mean pore size within scaffolds.

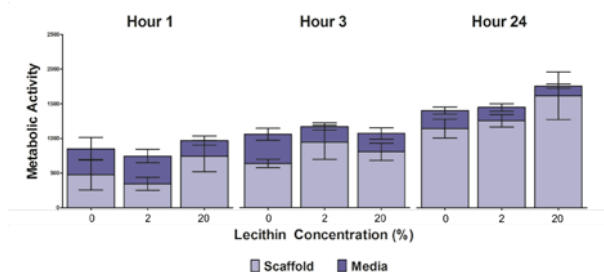


Figure 1. Cellular attachment. Metabolic activity of cells seeded on scaffolds composed of 0%, 2% and 20% lecithin vs media up to 24 hours post seeding.

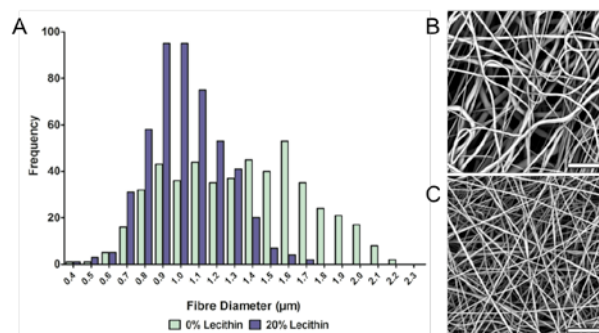


Figure 2. Fibre diameters. A) Histogram showing fibre diameter distribution of scaffolds composed of 0% and 20% lecithin. B) SEM of 0%. C) SEM of 20%. (Scale bar 20 μ m).

DISCUSSION & CONCLUSIONS: Increasing hydrophobicity of PCL fibres through lecithin addition allowed for greater cellular adhesion onto scaffolds. Reduction in mean fibre size led to increased surface area, which may also contribute to improved attachment. Heightened consistency of scaffolds allows for specific tailoring of electrospun scaffolds, making the process more efficient and more suitable for controlled differentiation. Furthermore all scaffolds conform to ISO 10993-5:2009 enabling their use in medical devices.

ACKNOWLEDGEMENTS: Funding body, EPSRC.

A mathematical model with the capacity to direct and accelerate the design of cellular peripheral nerve repair conduits

RH Coy¹, JB Phillips², RJ Shipley³

¹CoMPLEX, University College London, UK. ²Biomaterials & Tissue Engineering, UCL Eastman Dental Institute, University College London, UK. ³UCL Mechanical Engineering, University College London, UK.

INTRODUCTION: Therapeutic cell populations are used to promote neurite growth along the length of nerve repair conduits. The spatially-distributed density of such cells affects oxygen concentration levels. The resulting level of hypoxia determines vascular endothelial growth factor (VEGF) gradients along the conduits; however, excessive hypoxia results in cell death. Therefore a careful balance must be achieved: the distribution of VEGF along conduits is crucial for their vascularisation and long-term efficacy, but a sufficient level of cell viability must also be maintained. Therefore the initial seeding cell distribution used in such conduits is an important design factor.

However, exploring the many different possible initial cell seeding distributions experimentally would be a time consuming and expensive pursuit. Conversely, this task, and other similar spatial distribution problems within the field of nerve conduit design, is well suited to the application of mathematical and computational modelling techniques. The current study outlines a mathematical model, capable of quickly simulating changes in the spatial distributions of oxygen, VEGF and cell density along a nerve conduit with time, for different initial conditions.

METHODS: A model was designed to simulate the interactions between cell density, oxygen concentration and VEGF concentration along the length of a cylindrical nerve conduit. This involves three coupled differential equations, which incorporate the processes of diffusion, oxygen consumption, cell death and proliferation, and VEGF production. Estimates of parameters within the model were assigned using available experimental data.[1-3] The initial spatial distributions of the variables can be adjusted in order to investigate different possible conduit designs.

RESULTS: Solutions for the cell density, VEGF concentration and oxygen concentration were obtained as functions of time and space (distance along the conduit). It was found that the initial spatial distribution of cells had a large effect on the

subsequent spatial distributions of VEGF, oxygen and the seeding cell population, as shown in Fig. 1. The interactions were in some cases complex and not immediately intuitive.

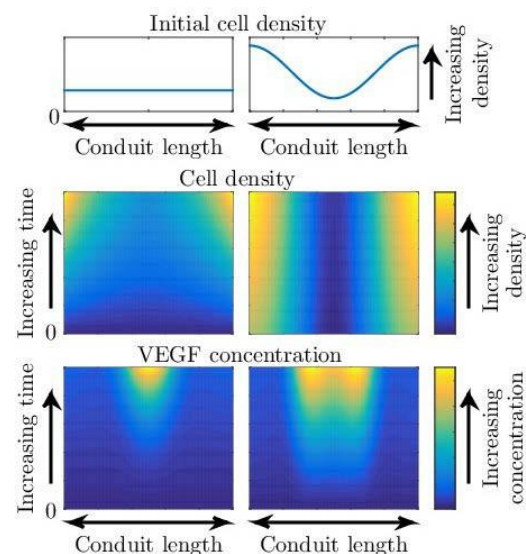


Fig. 1: Spatiotemporal (non-dimensional) results of model simulations with differing initial cell density distributions.

DISCUSSION & CONCLUSIONS: The model simulations demonstrate the potential for identifying optimal initial spatial cell seeding distributions by examining computationally how they affect other factors over time. The predictions obtained from such a model are capable of guiding the direction of further experiments; the outcomes of such experiments could in turn be used to refine the values of the various parameters used to define levels of cell death and proliferation, and VEGF production. This experimental-theoretical feedback loop is an exciting tool with the capacity to greatly improve both the efficacy and speed of conduit designs.

Directing cell differentiation through delivery of PLGA-nanoparticles loaded with bioactive molecules

EM Czekanska¹, J Geng², ND Evans¹, M Bradley², ROC Oreffo¹

¹ Bone & Joint Research Group, Centre for Human Development, Stem Cells and Regeneration, Faculty of Medicine, Southampton University, UK; ² School of Chemistry, University of Edinburgh, UK

INTRODUCTION: The intrinsic healing capacity of bone is compromised in cases of large segmental bone defects, avascular necrosis and non-unions. Given the limitations of bone grafts, including: i) limited availability, ii) donor site morbidity of autografts, iii) infection risk and iv) host response to allografts, there is a need for a novel strategies to aid bone healing. The combination of supportive biomaterials and bioactive factors to stimulate endogenous progenitor cells is of particular interest for clinical application for treatment of these conditions. The current work has examined a novel strategy for the temporal delivery of bioactive molecules encapsulated within biodegradable nanoparticles to develop smart materials to direct the differentiation of cells during bone regeneration.

METHODS: Poly(lactic-co-glycolic acid) (PLGA) nanoparticles (NP; 135-145nm diameter) containing either fluorescent dye, CFDA (NP_CFDA), or TGFβ₃ (NP_TGFβ₃) were prepared by a double emulsion process. C28/I2 cells (chondrogenic cell line) were incubated with 1, 10, 50 or 100μg/ml of the NP_CFDA supplemented to the cell culture medium (DMEM, 5% foetal bovine serum, 1% penicillin/streptomycin, 1xITS and 50μM ascorbic acid). NP_TGFβ₃ at the concentration 25, 50 or 100μg/ml were added to the culture medium and incubated with cells for 72 hours. Cell cultures with NPs with bovine serum albumin (BSA) or 1 and 5ng/ml TGFβ₃ protein served as controls. Internalisation of NPs after 1, 24 and 48 hours was analysed by flow cytometry. The concentration of gene expression of specific chondrogenic genes (Sox9, aggrecan, type II collagen) after 72 hours incubation with NP_TGFβ₃ was performed to evaluate NP functionality.

RESULTS: A time- and dose-dependent internalisation of NPs was observed, as evidenced by the number of fluorescent C28/I2 cells after the incubation with NP_CFDA. Consistently high level (>95%) of fluorescence was observed within 48 hours of incubation at a dose of 100μg NP_CFDA/ml. The gene expression of chondro-

genic genes of cells incubated with NP_TGFβ₃ was dose-dependent with the highest expression observed at 100μg NP_TGFβ₃ per ml (Fig.1). We observed a 2.0-, 2.3- and 2.2-fold up-regulation of aggrecan, type II collagen and Sox9 genes, respectively, in cells incubated with TGFβ₃ encapsulated NP compared to controls (Fig.1). The level of expression observed was comparable to expression in cells treated with 5ng/ml TGFβ₃. Calculations indicated the concentration of TGFβ₃ encapsulated within NPs was 3ng TGFβ₃/mg NP. Furthermore, we observed a 0.3ng of TGFβ₃ encapsulated in 100μg NP was sufficient to induce a comparable gene response in cells as 5ng TGFβ₃ per ml.

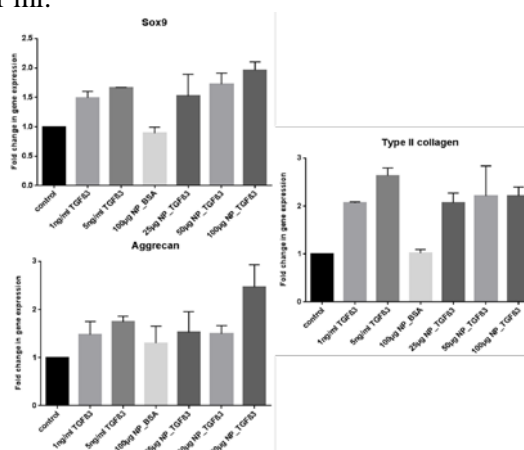


Fig.1: Gene expression of C28/I2 cells after treatment with NP_TGFβ₃.

DISCUSSION & CONCLUSIONS: These results indicate that PLGA nanoparticles can be successfully delivered into cells. Moreover, in conjunction with TGFβ₃, the NPs are able to modulate differentiation of cells and enhanced gene expression was observed with lower concentrations of TGFβ₃ following encapsulation and NP delivery. The delivery of growth factor encapsulated within NPs, offers the potential of reduced growth factor application during treatment as well as reduced therapeutic costs. Furthermore, our approach indicates the potential for the development and delivery of multiple growth factors within nanoparticles, with different degradation rates, providing a powerful strategy to enhance bone regeneration processes.

Hypothermic and cryogenic preservation of artificial neural tissue made using differentiated CTX human neural stem cells in collagen gels

AGE Day¹, KS Bhangra¹, C Murray-Dunning¹, L Thanabalasundaram², N Grace³, G Cameron³, L Stevanato², J Sinden², JB Phillips¹

¹*Biomaterials & Tissue Engineering, UCL Eastman Dental Institute, University College London, UK.* ²*ReNeuron Ltd, Guildford, Surrey, UK.* ³*TAP Biosystems, Royston, UK*

INTRODUCTION: Developments in tissue engineering offer tremendous potential for the future of regenerative medicine, however clinical translation of tissue-engineered devices remains associated with numerous barriers. In particular, there are concerns regarding the logistics involved in maintaining the structure and viability of cellular tissue-engineered constructs during storage and transport (O'Brien 2011). The aim of this study was to compare methods and media preparations for storing collagen constructs containing differentiated CTX (dCTX) cells under hypothermic or cryogenic conditions.

METHODS: Cellular collagen constructs were made in 24-well plates using RAFT™ absorbers (TAP Biosystems) to stabilise 2 mg/ml bovine collagen (Koken Co Ltd, Japan) hydrogels containing 2 million dCTX cells/ml. After stabilisation, gels were cut into 6 pieces, one control for immediate analysis and the others randomised between 5 different combinations of media and preservation conditions. Hypothermic conditions involved refrigeration for 48h at 4°C in (1) differentiation media (dmedia; Gibco, UK), (2) Hibernate-A (Gibco, UK), and (3) HypoThermosol-FRS (HTS-FRS; BioLife Solutions, Inc, USA). Cryogenic conditions involved controlled rate cooling and storage at -80°C for 24h then 24h in liquid nitrogen in (4) 90% dmedia + 10% DMSO, and (5) 90% HTS-FRS + 10% DMSO. After restoring them to 37°C, cell death in the test samples was analysed using Syto-9 (5µM) and propidium iodide (200 µg/ml) staining followed by fluorescence microscopy (% cell death in the relevant control sample was subtracted).

RESULTS: Constructs preserved in HTS-FRS under hypothermic conditions exhibited the lowest cell death ($7.2 \pm 1.4\%$), followed by those cryogenically preserved in 90% HTS-FRS + 10% DMSO ($11.9 \pm 3.6\%$) and 90% dmedia + 10% DMSO ($13.7 \pm 7.6\%$). More cell death was present in constructs that were refrigerated in Hibernate A ($33.6 \pm 7.2\%$) and dmedia ($64.3 \pm 7.6\%$) (Fig 1).

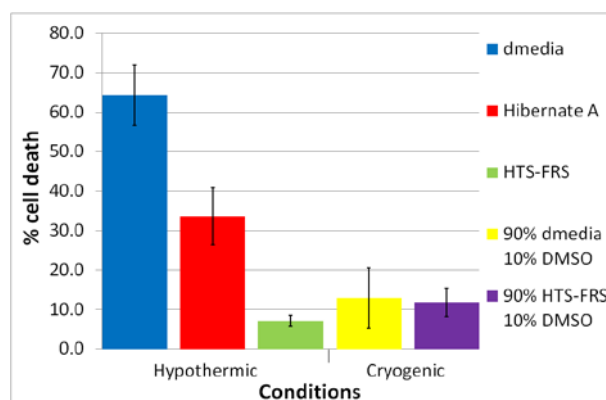


Fig. 1: Percentage of dCTX cell death in stabilised bovine collagen gels after 2 days in hypothermic or cryogenic preservation conditions (n=6, data are means ± SEM after subtraction of % cell death in relevant controls).

DISCUSSION & CONCLUSIONS: This study demonstrates that artificial tissues made using clinically relevant therapeutic cells in collagen gels can be subjected to hypothermic and cryogenic storage, with cell death varying according to media conditions. HTS-FRS in particular was used to preserve cells under hypothermic conditions and, with the addition of DMSO, under cryogenic conditions, with minimal cell death after 2 days. Further research is required to understand the effects of refrigeration and cryopreservation on the long-term viability of the cells, and the structure of the artificial tissue.

ACKNOWLEDGEMENTS:

This work was supported by funding from the UK Technology Strategy Board (101599).

Understanding the epigenetic mechanisms underlying anabolic and catabolic gene regulation in osteoarthritis

MC de Andrés¹, ROC Oreffo¹

¹*Bone and Joint Research Group, Centre for Human Development, Stem Cells and Regeneration, [Institute of Developmental Sciences](#), Southampton, UK.*

INTRODUCTION: Osteoarthritis (OA) is one of the most common degenerative joint diseases in the aging population affecting some two thirds of the elderly population. OA is characterized by the progressive loss of cartilage matrix, accompanied by deleterious changes in the synovium and subchondral bone. In OA disease, chondrocytes undergo phenotypic changes with altered patterns of gene expression that are stably transmitted to subsequent cell generations. Gene expression is regulated by epigenetic and non-epigenetic mechanisms and there is a growing body of evidence to support the role of epigenetics in the pathogenesis of OA. We have examined an essential feature of the underlying pathogenesis of OA, namely the imbalance of anabolic and catabolic activity leading to progressive loss and destruction of extracellular matrix of articular cartilage.

METHODS: Human articular cartilage samples were obtained from patients following hemiarthroplasty as a consequence of femoral neck fracture (NOF) and from OA patients who underwent total hip arthroplasty. *IL1B*, *iNOS*, *MMP13*, *COL9A1* and *IL8* expression levels and the percentage CpG methylation were quantified by qRT-PCR and pyrosequencing to compare OA patients with non-OA controls. The effect of CpG methylation on proximal promoter activities was determined using a CpG-free vector; co-transfections with expression vectors encoding crucial transcriptional factors in OA were subsequently undertaken to analyse for promoter activities in response to changes in methylation status. Furthermore, to determine the CpG sites critical for promoter activities, wild type promoter construct activities were compared against vectors containing mutations at different CpG sites. Chromatin immunoprecipitation assays were carried out to validate transcription factors binding to promoters and the influence of DNA methylation.

RESULTS: Relative expressions of catabolic genes (*IL1B*, *iNOS*, *MMP13*, and *IL8*) in OA patients were significantly higher than in NOF patients and, this was correlated with either

hypomethylated CpG sites in the proximal promoters or in a specific enhancer element for *iNOS* gene^{1,2}; in contrast, the relative expression level of the chondrocyte anabolic gene, *COL9A1*, was abolished in OA chondrocytes compared with healthy controls. This observation was correlated with hypermethylated CpG sites in its proximal promoter³. We now demonstrate for the first time, demethylation of an NF-κB enhancer element orchestrates *iNOS* induction in OA via cell cycle regulation (Figure 1).

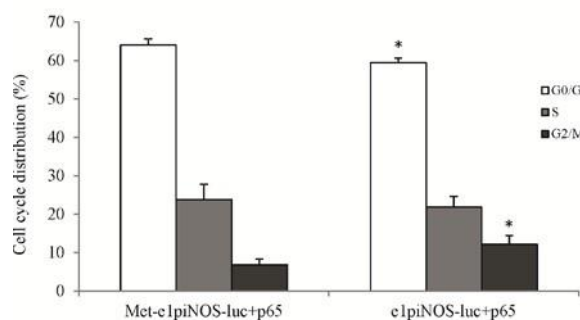


*Fig. 1: Cell cycle distribution is altered by NF-κB mediated iNOS transactivation in human chondrocytes. Values are expressed as mean ± SD (n = 3 independent experiments). *P<0.05.*

DISCUSSION & CONCLUSIONS: Epigenetic changes in OA involve hypomethylation and the consequent activation of aberrant, catabolic genes, as well as hypermethylation leading to silencing of at least 1 chondrocytic gene that contains sparse CpG sites at important regulatory domains. The current studies demonstrate that approaches that incorporate prevention or reversal of epigenetic changes offer significant therapeutic potential for OA in an increasing patient demographic.

ACKNOWLEDGEMENTS: The authors acknowledge the orthopaedic surgeons at Southampton General Hospital for provision of the femoral heads and BBSRC for funding.

Nanoelasticity and structure of collagen fibrils highly influenced by osmotic stress

S Desissaire¹, OG Andriotis¹, PJ Thurner^{1,2}

¹[TU Wien, Vienna, Austria.](#) ²[University of Southampton, UK](#)

INTRODUCTION: Proteoglycans are macromolecules with high negative charge, normally located in the vicinity of collagen fibrils. The high negative charge creates osmotic stress on the neighbouring collagen fibrils by retracting ions and consequently water from their intermolecular space. Therefore we hypothesized that both the structure and mechanics of collagen fibrils will also be influenced lower hydration levels due to osmotic stress.

METHODS: Collagen fibrils were obtained from a wild type mice tail tendon of 2 months old, deposited onto poly-L-lysine coated microscope glass slides, washed with distilled water and air-dried. Individual collagen fibrils were then subsequently imaged in air, in phosphate buffered saline (PBS) solution (1mM, pH7.4) and in polyethylene glycol (PEG; 200 gr/mol) solutions of 0.1M, 0.5, 1M, 5M and 10M concentrations (figure 1a). After imaging, the average diameter of individual collagen fibrils was estimated from height measurements of the cross-sections (figure 1b) from the AFM height topography images. Swelling was then defined as the fold-increase in fibril diameter when hydrating the samples in PBS from the air-dried state. Shrinking was defined as the fold-decrease in fibril height while increasing concentration of PEG from the fully hydrated state in PBS (D_{PEG}/D_{PBS}).

RESULTS: During hydration with PBS from the air-dried state the diameter increased by (1.54 ± 0.09) fold increase. Gradual dehydration with increasing the concentration of PEG only caused 14% to 22% of shrinking (figure 1c). But the increase in the transverse elastic properties of the collagen fibrils was substantial. The indentation modulus increased, from (9 ± 1) MPa in 0.1M of PEG to (364 ± 18) MPa (~42-fold increase) in 10M of PEG (figure 1d).

DISCUSSION & CONCLUSIONS: Reduction of the fibril diameter is caused because of dehydration, i.e. removing of ions and unbound water from the intrafibrillar space. As a result, the axial intermolecular distance decreases [1] and now collagen molecules are more densely packed. The increase in density explains why the mechanical properties are increased in the

transverse direction. Our results show that the osmotic stress influences the elasticity of collagen fibrils to a large extent. *In vivo*, osmotic stress may be preferentially increased or decreased by the amount of proteoglycans secreted from cells to tune cell functions. For example, increasing amount of secreted proteoglycan could increase cell mobility during wound healing [2]. This means that collagen in the form of fibrils is truly a functional material; and scaffolds based on collagen fibrils have a built-in mechanical tuning function for cells.

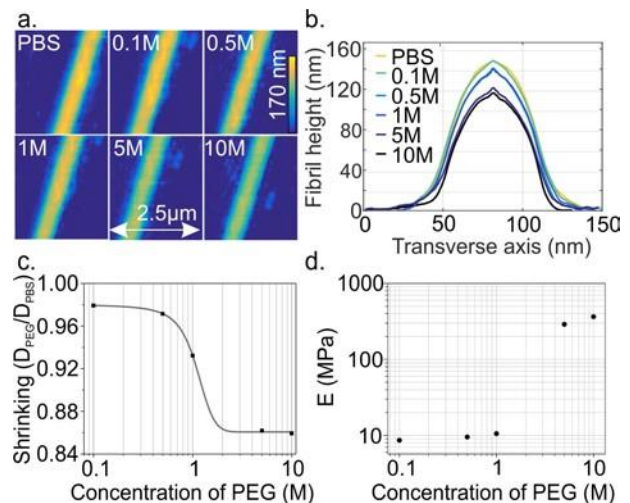


Fig.1: (a) AFM images of a collagen fibrils at different environments. (b) Representative cross-section profiles at increasing concentration of PEG. (c) Shrinking of collagen fibril diameter. (d) Increase in indentation modulus with increasing PEG concentration.

Designing and fabricating a functional *in vitro* neural circuit

M Dunn^{1*}, M Kamudzandu², R Fricker², P Roach^{1*}

¹ Guy Hilton Research Centre, Hartshill, Stoke-on-Trent, UK. ² Keele University, Keele, Staffordshire, UK.

INTRODUCTION: Cell damage or dysfunction within the brain can result in a number of debilitating and progressive neurodegenerative disorders. One example is the basal ganglia: losing dopamine neurons in this area is responsible for Parkinson's and Huntington's diseases. However, the basal ganglia is deep within the midbrain, and difficult to access without causing damage to outer parts of the brain. Even so, the neurons within are densely interconnected, meaning neural study *in vivo* is very challenging. By re-creating the basal ganglia *in vitro*, it will be much easier to study, but can a complex functioning circuit be created *in vitro*?

In this study, a five-port biomimetic device has been developed in an attempt to replicate a simplified version of the basal ganglia circuitry using different neural cell subtypes. By growing primary cells from the striatum, SNc, SNr, cortex and globus pallidus, and forcing them to connect from otherwise isolated ports via channels large enough for axons, a controlled network can be produced. The cells can be functionally assessed to determine any electrophysiological activity within defined populations and across the entire circuit. The complexity can be gradually increased to introduce surface chemical coatings, physical surface features (micro/nanotopographies) and surface mechanical properties similar to those presented to cells within the brain niche.

METHODS: The device itself is fabricated via photo- (SU8) and sequential soft-lithography. The cell culture wells are interconnected with micro-channels specifically designed to promote unidirectional connections. The devices were produced from this mould using polydimethylsiloxane (PDMS) and bonded to glass coverslips via oxygen plasma treatment. Primary embryonic rat neural cells from different neural subtypes were seeded into different ports, for axons to grow through the channels between ports in a unidirectional manner, connecting the ports. Cell attachment and morphology was assessed by via fluorescence imaging, and cell function (spontaneous activity) was assessed by electrophysiological measurements and calcium signalling. Ion channel blockers were used to halt the spontaneous activity. Fluorescent dyes were

used to assess connectivity and diffusion between culture wells.

RESULTS: The device supported attachment, alignment and viability of primary neurons. Neurons were interconnected via directed axons, observed extending through the micro-channels, creating a rudimentary circuit. Electrophysiological tests and calcium assays indicated that the cells were functional and producing spontaneous bursts of activity. This activity was halted by the use of an ion channel blocker, affecting not only the directly blocked cells but also in downstream adjacent populations – highlighting functional connectivity.

DISCUSSION & CONCLUSIONS: We demonstrate the fabrication and investigation of functional activity of specific neural cell interconnections within a fabricated neural circuit. By gradually increasing the complexity of the device it will be able to mimic the basal ganglia environment and be used as a powerful experimental platform to study an otherwise inaccessible area of the brain, as well as any other neural or cellular network.

ACKNOWLEDGEMENTS: We acknowledge funding support from the EPSRC Doctoral Training Centre in Regenerative Medicine. This template was modified with kind permission from eCM Journal.

Assessment of the gradient delivery of bioactive molecules to hydrogel-encapsulated cells using flow cytometric analysis

HM Eltaher^{1,2}, J Yang¹, JE Dixon¹, KM Shakesheff¹

¹ [Wolfson Centre for Stem Cells, Tissue Engineering and Modelling \(STEM\), Division of Advanced Drug Delivery and Tissue Engineering, School of Pharmacy, University of Nottingham, UK.](#)

² [Department of Pharmaceutics, Faculty of Pharmacy, Alexandria University, Egypt.](#)

INTRODUCTION: Cellular microenvironment accommodates various cell types that are exposed to physical and chemical cues regulating their behaviour and defining the overall tissue fate¹. Traditional 2D cultures are found to poorly represent the 3D environment to which the cells are exposed and hence 3D models have been extensively studied to evaluate factors affecting morphogenesis and differentiation in response to biologically active molecules². In particular, gradients of proteins can be employed to replicate this fine microarchitecture upon understanding cellular responses towards them. From this perspective and resuming our previous work^{3, 4}, gradients of GET proteins across 3D cell-laden hydrogels were developed and gradient cellular protein uptake was monitored as a function of distance away from source protein.

METHODS: Following gradient development via compartmental diffusion model, cells were retrieved from 5 successive 1 mm thick slices employing gel digestion protocol that involved heat and enzymatic treatment. Hoechst 33342 was added to the liquefied gel slices to stain cell nuclei. Samples were then analysed using a MoFlo™ DP (DAKO) Flow Cytometer using the green (561 nm) and violet (405 nm) lasers to detect staining for red fluorescent proteins and Hoechst 33342 respectively.

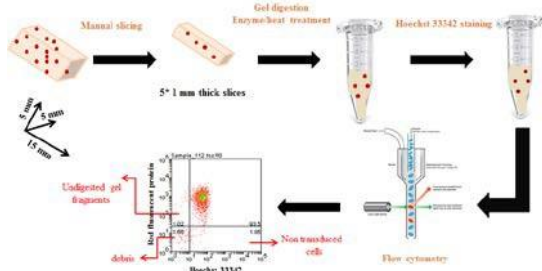


Fig. 1: Schematic representation of work flow to assess the gradient delivery of GET proteins to hydrogel encapsulated cells.

RESULTS: Intracellular gradient of red fluorescent proteins across the hydrogel width was achieved as a function of distance away from source GET protein (P21-mR-8R). In contrast, cells encapsulated within hydrogels through which reporter protein (mRFP) diffused, did not show

such gradient cellular uptake and behaved like cells from scaffolds exposed to culture medium.

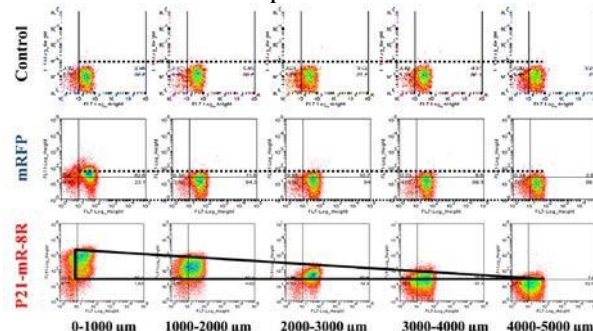


Fig. 2: Flow cytometric analysis of cells retrieved from digested gel slices as a function of distance away from source protein. A: levelled minimal red fluorescent proteins (upper right quadrants) in slices comprising control scaffold (upper panel). B: mRFP scaffold showing levelled fluorescent intensities for the last 4 slices with the first slice slightly higher. C: P21-mR-8R scaffold (lower panel) showing gradient cellular uptake of the red fluorescent protein across the hydrogel width.

DISCUSSION & CONCLUSIONS: Flow cytometric analysis revealed gradient cellular uptake of GET proteins as a function of distance, demonstrating the ability to control the intracellular delivery of functional GET proteins for directing cell behaviour and tissue fate.

ACKNOWLEDGEMENTS: We would like to thank Dr. David Onion (University of Nottingham) for helpful discussions and the Ministry of Higher Education in Egypt for the PhD scholarship.

The effect of substrate coating on pseudoislet formation

A Elttayef¹, L Lyu¹, C Kelly², Y Yang¹,

¹Institute for Science & Technology in Medicine, Guy Hilton Research Centre, Keele University, Stoke-on-Trent, UK. ²NI Centre for Stratified Medicine, Ulster University, Altnagelvin Hospital Campus, Derry/Londonderry, UK

INTRODUCTION: The architecture of pancreatic islets of Langerhans plays a central role in their physiological function. Pancreatic beta cells communicate to each other through gap junction channels. The three-dimensional (3D) structure of islets is essential for the maintenance of normal patterns of insulin secretion and action. Artificial reconstruction of isolated beta cells into islets of Langerhans through 3D cell aggregation has led to the formation of pseudoislets (PIs) by regenerative medicine/tissue engineering approaches. However, the life span of current PI models is approximately 7 days, after which central necrosis has been reported¹. The aim of this study is the generation of PIs through treatment of suspension plates, which can be maintained in culture for extended periods of time with high viability.

METHODS: The pancreatic beta cell line, BRIN-BD11, was used for all experiments. BRIN-BD11 cells are of rat origin and were generated through the electrofusion of primary rat pancreatic islets with the insulinoma-derived RINm5F cell line. BRIN-BD11 cells are traditionally grown as monolayers. Thus, PIs were formed on suspension culture plates with different coating as following: Ultra-low attachment 6 well plates (Corning, 2 x 10⁵ cells/well); 24 well suspension culture plates (32 x 10³ cells/well) coated with 1% gelatin A, 2% F127, or various mixtures of the two including 98% gelatin A and 2% F127 (group A), 95% gelatin A and 5% (group B); and 90% gelatin A and 10% F127 (group C). Cell viability/proliferation was assessed using MTT assays. Insulin secretion in response to 16.7 mM glucose stimulation for 20 min was measured using a commercially available ELISA kit.

RESULTS: PIs' size varied depending on the type of plate and the coating used. Ultra-low attachment

plates formed PIs size of 293.2 ± 44.2 μm (N=18), while suspension tissue culture plates coated with 2% F127 produced PIs size of 789.9 ± 115.2 μm (N=5). The coating mixture of gelatin A and F127 generated PIs with different sizes. Group A was 146.2 ± 18.1 μm (N=17); Group B was 155.7 ± 22.6 μm (N=11) and Group C was 205.0 ± 29.6 μm (N=11) (Fig 1). PIs grown on coating of 1% gelatin A anchored to the surface of the suspension tissue culture plate. The viability of PIs compared with monolayer controls were 49.0% (Group A), 46.6% (Group B) and 34.8% (Group C). The highest insulin secretion was noted in the PIs from group A which was 3.29 pg insulin/2 μg protein/20min.

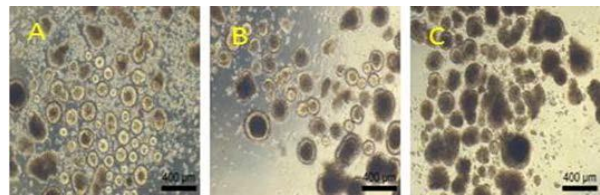


Fig. 1: Live images of PIs in suspension with different coating (A) group A; (B) group B; (C) group C at day 7 culture.

DISCUSSION & CONCLUSIONS: Changing the surface chemistry of the culture substrate through coating with a mixture of gelatin A and F127 may be used to control PIs' size, cell viability and insulin secretion capacity.

ACKNOWLEDGEMENTS: Funding of this project was provide by the Iraqi Ministry of higher education and scientific research.

Examining tissue invasion in an organotypic ameloblastoma model

T Eriksson¹, S Fedele², R Day³, V Salih⁴

¹Biomaterials and Tissue Engineering, ²Oral Medicine, ³Applied Biomedical Engineering; all University College London, UK; ⁴Plymouth University Peninsula School of Medicine and Dentistry, UK;

INTRODUCTION: Ameloblastoma (AM) is a benign but destructive oral tumour with up to 70% recurrence potential depending on tumour type¹. Therapy requires a large resection of the jawbone and surrounding soft tissues, to minimise the risk of incomplete excision, as recurrences are caused by the presence of cell islands surrounding the main tumour². We have used tissue engineering to make an organotypic soft tissue model to study the invasive behaviour of AM in vitro.

METHODS: Compressed collagen scaffolds (2ml collagen to 1ml Corning Matrigel[®]) seeded with gingival fibroblasts (GF) formed the basis of the model. Ameloblastoma cells (AM-1 cell line³) were incorporated into a collagen-only gel and co-cultured with the fibroblast gel. Cell interactions were examined using immunocytochemistry: fibroblast surface protein antibody (Abcam), AlexaFluor 488 antibody and Live/Dead staining (all Life Technologies). Cell Titre Glo 3D assay (Promega) was used to quantify cell proliferation. Quantitative RT-PCR for MMPs was carried out using Trizol[®]-extracted RNA and a high-capacity RNA-to-cDNA mastermix (Applied Biosystems). The Mastermix and primers used for qRT-PCR were from Applied Biosystems with GAPDH as an internal control.

RESULTS: Immunocytochemical staining showed a close interaction between the fibroblasts and AM-1 cells in the co-culture models (fig.1).

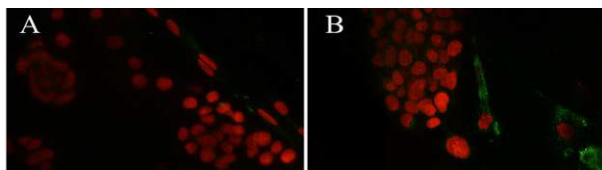


Fig. 1: Interactions between the two cell types in the co-culture scaffold were observed. A: On day 7, green GF cells are elongated close to the red nuclei of AM-1 cells (clustered). B: GF and AM-1 cells in close contact with each other in mixed populations in gels by day 14. N =3.

A significant increase ($p < 0.05$) in MMP-2 levels was seen in the AM part of the model (Fig. 2),

indicating increased tissue remodelling and invasion potential.

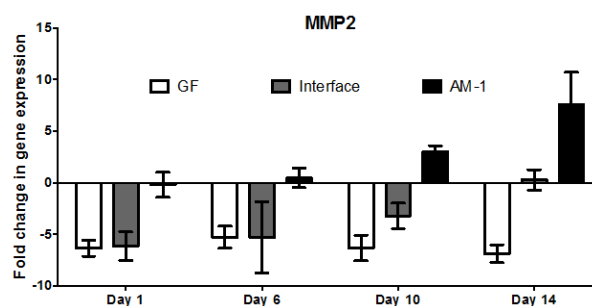


Fig. 2: MMP2 levels increase over time in the AM part of the co-culture and the gel interface when compared to the GF part. N =3.

DISCUSSION & CONCLUSIONS: Both the spatial localisation of the two cell types, and the increase in MMP2 levels in the AM part of the

model, indicate that AM cells can interact with GF and invade the soft tissue matrix. MMP2 has previously been reported to be over-expressed at the edges of AM tumours, presumably due to its contribution in tumour invasion⁴. There may also be a link between the interactions between the cells and tumour-associated fibroblasts being recruited by the AM cells, although this needs further investigation. As MMP activation is common in tumours, there are many therapeutic agents available. This model enables screening of these compounds to assess their effect on tumour growth, which could be used to limit AM invasion both in this model, and in conjunction with surgery in future clinical use.

ACKNOWLEDGEMENTS: This study was sponsored by a UCL Impact Scholarship from the Biss-Davies charitable foundation and the UCL Development Office. AM-1 cells were donated by Prof. H. Harada, Iwate Medical University, Japan.

Engineering a capillary bed bioreactor for dermal bioavailability and toxicity testing: caffeine permeation across novel hollow fibre membranes

PP Esteban¹, C Moore², A Scott², MJ Ellis¹

¹ [Department of Chemical Engineering, University of Bath, UK.](#) ² [Safety and Environmental Assurance Centre, Unilever, Bedford, UK](#)

INTRODUCTION: Traditionally, the estimation of dermal bioavailability and cutaneous toxicity of ingredients in cosmetics has been carried out using animal testing. Nowadays, there is a strong need for alternatives due to more strict regulations when animal testing is involved. In fact, the use of animals to test cosmetic products is banned in the UK and all other members of the EU, and commercialisation of products that have been tested on animals is illegal since March 2013. Toxicological assessment and skin penetration studies *in vitro* do not reproduce physiological conditions for two reasons: they do not consider the resistance to flow opposed by the blood vessels, and the position of the skin vasculature *in vivo* is much closer to the skin surface than that achieved *in vitro*. We propose a novel strategy to mimic skin vascularisation using hollow fibres fabricated with biocompatible materials. As a proof of concept we show that caffeine, a standard compound used in skin penetration studies, permeates through porous hollow fibres, similarly to the clearance that would occur in dermal capillaries.

METHODS: Hollow fibres were fabricated by wet spinning as described elsewhere¹. Casting solutions were formulated using various *PolymerX (PX)* fibres (a new membrane material developed in-house) with different pore sizes. Caffeine permeation studies were performed using a custom-made glass bioreactor, where 0.5 ml of a caffeine solution (7.5 mg ml^{-1}) was dosed in the outer part of the hollow fibre, and deionised water was circulated through the lumen of the fibre at a flow rate of 2.5 ml h^{-1} . Samples were taken every 10 minutes for a period of two hours, and the concentration of caffeine was measured via HPLC.

RESULTS: Figure 1 shows an SEM micrograph of a *PX20*. The porous structure can be seen to have a desirable asymmetric morphology with interconnected pores. Figure 2 shows cumulative mass of caffeine that permeates through the porous outer surface collected over a period of 2 hours.

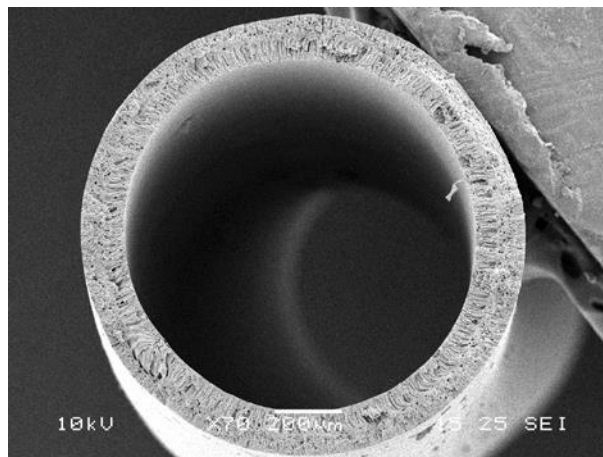


Fig. 1: SEM micrograph of PolyX20 hollow fibre.

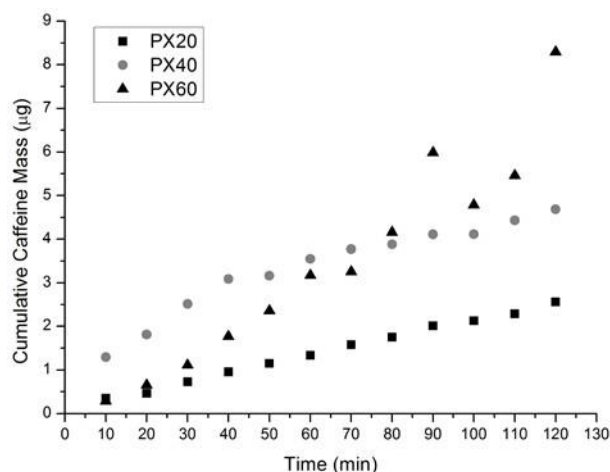


Fig. 2: Representative data for the cumulative mass of caffeine that permeates through the pores of *PX20*, *PX40* and *PX60* fibres.

DISCUSSION & CONCLUSIONS: It is clear that caffeine permeates through the hollow fibres, and the cumulative mass collected is higher for the more porous fibres. These results demonstrate the suitability of the membranes for the design of a capillary bed bioreactor for skin pseudo-vascularisation.

ACKNOWLEDGEMENTS: We thank InnovateUK, NC3Rs and EPSRC for funding.

DNA minicircle vector technology: a new solution to overcome plasmid size restrictions on magnetic particle based gene delivery to neural stem cells

AR Fernandes & DM Chari

Cellular and Neural Engineering Group, Institute of Science and Technology in Medicine, Keele University

INTRODUCTION: The central nervous system (brain and spinal cord) has limited regenerative capacity. Genetically engineering transplant cells to release therapeutic molecules can augment their regenerative capacity and promote neural regeneration [1].

Current genetic engineering approaches (viral and non-viral) have significant drawbacks for clinical translation (low transfection and high toxicity). Magnetofection (magnetic particles [MPs] deployed with oscillating magnetic fields) is a well-established approach for **safe and reliable** gene transfer to NSCs [2]. However, we recently reported an inverse relationship between transfection efficiency and plasmid size [3], representing a **major challenge for therapeutic gene delivery** which inevitably results in increased plasmid size. This study presents a **novel solution** using minicircle DNA technology. Minicircles are small vectors devoid of a bacterial backbone offering significant clinical benefits (safety, efficient gene transfer and long-term biomolecule expression).

METHODS: Reporter gene delivery was assessed using minicircles expressing green fluorescent protein (GFP). For *therapeutic* gene delivery, minicircles were engineered in-house to express brain-derived neurotrophic factor (BDNF), a pro-regenerative biomolecule. Minicircle/iron oxide MP complexes were added to primary neonatal murine NSCs and incubated for 48 hrs with an oscillating magnetic field (4Hz) applied for the first 30 minutes.

RESULTS: We report up to 49% transfection efficiency with minicircle reporter gene delivery, **the highest non-viral transfection levels reported to date in primary NSCs [Fig. 1]**. Further, for the first time, we demonstrate 1) safe therapeutic gene transfer to NSCs; 2) high therapeutic transfection efficiency (>30%) [Fig. 1]; and 3) sustained BDNF secretion.

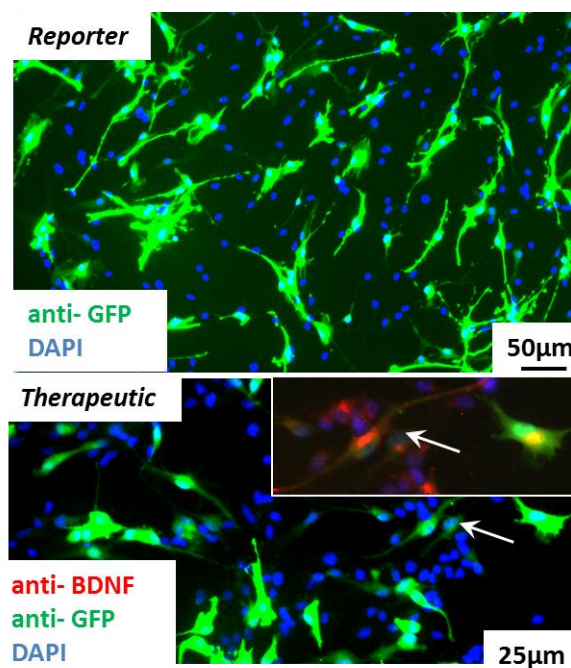


Fig.1: Top panel depicts high levels of reporter GFP expression in NSCs magnetofected with minicircles (top). Bottom panel illustrates efficient therapeutic gene delivery: BDNF (inset) and GFP expression (main image) is co-localised indicating successful overexpression of the neurotherapeutic biomolecule. Arrows indicate the same cell.

DISCUSSION & CONCLUSIONS: Safe, efficient and sustained gene transfer to NSCs - a key transplant population - is a major goal for regenerative neurology. We have developed a clinically-compatible strategy to genetically engineer hard-to-transfect NSCs by combining minicircle and magnetofection technologies. We consider that our finding is of wide benefit to the neural tissue engineering community.

ACKNOWLEDGEMENTS: This project is supported by a BBSRC grant – BB/JO17590/1.

MICA genotype, serum and expression level effects on the outcome of HSCT

R Gam*¹, J Norden¹, R Crossland¹, K Pearce¹, C Lendrem¹, E Holler², R Dressel³, AM Dickinson¹

¹Department of haematological sciences, Newcastle University, Newcastle-Upon-Tyne, United Kingdom, ²Department of Haematology and Oncology, University Clinic Regensburg, Regensburg, ³Department of Cellular and Molecular Immunology, University of Göttingen, Germany

INTRODUCTION:

Graft-versus-host disease (GvHD) is a serious complication of allogeneic haematopoietic stem cell transplantation (allo-HSCT). The immunopathology of GvHD involves secretion of proinflammatory cytokines with subsequent expression of danger signals by the affected tissues. MHC class I chain-related gene A (MICA), is a stress induced molecule that acts as danger signal to alert NK and $\alpha\beta$ or $\gamma\delta$ CD8 T cells through engagement of the activating NKG2D receptor.

We investigated MICA genotype together with serum and mRNA expression levels in the development and progression GvHD.

METHODS:

We analysed the MICA SNP (rs1051792) Val129Met in n=1384 patient-donor pairs. Genotyping was performed by KASP, based on competitive allele specific PCR (LGC Genomics, UK).

MICA expression levels were investigated in n=180 gut biopsies with SYBR GREEN® qRT-PCR. Histological grades of the gastrointestinal GvHD (GI GvHD) were determined by the pathology department at the University Clinic, Regensburg and severity was grouped by assigning an apoptotic score (0 = absence of apoptosis, 3 = maximum apoptosis). A Protein Biochip Array (Evidence Investigator®, RANDOX) was utilised for measuring MICA serum levels and evaluated in n=129 samples from allo-HSCT patients collected at pre-transplantation, day-7, day+14, day+28 and 3 months post transplantation

RESULTS:

Our analysis showed that the Methionine allele in rs1051792 was associated with an increased risk of relapse (p=0.029). The same allele was also found to be associated with a reduced overall survival (p=0.041) which was more severe for non-T cell-depleted allo-HSCT (p=0.001). Vice, versa, the presence of the Valine allele was associated with the development of aGvHD (p=0.044).

In the gut, MICA expression was investigated in patients treated with low doses of steroids (\leq

20mg/kg), as high dose steroid treatment strongly suppressed MICA expression. Higher levels of MICA were associated with an apoptotic score=0 (no apoptosis) (p=0.044) and the absence of active GI GvHD (p=0.046).

Increased soluble MICA levels at 3 months post-transplantation were significantly associated with aGvHD (p=0.0123).

DISCUSSION & CONCLUSIONS:

MICA molecules have been shown to play prominent roles in immune processes and therefore are also potential aGvHD biomarkers. In this study, we showed that the Methionine (MICA-129Met) allele was associated with the incidence of relapse while the Valine (MICA-129Val) allele was associated with an increased risk aGvHD. A low overall survival for patients who did not have had the T cell depletion treatment was also associated with the presence of the Methionine (MICA-129Met) allele. In the gut of patients treated with low doses of steroid, MICA gene expression levels were higher with the absence of GvHD. This may indicate that the isoforms are able to mediate NK cell and T cell

DISCLOSURE OF INTEREST:

R. Gam Funding from: This work was done under the framework of CellEurope project (FP7-People-2012-ITN, No. 315963) coordinated by Professor Anne Dickinson from University of Newcastle upon Tyne, J.

Norden: None Declared, R. Crossland: None Declared, K. Pearce: None Declared, E. Holler: None Declared, R. Dressel:

None Declared, A. M. Dickinson: None Declared

KEYWORDS:

Biomarkers, GvHD, HSCT, single-nucleotide polymorphism

Comparison of the potential of human chondrocytes, bone marrow, adipose and synovial fluid derived mesenchymal stem cells from arthritic joints for osteochondral repair

J Garcia¹, C Mennan¹, J Richardson¹, S Roberts¹, K Wright¹

¹ISTM, Keele University based at the RJAH Orthopaedic Hospital, Oswestry, Shropshire, UK

INTRODUCTION: Autologous chondrocyte implantation (ACI) is a cell based therapy option used to treat defects in articular cartilage. However, donor sight morbidity is a potential risk associated with harvesting healthy cartilage for ACI, which could contribute to joint degeneration. As a result, cells obtained from easily accessible alternative tissue sources such as bone marrow adipose tissue and synovial fluid are currently being assessed for cartilage repair.

METHODS: Chondrocytes, bone mesenchymal stem cells (BMSCs), subcutaneous fat adipose stem cells (SC-ASCs), infrapatellar fat pad adipose stem cells (FP-ASCs) and synovial fluid mesenchymal stem cells (SF-MSCs) were obtained from 6 donors. Flow cytometry was used to assess their MSC immunoprofile, a panel of putative chondrogenic markers (CD44, CD166, CD49c, CD271, CD151, CD39, FGFR3 and ROR2) and the immunomodulatory marker CD106, while their chondrogenic capacity was assessed using a standard pellet culture differentiation protocol¹. Culture doubling time (DT) was calculated to determine growth kinetics. To evaluate the immunogenic nature of FP-ASCs and SF-MSCs, immunopositivity for CD40, CD80, CD86 and HLA-DR was evaluated before and after stimulation with IFN- γ .

RESULTS: Chondrocytes, BMSCs, SC-ASCs, FP-ASCs and SF-MSCs adhered to the immunoprofile criteria for MSCs derived from bone marrow and adipose tissues^{2,3}. All cell types were constitutively immunopositive for CD44 and CD151 and negative for CD271, FGFR3 and ROR2. Whereas, CD166, CD49c, CD39 and CD106 were differentially expressed between cell types and across donors.

Histological assessment showed that chondrocytes and FP-ASCs produced larger pellets with a higher glycosaminoglycan (GAG) content compared to BMSCs and SC-ASCs (Figure 1). Preliminary analyses suggest that CD49c and CD39 immunopositivity on chondrocytes and FP-ASCs may indicate increased chondrogenic potency with regard to pellet GAG content.

FP-ASCs were shown to have a significantly shorter population doubling time than SF-MSCs cells over ten passages ($p=0.018$). After 48 hours of stimulation with IFN- γ , neither cell type increased positivity for the co-stimulatory markers CD40, CD80 or CD86, but both showed significantly higher levels of HLA-DR when compared to untreated controls.

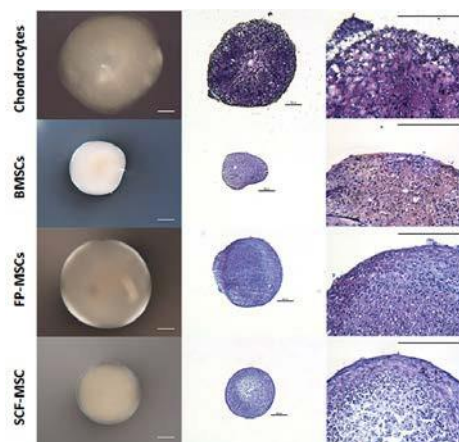


Fig. 1: Images of chondrogenic pellet sections stained with Toluidine blue. Scale bars=200 μ m

DISCUSSION & CONCLUSIONS: Taken together, our results indicate that MSCs can be isolated from bone marrow, adipose tissues and synovial fluid and that these MSCs are not themselves pro-inflammatory. However, FP-ASCs show the most promise as an alternative cell resource for autologous cartilage therapies, due to their apparent superior ability to produce GAGs in pellet culture compared to BMSCs and SC-ASCs. CD49c and CD39 are interesting markers which may be used to select subpopulations of cells with a high chondrogenic potency.

ACKNOWLEDGEMENTS: We would like to thank Arthritis Research UK (Grant Numbers 19429 and 20253) and the EPSRC Centre for Doctoral Training at Keele University for supporting this work.

Towards an allogeneic olfactory ensheathing cell line for spinal cord injury

M Georgiou¹, JD Reis¹, R Wood¹, D Li², D Choi², I Wall¹

¹ [Biochemical Engineering](#), University College London, London, UK. ² Institute of Neurology, University College London, London, UK.

INTRODUCTION: Regeneration within the central nervous system (CNS) generally does not occur. One exception is the olfactory system, where neuronal regeneration is permissive throughout life. Olfactory ensheathing cells (OECs) play a key role in guided regeneration of sensory neurons from the peripheral nervous system into the CNS, thus making them an ideal candidate for spinal cord repair. Transplantation of autologous OECs following spinal cord injury has shown promise in man [1, 2]. However, OEC yield from individual patients varies considerably and so it is not feasible to establish a robust process to generate autologous material. To overcome this, we aim to generate cell lines from OECs by genetically modifying them using the clinically approved and tested c-mycER molecular control switch [3]. Our first project aim was to define an enrichment process to obtain a high yield of OECs from primary tissue for cell line production.

METHODS: Olfactory mucosa was obtained from Sprague-Dawley rats and digested with Dispase II (45 mins) and Collagenase I (15 mins) at 37°C, 5% CO₂. Tissue digests were plated onto tissue culture plastic (TCP) for 24 hrs to remove rapidly adherent fibroblast cells and the resulting supernatant then plated in a matrix of different process conditions, including matrix, serum concentration and growth factor supplement. After 14 days cells were characterised after fixing, by labelling with antibodies for p75NTR and CD90. Next, the effect of oxygen level during culture was assessed using optimal conditions defined earlier. Finally, human mucosa material was harvested and candidate cell lines generated using c-mycER.

RESULTS: Rat tissue digests were subjected to pre-selection using differential adhesion to TCP (to remove most of the contaminating fibroblasts). After 14 days culture, immunolabelling revealed that 2% serum culture with NT-3 growth factor addition was necessary to obtain high purity and yields of OECs. OECs obtained by culturing on PDL and laminin produced distinct morphologies (Fig. 1). Analysis of oxygen effects revealed that ambient oxygen improved yield of OECs significantly compared with physiologic (2-8%) oxygen.

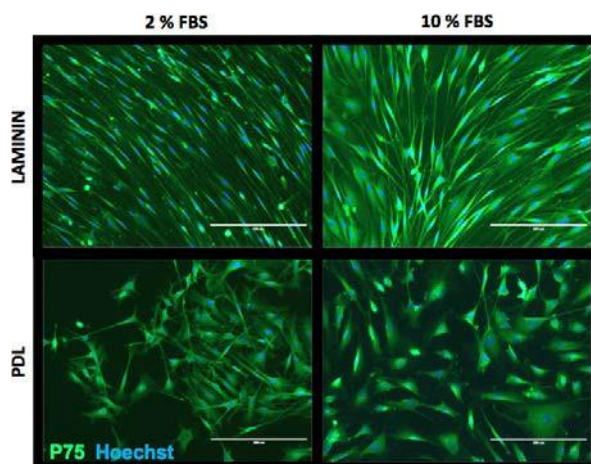


Figure 1. Fluorescent micrographs of rat mucosa-derived cell cultures at day 14 stained to detect p75NTR under different culture conditions.

DISCUSSION & CONCLUSIONS: It was hoped to define optimal process conditions using rat tissue for subsequent use to enrich human OECs, which are difficult to obtain in culture. By screening a matrix of different cell culture conditions it was possible to define a candidate set of optimal process conditions in which to enhance the yield and purity of OECs from primary tissue preparations. NT-3 was found to be critical for OEC expansion. A differential adhesion step to reduce contamination by fibroblasts further enabled enrichment. On testing the optimised process on human cells, it was not possible to obtain comparable yields and so primary populations were used to create cell lines with c-mycER. Clonal expansion and characterisation of these novel human cell lines is ongoing.

ACKNOWLEDGEMENTS: Research was funded by a BBSRC/EPSRC BRIC project grant.

Biological active compound from Green propolis for wound healing

A Giacaman¹, D Pritchard², A Cameron¹, FRJ Rose¹.

¹ [Division of Drug delivery and Tissue Engineering](#), ² [Immune Modulation Group, Division of Molecular and Cellular Science](#), School of Pharmacy, University of Nottingham, Nottingham, England

INTRODUCTION:

Wound healing is a complex and coordinated response where the skin repairs itself. The prolongation or failure of wound healing may result in a chronic wound condition. In this study, it is hypothesized that bioactive molecules, such as quercetin, rutin and artemisinic acid, isolated from green propolis may have a beneficial effect on wound healing and could be included as a bioactive molecule within a synthetic matrix to support wound closure.

METHODS:

Cytotoxicity (Alamarblue and Propidium iodide/Hoeschst staining) and migration assays were carried out using 3T3 fibroblasts, testing a range of concentrations of green propolis, quercetin, rutin and artemisinic acid solutions. Scratch assays were used as a model of wound healing; migration was monitored using time-lapse microscopy.

RESULTS:

Findings indicate that propolis does not significantly enhance fibroblast migration. Furthermore, at high concentrations (46-187 µg/mL) it significantly inhibits fibroblast migration. Cytotoxicity assays revealed a dose and dependent effect of propolis on cells. In cells treated with low doses of propolis, relative metabolic activity (%) was significantly enhanced. However, at high concentrations (46-187 µg/mL), propolis had a negative effect on cell viability. Quercetin did not show any effect on fibroblast migration at concentrations below 10 µM. However, concentrations above 30 µM inhibited cell migration and relative metabolic activity in a dose dependent manner. Rutin did not show any effect upon fibroblast migration however, it inhibited relative metabolic activity at all the tested concentrations. Finally, artemisinic acid was shown to enhance fibroblast migration after 24 h at 1 µM, whilst relative metabolic activity was inhibited at concentrations of 10 µM and above.

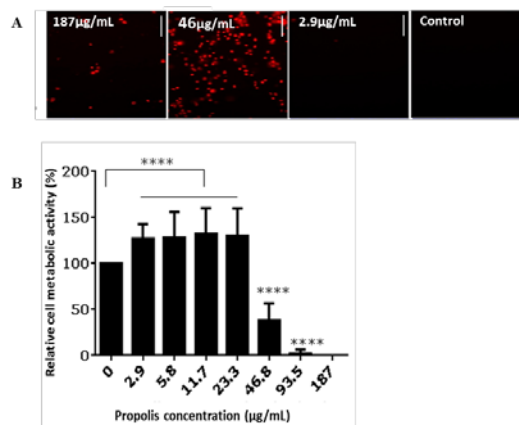


Fig. 1: (A) Dose dependent cell viability of NIH3T3 cells treated with propolis. Cells were stained with Propidium Iodide; red indicates dead cells. Magnification: $\times 20$; scale bar: 10 µm (B) Alamarblue® assay ($n=3$, mean \pm SD, **** $P \leq 0.0001$ one-way ANOVA).

DISCUSSION & CONCLUSIONS:

Findings are in agreement with previous literature suggesting that propolis has a dose, time and phenotype dependent effect¹. Propolis' capacity to influence wound healing could be associated to the presence of flavonoids which work as anti-inflammatory and antimicrobial agents². At present, no evidence has been found to establish that propolis or its compounds artemisinic acid, rutin or quercetin are able to improve wound healing by enhancing cell migration. Our results suggest that propolis may positively influence wound healing by controlling the inflammatory response and infection.

ACKNOWLEDGEMENTS: The present work has been supported by a grant from 'CONICYT'.

Bone formation at physiological doses of BMP through clay hydrogel localisation

DM Gibbs¹, CRM Black¹, G Hulsart-Bilstrom¹, ROC Oreffo¹, JI Dawson¹

¹Bone and Joint Group, Institute of Developmental Sciences, University of Southampton

INTRODUCTION: Bone Morphogenic Protein (BMP) has been used to stimulate fracture healing and spinal arthrodesis. However, difficulty in maintaining BMP activity at the target site has necessitated large supra-physiological doses with associated adverse effects. Clay (Laponite) hydrogels can bind growth factors for localised efficacy [1-2]. Our objective was to investigate if localisation of BMP by clay gels would reduce the dose required to mediate bone formation.

METHODS: Localisation of BMP-2 by clay gels was assessed *in vitro* via staining for BMP-2 induced alkaline phosphatase activity in C2C12 cells. *In vivo* 'low' (500ng) or 'super low' (40ng) doses of BMP-2 mixed in Laponite or an alginate control were applied to a collagen sponge before subcutaneous implantation in a mouse model. Micro Computed Tomography was used to assess bone formation fortnightly. At 8 weeks the mice were culled and underwent histological analysis.

RESULTS: Enhanced BMP2 induced APA ($p < 0.0001$) was localised to cells seeded upon clay gels in a BMP2 dose dependent manner. *In vivo*, only Laponite, not alginate, sustained ectopic bone formation at 'super low' doses of BMP2. Significantly greater bone volume per ng BMP was achieved with 'super low' doses of BMP2 in Laponite, compared to alginate and Laponite gels with 'low dose' BMP ($p < 0.0001$).

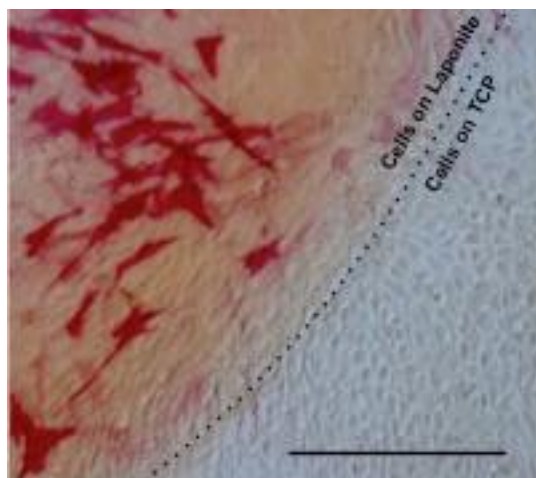


Fig. 1: Laponite gels bind BMP2 from media to locally enhance APA in C2C12 cells. Scale bar 200 μ m

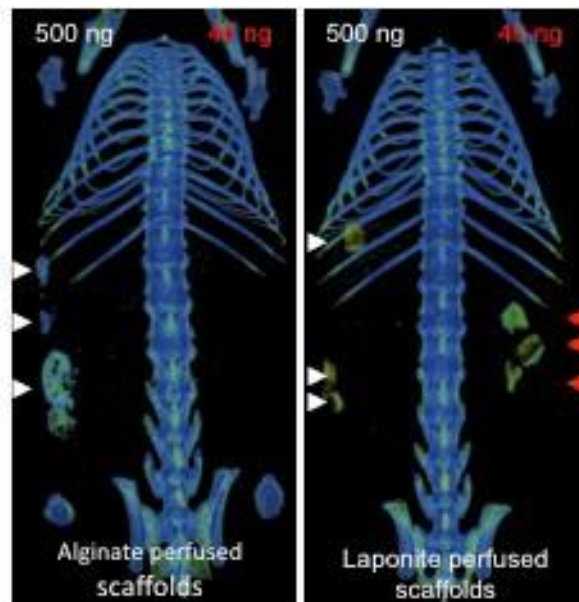


Fig. 2: Only Laponite not alginate gels sustain ectopic bone on collagen scaffolds at 40ng doses of BMP2.

DISCUSSION & CONCLUSIONS: Laponite gels are able to localise BMP2 and reduce, by several orders, the effective dose of BMP required to mediate ectopic bone formation compared to current gold standard methods of BMP delivery. Critically bone formation was observed *in vivo* at doses within range of the 10^{-4} mg/ml concentrations required for cellular responses *in vitro*. Clinical translation of this finding offers, potentially, great significance to orthopaedic surgery.

ACKNOWLEDGEMENTS: Funded by grants from EU(FP7)Biodesign, Rosetrees Trust, BBSRC and EPSRC

Cloning rings do not necessarily generate cellular clones, implications and recommendations for stem cell tissue engineering

A Glen

Department of Material Science and Engineering, The University of Sheffield, UK.

INTRODUCTION: A variety of experimental methods are reported for use in tissue engineering strategies to minimise the cellular and phenotypic heterogeneity of mixed cell populations, in particular stem cells. The goal of these procedures is to both maximise the selection of therapeutically useful cell types and minimise phenotypic variation resulting from starting heterogeneity. The most commonly used methods reporting to generate clonal cell lines include microscopically picking individual cells, cloning by limiting dilution, and the use of cloning rings. Cloning rings are cylindrical rings used to physically isolate colonies of cells for enzymatic removal and subculture. A major underlying assumption regarding the formation of colonies is that colonies are derived from a single progenitor cell and therefore fulfil the definition of clonality. Directly observing stem cell colony formation highlights the dynamic nature of stem cells and indicates that colonies isolated using cloning rings are not necessarily clonal.

METHODS: Human embryonic stem cells (H7.S6) were seeded on matrigel coated tissue culture plastic and imaged using time lapse microscopy as described¹.

RESULTS: Colonies at sizes considered to be clonal can be observed to fuse and generate progeny which can join independently forming colonies.

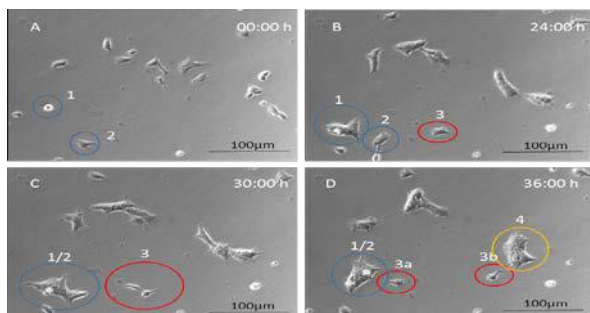


Fig. 1: Cells in A1 and A2 form small colonies (B) and merge in (C). Cell B3 forms daughters which then merge with colony 1/2 and colony 4.

DISCUSSION & CONCLUSIONS: By following the fate of individual human embryonic stem cells using time lapse microscopy it was observed that the progeny of dividing ‘clonal’ cells

and discrete colonies could join independent colonies. Whilst cloning rings are likely to reduce gross heterogeneity these observations challenge the notion reported in many published tissue engineering studies that cloning rings definitively generate clonal cell populations. This has implications not only for experimental interpretation when comparing ‘clonal’ cell populations but indicates that additional parameters need to be standardized and reported when utilizing cloning rings. These features include seeding density, colony size, distance between colonies and proliferative/locomotive rate under clonogenic conditions.

The following recommendations are therefore made:

Ideally, where possible individual cells should be microscopically picked and visually identified as individual cells and cultured in isolation from other clones.

If cloning rings are essential, such as in cases where single cell survival is poor, multiple rounds of cloning should be undertaken in order to maximize the probability of clonality.

When utilizing cloning rings the seeding density of cells and their migration rates in clonal conditions need to be carefully considered and reported in order to minimize the probability of non-clonal colonies.

Finally, it is recommend that the nomenclature regarding ‘cloning ring’ be changed to ‘colony ring’ as this is a likely source of misinterpretation relating to cloning rings definitively generating clonal cells. Current work mathematically modelling clonality is ongoing.

ACKNOWLEDGEMENTS: Prof Peter Andrews, Dr Ivana Barbaric, Dr Veronica Biga and Dr Himanshu Kaul for useful discussion.

MicroCT facilitated analysis and design of next generation nerve guide conduits

A Glen^{1*}, L Zilic¹, C Taylor¹, R Diez-Ahedo², X Bazan², F Claeysens¹, JW Haycock¹.

¹Department of Materials Science and Engineering, The University of Sheffield, UK. ²[NEURIMP consortium](#), IK4 Tekniker, Eibar, Spain.

INTRODUCTION: Peripheral nervous system injury affects 1/1000 individuals/year, with significant morbidity and socioeconomic consequences. Nerve autograft repair is the main form of treatment to bridge injury gaps, but is associated with donor site morbidity and incomplete recovery of both motor and sensory function. Nerve guide conduits, consisting of simple tubular structures manufactured from synthetic and biological materials, are emerging as comparable alternatives to autologous nerve grafts¹. Current histological and microscopy techniques used to inform the design and assess conduits suffer from destructive image processes and losses in internal *in situ* structure features which lack complete dimensionality. The aim of this work was to combine computed tomography (CT) scanning of peripheral nerves/conduits and laser based 3D structuring (microstereolithography, MSL) of polymeric photocurable resins for designing the next generation of nerve guide conduits.

METHODS: Nerve guide conduits¹ and electrospun fibres² were produced from PEG and PCL as previously described with electrospun fibres being threaded into nerve guide conduits or intra luminal channels created using a UV wire casting system. Porosity was introduced into conduits using a poragen leaching process. Porcine sciatic nerve tissue was dissected from adult Yorkshire pigs and fresh frozen or embedded in paraffin wax prior to CT imaging. MicroCT was performed on a Skyscan 1272 (Bruker, Belgium) by securing samples in a polypropylene tube and scanned at 50kV/200µA (0.7° increments over 360°). Images were reconstructed, analysed and rendered with Nrecon (v 1.6.9.8 Bruker, Belgium), CT analyzer (v 1.14.4.1 Bruker, Belgium) and CTvol (v2.2.3.0 Bruker, Belgium) or Drishti (v2.4) respectively.

RESULTS:

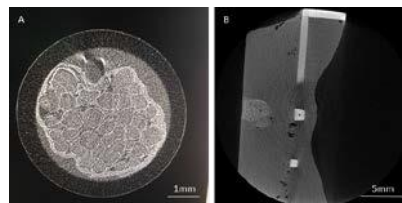


Fig 1: MicroCT imaging of fresh frozen rat sciatic nerve within a polypropylene mounting tube (A) and rat sciatic nerve tissue embedded in paraffin wax on a standard histological embedding cassette (B) identified overt microstructures without the need for exogenous contrast agents.

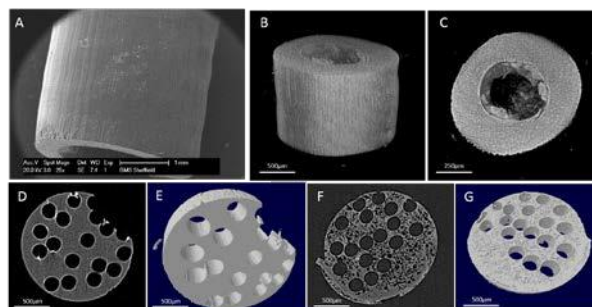


Fig. 2: Manufacture of synthetic polymeric nerve guide conduits by MSL (A, B, C) or UV casting (D, E, F, G) imaged with SEM (A) and rendered longitudinal (B) or transverse (C) microCT data with internal electrospun material and raw (D, F) or rendered (E, G) microCT data of conduits with intraluminal channels (D, E, F, G) with (F, G) or without porosity (D, E).

DISCUSSION & CONCLUSIONS: Traditionally within biomedical research microCT has predominantly been utilised for fields interested in morphometric analysis of hard tissue such as bone. MicroCT imaging enabled unperturbed and non-destructive retrieval of internal and external macrostructure from fresh, archived peripheral nerve tissue and synthetically manufactured nerve guide conduits. The use of microCT imaging represents a novel and underutilised resource in synthetic scaffold production and neural tissue engineering which can be applied to analysis of archived biological samples in other areas of soft tissue engineering, and beyond.

ACKNOWLEDGEMENTS: Funding from the European Community's Seventh Framework Programme (FP7-NMP-2013-SME-7) under grant agreement no 604450. Also thanks to Ms Holly Evans and Dr Shelly Lawson for training and access to the microCT platform respectively.

3D imaging of osteocytes using serial block-face scanning electron microscopy

P Goggin¹, KC Zygalkakis², ROC Oreffo³, P Schneider¹

¹Bioengineering Science Research Group, Faculty of Engineering and the Environment, University of Southampton (UoS), UK. ²Mathematical Sciences, Faculty of Social and Human Sciences, UoS. ³Institute of Developmental Sciences, Faculty of Medicine, UoS

INTRODUCTION: Osteocytes, the most abundant bone cells, are embedded within a hard mineralised matrix. By sensing and integrating local mechanical and chemical signals, they play a key role for bone homeostasis by regulating bone modelling and remodelling¹. Abnormalities of the osteocyte network and the encasing lacuno-canalicular network (ON&LCN) have been associated with bone diseases such as osteoporosis². Controversy remains as to how mechanical loading is transferred to osteocytes. Thus, to characterise the ON&LCN and to better understand osteocyte function through *in silico* modelling, high-resolution 3D imaging techniques for bone are urgently needed. However, high-resolution 3D examination of the ON&LCN is in its infancy³. Serial block-face scanning electron microscopy (SBF SEM) offers a promising approach. Using a remotely controlled ultramicrotome within an SEM, nanoscopic layers are removed from a tissue block, which is consecutively assessed to extract morphologies at spatial resolutions comparable to transmission EM⁴. SBF SEM can cover large fields of view (~1mm²) and provides imaging contrast for soft and hard tissues simultaneously, such as the ON and the LCN, respectively. This study adapts and extends SBF SEM to assess the ON&LCN.

METHODS: A 2mm³ block from a 10-week-old C57BL/6 mouse tibia was fixed, decalcified and prepared using a modified 'Ellisman' protocol⁵ permeating the tissue with heavy metals, providing electrical conductivity and contrast. A 100µm² area containing several osteocytes was chosen. The block was trimmed and the surface metal coated to further enhance conductivity and reduce charging. The 3View[®] system of Gatan Inc. (Pleasanton, USA) within an FEI Quanta 250 FEG-SEM was used to produce a stack of 600 images at 2.5kV, spot size 3, slice thickness 50nm and vacuum 40Pa. A median filter was applied to reduce noise and Reconstruct⁶ was employed to trace the surfaces of the ON&LCN semi-automatically.

RESULTS: Figure 1 shows a SBF SEM slice and corresponding 3D reconstructions. The ON was clearly resolved, along with the pericellular space and the bone matrix.

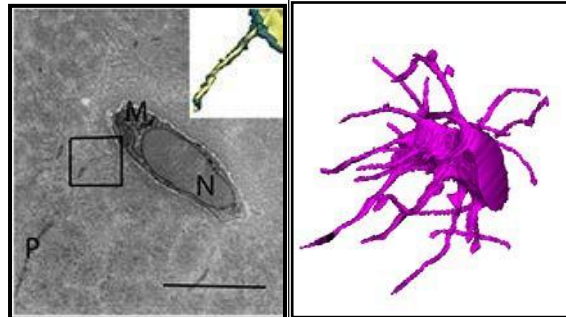


Fig. 1: (Left) SBF SEM slice showing an osteocyte including its nucleus (N), mitochondria (M), cell processes (P) and decalcified bone matrix (scale bar = 2µm). The inset shows cell process (yellow) and the pericellular space (green). (Right): Osteocyte derived from 250 SBF SEM sections.

DISCUSSION: SBF SEM can produce high-resolution 3D images of the ON&LCN and offers automation of sectioning and imaging. Complex sample preparation has to be noted, along with the destructive nature of this emerging method. Importantly, SBF SEM allows for simultaneous imaging of the ON and LCN (soft and hard tissue). SBF SEM will enable the quantitative assessment of healthy and diseased bone on a cellular and sub-cellular level. ON&LCN models based on experimental 3D data will allow for more realistic computational modelling in bone mechanobiology. SBF SEM will enhance our understanding of the osteocyte's role in bone health, development and pathology, helping to identify new targets for the diagnosis and treatment of bone diseases.

Graded organisation of fibronectin on polymer surfaces to tune cell response

E Grigoriou¹, M Cantini¹, M J Dalby², M Salmeron-Sanchez¹

¹ Division of Biomedical Engineering, School of Engineering, University of Glasgow. ² Centre for Cell Engineering, Institute for Molecular, Cell and Systems Biology, University of Glasgow

INTRODUCTION: Cell behaviour is largely controlled by mechanochemical cues coming from the extracellular matrix (ECM). Fibronectin (FN), a major component of the ECM, binds to cell receptors and other ECM proteins and therefore plays a prominent role in regulating cell fate. Exploring biomaterial-cell interactions is an effective way to elucidate ECM-cell interactions and to engineer materials mimicking cell natural environment. The chemical composition of biomaterials surfaces can alter the conformation of adsorbed proteins which subsequently affect cell response¹. We are interested in investigating how biomaterial surfaces with well-defined chemistries elicit specific responses of human mesenchymal stem cells (hMSCs) such as adhesion, differentiation and migration.

METHODS: Copolymers with controlled ratios of PMA and PEA were used: 100/0, 70/30, 50/50, 30/70, 0/100. Surfaces and FN adsorption were characterised by water contact angle (WCA), AFM imaging and immunostaining. ELISAs were also carried out using monoclonal antibodies against the integrin binding domain of FN. A short attachment assay was carried out in which hMSCs were seeded at a high density on FN coated samples. After initial attachment for 20 min, cells were counted by staining the nuclei. Cells adhesion was further explored by analysing the formation of focal adhesions (FAs) after 3 hours and 1 day. Cells were stained against vinculin and images were analysed to determine size distribution.

RESULTS: WCA measurements show that hysteresis of the samples is higher after FN adsorption on material surfaces, which indicates that samples become more hydrophilic. AFM images demonstrate that FN forms fibrillar networks on PEA which are distributed at increasing concentrations of PMA, finally forming globular aggregates on PMA (Fig.1). These copolymers are a way to control the degree of organization of fibronectin on material surfaces – from interconnected nanonetworks on PEA to globular aggregates on PMA.

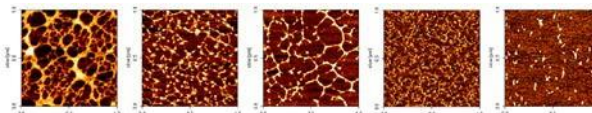


Fig. 1: Phase AFM images of FN distribution on spin coated samples. The size of the images is $1 \times 1 \mu\text{m}^2$.

ELISAs show the differential availability of the integrin binding domain upon adsorption of FN on the polymer surfaces. Focal adhesions are well formed on all surfaces. Area and length distributions of FAs were quantified by analyzing fluorescent images (Fig.2).

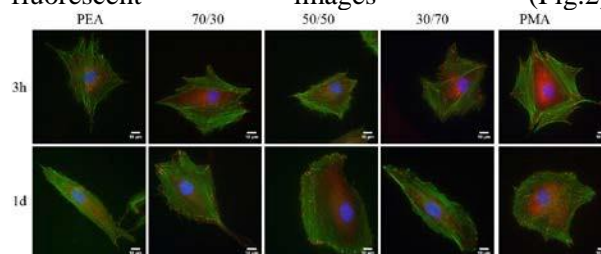


Fig. 2. Cell adhesion of hMSCs on protein coated samples 3h and 1d after seeding. Fluorescent staining of focal adhesions (red), actin cytoskeleton (green) and nuclei (blue).

DISCUSSION & CONCLUSIONS: This work aims at deciphering how surface-dependent FN organisation can influence cell-biomaterial interactions in general and stem cell differentiation in particular. A graded organisation of FN is obtained upon adsorption on p(MA-co-EA) copolymers. The family of surfaces promote cell attachment and focal adhesion formation, and might trigger different cell response in terms of, e.g, differentiation and migration.

ACKNOWLEDGEMENTS: The support from ECR through HealInSynergy 306990 is acknowledged.

Towards an *in vitro* stem cell niche using surface chemistry and mesenchymal stem cells

RB Gurden^{1,2}, P Sweeten^{1,2}, LA Turner¹, CC Berry¹, M Salmeron-Sanchez², ROC Oreffo³, MJ Dalby¹

¹ [Centre for Cell Engineering](#), Institute of Molecular, Cell, and Systems Biology, University of Glasgow, UK ² [Microenvironments for Medicine](#), School of Engineering, University of Glasgow, UK ³ [Bone and Joint Research Group](#), Institute of Developmental Sciences, University of Southampton, UK

INTRODUCTION: Control of stem cell fate and function is critical for clinical and academic work, for example manipulation of mesenchymal stem cell (MSC) phenotype *in vitro* to provide conditions to best study the cells. We use surface chemistry-driven extracellular matrix assembly to build an *in vitro* MSC niche designed to control MSC phenotype. The distribution of the ECM glycoprotein fibronectin (Fn) is different when adsorbed onto poly(methylacrylate) (PMA) compared to poly(ethylacrylate) (PEA), where it has been reported to form globular aggregates or physiological fibrillar networks, respectively [1]. It has previously been shown that the conformation of this Fn layer impacts cell behaviours, including osteoblastic differentiation of MSCs in 2D [1]. Here, we test how absorption of growth factors (BMP2 and VEGF) to the synergistic adhesion/growth factor binding site of Fn effect MSCs. Furthermore, we move our niche into 3D. In this study we look at a range of niche-behaviour related proteins (phenotype-related, chemokine / cytokine related and stem cell maintenance related).

METHODS: Toluene-dissolved PMA and PEA were spin coated onto glass coverslips before solvent extraction *in vacuo* and UV sterilisation. 20 mg/ml human plasma Fn was adsorbed onto the surfaces followed by 25 ng/ml recombinant human VEGF and BMP2. Fn conformations were characterised by atomic force microscopy (AFM). For 3D systems, a collagen hydrogel was placed above the substrate. Adult human bone marrow STRO-1+ MSCs were cultured on substrates (with and without growth factors) for 3 weeks in supplemented DMEM. Expression of MSC multipotency and stem cell maintenance factors were analysed by immunofluorescence microscopy or in-cell western assay.

RESULTS: To establish the best combination of polymer, Fn distribution and GF, expression of MSC multipotency (ALCAM and NESTIN) and stem cell maintenance (SCF and VCAM1) factors were measured. In the 2D environments, in-cell western analysis (Fig. 1) showed that expression of

VCAM1 and SCF was increased on all substrates compared to glass, and ALCAM was also increased on all substrates except PEA with Fn compared to glass. NESTIN expression was reduced on all substrates compared to glass. Immunostaining highlighted that SCF was expressed across all conditions in 3D. (Fig. 2).

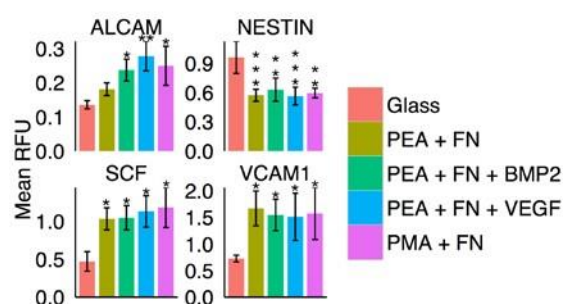


Fig. 1: Expression of multipotency and stem cell maintenance proteins by MSCs cultured on substrates; quantified using in-cell western. Error bars are standard deviation, asterisks show significance compared to glass (* $p < 0.05$, ** $p < 0.01$, *** $p < 0.001$). RFU = relative fluorescence units; fluorescence normalised to cell number.

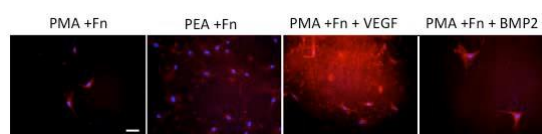


Fig. 2: Fluorescence images showing SCF expression in 3D cultures.

DISCUSSION & CONCLUSIONS: Initial results show that the Fn distributions induce the expression of multipotency and stem cell maintenance factors by MSCs in both 2D and 3D.

ACKNOWLEDGEMENTS: Julia Wells kindly provided MSCs. Funding for PhDs for RG and PS awarded from BBSRC and EPSRC. LAT supported by BBSRC BB/K011235/1 and MSS and MJD supported by MRC MR/L022710/1.

Three dimensional printing of hydrogels, growth factors and mammalian cells to create a biomimetic environment for nervous tissue formation *in vitro*

OA Hamid, J Yang, HM Eltahir, KM Shakesheff

Drug delivery and tissue engineering division, School of Pharmacy, University of Nottingham

INTRODUCTION: Recapitulating the complex conditions that lead spinal neurons formation could provide a promising approach for generating nervous tissue grafts *in vitro*. These conditions are mainly represented by the molecular gradient of growth factors which are responsible for neuronal differentiation during neural tube development [1]. Recent advances in three dimensional (3D) printing technology offer an interesting opportunity for the replication of the intrinsic complexity of native tissues *in vitro* by precise positioning of multiple cell types, hydrogels and bioactive molecules [2]. However, 3D printing of a model simulating the complex conditions that lead to spinal cord neurons development has many challenges including fabrication of a hydrogel tubular structure with clinically relevant size, the spatial delivering of bio-active molecules to generate concentration gradient and preserving cell viability during the printing process.

The aim of this research is to develop a 3D hydrogel tubular model with a controlled molecular gradient using 3D printing. In addition, the impact of 3D printing process on cell viability is characterized.

METHODS: An extrusion based multi-head 3D printer (Regen HU, Switzerland) was used for 3D printing a hollow tubular construct from polycaprolactone (PCL, MWT 45 kDa; Sigma-Aldrich, UK) and semi-cross linked alginate hydrogel (1.5%) (FMC BioPolymer, Ireland). The scaffold consisted of two concentric cylinders of PCL (12 and 8 mm in diameter) with alginate filling the annulus space. A concentration gradient of fluorescein isothiocyanate-labelled albumin (FITC-BSA), as a model, was printed in the annulus. The hydrogel annulus was printed using two printing heads, one for FITC-BSA-mixed alginate gel and the other for alginate gel. The gradient was created by gradual reduction in the number of the layers that contain FITC-BSA as a function of tube distance; consequently, the diffusion between layers will generate the gradient. The gradient was quantified as a function of tube distance by sectioning the tube into segments followed by fluorescent intensity assay. In addition, the effect of printing nozzle's internal diameter on mammalian cell (3T3) viability was examined using live/dead assay.

RESULTS:

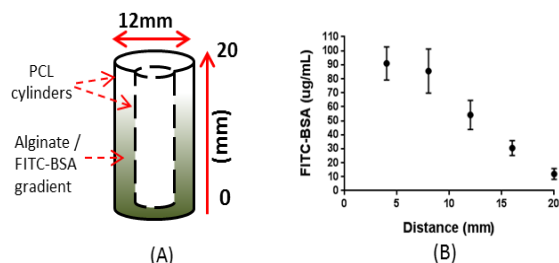


Fig. 1: (A) Schematic diagram of the hollow PCL-alginate gel tubular construct with gradient of FITC-BSA (green colour); (B) Concentration of FITC-BSA as a function of tube distance.

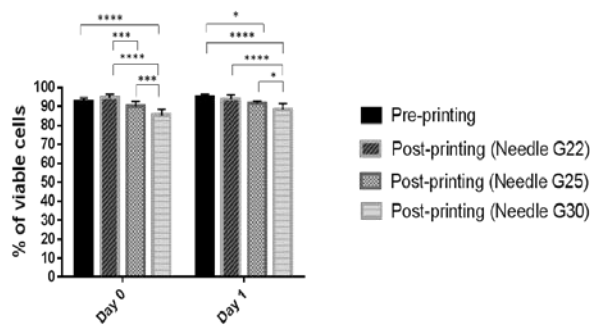


Fig. 2: Pre and post printing 3T3 cell viability.

DISCUSSION & CONCLUSIONS: Multi-head 3D printer provided an opportunity to fabricate a mechanically stable PCL-hydrogel tubular structure with a controlled molecular gradient. In addition, 3D printing process showed a limited negative effect on cell viability. This *in vitro* 3D model will help to improve the understanding of neuronal cells development for nerve regenerative applications.

ACKNOWLEDGEMENTS: this work was sponsored by the higher committee for education development in Iraq.

Isolation of colonic smooth muscle cells from neonatal rats: Can ultrasound induce contractions?

X He¹, SE Thomson¹, AL Bernassau², SJ Moug³, MO Riehle¹

¹ [Centre for Cell Engineering](#), Institute of Molecular Cell and Systems Biology, University of Glasgow, UK. ² [School of Engineering & Physical Sciences](#), Herriot Watt University, Edinburgh, UK. ³ [Royal Alexandra Hospital Paisley](#), UK.

INTRODUCTION: To investigate if colonic smooth muscle cells (CSMC) could be stimulated to contract by medical ultrasound. The motivation is to improve patients' recovery from ileus after abdominal surgery. A technique to isolate CSMC from neonatal rat pups was established in the lab, and these used to examine how the contractility of CSMC could be monitored on a deformable polyacrylamide substrate (1) by ultrasound (US).

METHODS: By using microsurgery and trypsin digestion it was possible to reliably isolate and culture CSMC using a method substantially modified from Batista *et al.* (2). The CSMC were identified by morphology, the presence of smooth muscle α -actin by immunofluorescence staining, and sensitivity to acetylcholine induced contraction. The CSMC were subsequently treated with 4MHz US at three different amplitudes (2, 5, 10V peak-peak), to evaluate if US could stimulate contraction.

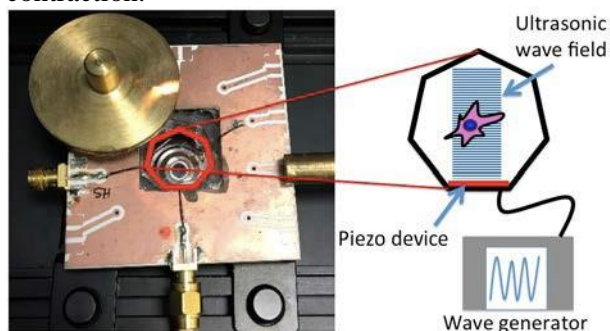


Fig. 1: US exposure of CSMC. The heptagon shaped US device (3) linked by a wave generator was placed over the cultured cells. Heptagon outlined in red, the centre of the objective was where cells were observed, sitting in the middle of the US beam (5 mm wide).

RESULTS: The CSMC in culture had a typical spindle shape and reached confluence within 10-12 days. Immunofluorescence showed that 87% of cells were positive for smooth muscle α -actin. Acetylcholine (5.5 μ M) leads to a contraction of the isolated cells, confirming SMC status. Applying US to CSMC resulted in contraction of 4 out of 5 cells tested. There was an indication that the intensity of the US modulated the response (Figure

2).

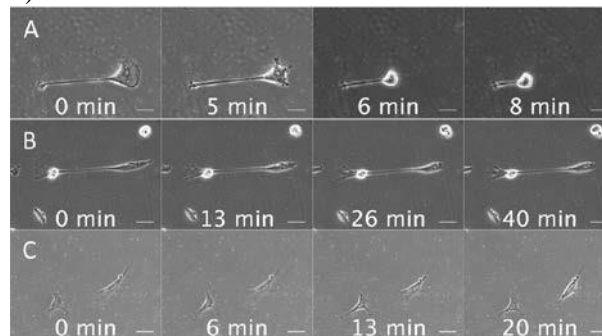


Fig. 2: CSMC stimulated to contract by 4MHz ultrasound. (A) The cells contracts continuously until it is completely rounded up. (2 Vpp) (20x). (B) Two individual CSMC linked to each other contract, the left one toward the middle; whereas the right large one contracts and visibility tenses up. (5 Vpp) (20x). (C) The left cell does not respond, whereas the right cell does contract (10 Vpp) (20x). Scale bar, 50 μ m.

DISCUSSION & CONCLUSIONS: The most significant finding in this study is that US can induce contraction of CSMC. As the frequency tested is in the range of medical ultrasound, this could be translated into clinical use.

ACKNOWLEDGEMENTS: XH would like to thank the people at CCE for their help & support.

Remotely controlled mechanotransduction via magnetic nanoparticles: applications for injectable cell therapies.

JR Henstock¹, M Rotherham¹, AJ El Haj¹

¹[Institute for Science and Technology in Medicine, University of Keele, UK](#)

INTRODUCTION: Bone requires dynamic mechanical stimulation to form and maintain functional tissue, yet mechanical stimuli are often lacking in many therapeutic approaches for bone regeneration. Magnetic nanoparticles provide a method for delivering these stimuli by directly targeting cell-surface mechanosensors and transducing forces from an external magnetic field, resulting in remotely controllable mechanotransduction. In this investigation, functionalised magnetic nanoparticles were attached to the mechanically-gated TREK-1 K⁺ channels of human mesenchymal stem cells. These cells were microinjected into an *ex vivo* chick foetal femur (e11) as a model for endochondral bone formation¹. An oscillating 25mT magnetic field was used to induce mechanotransduction in the injected MSCs *via* the nanoparticles. Further analysis was performed *in vitro* in both monolayer and 3D hydrogel cultures.

METHODS: Human MSCs labelled with TREK1-antibody-conjugated magnetic nano-particles were seeded into collagen hydrogels and cultured in an osteogenic media for 28 days. An oscillating magnetic field was applied for 1 hour per day to remotely activate TREK-1 signalling.

RESULTS: Control hMSCs did not significantly mineralise the hydrogel construct, whereas hMSCs labelled with nanoparticles showed significant increases in extracellular matrix production and mineralisation (*fig. 1*). Repeating these experiments with exogenous BMP2 (released from microparticle carriers) demonstrated a synergistic increase in bone formation over either nanoparticles or growth factors alone.

DISCUSSION & CONCLUSIONS: In these experiments we demonstrated the effectiveness of targeting the TREK1 ion channel to remotely activate mechanotransduction and promote osteogenesis in tissue engineered scaffolds. By targeting mechanotransduction as a synergistic therapy, we have demonstrated that these combination approaches (stem cells, growth factors, biomaterials and cell biomechanics) are a valid method for optimising cell-based therapies for clinical applications.

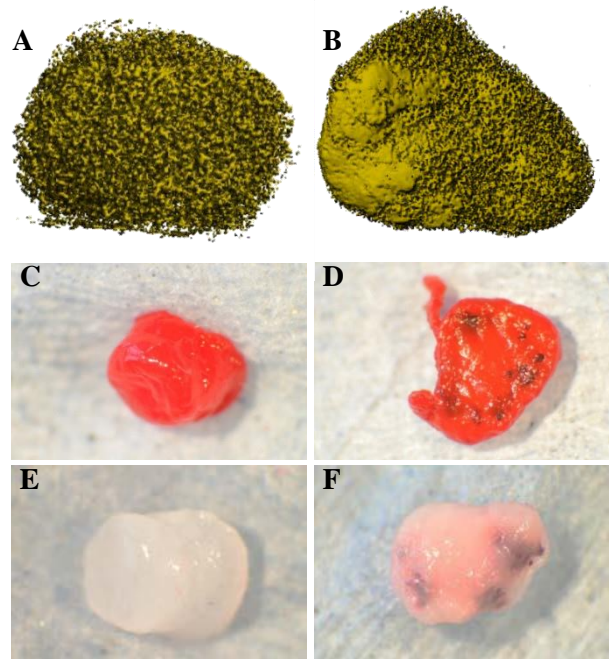


Fig. 1: Tissue engineered collagen hydrogels containing hMSCs (left) and hMSCs labelled with magnetic nanoparticles (right). Remote activation of the mechanosensitive ion channel TREK1 by nanoparticles resulted in substantial formation of mineralised extracellular matrix, quantified by μ CT (3D reconstruction of internal mineralisation, A & B), collagen staining (C & D) and Calcium staining (E & F).

FURTHER WORK: Following validation of the nanoparticles-based approach, this technique is now being trailed in a pre-clinical large animal model (sheep) for treatment of a bone critical-sized defect

ACKNOWLEDGEMENTS: This work was supported by the BBSRC (sLoLa grant). We would like to thank our collaborators in groups led by Prof. Richard Oreffo, Prof. Kevin Shakesheff and Prof. Molly Stevens for their contributions to this project.

Screening growth factor loading capacity of distinct biomaterials using a high-throughput *ex vivo* avian model

SG Hulsart Billström¹, S Inglis¹, ROC. Oreffo¹

¹*Bone and Joint Research Group, Centre for Human Development Stem Cells and Regeneration, Institute of Developmental Sciences, University of Southampton, UK,*

INTRODUCTION: Biomaterials research generates a plethora of novel materials, with the ultimate aim of application in the reparation and replacement of damaged tissue. The biocompatibility and functionality of these materials requires careful analysis. We have developed and applied a high-throughput screening model as a replacement and reduction for in vivo model evaluation. The current study has examined using a high throughput *ex vivo* model the BMP-2 loading capacity of three pre-formed hard materials. The study examined the BMP-2 loading capacity of a poly lactic glycolic acid (PLGA), a calcium phosphate cement (CaP) and a pegylated fibrinogen (PEGF), using an *ex vivo* chick femoral defect cultured on the chick embryo chorioallantoic membrane (CAM) in ovo.

METHODS: The chick femoral CAM model¹ was utilized to assess the BMP-2 loading capacity of various biomaterials. The biomaterials were soaked in 10 μ l of PBS with and without BMP-2 (2 ng/implant) after which materials were implanted into 1 mm drill defects in chick femurs previously explanted from E 18 chicks. The femurs were scanned in a Skyscan 1176 prior to CAM culture using the following settings: source voltage: 45 kVp; current: 556 μ A; filter: Al 0.2 mm; exposure time: 94 ms; frame averaging: 1; rotation step: 0.74. The chick femurs were harvested after 8 days and bone forming potential assessed using μ CT using the same settings. The software NRecon was used for reconstruction with correction for misalignment, ring artefacts and beam hardening. The biomaterials were evaluated with pre-scans as controls for the post-scans, thereby assessing the bone forming capacity of each individual material in the presence and absence of growth factor. The data were analysed using Otsu-thresholding in CTAn and 3D co-registration in DataViewer. The differences between pre and post scan were visualized in CTVol and CTvox (SkyScan and Bruker, Kontich, Belgium). The femurs were paraffin embedded, sectioned and stained with Alcian blue/Sirius red (A/S) to confirm CT data histologically.

RESULTS: All the biomaterials examined displayed excellent biocompatibility with good cell infiltration. The PEGF was the only material that showed a significant difference in bone volume after 8 days of CAM culture (Figure 1). Gross examination showed CAM integration of all the biomaterials and histology revealed cells infiltrating the biomaterial where remnants of the biomaterial remained visible.

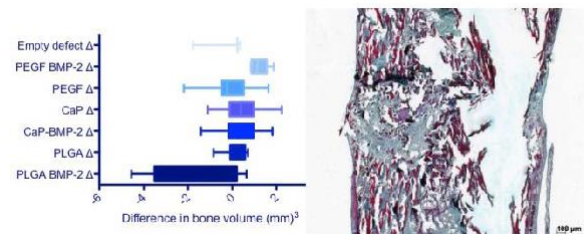


Fig. 1(left) Variation in bone volume between pre and post-CAM culture at 8 days (mean \pm min/max whiskers). Three pre-formed materials were evaluated; biomaterials were soaked with and without BMP-2 and implanted into drill defects in E18 chick femurs and analysed pre and post CAM via μ CT; (right) A/S staining of E18 femoral drill defect with PEGF.

DISCUSSION & CONCLUSIONS: The current studies indicate the potential of the chick femur defect CAM model to i) serve as a high-throughput screen for biomaterials and engineered constructs, ii) evaluate biomaterial compatibility and, iii) to assess the bone forming potential of an implanted construct within the defect. The current model, in combination with μ CT, provides a visualization of the bone tissue response. The current work has enabled the evaluation of a range of BMP-2 loaded pre-formed biomaterials.

ACKNOWLEDGEMENTS: We acknowledge the provision of materials from members of EU Biodesign – without whom this work would not have been possible (Jöns Hilborn, Alicia El Haj, Martin Stoddart, Dror Seliktar, Håkan Engqvist, Mathias Lutolf).

3D Human bone marrow and endothelial cell pellets induce osseointegration and differentiation in organ cultures of E18 chick femur drill defects

[S Inglis](#)¹, [JM Kanczler](#)¹, [SG Hulsart Billström](#)¹, [ROC Oreffo](#)¹

¹

Bone and Joint Research Group, Centre for Human Development, Stem Cells and Regeneration, Institute of Developmental Sciences, University of Southampton, UK.

INTRODUCTION: 3-dimensional pellet cultures of skeletal cells offer a beneficial tool to further examine in-vitro bone formation¹ enhancing information typically drawn from 2-dimensional co-culture studies. We have developed an ex vivo model using staged (E18) embryonic chick femurs with precision drill defects that allow the examination of the regenerative capacity of 3D pellet constructs. In the current study, we have investigated 3D co-culture pellets of human bone marrow cells (HBMC) and human umbilical vein endothelial cells (HUVEC) to ascertain the potential of HBMC-endothelial co-cultures to drive bone formation and the interactions and temporal cues for bone repair and regeneration therein.

METHODS: HBMCs and HUVECs were pelleted and examined at a 1:1 ratio. Controls of mono-cell pellets of HUVECs and HBMCs were run in parallel to the co-culture pellets. After 48 hrs of incubation, pellets were placed within 1mm drill-hole defect created in the centre of the diaphysis of E18 chick femurs. Femurs were maintained in an organotypic culture for a period of 10 days after which samples were assessed for osteogenesis using a micro CT scanner. Femurs were subsequently processed for histological analysis for the presence of collagen and proteoglycan production using Alcian blue/Sirius red (A/S) staining. Tissue calcification was assessed using von Kossa staining and the presence of Type-I and Type-II collagen antigen was confirmed using immunostaining.

RESULTS: Histological analysis revealed good integration and fusion of pellets into the bone defects. This was particularly evident in the co-culture pellets. In contrast, migratory activity into the surrounding tissue was visible in defects containing HUVEC or HBMC pellets alone. A/S staining of the femurs revealed extensive collagen staining (Fig.1). This was confirmed by Type I collagen immunocytochemistry, which was particularly pronounced in the tissue surrounding the defect as well as Type-II collagen which was observed within the pellets and noted to extend into the surrounding tissue. Co-culture pellet constructs within the drill defect femurs showed

extensive areas of calcification, evident by von Kossa staining. Interestingly, we observed extensive Type II collagen expression in HUVEC-pellet femurs. Micro CT analysis revealed increases in Bone Volume (BV) and Bone Volume to Tissue Volume (BV/TV) ratio in HUVEC and HBMC treatment groups. Surprisingly the greatest increase was evident in BV and BV/TV was detected in the femurs with HUVEC-pellets alone. BV at D10: HUVEC 2.5±0.25, HBMC 2.3±0.23, CO 2.05±0.24, CTRL 1.7±0.07.

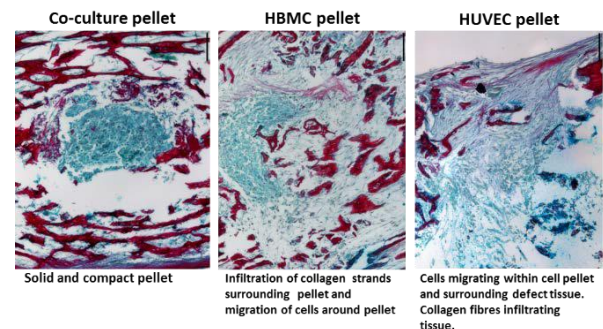


Fig. 1: A/S staining of E18 chick femur drill defects with implanted co-culture and mono-cell pellets.

DISCUSSION & CONCLUSIONS: Extensive cell integration of the pellet within the defect was observed in this 3D organotypic model. Bone formation was observed in HUVEC pellet constructs, indicating the importance of endothelial cells within this model. In contrast, enhanced cell migration was observed in HUVEC or HBM pellet only constructs. Co-culture samples displayed enhanced integration and were observed to be compact in structure. Dissection and understanding of the component cell interactions and the role of exogenous factors in driving the osteogenic process observed in this defect model will provide the potential information to successfully regenerate bone in conjunction with neo-vascularisation in clinical orthopaedic related bone loss.

ACKNOWLEDGEMENTS: The authors would like to thank EU FP7 (BIODESIGN) for funding this research.

Association of Wnt3A growth factor with PEGylated liposomes for bone tissue regeneration

[AA Janeczek](#)¹, [MH Horrocks](#)³, [RS Tare](#)¹, [E Scarpa](#)¹, [TA Newman](#)², [ROC Oreffo](#)¹, [SF Lee](#)³, [ND Evans](#)¹

¹Bone and Joint Research Group, Centre for Human Development, Stem Cells and Regeneration, University of Southampton, UK; ²Clinical Neuroscience, University of Southampton, UK;

³Chemistry Department, University of Cambridge, UK

INTRODUCTION: With more than 3.5 million osteoporotic bone fractures each year at an EU cost of ~€37 billion/pa there is a strong demand for therapies that enhance bone regeneration. The currently available treatments are insufficient and often cause side-effects. As Wnt signalling has been implicated in the regulation of mesenchymal stem cells (MSCs) and osteoprogenitors¹, responsible for bone healing, we are proposing to deliver Wnt growth factor specifically to MSCs to enhance bone regeneration. To ensure safety and efficacy of our approach through spatiotemporal delivery, we entrapped the hydrophobic Wnt in nanoparticles, such as liposomes², which may be preferentially retained at the bone fracture site.

METHODS: We fabricated 100 nm stealth (5 mol% PEGylated) DMPC and DOPC liposomes via extrusion. Following incubation with Wnt3A protein (2 µg of protein per ~10¹³ liposome particles), the preparations were ultracentrifuged at different time points, and the pellets and supernatants analysed for protein presence (Western blot and protein quantification) and activity (luciferase assays) to calculate loading efficiency and retention. To characterise Wnt association with liposomes, we fluorescently tagged the protein and incorporated it within dye-labelled liposomes, after which we studied them at a single molecule spectroscopy level with the use of TIRFM and TCCD techniques. All statistical analysis was conducted using GraphPad Prism software with significance set at p<0.05.

RESULTS: Incubation of Wnt with different formulations of liposomes resulted in association of majority of the protein with the nanocarriers (Figure 1A). Encapsulation in PEGylated DOPC lipid-based nanoparticles enhanced Wnt protein activity (131 ± 3% p<0.001 vs. neat Wnt3A protein, n = 3) (Figure 1B). The degree of association of Wnt with liposomes measured at a single molecule level was 10x higher (n = 3) than that of a control protein (Figure 1C).

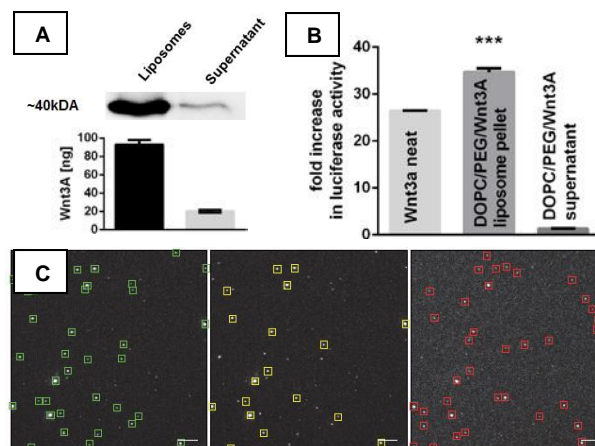


Fig. 1: WB and protein quantification (A) for Wnt protein in liposomal pellet and supernatant after Wnt incorporation and its *in vitro* activity (B). TIRFM images (C) of DiO-labelled liposomes (left) and Atto680-labelled Wnt (right). 24% of the spots were coincident (centre) after 5 min incubation. Scale bars are 5µm.

DISCUSSION & CONCLUSIONS: Due to its hydrophobicity, liposomal encapsulation of Wnt3A is advantageous for the stability and hence efficiency of the protein. Wnt preferentially associates with lipid carriers and the association in PEGylated formulations is stable. Forthcoming *in vivo* data will provide evidence of the safety, efficacy and selectivity of liposome-encapsulated Wnt for bone regeneration purposes.

ACKNOWLEDGEMENTS: We acknowledge the support of MRC. AAJ was the recipient of a Barbara Mawer Travel Fellowship from the BRS and TCES Short Scientific Mission Award to enable biophysical measurements of liposomes.

Muscle organoid standardization: an *in vitro* 3-D study

JM Jones¹, DJ Player², NRW Martin², R Brown¹, MP Lewis², V Mudera¹

¹*Institute of Orthopedics and Musculoskeletal Science, University College London.*

²*School of Sport, Exercise and Health Sciences, Loughborough University.*

INTRODUCTION:

3Rs of research (replace, reduce, refinement) are the driving force behind the use of our revised muscle model. Cellular attachment is fundamental to cell viability. Previous models reported have often-required use of customary tools in order to achieve expected outcomes.^[1,2] We are focusing on optimization cellular attachment to enable quicker production of a mature muscle tissue 3D construct for testing. We now report a comparative view between our previously reported custom designed model^[1] and our revised organoid model constructed from standard lab equipment. The use of our revised model is one that has the potential to be a high throughout model for testing of novel biomaterials.

METHODS:

Neutralized 3D collagen hydrogel constructs 85% Type I collagen (2.05 mg/mL), 10x MEM, were seeded with C2C12 mouse myoblasts at 4 million cells/ml. Cells passage between 2-20, in 20% FCS high glucose DMEM. Comparative models; custom designed cuboidal model^[1], 30mm x 1.4mm x 1mm; revised model 48 well-plates, 11.0mm x 5mm. This study was scaled down to reduce resources, whilst maintaining basic tethering by creating lines of longitudinal isometric tension using custom polythene mesh floatation bars. The round multi well plate had stainless steel staple posts fixed (Superglue & silicone) to bottom. Observations of early cellular attachment constructs over the first 28 hours post seeded (at timed intervals 0, 2, 4, 8, 22, 28). Images taken under calcein and ethidium homodimer staining at 0hrs, 22hrs, 28hrs.

RESULTS:

In the revised model samples were tested tethered and untethered gels. All measurements were taken over the time course (tethered data reported). Cellular contraction within hydrogel of revised model sees wastage of construct ~58.2% reduction from original size in post gels. At 0 hours cells are live, but by end of 28 hours period fluorescence staining shows there was a significant decrease in cell viability within the revised model (fig.2).



Fig1. Time-lapse image: 48well-plate bottom showing seeded hydrogel contraction over 28hours.

However, pH test showed constant readings between 8.0-6.5 over 12hrs, before media change. Measurements: cell roundness, area, and perimeter, are preliminary methods of quantifying cellular attachment. Preliminary results: Cell roundness decreases over time, as cells attach (post and no post gels). Bimodal distribution at 22hrs accounts for dead (round) cells (Mann-Whitney U test P=0.007).

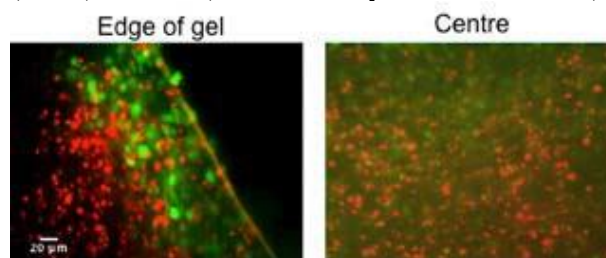


Fig. 2: Live Dead Staining (48-well plate) two fixed posts tethered samples 28hrs. Live cells (calcein-Green) & dead cells & (ethidium homodimer-red).

DISCUSSION & CONCLUSIONS:

Perfusion & media turn-over time is a limitation of the revised model. Custom designed model had faster cellular attachment at 4hrs, with directional cellular projections along the longitudinal lines of tension, but visualized contraction (wasting) of hydrogel was not observed until days 5-7^[1] The revised model un/tethered gels, cellular viability was significantly decreased compared to the custom designed model.^[2] Our revised model offers a rapid contraction and deformation of construct, cellular attachment and alignment in a bid for faster muscle maturity.

ACKNOWLEDGEMENTS: E.U. Framework 7 BIODESIGN programme for providing financial support to this project.

Assessment of aggrecanase- and MMP-driven cartilage degradation following MSC treatment for Rheumatoid Arthritis.

AG Kay¹, S Parida¹, A Stefan¹, L Rump¹, J Middleton², O Kehoe¹

¹Keele University, ISTM at RJA Orthopaedic Hospital, Oswestry, Shropshire, UK ²University of Bristol, Faculty of Medicine and Dentistry, Bristol, UK

INTRODUCTION: Rheumatoid arthritis (RA) is a debilitating and painful disorder affecting more than 400,000 people in the UK. Recent advances using biologic drugs have had significant impact on the treatment of RA patients although many patients do not respond and 50% discontinue the drug after 2 years. Mesenchymal stem cells (MSCs) possess anti-inflammatory and immunosuppressive properties which could function as a therapy in RA¹. Cartilage degradation occurs in RA due to catabolic enzymes: a disintegrin and metalloproteinase with thrombospondin motif 5 (ADAMTS5) in early stage; and matrix metalloproteinases (MMP) during late stage degradation.

Monoclonal neopeptide antibodies allow specific C terminus cleavage sites for Aggrecanase-driven (NITEGE373↓374ARGSV) or MMP-driven (DIPEN341↓342FFGVG) cartilage degradation².

METHODS: Animals with Antigen Induced Arthritis were treated with a single intra-articular injection of 5.0×10^5 murine mesenchymal stem cells (mMSCs) and knee joints were retrieved at 3, 7 and 14 days post-arthritis induction³. Contralateral joints without therapeutic injection represented controls. Joints were dissected and processed for immunohistochemical staining for the presence of NITEGE and DIPEN neopeptides (Figure 1). Quantitative assessment was achieved through calculation of percentage cells displaying extracellular neopeptide staining in cartilage matrix⁴.

RESULTS: Significant reductions in NITEGE neopeptide at 3 days post treatment and in DIPEN 7 days post treatment were seen in MSC treated mice compared to AIA untreated controls ($p < 0.05$, student's t-test). No differences were found between time points for NITEGE or DIPEN individually although there was a trend in controls for reductions in neopeptide detection; and greater DIPEN detection in comparison to NITEGE at each time point.

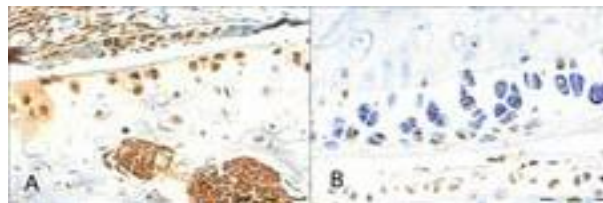


Fig. 1: Positive NITEGE detection in early stage (day 3) control treated tissue (A) shows ECM stain whilst later stage control tissue (B) has only intracellular staining.

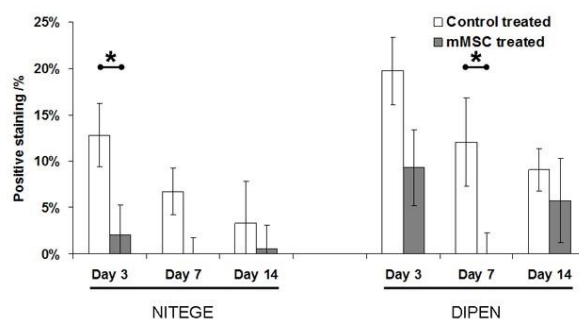


Figure 2: Neopeptide staining for NITEGE and DIPEN in control treated and mMSC treated tissue (Error bars = SEM).

DISCUSSION & CONCLUSIONS: Proteinase mediated degradation of cartilage is reduced at early (day 3, aggrecanase) and late (day 7, MMP) stages following administration of mMSC to the joint. This study demonstrates the potential application of stem cells as cell therapy to reduce the damage to cartilage in sufferers of RA.

ACKNOWLEDGEMENTS: Research was funded by the Dowager Countess Eleanor Peel Trust, the Institute of Orthopaedics Ltd and Oswestry Rheumatology Association. We thank John Mort for providing antibodies; Pat Evans, Martin Pritchard and Nigel Harness for their histological expertise; and the LSSU of Liverpool John Moores University for housing the mice.

Physical substrate factors, NGF concentration and Rho-ROCK inhibition affect outgrowth response in individual neurons

D Kredi¹, MO Riehle¹

¹ [Centre for Cell Engineering](#), University of Glasgow, Glasgow, UK.

INTRODUCTION: The mechanisms underlying the process of axon regeneration are poorly understood therefore, in order to improve the regenerative potential of nerve repair conduits, it is important to understand these mechanisms to optimise the design of nerve repair tubes. Previous work in our group has shown that the combinational modulation of substrate topography, stiffness and neurotrophic support, affects axonal outgrowth in whole rat dorsal root ganglia (DRGs). In this study we used individual sensory neurons dissociated from the DRGs, to see if these factors similarly affect axonal outgrowth at the single cell level. This was achieved by seeding DRG neurons onto polydimethylsiloxane (PDMS) substrates with or without micro-grooves, and cultured with varying NGF concentrations. Rho associated protein kinase (ROCK) and myosin II inhibitors, which affect cytoskeletal contractility, were used to influence growth cone traction forces.

METHODS: Neonatal rat DRG's were dissected and dissociated using trypsin/DNAase. The cells were seeded on either flat or grooved (4.1 MPa) PDMS coated with poly-L-lysine (PLL), and cultured in neurobasal media containing 10, 50 or 100 ng/ml of NGF. For inhibitor studies, cells were allowed to attach, then inhibitors were added. Fluorescence staining was used to assess axonal length (β -3 tubulin), actin organization (Phalloidin) and focal adhesions (talin). Image J (1), with the Neuron J plugin (2) was used to measure axon length. Statistical significance was identified using Student's T-test.

RESULTS: When studying the response of explants, more than 5 different cell types could have been responsible for the modulation observed. Here we show that the difference in response to NGF on grooved versus flat is not a collaborative effect involving other cell types. The individual neuron is responsible for the differences observed in axonal outgrowth on flat versus grooved topography, where on flat PDMS, axonal outgrowth **increased** with increasing NGF concentration while outgrowth **decreased** with increasing NGF concentrations on grooved PDMS. To understand if cytoskeletal contractility was responsible for the observed differences in axonal

outgrowth, ROCK was inhibited (Y-27632). Upon addition, the outgrowth observed on the control (fig 1A) was inhibited (fig 1B). When myosin II was inhibited (blebbistatin), outgrowth was accelerated, but the underlying actin was damaged (fig 1C). This suggests that growth cone dynamics, and the generation of traction forces, emerge as a result of a difference in NGF signalling and topography. This leads to an overall change in the axonal outgrowth in the conditions tested.

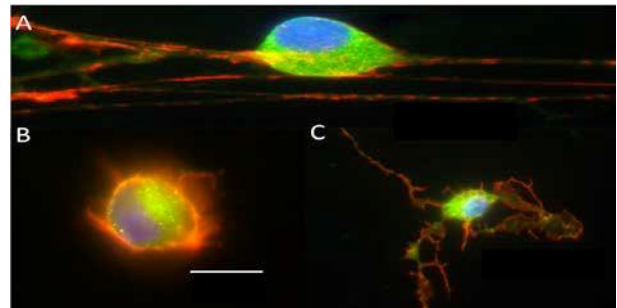


Fig. 1: Images of individual rat sensory neurons. A) Non- treated control, B) treated with Y-27632 and C) Blebbistatin [50µM]. Phalloidin (red), Talin (green) and DNA (blue). Scale bar = 10µm

DISCUSSION & CONCLUSIONS: The interaction between physical cues provided by microgrooved substrates, and the influence of growth factor concentrations are all important factors to be considered for nerve repair. We have shown that these factors work in combination by interfering with growth cone dynamics creating a difference in axonal outgrowth at the single cell level. This will help us refine the best parameters for future *in vivo* studies.

ACKNOWLEDGEMENTS: The authors would like to acknowledge funding of D. Kredi by the EPSRC DTC in Cell and Proteomic Technologies (EP/F500424/1).

Adult and foetal tenocytes display phenotypic variation in relation to cell attachment, spreading and their cytoskeleton

JK Kular¹, MJ Ellis¹, RI Sharma¹

¹Department of Chemical Engineering, University of Bath, Bath, BA2 7AY, UK

INTRODUCTION: Adequate healing of tendon injuries in adults remains a significant challenge to resolve. Scar formation can impede the proper restoration of tendon, due to the disruption of the collagen fibres at the injury site¹. Foetal tendon injuries undergo scarless healing and repair at a faster rate than in adults². The aims of this study were to investigate whether adult and foetal tenocytes displayed discernible differences in their morphology and the influence of particular substrate properties and shear flow on their adhesion strength behaviour.

METHODS: Cell morphology assays were performed by seeding adult and foetal tenocytes at 5000 cells/cm² on an untreated coverslip, a coverslip pre-coated with PBS and a coverslip pre-coated with FBS, for 6 hours and 24 hours at 37°C. Cells were fixed, permeabilised and stained with FTIC conjugated phalloidin for the actin cytoskeleton and DAPI for the nuclei. Images were acquired on an AMG EVOS inverted fluorescence light microscope with a 10x objective. Using ImageJ, average area of the cells and circularity were measured to indicate how spread the cells were. Circularity values range from 1.0-0.0 with 1 indicating a perfect circle, and 0 a progressively elongated cell shape. Circularity was calculated using the equation:

$$\text{Circularity} = 4\pi^2/\text{Perimeter}^2$$

Tenocytes were seeded in a convergent flow chamber (Fig. 2) at 10,000 cells/cm², and incubated at 37°C for 3hrs. Images were taken before the flow was applied; then the desired flow rate of 66 ml/minute was applied for 15 minutes. The range of shear stress was from 1.02 dyne/cm² to 0.27 dyne/cm². A matching set of images were taken to compare the effects of shear on the cells.

RESULTS: Overall the adult tenocytes became more elongated and larger over time, becoming more evident when the cells were seeded onto coverslips adsorbed in serum. In contrast the foetal tenocytes remained almost unchanged in both their size and shape, after both 6 hours and 24 hours (Fig. 1). Cell attachment for both the adult and foetal tenocytes did not fall below 50% across the range of shear stress applied.

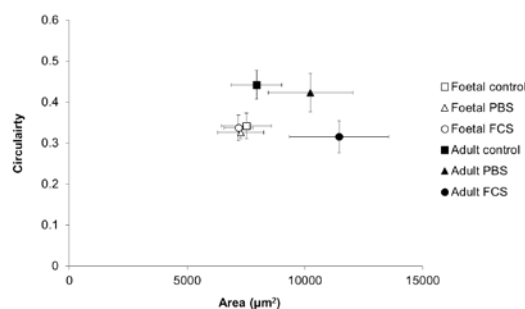


Fig. 1 Scatter plot comparing cell morphology of in adult and foetal tenocytes at 24 hours attachment ($n = 3$ $N = 24$) Error bars are \pm SEM.

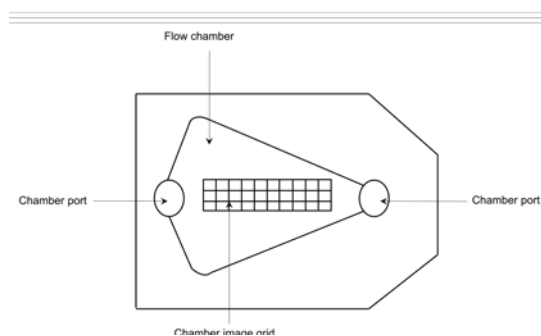


Fig. 2. Flow chamber apparatus for shear stress assay.

DISCUSSION & CONCLUSIONS: Age related morphological differences between adult and foetal tenocytes were demonstrated in this study. Unlike adult tenocytes, foetal tenocytes were able to retain their morphology even with changes in substrate properties. Foetal and adult tenocytes were also able to display disparities in the strength of their cell adhesion in response to shear. The ability of foetal tenocytes to maintain this behaviour despite environmental influences, could be linked to regenerative behavior in foetal tendon.

ACKNOWLEDGEMENTS: This research is funded by a University Research Scholarship (URS) by the University of Bath. We thank Dr. Robert Williams from Biology and Biochemistry for providing tendon tissue.

Injectable peptide hydrogel for the treatment of Barrett's oesophagus

D Kumar¹, V L Workman², L C Diaz², F Rose³, A Miller², A Saiani² and J E Gough¹.

¹ School of Materials, Materials Science Centre, University of Manchester, UK. ² Polymer and Peptides Group, Manchester Institute of Biotechnology, University of Manchester, UK. ³ Centre for Biomolecular Sciences, School of Pharmacy, University of Nottingham, UK

INTRODUCTION: Barrett's is a precancerous condition whereby a change in the epithelium is observed caused by gastro-oesophageal reflux disease¹. Current surgical treatments elicit rapid inflammatory responses resulting in subsequent strictures. Though this can be suppressed by direct injection of steroids, an intervention is required to improve treatment outcome. In this study, we propose the use of synthetic peptide hydrogels, which are injectable, mimic nano-architectural structure of extracellular matrix, are able to provide a protective barrier to the treated tissue area and encourage rapid re-epithelialisation.

METHODS: A variety of synthetic peptides were dissolved at 30mg/mL in HPLC grade water and neutralized to allow hydrogel formation. Following buffering in culture media overnight, primary rat oesophageal fibroblasts (rOFs) were incorporated into the peptide hydrogels, whereas epithelial cells (rOECs) were seeded on top mimicking the *in vivo* arrangement of these cell types. Cell-gel constructs were cultured for 3 days after which, cell viability and metabolic activity were monitored. Epithelial cells were also characterised for typical markers including ZO-1, Cytokeratins. Mechanical and degradation properties of hydrogels were also assessed in acellular conditions.

RESULTS: The inherent mechanical properties and peptide sequence of the hydrogels influenced cell viability (rOFs and rOECs). Stromal fibroblasts were homogeneously incorporated into hydrogels and demonstrated good cell viability and typical morphology after 3 days of culture. Greatest fibroblast viability was observed in peptide #3 although better homogenous distribution of cells was witnessed on peptide #2 (Fig.1). rOECs proliferated well and formed a sheet on top of the hydrogels, whilst retaining morphology and cell-cell tight junctions. Greatest area coverage of peptide surface by epithelial cells was observed on peptide # 1, 3 and 5 (Fig 2).

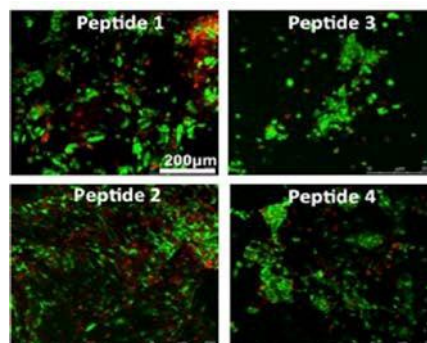


Fig. 1: Cell viability of rOFs cultured within self-assembled peptide hydrogels for three days.

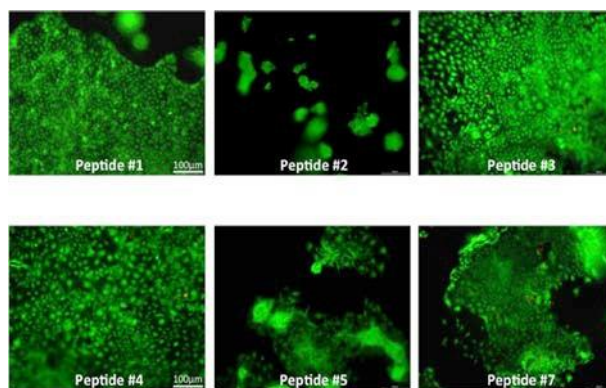


Fig. 2: Cell viability of rOECs cultured on top of self-assembled peptide hydrogels for three days.

DISCUSSION & CONCLUSIONS: Assessment of these peptides provides a platform to further develop a composite hydrogel system (Fig 3) with incorporated anti-inflammatory properties, which will be tested further under simulated gastric conditions and under air-liquid interface.

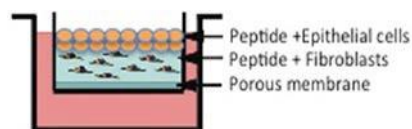


Fig. 3: *In Vitro* Oesophagus Model.

ACKNOWLEDGEMENTS: Funded by a grant from the UK Regenerative Medicine Platform.

3D culture model of human corneal epithelial-stromal cell interactions in the limbal niche.

AK Kureshi¹, M Dziasko¹, JL Funderburgh², JT Daniels¹

¹Ocular Biology & Therapeutics, Institute of Ophthalmology, University College London, London, United Kingdom. ²Department of Ophthalmology, UPMC Eye Centre, University of Pittsburgh, Pittsburgh, Pennsylvania, USA.

INTRODUCTION: In this study we used RAFT (Real Architecture For 3D Tissue) tissue equivalents (TEs) as a 3-dimensional (3D) substrate for co-culturing human limbal epithelial cells (HLE) and corneal stromal stem cells (CSSC). HLE and CSSC reside in close proximity *in vivo* in the corneal limbal stem cell niche. Our aim was to re-create this cell-cell juxtaposition of the native environment *in vitro*, to provide a tool for investigation of epithelial-stromal cell interactions and to optimize HLE culture conditions for potential therapeutic application.

METHODS: RAFT TEs were used as a biomimetic substrate to co-culture a mixed population of HLE and CSSC. Briefly, rat-tail type I collagen solution (80% of total volume) was mixed with 10xMEM (10%), neutralizing solution (5.9%) and DMEM (4.1%). This was cast into 24-well plates and allowed to set for 30 minutes prior to gentle wicking of water using hydrophilic porous absorbers (TAP Biosystems). RAFT TEs were cultured at 37°C and 5% CO₂ in CSSC media for 13 days. Cell morphology, HLE and CSSC marker expression, HLE confluence and epithelial and stromal cell physical interactions were assessed with light microscopy, immunohistochemistry, fluorescein-diacetate staining and transmission electron microscopy analysis respectively.

RESULTS: A monolayer of HLE that maintained positive expression of p63 α , a characteristic of limbal basal epithelial cells, formed on the surface of RAFT TEs within 13 days of culture. CSSC remained in close proximity to HLE and maintained positive expression of mesenchymal stem cell markers. The onset of epithelial cell layering and differentiation was also observed. TEM micrographs demonstrated a close physical interaction of CSSC with HLE cultured on RAFT TEs.

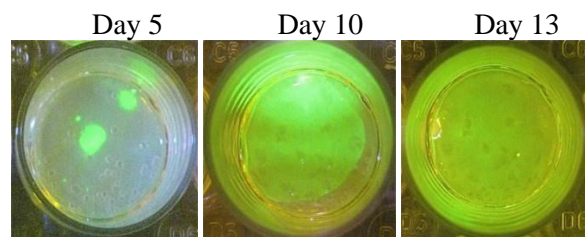
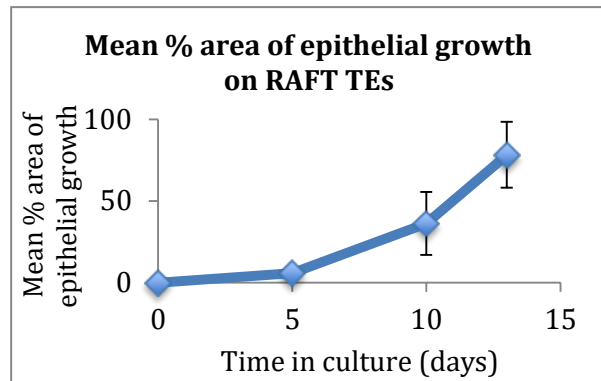


Fig. 1: a) Graph illustrating mean percentage area of LEC growth on RAFT TEs (n=4 donors) over 13 days of culture. b) Photographs of fluorescein diacetate (Fda)-stained RAFT TEs with mixed population of CSSC and HLE on surface. A confluent monolayer of HLE is achieved by day 13.

DISCUSSION & CONCLUSIONS: We have demonstrated a reproducible, 3D co-culture method to support the cultivation of HLE using CSSC on RAFT TEs. This approach may be useful in the investigation of epithelial-stromal cell interactions in the limbal niche. This simple technique has a short preparation time of only 15 days and supports the growth of multi-layered epithelium. Furthermore, co-cultivation of HLE with another niche cell type (CSSC) directly on RAFT TEs, eliminates the requirement for animal-derived feeder cells. RAFT TEs may be useful for future therapeutic delivery of multiple cell types to restore the limbal stem cell niche following ocular surface injury or disease.

ACKNOWLEDGEMENTS: This study was funded by Special Trustees of Moorfields Eye Hospital and in part by NIHR Moorfields Biomedical Research Centre.

Development of a tissue engineered co-culture model to study neurodegeneration

C Lee-Reeves¹, JB Phillips², C O'Rourke²

¹*Institute of Neurology, University College London, UK.* ²*Biomaterials and Tissue Engineering, UCL Eastman Dental Institute, University College London, UK.*

INTRODUCTION: Neurodegenerative diseases remain poorly understood; extensive research is required to investigate the mechanisms by which cellular loss can be decelerated or prevented, in order to be able to develop effective therapies. There is an unmet need for more physiologically relevant in vitro models in which potential treatments can be tested without the limitations associated with traditional monolayer cell culture. Tissue engineering provides an opportunity for building artificial CNS tissue in which both neurons and glia grow in 3D co-culture in an organised manner [1]. The alignment of these cells mimics the anisotropic architecture of the CNS and facilitates the quantitative measurement of neurite length.

The aim was to optimise an aligned 3D co-culture model to enable quantifiable simulation of neuronal degeneration in vitro, thereby producing a replicable model of pathology, which could help to reduce the use of animals in neurodegenerative disease research.

METHODS: Artificial neural tissue was engineered through creation of 3D collagen hydrogels, which were tethered to achieve glial cell self-alignment that allowed for neuronal processes to follow these structural cues. Growth was stimulated with NGF over the course of 3 or 5 days. Degeneration was induced through the addition of neurotoxic compounds at different concentrations for a period of 24hrs and these effects were quantified through the measurement of change in neurite length over time. The model can be constructed using glial cell lines and different neuronal cell sources including PC12, rat DRG and hiPSC. Neurite degeneration can be triggered using compounds such as Okadaic Acid [2], MPP+ and methyl mercury.

RESULTS: Robust aligned neurite growth that was compatible with quantification was observed in co-cultures (Fig. 1). Neurite length increased over time and was greater in the presence of NGF (Fig. 2). Preliminary dose response data reveal progressive neurite degeneration as the toxic concentration increases.

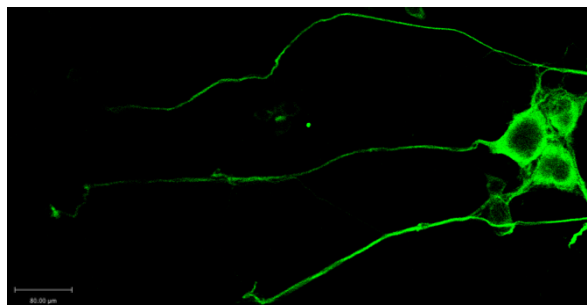


Fig. 1: Aligned neurite growth in PC12 cells in co-culture, following addition of NGF after 5 days.

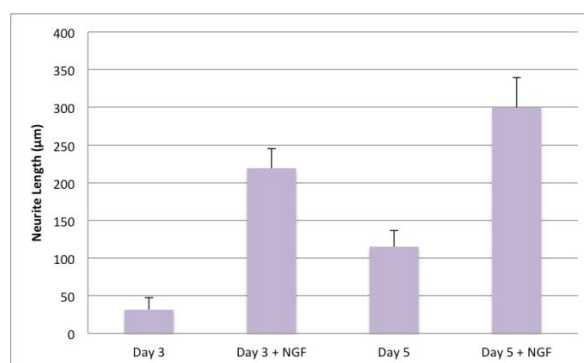


Fig. 2: Neurite length (μm) in the presence and absence of NGF after 3 and 5 days (mean \pm SEM).

DISCUSSION & CONCLUSIONS: The aligned co-culture model supported robust and replicable neurite growth. The 3 day time point in the presence of NGF was determined to be sufficient to provide an experimental platform in which neurodegeneration can be studied and potential neuroprotective applications may be tested. The 3D model may be adapted to suit individual research specifications through the use of different cell lines and degenerative compounds.

The magnetic labelling of stem cells to develop a functional hematopoietic stem cell niche *in vitro*

N Lewis¹, E Lewis¹, M Dalby¹, C Berry¹

¹Centre for Cell Engineering, University of Glasgow, Glasgow

INTRODUCTION: Hematopoietic stem cells (HSCs) are the parent cells of all cellular constituents of the blood. They reside within a specialised niche area in the bone marrow (BM). These cells have tremendous clinical relevance in treating disorders of the blood, as they are able to replace defective blood cells in patients with blood disorders and leukaemia. However, HSC population expansion and long-term culture *ex vivo* is not currently possible, meaning that reliance on donors and small yields have reduced BM transplant success. The ability to manipulate HSCs *ex vivo* could improve transplant success, and would be invaluable for studying HSC interaction with niche cells and elucidating mechanisms involved in HSC control within the BM. The fact that HSCs are supported in the niche by other BM cell types is a long established concept¹. More recently, the focus has been on nestin-positive mesenchymal stem cells (MSCs) as the main supportive cell type for HSCs, as these co-localise with HSCs in both endosteal and perivascular regions of the bone marrow². This project expands a novel 3D MSC niche model developed in our lab to include HSCs.

METHODS: MSCs and HSCs were obtained from primary human bone marrow samples via magnetic cell sorting. MSCs were loaded with either unlabeled or green fluorescently labelled magnetic iron oxide (FeO₃) nanoparticles (200 nm diameter) at a concentration of 0.1 mg ml⁻¹, and subsequently incubated for 30 min over a magnet to enhance cellular uptake. The cells were then washed with HEPES saline to remove excess nanoparticles and detached via trypsin. The resulting cell suspension was centrifuged (4 minutes, 1400 rpm), the supernatant was removed and the cells were resuspended in fresh medium. This suspension was then transferred to 6-well plates at a concentration of 1x10⁴ cells ml⁻¹, with magnets fixed to the culture plate lid to attract the magnetically labeled cells together. Spheroids formed within several hours and were subsequently implanted into 2 mg ml⁻¹ collagen gel. HSCs were loaded with red nanoparticles via incubation with suspension, and then introduced to the gel containing the spheroid. Immunostaining, BrdU

and viability assays were performed to characterise the cells.

RESULTS: Calcein/ ethidium homodimer tests were used to assess cell viability of MSCs in monolayers as compared to spheroids. Cells in both monolayers and spheroids remain viable up to 7 days in culture. MSCs in monolayers and spheroids were stained with antibodies for: STRO-1, an MSC marker; SDF-1 (CXCL-12), a secreted factor which is instrumental in HSC homing; and nestin, as a rare subset of MSCs expressing this cytoskeletal component is thought to be the main support of HSCs *in vivo*. Quiescence was assessed using BrdU staining. MSCs in spheroids retain a higher level of expression of STRO-1, SDF-1 and nestin for 7 days compared to MSCs in monolayers. The BrdU assay shows that the MSCs are more quiescent in spheroids as compared to monolayers.

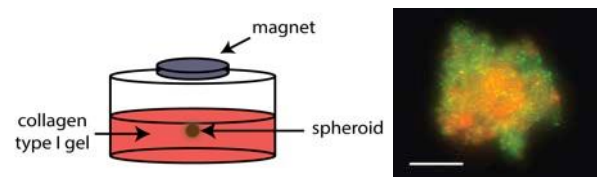


Fig. 1: Schematic of the spheroid culture system and fluorescence microscope image of a co-culture spheroid. Green nanoparticles: MSCs, red nanoparticles: HSCs. Scale bar=100µm.

DISCUSSION & CONCLUSIONS: Proof of principle studies are promising for the success of the proposed niche model. MSCs express a higher level of MSC markers and retain quiescence when they are in spheroids as compared to monolayers: they are themselves in a more stem-like state. In addition, they express a higher level of the important HSC niche factor SDF-1α, which facilitates HSC migration and retention.

ACKNOWLEDGEMENTS: This research is funded by the BBSRC.

***In utero* vitamin D depletion reduces femoral bone area and strength of offspring at 21 days of age**

T Li^{1,2}, T Jenkins², SA Lanham¹, D Sreenivasan³, J Fernandez³, PJ Thurner^{2,4}, ROC Oreffo¹

¹*Bone and Joint Research Group, University of Southampton, UK.* ²*Bioengineering Research Group, University of Southampton, UK.* ³*Auckland Bioengineering Institute, University of Auckland, New Zealand.* ⁴*Institute for Lightweight Design and Structural Biomechanics, Vienna University of Technology, Austria.*

INTRODUCTION: Bone quality is determined by a framework of factors (most notably size, material properties and structural features) that, along with bone mass, all affect mechanical behaviour. These factors are governed by the bone biology environment and we have previously utilised an experimental approach on rat femora that measures a number of these parameters within one sample. We have applied this approach to analyse a model of *in utero* vitamin D deficiency (VDD), with the aim to test whether and how VDD disrupts bone formation and the consequences on bone health at 21 days of age. We hypothesise that VDD will cause a restriction in bone cell activity that leads to a degradation in bone strength through impaired bone quality.

METHODS: Femora from day 21 old rats on either control or VDD diet conditions during *in utero* life were analysed ($n = 8$ for control and VDD groups for each gender). Osteogenic gene expression (*Runx2*, *Coll*, *Opn* and *Ocn*) was measured by RT-qPCR, microarchitecture and bone mineral density by μ CT scanning, fracture toughness by notched three-point bend testing and overall bone strength by three-point bend testing. A subset of male μ CT midshaft scans ($n = 5$ for control and VDD) was used to generate finite element models for simulated compression tests to predict the role of bone architecture towards strength when material properties are normalised.

RESULTS: Femora from male VDD background rats were found to have a reduced midshaft area when compared to controls (figure 1, 14.9% reduction, $p = 0.03$) despite no detected difference in bone volume. The computational modelling predicted lower forces to reach the average von Mises failure stress threshold in the VDD femora (7.0 N vs 5.2 N, $p = 0.04$). This was confirmed experimentally in the three-point bend data, where VDD femora failed at lower loads compared to controls (11.4 N vs 8.3 N, $p = 0.04$). No differences were found within osteogenic gene expression, BMD, fracture toughness or cortical

thickness. Within the female cohort, no differences were found for any of the measured parameters.

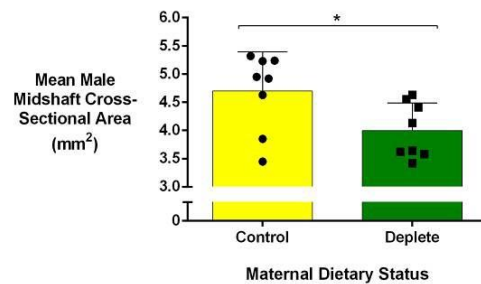


Fig. 1: Male femora from an *in utero* vitamin D deficiency background were found to have a reduced midshaft cross-sectional area.

DISCUSSION & CONCLUSIONS: The results obtained demonstrate that *in utero* vitamin D deficiency is linked to a reduction in mean cross-sectional area at the femur midshaft and femur maximum load in strength tests of male samples at 21 days old. No differences were found in bone content or bone mineral density, suggesting that femur shape is solely adapted in cases of vitamin D challenge. The impact of this was supported by the computational models, whereby reduced midshaft area predicted lower compression loads for failure stress to be reached when material properties were held constant. No other significant differences were detected in the other bone metrics or in the female cohort, possibly highlighting the role of *in utero* vitamin D in specific areas of bone health (femur midshaft morphology in this instance) and gender specificity. This data and the methods employed emphasise the importance of applying multi-disciplinary approaches to evaluate bone tissue formation and the elucidation of key factors in bone mechanical strength for effective regenerative medicine strategies.

ACKNOWLEDGEMENTS: This work is funded by the EPSRC UK and the University of Southampton. Collaborative work partially funded by EU FP7- 'SkelGEN' under grant agreement n° [318553]. The authors have no conflict of interest.

Silk fibroin/gelatin blended materials as osteogenic scaffolds for tissue engineering

[KA Luetchford](#)¹, [JB Chaudhuri](#)², [PA De Bank](#)¹

¹Centre for Regenerative Medicine, Department of Pharmacy & Pharmacology, University of Bath, U.K.

²School of Engineering and Informatics, University of Bradford, U.K.

INTRODUCTION: Silk fibroin (SF) is a biocompatible, light-weight, and strong material that can be processed into many formats [1]. While there are reports of successful cell adhesion and proliferation on SF materials, there are a number of instances where SF has been blended with other biopolymers such as collagen and gelatin to improve its properties, specifically cell adhesion [2]. This work investigates SF/gelatin (SF/G) blends as osteogenic cell scaffolds.

METHODS: An aqueous solution of SF was generated following extraction from the cocoons of *Bombyx mori* silkworms. Following lyophilisation, SF was dissolved in HFIP at 2% w/v, and blended with porcine Type A gelatin (2% w/v, in HFIP) at ratios of 75:25, 50:50 and 25:75. 2D films were cast from these solutions and cross-linked with 50 mM EDC in methanol. SF/G blended microparticles were created from aqueous solutions of SF/G using microfluidic flow focussing and cross-linked the same way. Mesenchymal stem cells (rMSCs), harvested from the bone marrow of juvenile Wistar rats, were maintained in MEM with 10% (v/v) fetal bovine serum, 2 mM L-glutamine, 100 U/mL penicillin and 100 µg/mL streptomycin, at 37°C in a 5% CO₂ atmosphere. Osteogenic differentiation medium (ODM) consisted of basal medium supplemented with 0.1 µM dexamethasone, 0.2 µM ascorbic acid 2-phosphate, and 10 mM glycerol 2-phosphate. Cells were cultured in either basal medium or ODM for a minimum of 14 days. Osteogenic differentiation was confirmed by positive alkaline phosphatase (ALP) activity (BCIP/NBT assay), and osteocalcin and osteopontin expression.

RESULTS: Cell attachment to the films was improved by the inclusion of gelatin, as determined by the MTS assay three days after seeding. This was reflected in 3D by increased seeding efficiencies of cells on microparticles. Osteogenic differentiation on the SF/G films was confirmed by ALP activity, osteocalcin expression and osteopontin expression (Fig. 1). All SF/G blends supported osteodifferentiation at a level equivalent to that on tissue culture plastic (TCP). Interestingly, SF alone appeared to support a higher degree of differentiation, suggesting that where cells do adhere, the surface is highly

osteogenic. However, this is hindered in real terms by the reduced cell adhesion in comparison to SF/G blends. Differentiation of rMSCs on microparticles was confirmed initially by ALP activity (Fig. 2)

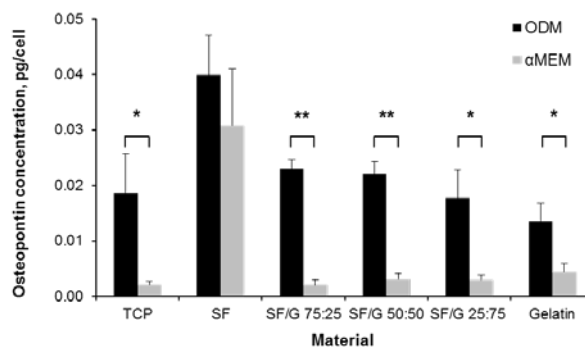


Fig. 1: Osteopontin expression of rMSCs cultured on SF, SF/G, and gelatin films for 14 days. Data shown represents mean + standard error, n=3. ** p<0.001; * p<0.05.

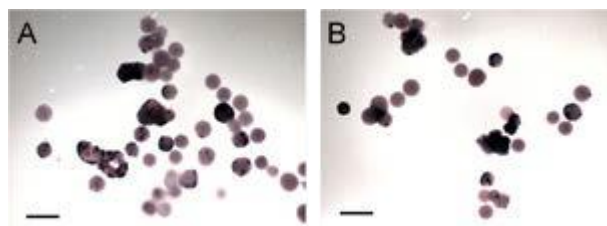


Fig. 2: Positive purple staining for ALP activity in rMSCs cultured on SF/G 25:75 microparticles in basal media (A) or ODM (B). Scale bar = 500 µm.

DISCUSSION & CONCLUSIONS: SF/G blends are shown to support cell attachment in 2- and 3D at higher levels than SF alone. The blends of materials are also shown to support osteodifferentiation, suggesting these biomaterials could be useful scaffolds for bone tissue engineering or repair.

ACKNOWLEDGEMENTS: This work was financially supported by the Medical Research Council.

A simplified, *in vitro*, 3D printed dry eye model and its application in the assessment of therapeutic ocular lubricants

N Madarbox¹, S Shafaie¹, M Bloomfield², MB Brown¹, V Hutter¹, DYS Chau¹

¹The Research Centre in Topical Drug Delivery and Toxicology, Department of Pharmacy, University of Hertfordshire, Hatfield, UK. ²The Digital Hack Lab, School of Creative Arts, University of Hertfordshire, Hatfield, UK

INTRODUCTION: The ethical constraints associated with human and/or animal models make it a less favourable method for performing toxicity assessments on novel drug compounds. Instead, *in vitro* cell-based models are the preferred method of use. Traditionally, cell culture is performed on flat tissue culture plates (TCP) although it is now considered not to be truly representative of the real 3-dimensional (3D) surfaces, *in vivo*. Consequently, it is proposed to develop a novel *in vitro* model of the eye by combining ocular cells with a 3D printed curved scaffold. This model seeks to support long term cell growth while providing a more accurate representation of the ocular surface due to the surface curvature. Further to this, it is intended to this *in vitro* construct as a novel model to represent dry eye syndrome (DES) whilst assessing the efficacy of four commercially available ocular lubricants.

METHODS: 3D poly-lactic acid (PLA) scaffolds were designed and developed using an Up!® Plus 2 3D fused deposited modelling printer. Human ocular epithelium cells (CRL-2302, ATCC) were cultured in DMEM-F12 media in a humidified-incubator at 37°C and 5% v/v CO₂. 20,000 cells were placed onto each 3D scaffold and following 24h equilibration, the media was removed and cells were allowed to air dry for 30 minutes to mimic DES. These cells were then exposed to four ocular lubricants (i.e. 0.3% w/v hypromellose, Liquifilm Tears®, Optrex® and Viscotears® Liquid Gel) before being assessed for cellular activity and viability using the Cell Titer AQ Proliferation/MTS assay (Promega) and CytoTox-ONE LDH assay (Promega), respectively.

RESULTS: 3D printed scaffold were successfully fabricated with the correct dimensions. The biological assays demonstrated that the most effective ocular lubricant was Optrex® which documented the greatest cell viability and lowest cell toxicity. In contrast, 0.3% w/v hypromellose was seen to be the least effective ocular lubricant by showing a significantly lower viability measurement. Liquifilm Tears® and Viscotears® Liquid Gel displayed moderate therapeutic activity (Figure 1).

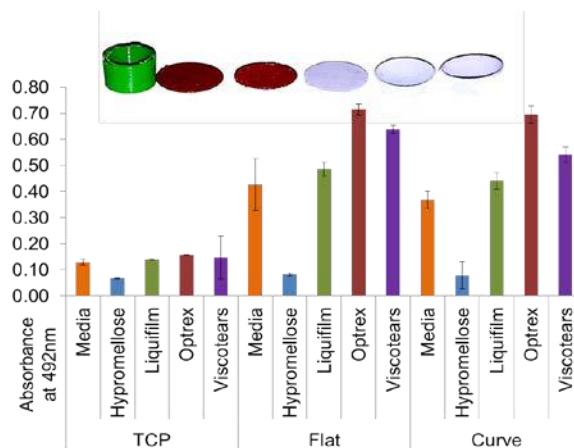


Figure 1: Mitochondrial activity of cells cultured on different scaffolds and exposed to lubricants. Insert: 3D printed scaffold supports: PLA cylinder; PLA flat, PLA curved, nylon flat, nylon curved-1, nylon curved-2 (L-R)

DISCUSSION: Cells cultured on a “curved” substrate demonstrated enhanced growth and differentiation characteristics i.e. representative of the native eye. The cell response to each lubricant was related to their formulations and can be seen to be reflected by the corresponding cellular activity (MTS) and higher cell death (LDH) values.

CONCLUSIONS: Ocular cells were successfully cultured on 3D printed curved scaffolds. There was a greater cell growth and lower cell death in comparison to those cultured on flat TCP. DES was also successfully replicated and the efficacy ocular lubricants demonstrated varying levels of cell viability and/or prevention of cell death.

ACKNOWLEDGEMENTS: The authors would like to thank the University of Hertfordshire for funding.

A serum-free and feeder-free protocol for expanding human keratinocytes on biodegradable microcarriers for the treatment of severe burn injuries

YH Martin^{1,2}, AD Metcalfe^{1,2}

¹ *Blond McIndoe Research Foundation, East Grinstead, UK* ² *The Brighton Centre for Regenerative Medicine, University of Brighton, Brighton, UK*

INTRODUCTION: Autologous keratinocytes are used in the treatment of severe burns to augment wound healing. Cells are commonly expanded in serum-containing medium in the presence of lethally irradiated mouse fibroblast feeder cells. Application to the wound bed in single cell suspension is damaging to the cells and often results in significant cell loss. We previously demonstrated improved wound healing outcomes in the porcine model of wound repair with cells delivered using biodegradable gelatin microcarriers instead of as cell spray¹. We present here an improved method of culturing human keratinocytes on biodegradable microcarriers under serum-free and feeder-free conditions.

METHODS: Keratinocytes were isolated from discarded human skin and cultured in serum-free, feeder-free CnT-07 medium (CellnTech) until sub-confluent (5-6 days). Gelatin Cultispher-G microcarriers (Sigma-Aldrich) were seeded with 5×10^6 cells and cultured for a further 4 days in a stirring glass bioreactor. Cell phenotype was assessed by microscopy, proliferation assay (CCK-8, Sigma-Aldrich) and qRT-PCR (Bio-Rad).

RESULTS: Using a serum- and feeder-free culture medium, we obtained gelatin microcarriers with sub-confluent keratinocyte cultures after 4 days.

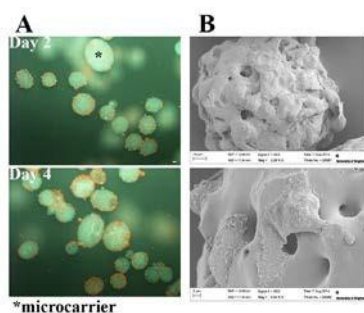


Fig. 1: Microscopy reveals sub-confluent keratinocyte cultures. (A) Acridine orange staining indicates proliferating cells (RNA – orange, DNA – green, scale bar = 100 μ m). (B) Scanning electron microscopy indicates distribution and cell shape of keratinocytes on microcarriers, scale bars as indicated.

Proliferation over the 4 day culture period was rapid. Cell phenotype on microcarriers (MC) was

assessed by qRT-PCR and compared to cells prior to culturing (P0) and cells on tissue culture plastic at passages 1 (P1 TCP) and 2 (P2 TCP). Significant differences were detected between cells prior to and after culturing, but not between cells grown on tissue culture plastic and those grown on microcarriers.

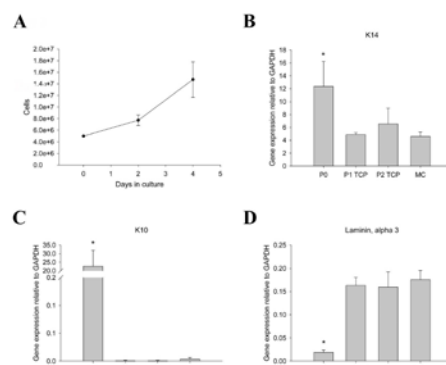


Fig. 2: Cell growth and phenotypic analysis. (A) Proliferation assay indicates rapid growth on microcarriers. (B) qRT-PCR of cytokeratin 14 (K14), cytokeratin 10 (K10) and Laminin, alpha 3 indicates no significant differences between cells grown on microcarriers and on tissue culture plastic, n=3, p<0.05.

DISCUSSION & CONCLUSIONS: Severe burns are often treated with autologous keratinocytes within 10 – 20 days of hospital admission. Using the culture protocol reported here, highly proliferative keratinocytes are available within 10 days. The use of biodegradable microcarriers for transplantation ensures the cells are not damaged by enzymatic digestion during removal from tissue culture flasks. Using a serum-free and feeder-free medium system would further limit the risk to patients associated with use of xenobiotic substances.

ACKNOWLEDGEMENTS: This work was funded by The Charles Wolfson Charitable Trust.

Tissue engineered skeletal muscle exhibits hypertrophy in response to supplementation with the amino acid L-Leucine

NRW Martin, DJ Player, MC Turner, MP Lewis

National Centre for Sport and Exercise Medicine, School of Sport, Exercise and Health Sciences, Loughborough University, UK.

INTRODUCTION: The field of skeletal muscle tissue engineering has expanded considerably in the past decade, and the development of biomimetic tissues with aligned multinucleate myotubes which can be stimulated to produce force are now well established. These tissues provide an ideal platform for pharmaceutical and nutritional testing, however, to date it has not been fully demonstrated that engineered muscle responds to specific stimuli in a manner known to occur *in vivo*. Here we sought to determine the effects of the known anabolic amino acid L-leucine¹ on the morphology and function on fibrin based tissue engineered skeletal muscle.

METHODS: Fibrin hydrogels were prepared as previously described², adding 20mg/ml Fibrinogen to a thrombin based solution and seeding the cells on top of the gel once polymerised. After 9 days in culture, extensive myotube formation was apparent within the hydrogels, which had delaminated and formed 3D structures. At this point, gels were treated with L-Leucine (1, 5 or 20mM) or control medias, and cultured for a further 5 days (14 day total culture period). At the end of the culture period gels were either taken for functional testing and subsequently fixed for immunostaining to determine myotube size or lysed for western blotting for p-mTOR^{ser2448}.

RESULTS: Skeletal muscle hydrogels cultured in the presence of L-Leucine generated greater tetanic force in comparison to control gels. Indeed relative force production was $161.8 \pm 8.4\%$, $143.1 \pm 29.6\%$ and $184.3 \pm 13.5\%$ in hydrogels cultured with 1, 5 and 20mM L-Leucine respectively. Furthermore, myotube width was increased in constructs cultured in the presence of L-leucine (Figure 1). Since skeletal muscle growth is directed through the Akt-mTOR signalling cascade, western blotting was performed on protein lysates derived from constructs cultured with or without L-leucine. Exposure to this amino acid led to increased phosphorylation of mTOR^{ser2448}.

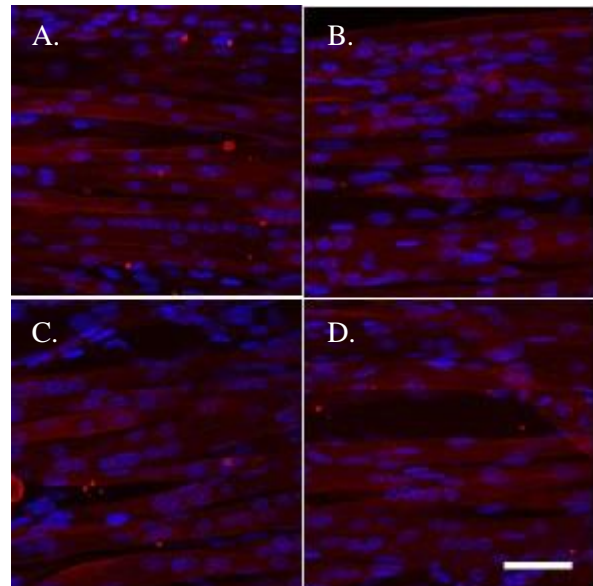


Fig. 1: Myotubes in engineered skeletal muscle undergo hypertrophy in response to L-Leucine supplementation. A-D; Control, 1mM, 5mM and 20mM L-Leucine. Scale bar = 50µm.

DISCUSSION & CONCLUSIONS: Here we have shown that biomimetic engineered skeletal muscle can respond to a known anabolic nutrient (L-leucine) in a manner akin to that of native skeletal muscle, and thus forms a critical validation step in the utility of such tissues. This work paves the way for future use of engineered skeletal muscle as a model for further nutritional and pharmacological testing.

ACKNOWLEDGEMENTS: This work was funded by the Gatorade Sports Science Institute (GSSI).

The use of magnetic nanoparticles to encourage new bone growth in a large animal model.

JS M^cLaren^{1,3}, H Markides², JR Henstock², BE Scammell³, KM Shakesheff¹, AJ El Haj²

¹Centre for Biomolecular Sciences, University of Nottingham, Nottingham, UK. ²Institute for Science and Technology in Medicine, Keele University, Stoke-on-Trent, UK. ³Academic Orthopaedics, Trauma and Sports Medicine, University of Nottingham, Nottingham, UK.

INTRODUCTION: We investigated the extent of bone repair in a critical size defect model in the medial femoral condyle of sheep by remotely applying localised mechanical stimulation directly to implanted stem cell populations. Magnetic nanoparticles are attached to specific receptors on the cell membrane which respond to the application of an external magnetic field thus promoting conformational changes in the membrane. This subsequently induces a series of signal cascades which results in controlled cell responses. This technology has successfully been demonstrated to aid in the production of cartilage and bone *in vitro* and *in vivo* (small animal studies) by controlling the differentiation of human mesenchymal stem cells¹.

This product has the potential to enhance bone repair above gold standard measures by remotely applying localised mechanical loading directly to the cells *in vivo* therefore promoting bone repair.

METHODS: Bone marrow was aspirated from the sternum of sheep (Fig. 1A) and processed to isolate cells expressing Stro-4. After a 2 week period of expansion 5×10^6 cells were labelled with magnetic nanoparticles and returned within decellularised extra cellular matrix to the bone defects. 8mm wide by 15mm deep bone defects were created in the cancellous bone of both medial femoral condyles in skeletally mature sheep (Fig. 1B).

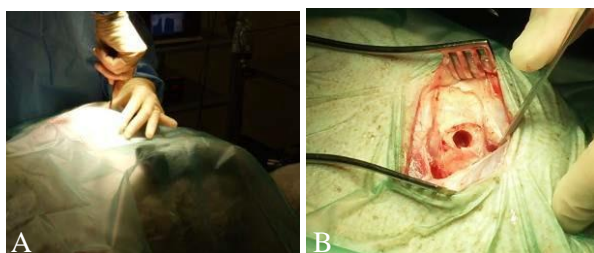


Fig. 1: A) Sternal aspiration of bone marrow B) Bone defect in the sheep femoral condyle.

The implanted cell populations were stimulated for 3 hours a day, 5 days a week for 13 weeks by magnetic arrays contained within a sheep harness (Fig. 2). Previous work has shown that cyclical use is more effective than continuous use. Sheep were sacrificed at 13 weeks and the femoral condyles

scanned using micro-computed tomography to assess new bone growth.



Fig. 2: A) The sheep harness, B) magnet and C) magnet applied to the defect site.

RESULTS: Preliminary micro-computed tomography data show an increase in new bone fill when cells labelled with magnetic nanoparticles were stimulated with a magnetic field compared to an empty defect ($p=0.038$). In addition a positive (bone graft) and negative control (empty defect) were carried out and a significant difference was detected between the two ($p=0.005$).

DISCUSSION & CONCLUSIONS: We were successful in managing to stimulate stro-4 positive cells labelled with magnetic nanoparticles by an external device, and in turn cause a significant increase in new bone formation within the defect.

ACKNOWLEDGEMENTS: This work was funded by the UK Regenerative Medicine Platform (BBSRC, EPSRC and MRC).

The role of hMSCs-secretome in attenuating the immune response using Jurkat cells as an in vitro model

MM Merkhan¹, NR Forsyth¹

¹ *Institute of Science and Technology in Medicine, Keele University, Stoke-On-Trent*

INTRODUCTION: Human mesenchymal stem cells (hMSCs) are in clinical trials for widespread indications including musculoskeletal, neurological, cardiac and haematological disorders¹. Though the mechanism of action is unclear in many of these indications it is apparent that hMSCs may have a paracrine, rather than cell-to-cell contact or functional role, including immunomodulation.

METHODS: hMSCs were isolated from bone marrow using an adherence-based methodology in either hypoxia (2% O₂) or normoxia (21% O₂)². Multilineage differentiation (bone, cartilage, fat) and expression of appropriate CD markers was assessed. Conditioned media (CM) were collected by conditioning serum-free (SF) media overnight on 70% confluent T75 flasks of hMSC and protein concentrations of SF-CM determined. Constituent components of SF-CM were then determined with cytokine arrays. To investigate the potential of hMSC secreted factors in immunomodulation SF-CM was evaluated during T cell line (Jurkat) activation. Cell counts, MTT, RTPCR and IL2 levels were evaluated as indicators of proliferation, activation and differentiation.

RESULTS: Cytokine array-based analysis of SF-CM indicated that hMSCs produced a range of cytokines in an oxygen-dependent manner (Figure 1A) which correlated closely with their transcriptional profile. Some of these paracrine factors (IGF-1, b-NGF, MCP-1) were secreted in significantly (P<0.05) higher amounts in hypoxia than normoxia and the secretion of others (IL2, IL17a, EGF, Adipo, Rantes) is merely restricted to hypoxia environment.

Furthermore SF-CM appeared to successfully block T cell line activation as evidenced by blockage of IL2 secretion irrespective of oxygen condition and substantially altered transcriptional profiles following activation (Figure 1B and 1C) when compared to serum free-non conditioned media (SF-NCM).

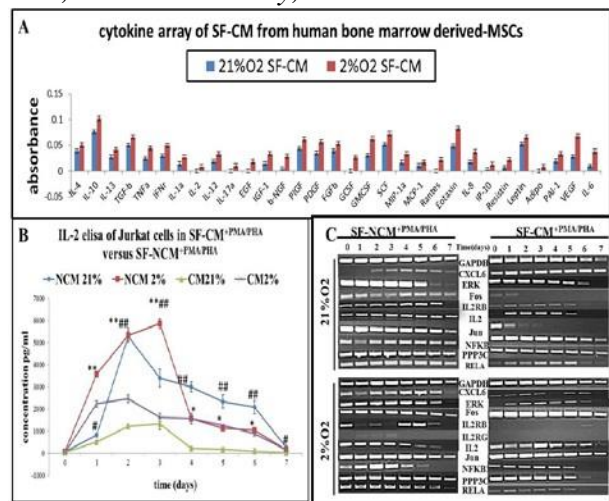


Figure 1: (A) cytokine concentration in SF-CM in hypoxia versus normoxia. (B) IL2 concentration in SF-CM versus SF-NCM following Jurkat cell activation. (C) gene transcriptome of Jurkat cell in SF-CM versus SF-NCM following activation

DISCUSSION & CONCLUSIONS: In this study, SF-CM was used as a model to characterize the paracrine role of hMSCs. SF-CM of hMSCs contains various cytokines which may play an important role in the suppression of inflammation. This property may be harnessed to produce biological agents which have immunomodulatory actions similar to hMSCs, leading to production of the “off-the-shelf” biological products. These findings support the notion for clinical application of hMSCs and/or their secretory factors as a pharmacoregenerative modality for the treatment of rheumatoid arthritis, Crohn disease, myocardial infarction and advanced critical limb diseases.

ACKNOWLEDGEMENTS: Funding for this project was provided by the Iraqi Ministry of Higher Education and Scientific Research.

Novel GET proteins for efficient gene transfer

G Osman¹, C Denning², KM Shakesheff¹, JE Dixon¹

¹ School of Pharmacy, University of Nottingham, Nottingham, United Kingdom, ² School of Medicine, The University of Nottingham, Nottingham, United Kingdom

INTRODUCTION: A major scientific goal is the development of non-viral DNA delivery platforms. CPPs (cell penetrating peptides) are intracellular delivery vehicles that have been used for transfection of nucleic acids.¹ Clinical adoption of CPPs have been inhibited by their low efficiency of transduction into cells. In previous work we demonstrated that the modification of CPPs to include a heparan sulphate-glycosaminoglycan (HS-GAG) cell surface binding region increased uptake of a reporter protein by 2 orders of magnitude. This phenomenon was termed GAG-binding enhanced transduction (GET). Due to their ability to deliver cargo into cells much more efficiently than unmodified CPPs, GET proteins may provide a powerful tool for the delivery of exogenous DNA into cells.

METHODS: A DNA-binding GET protein, termed P21 LK15 8R, was synthesized using solid phase t-Boc chemistry (Novabiochem (Beeston, Nottinghamshire, UK)).² Optimal DNA binding ratio of P21 LK15 8R and reporter gene (pSIN GFP) was determined using YOPRO1 fluorescence-based assay. Transfection parameters including transfection time, transfection media and amount of DNA were evaluated. Transfection efficiency was determined by analyzing the number of GFP positive cells using flow cytometry. Total number of cells and cell viability were determined using trypan blue assay. The transfection of commercial transfection reagent lipofectamine2000 was optimized according to the manufacturers guide.

RESULTS: Optimal ratio of P21 LK15 8R:pSIN GFP was determined as 2:1, respectively. GET protein exhibited serum resistant transfection of up to $38.1 \pm 1.8\%$, indicating potential *in-vivo* efficacy. Cells were transfected with P21 LK15 8R over a 3 day serial transfection. Cells treated with optimised Lipofectamine 2000 showed inhibited cell growth and lower cell viability than cells treated with P21 LK15 8R. 4-fold more GFP positive cells were detected using GET protein compared to Lipofectamine 2000.

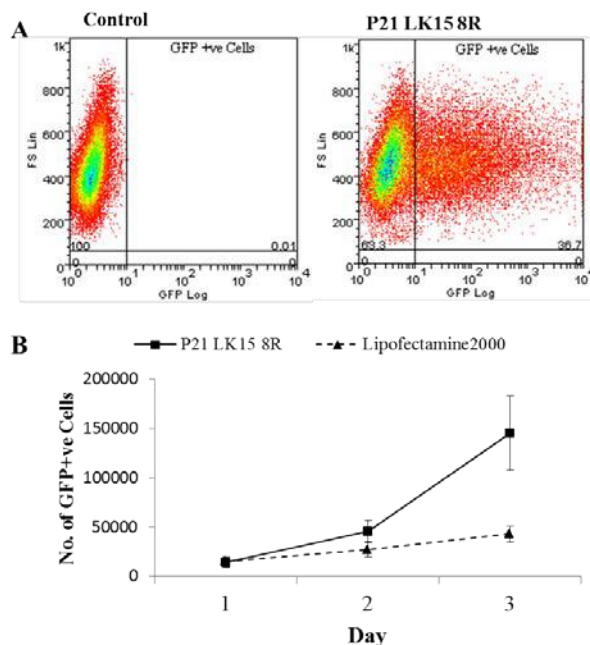


Fig. 1: Transfection efficiency was analysed by flowcytometry (A). Following a 3-day serial transfection 4-fold more GFP positive cells were determined using GET protein compared to commercial reagent Lipofectamine2000 (B).

DISCUSSION & CONCLUSIONS: In conclusion we have developed a serum-resistant transfection system that could potentially be applied *in-vivo* which is not cytotoxic and doesn't affect proliferation/expansion of cells. We believe that our system could facilitate new approaches for *in vivo* cell programming, gene correction, and in regenerative medicine.

ACKNOWLEDGEMENTS: This work was supported by the EPSRC.

Modelling the development of human tissue *in vitro* from pluripotent stem cells

DDG Owens¹, SA Przyborski^{1,2}

¹*School of Biological and Biomedical Sciences, Durham University, Durham, UK, DH1 3LE*

²*Reprocell Reinnervate, NETPark, Thomas Wright Way, Sedgfield, Co. Durham, UK, TS21 3FD*

INTRODUCTION: Newly derived pluripotent stem cell lines must be characterised to determine their pluripotent status and differentiation potential. Using the classical embryoid body approach, 3D aggregate cultures facilitate enhanced multi-lineage differentiation of pluripotent stem cells compared to 2D culture [1]. However, such cellular aggregates can become necrotic over prolonged culture in suspension, reducing their ability to form complex tissues [1]. 3D scaffolds offer an alternative method to culture aggregates and are being investigated for their ability to maintain the development of stem cell aggregates over prolonged *in vitro* culture.

METHODS: Aggregates of human embryonal carcinoma (hEC) cell line TERA2.cl.SP12 and murine embryonic stem cell line CGR8 were generated by spontaneous aggregation or using indented solid microspheres (Aggrewell[®] plates), respectively. Aggregates were cultured in suspension for between 5 and 21 days and then maintained using Alvetex[®] 3D polystyrene scaffold membranes for up to 14 days (Figure 1).

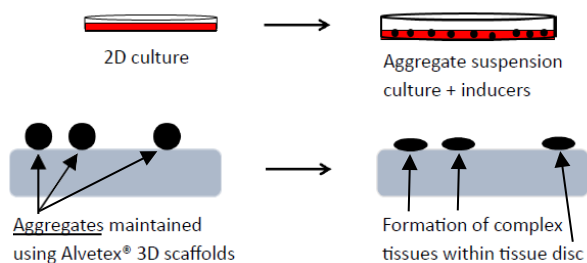


Fig. 1: Schematic of the method for culturing aggregates as tissue discs in 3D using Alvetex[®] scaffold membranes.

Aggregates were cultured in the presence of morphogens including retinoids and bone morphogenetic proteins in order to direct the differentiation of stem cells *in vitro*.

RESULTS: Pronounced effects on aggregate morphology were observed in hEC aggregates cultured in suspension for 21 days in the presence of a synthetic all-*trans*-retinoic acid analogue (ec23) [2] and cultured for a further 7 days using Alvetex[®] 3D scaffolds with pore sizes of either 40 μ m, 20 μ m, or 4 μ m (Figure 2).

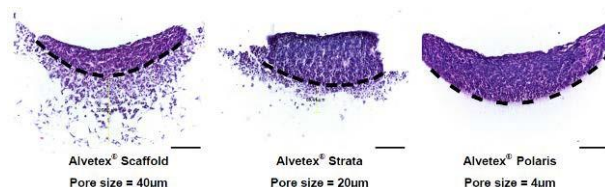


Fig. 2: Haematoxylin and eosin staining of hEC aggregates maintained in 3D using Alvetex[®] scaffold membranes. Scale bars represent 100 μ m.

Using Alvetex[®] Polaris as a growth substrate allowed aggregates to be maintained as an intact tissue disc (Figure 2). Aggregates treated with [10 μ M] ec23 and maintained in 3D underwent neural differentiation and expressed the neural marker β -III-tubulin (TUJ1) (Figure 3).

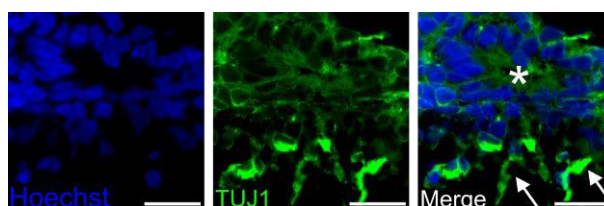


Fig. 3: TUJ1 immunofluorescence revealed morphological features typical of neural development including neural rosettes (*) and neurites (arrows). Scale bars represent 20 μ m.

DISCUSSION & CONCLUSIONS: Stem cell aggregates can be maintained for extended periods as tissue discs in 3D culture which maintains their viability and development potential. Differentiating pluripotent stem cells into complex tissues *in vitro* may provide an alternative to the current ‘gold standard’ teratoma formation pluripotency assay. Additionally, the role that morphogens and small molecules play in development can be investigated using this unique culture system, providing a novel approach to study aspects of human embryonic development.

ACKNOWLEDGEMENTS: Funding for this work was provided by The Grevillea Trust and Durham University.

Exploration of new anisotropic scaffolds for articular cartilage regeneration

HA Owida, N Kuiper and Y Yang

Institute of Science and Technology in Medicine, Keele University, UK

INTRODUCTION: Articular cartilage is a thin hydrated tissue, which covers articulating surfaces. It has an anisotropic, zonal-specific structure, extending from the articular surface to the subchondral bone¹. Cellular variations of the zones include cell shape, extracellular matrix (EMC) content and the orientation of collagen fibrils within the matrix, which leads to different mechanical proper and function of the zones².

The main challenge associated with cartilage tissue engineering is to generate the tissue with compositional and functional similarity to the native counterpart. The aim of this project is to fabricate and utilize nanofibrous scaffolds with different fiber organizations to mimic the native variations of ECM between zones, enabling a better cartilage tissue formation.

METHODS: Bovine chondrocytes extracted from knee of cows freshly slaughtered in a local abattoir were used with passage number up to 4. Electrospinning technique established in the lab³ has been used to produce nanofibrous zonal-specific scaffolds. 2% poly (lactic acid) solution has been use to obtain nanofibers. The nanofiber organization and density were changed to replicate the ECM structure at different zones (superficial, middle and deep zones) in articular cartilage. The chondrocytes were seeded in the nanofiber scaffolds encapsulated by agarose hydrogel. Various characterisation assays including live images to assess cell morphology, MTT for cell proliferation and DMMB assay to quantify GAG production have been conducted.

RESULTS: Nanofibrous scaffolds with aligned fiber (for superficial zone), random fiber (middle zone) and bundle-like fiber arrangement (for deep zone) have been produced. The seeded chondrocytes grown on aligned nanofiber scaffold exhibited elongated, highly proliferated cell morphology and low GAG production; whilst bundle-like fiber scaffold produce aligned chondrocyte clusters with high GAG production; random aligned nanofiber scaffold had the cellular behaviour between other two types of scaffolds (Figure 1 and 2).

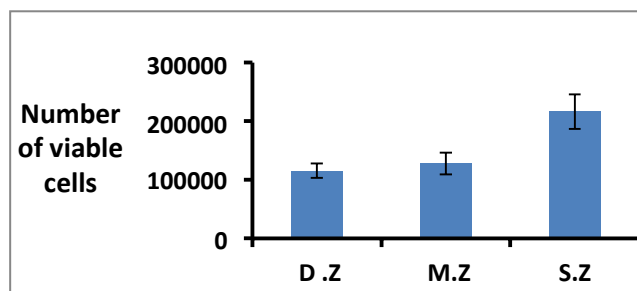


Figure 1: Cell proliferation outcome from MTT in different zonal scaffolds; D.Z: Deep zone, M.Z: Middle zone, S.Z: Superficial zone.

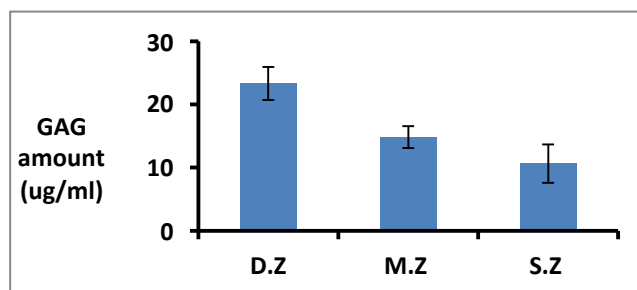


Figure 2: GAG production results in different zonal scaffolds; D.Z: Deep zone, M.Z: Middle zone, S.Z: Superficial zone

DISCUSSION & CONCLUSIONS: Nano-fabricated zonal-specific 3D scaffolds have induced distinct cellular response of chondrocytes, which demonstrates the hope to generate structural and functional cartilage tissue similar to native counterpart.

Novel clay gels as regenerative microenvironments for the treatment of diabetic foot ulcers

DJ Page^{1,3}, JI Dawson¹, R Mani⁴, ROC Oreffo¹, CE Clarkin², ND Evans^{1,3}

¹Centre for Human Development and Health, Stem Cells & Regeneration, Faculty of Medicine, University of Southampton, U.K.; ²Centre for Biological Sciences, Faculty of Natural and Environmental Sciences, University of Southampton, UK; ³Department of Bioengineering, Faculty of Engineering and the Environment, University of Southampton, UK
⁴Medical Physics & Bioengineering, University Hospital Southampton NHS Foundation Trust, UK

INTRODUCTION: People that suffer with diabetes have a high risk of developing a chronic wound known as a diabetic foot ulcer (DFU). There has been recent interest in treating DFUs with biological agents to improve wound healing. However, delivery of biological agents in an active form remains a significant clinical challenge. To address this problem we propose using a synthetic clay biomaterial called Laponite; its unique layered silica/metal cation structure allows formation of a hydrated gel network which retain and deliver biological agents¹. Thus, our aim is to test the efficacy of Laponite to deliver active biological agents as a means to improve chronic wound healing rates. Herein, we tested i) the uptake and retention of a small molecule Wnt signal agonist; 6-bromindirubin-3-oxime (BIO) by Laponite and ii) whether Laponite could be retained at skin injury sites in a murine model.

METHODS: In vitro BIO uptake and release study: To test BIO uptake by Laponite, 3% Laponite hydrogel capsules were added to media containing 50 μ M of BIO. Release assays involved adding Laponite capsules premixed with 5 μ M of BIO to media. A control assay was performed in parallel with untreated media spiked with BIO (5 μ M) upon recovery. Recovered media was used to culture 3T3 mouse fibroblast cells and BIO concentration was determined using the Enzo Leading Light® Wnt Reporter Assay kit. In vivo full-thickness skin wound healing study: two left and two right side surgical wounds were created on the dorsum of male MF1 mice and a Tegaderm dressing applied. One day post wounding, left wounds were treated with 3% Laponite hydrogel and right wounds with PBS. Wound tissue samples were taken at 3, 5, and 7 days, fixed with 4% PFA, paraffin embedded, sectioned and stained.

RESULTS: In vitro BIO uptake and release study: Preliminary results showed that Laponite hydrogel adsorbed exogenous BIO following 0.5 and 2 minutes of treatment versus controls ($p < 0.05$), however no significance was measured at the remaining time points (Figure 1A). BIO was also

successfully retained by Laponite hydrogels with no evidence of release (Figure 1B). Control assays showed Laponite hydrogels did not negatively impact the 3T3 cell growth media. In vivo full-thickness wound healing study: Preliminary results showed that Laponite hydrogel was retained within the wound bed over 7 days. There was also an indication of increased cellular infiltration compared to the PBS control by day 7.

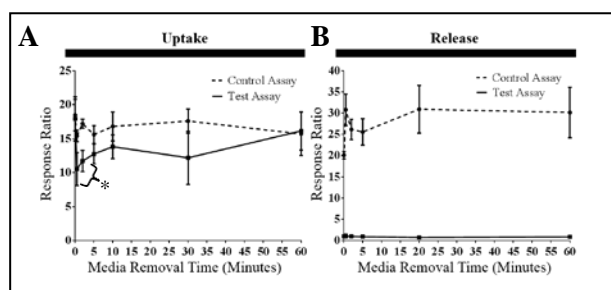


Fig. 1: BIO release/uptake test assay data (* denotes $p < 0.05$, uptake test assay data)

DISCUSSION & CONCLUSIONS: Our *in vitro* study highlights successful uptake and retention of BIO by Laponite. In addition, our *in vivo* study demonstrated the successful retention of Laponite hydrogel over 7 days; this may provide significant clinical potential to directly localise biological agents such as Wnt agonists to chronic wounds. Furthermore if successfully translated *in vivo*, Laponite could potentially stimulate stem cells that are known to exist in the dermis and hair follicle bulb of skin tissue, encouraging regeneration of proliferative cells²⁻³. Overall, this project will continue to elucidate whether Laponite can act as a suitable carrier of key stimulatory biological agents and ultimately become a novel method for treating diabetic foot ulcers.

ACKNOWLEDGEMENTS: Many thanks to Tizard, Grundy Educational Trust, and Novo Nordisk for providing funding for this project.

On course to the next generation of prosthetics: Chemical functionalised substrates for neuronal guidance

[MM Pardo-Figuerez](#)^{1,2}, NRW. Martin¹, DJ Player¹, SDR Christie² and MP Lewis¹

¹ School of Sport, Health and Exercise Sciences, ² Department of Chemistry, School of Science
Loughborough University, Loughborough, LE11 3TU

INTRODUCTION: The “next generation” of prosthetics aims to restore natural human functions through interaction with existing structures¹. One of the most challenging of these areas is the integration of a prosthetic device with the existing neuromuscular system of a patient via neurons grown *in vitro*. The optimisation of this process starts by finding a substrate which can support the growth and behaviour of the neurons, particularly neurite extension including length and directionality; these are known to be highly dependent on environmental conditions. Chemical coatings have proved applicable in a wide variety of situations for cell support. In addition, engineering techniques can be incorporated with such coatings, and thus the potential to guide neuronal cells in a specified direction could be achieved^{1,2}. We aimed to find different chemical coatings which could both support and inhibit cell growth and neurite extension (length and directionality). The next steps would then be to use varying combinations of these coatings to achieve precise control over cellular response.

METHODS: Glass slides were chemically modified by attaching different polymer chains onto the surface via a “grafting from” method. A variety of coatings (see table 1) were tested by looking at the viability (LIVE/DEAD® Cell Viability assay), neurite length and cell proliferation (alamarBlue® assay, Quant-iT™ PicoGreen® dsDNA assay) of the SHSY-5Y cell line. After this characterisation, coatings were chosen as either “permissive” or “non-permissive” substrates and were patterned by MIMIC technique³.

Acronym	Name of the chemical coating
BIBB	2-bromoisobutyryl bromide
APTES	3-Aminopropyltriethoxysilane
PKSPMA	Poly(potassium 3-sulfopropyl methacrylate)
PMETAC	Poly[2(methacryloyloxy)ethyltrimethylammonium chloride]
PHEMA	Poly(2-hydroxyethyl methacrylate)
PMMA	Poly(methyl methacrylate)

Table 1. Chemical coatings used in this study.

RESULTS: SHSY-5Y cells were cultured on the coatings until 50% confluent was reached, then cell differentiation was induced by the addition of

10µM retinoic acid. APTES and BIBB promoted neuronal differentiation as assessed by neurite length whilst neurons cultured on PMETAC and PKSPMA failed to adhere to the surface. LIVE/DEAD® staining was used to confirm that PMETAC caused cellular death which PKSPMA did not, suggesting that cells simply were unable to attach to this substrate. The “micromolding in capillaries” technique was then used in order to pattern substrates to promote cell directionality, using PKSPMA as an ideal substrate to restrain neuronal outgrowth and APTES/BIBB, which were shown to be good options for the cell-attractive zones. A binary coating formed by BIBB/PKSPMA showed that cells adhered to the BIBB zone, whilst avoiding the zones formed by PKSPMA (Figure 1).

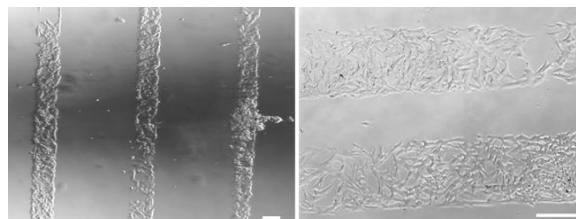


Fig. 1. Binary coating created by BIBB/PKSPMA after 4 days in growth media. Scale bar=200 µm

DISCUSSION & CONCLUSIONS: The formation of a binary pattern by selecting “permissive” or “non-permissive” coatings previously characterised allowed us to guide and restrain the growth of neuronal cells. In the long term, this system will be incorporated into a larger scale manufacturing process with the aim of developing the next generation of smart prosthetics.

ACKNOWLEDGEMENTS: Thanks to Loughborough University for supporting this project.

Ti/Co doped phosphate bioactive glass microcarriers: effect on hBM-MSCs osteogenic and angiogenic responses

C Peticone¹, JC Knowles^{2,3}, M Micheletti¹, JJ Cooper-White^{4,5,6}, IB Wall^{1,3}

¹Department of Biochemical Engineering, UCL, UK ²UCL Eastman Dental Institute, UK

³Department of Nanobiomedical Science, Dankook University, Cheonan, South Korea, ⁴Australian Institute for Bioengineering and Nanotechnology, The University of Queensland, Australia ⁵School of Chemical Engineering, The University of Queensland, Australia, ⁶Division of Materials Science and Engineering, CSIRO, Clayton, Australia

INTRODUCTION: The establishment of a robust and reproducible bioprocess for the production of functional bone tissue is still an unmet clinical challenge. A “bottom-up” approach, in which modular micro-units of tissue are used as building blocks to produce larger tissue, could be used as a valid alternative to a more traditional “top-down” approach, involving the use of scaffolds of predefined size. For example, microcarrier-based tissue engineering could represent a potential strategy to address osseous defects of different sizes and shapes. In particular, the use of microcarriers composed of a suitable scaffold material for bone tissue engineering meet the dual requirements of scalable cell expansion and commitment towards an osteogenic phenotype, within a single bioprocessing step.

In this study, the use of bioactive phosphate glass microcarriers for bone tissue engineering applications was investigated. As this material is completely soluble and non-toxic, it can be implanted *in vivo* together with cells. Furthermore, the tunable glass composition can be easily engineered to induce specific structural and biological properties¹. Here, we studied the effect of doping the glass with titanium and cobalt, as these ions have been shown to induce osteogenesis¹ and angiogenic growth factor secretion², respectively.

METHODS: Human bone marrow mesenchymal stromal cells (hBM-MSCs) were cultured on phosphate bioglass microspheres. Two glass compositions were used, one doped with titanium only and one doped with titanium and cobalt. Effects on cytotoxicity, proliferation, osteogenic differentiation and angiogenic responses were assessed over a two-week period.

RESULTS: hBM-MSCs were found to proliferate on both glass compositions, confirming the biocompatibility of the substrates. The formation of macroscale ‘tissue-like’ aggregates and upregulation of osteogenic markers i.e. alkaline phosphatase (ALP), type I collagen and matrix

mineralization were shown in the absence of cobalt. Enhanced angiogenic responses including VEGF upregulation and fibronectin secretion were also observed in response to cobalt.

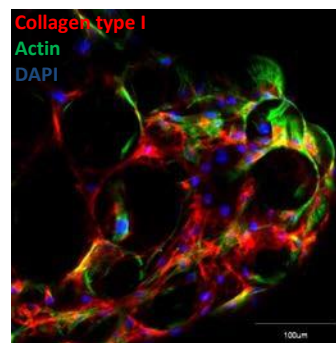


Fig. 1: hBM-MSCs cultured for 1 week on Ti-doped bioactive glass microcarriers, presenting upregulation of type I collagen secretion in the ECM.

DISCUSSION & CONCLUSIONS: This study addressed the potential use of metal-doped phosphate bioactive glass microspheres for the production of functional micro-units of tissue for bone regeneration. Both compositions were found to be cytocompatible, but induced different responses on hBM-MSCs. While differentiation towards an osteogenic pathway was enhanced in titanium-doped bioactive glass, the addition of cobalt had a main effect on angiogenic responses. Identifying an optimal ratio between microcarriers of different compositions could underpin a possible strategy to control both responses simultaneously, enabling the establishment of a scalable platform for *in vitro* vascularized bone manufacturing.

Mechanical unloading induces tissue and cellular responses in engineered skeletal muscle

DJ Player^{1,2}, NRW Martin¹, MP Lewis^{1,2},

¹School of Sport, Exercise and Health Sciences, Loughborough University, UK, ²Arthritis Research UK Centre for Sport, Exercise and Osteoarthritis.

INTRODUCTION: Recent reports suggest that the onset and development of osteoarthritis (OA) may reflect degeneration of the functional and structural properties of skeletal muscle¹. This is thought to occur through processes associated with mechanical unloading of the affected limb and local and systemic inflammation, contributing to reduced joint stability and varus-valgus movement². We have used tissue engineered skeletal muscle to investigate mechanical unloading and its role in the contribution to skeletal muscle degeneration.

METHODS: Tissue engineered skeletal muscle constructs were fabricated as previously described³, with slight modifications. Briefly, 4×10^6 C2C12 muscle precursor cells (MPC's) were seeded in 1 ml type-1 rat-tail collagen hydrogels and allowed to develop for 14 days until aligned myotubes were present ($n = 6$ constructs per condition). At 14 days, experimental constructs (unloaded condition, UNL) were reduced in length by ~33% of original length for a further 7 days to induce a reduction in mechanical loading. Control constructs (CON) remained at the original length for the 7 day experimental period. Macroscopic observations were recorded throughout the experimental period and following 7 days unloading, constructs were fixed and stained for the actin cytoskeleton.

RESULTS: Macroscopic observations demonstrated UNL constructs rapidly remodel the collagen matrix, to restore the inherent tension within the system (Fig. 1). Despite construct length being altered, there was no change in construct width ($p > 0.05$) compared to CON, indicating reorganisation of the matrix in the longitudinal axis.



Fig. 1. Matrix remodelling following 7 days mechanical unloading. A = CON, B = UNL. Scale bar = 10 mm.

Histological analyses revealed a high degree of alignment and multinucleate differentiation of seeded cells in CON (Fig. 2, A). UNL constructs displayed significantly reduced myotube width compared to CON (Fig. 2 B, $p < 0.05$), evident with the 'spindle-like' morphology. Furthermore, multinucleate spherical cell masses (arrows) were evident in UNL constructs, consistent with myotubes detaching from the matrix.

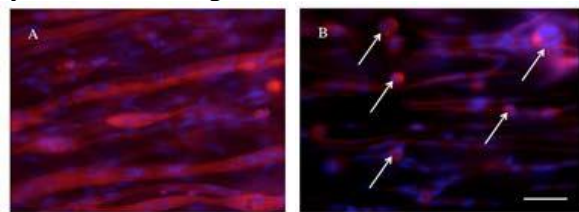


Fig. 2. Morphological analyses of control (A, CON) and unloaded (B, UNL) constructs. Arrows indicate presence of multinucleate cell masses. Scale bar = 50 μ m.

DISCUSSION & CONCLUSIONS: The phenomenon of matrix remodelling following unloading is thought to exist as a homeostatic mechanism to maintain tension within the model. The mechanism by which this occurs is thought to be mediated by both MMP's, active (actin-myosin) and passive cytoskeletal-extracellular matrix (desmin, titin, integrins etc.) components. Future work will seek to investigate the fate of the detached cell masses. This model can be used in future investigations to understand the role of mechanical unloading in the development of clinical conditions including OA.

ACKNOWLEDGEMENTS: This study was supported financially by the Arthritis Research UK Centre for Sport, Exercise and Osteoarthritis (Grant reference 20194).

Hydrostatic preconditioning of hMSC-collagen scaffolds enhances fracture repair in an ex vivo nonunion defect

J Price, JR Henstock, AJ El Haj

Institute of Science and Technology in Medicine, University of Keele, Stoke-on-Trent, United Kingdom.

INTRODUCTION:

Mechanical loading of bone *in vivo* results in the generation of hydrostatic forces as bone compression is transduced to fluid pressure in the canalicular network. It has been shown previously that physiological hydrostatic loading regimes result in superior bone growth in *ex vivo* embryonic chick femurs [1]. The aim of this study was to investigate the effect of physiological loading for pre-conditioning hMSC collagen hydrogels prior to implantation in an embryonic chick femur fracture repair model.

METHODS:

A hydrostatic pressure regime of 0-279kPa at 1Hz, was applied to hMSC seeded collagen gels for 1hour per day for 1,3 and 5 days per week. After 28 days the hydrogels were implanted into organotypically cultured chick femurs to simulate the fracture repair. The constructs were organotypically cultured for a further 14 days before analysis of new bone formation in the defect was performed. New bone formation was assessed by X-ray microtomography and qualified by histology.

RESULTS:

After 28 days, hydrostatic preconditioning increased hydrogel density with increasing days/week stimulation. Preconditioned hydrogels linearly increased defect mineralization after implantation into femurs, with significant increases in new bone formation in 1, 3 and 5days/week vs static controls ($P<0.05$).

DISCUSSION & CONCLUSIONS:

Hydrostatic preconditioning increases bone volume in collagen - hMSC implants in ex vivo chick femurs after 14 days culture. The study demonstrates that mechanical conditioning of cell seeded scaffolds prior to implantation could potentially be used to enhance bone regeneration in a clinical setting.

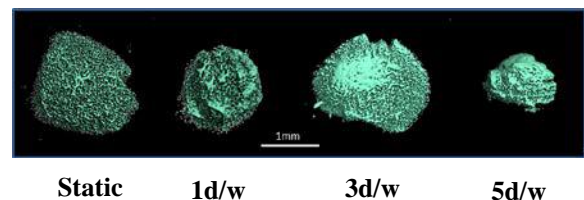
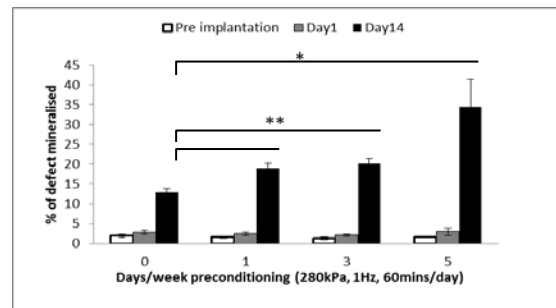


Fig. 1. Assessment of mineralization by μ CT demonstrated a linear increase in new bone formation due to hydrostatic preconditioning. Image reconstructions of the defect site region reveal extensive formation of dense mineralized tissue in hydrogels preconditioned prior to implantation. Scale bar = 1mm

ACKNOWLEDGEMENTS:

The author would like to acknowledge TGT/Inston and the EPSRC DTC in regenerative medicine.

DISCLOSURES:

There is no conflict of interest with this work

Impact of substrate topography on the growth of pluripotent stem cells cultured in three dimensions

RH Quelch¹, SA Przyborski^{1,2}

¹ School of Biological and Biomedical Sciences, Durham University, UK. ² ReproCELL Reinnervate Ltd., Sedgefield, UK.

INTRODUCTION: The environment in which cells are cultured impacts cellular morphology and signaling pathways¹. A number of three dimensional (3D) methods of culturing cells have been developed in recent years in order to maintain cells in a format that bridges the gap between *in vitro* and *in vivo* biological research². This area is of particular importance in stem cell biology whereby the developmental potential of cells is directly influenced by their microenvironment³. It is hypothesised that by maintaining pluripotent stem cells in a 3D environment that is more like the inner cell mass in blastocysts, and allows cells to group close together, and their structure and behaviour will more closely mimic that of the cells *in vivo*. It is thought that this will result in a more rounded 3D morphology, enhanced stem cell phenotype and ultimately increased developmental potential and differentiation.

METHODS: To test this TERA2.cl.SP12 embryonal carcinoma cells were first used. Cells were seeded onto Alvetex[®] Polaris at a density of 0.25 million cells per insert. After 5 days, cells were removed from inserts (using a combination of 0.25% Trypsin EDTA and pipette flushing of the media), counted and reseeded, completed in parallel with cells cultured in 2D. Cells upon inserts were visualised by H&E staining of OCT-embedded cryosectioned samples. Cell shape descriptors (cell circularity and area) were quantified and levels of cell surface marker expression were assessed by flow cytometry and immunocytochemistry.

RESULTS: A protocol has been optimised to maintain pluripotent stem cells in 3D culture. The approach allows a dense layer of cells to be maintained upon the substrate surface (as visualised in Figure 1 A & B). Propagation and maintenance of cells in 3D has resulted in a change in morphology represented by a significant increase in cell circularity and decrease in cell area (Figure 1 E & F). This change in morphology also correlates with an increase in pluripotency marker expression (Figure 1 C & D).

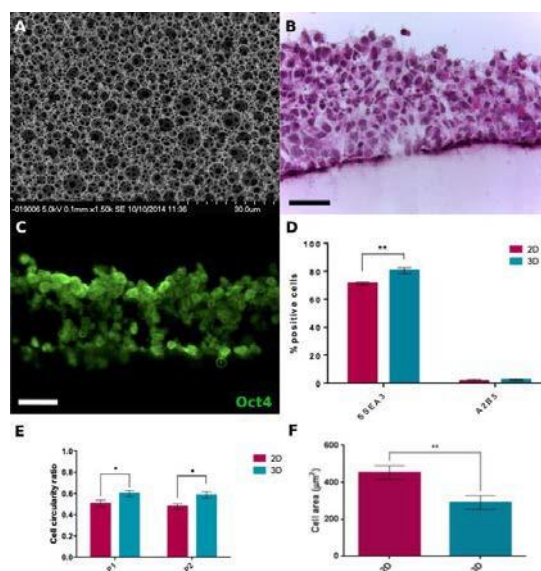


Fig. 1: Maintenance and propagation of human pluripotent stem cells in 3D culture. (A) SEM showing the structure of Alvetex[®] Polaris; (B) Stem cells maintained in 3D on the surface of Polaris (H&E); (C) Cells on Polaris express high levels of stem cell markers (Oct4); (D) Flow cytometric analysis shows significant increase in stem cell marker expression after only two passages in 3D and absence of differentiation marker A2B5; (E&F) Measurement data show that cells maintained on Polaris change their morphology and acquire a more 3D phenotype. Scale: 50 µm.

DISCUSSION & CONCLUSIONS: We demonstrate that pluripotent stem cells can be propagated and maintained in 3D culture resulting in changes to the stem cell phenotype. We are currently applying this technology to examine the impact of 3D propagation on stem cell developmental potential, including the use of embryonic and induced pluripotent stem cells.

ACKNOWLEDGEMENTS: This research is funded by a BBSRC industrial case studentship in partnership with ReproCELL Reinnervate Ltd.

Mechanical and topographical cues affecting the stem cell fate for bone tissue engineering

Y Reinwald¹, AJ El Haj^{1*}

¹*Institute of Science and Technology in Medicine, University of Keele, Stoke-on-Trent, United Kingdom.*

INTRODUCTION: Topographical and chemical cues are vital for cell adhesion, proliferation and differentiation and hence tissue maturation. In addition, for the generation of functional tissues it is of great importance to replicate the structural as well as the mechanical environment cells experience *in vivo*. Bioreactors are widely recognized as tools which provide a physical growth environment for cells and tissue constructs enabling the investigation of cell fate and tissue maturation [1-4]. This study aims to investigate the combinatory effect of topographical, chemical and physical cues on stem cell differentiation for bone tissue regeneration when seeded on different cell culture formats.

METHODS: Bone marrow derived human mesenchymal stem cells (hBMSC) were seeded onto standard tissue culture well plates (TCP) and commercial electrospun random (R) and aligned (A) PCL nanofibres. Tissue culture formats were subjected to hydrostatic pressure for 21 days at 270 kPa, 1Hz for 1 hour daily and compared to non-stimulated samples. All tissue culture formats were cultured in osteogenic medium. MTT assay and live/dead stain were performed to assess cell viability and cell metabolic activity. To investigate fiber morphology and for the chemical characterization of fibrous scaffolds after 21 days SEM and EDX analysis were utilized. qPCR and alizarin red stain were applied to determine changes in gene expression and calcium deposition.

RESULTS: SEM imaging revealed that PCL fibre diameters ranged between 200 nm to 3.0 µm with the majority of random fibers being smaller than 800 nm. Aligned fiber diameters exhibited a narrower diameter range with over 70% being smaller than 1.2 µm. Mechanical stimulation resulted in increased cell proliferation on all tissue culture formats compared to non-stimulated controls. Cell elongation and spreading was affected by fiber orientation. Positive alizarin red stain was observed on all culture substrates indicating calcium deposition by cells. Furthermore, EDX analysis revealed the presence of calcium phosphate on aligned and random fibers. The up-and down regulation of RUNX-2, SOX-9 and ALP were influenced by mechanical stimulation and fiber orientation.

DISCUSSION & CONCLUSIONS: This study aimed to investigate the effect of topographical cues in combination with hydrostatic pressure on the osteogenic potential of hBMSC seeded onto different cell culture formats. It has been demonstrated that mechanical stimulation resulted in clear trends in the expression of osteogenic markers, calcium deposition, cell viability

and metabolic activity. Hydrostatic pressure enhanced the osteogenic potential of hBMSC, cell proliferation and has previously been shown to enhance mineralization⁴. In summary, chemical and topographical cues together with mechanical stimulation effect stem cell proliferation and differentiation and are essential stimuli for bone formation.

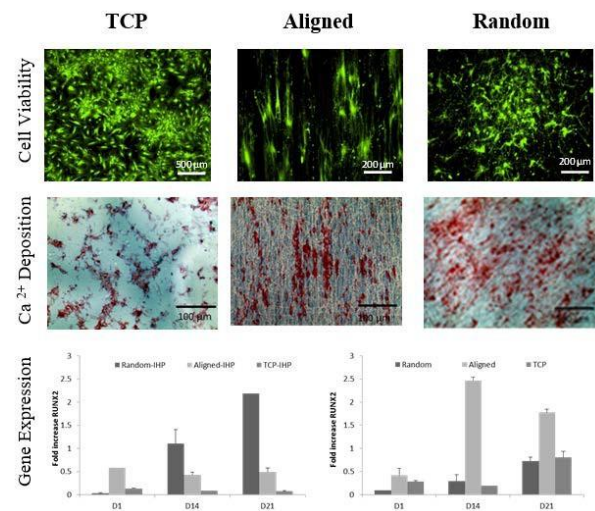


Figure 1: Cell viability and calcium deposition of mechanically stimulated TCP, aligned and random PCL fibers on day 21. Scale bars = 100 µm, 200 µm and 500 µm respectively. Expression of RUNX-2, for mechanically stimulated (left) and unstimulated (right) culture formats over 21 days, expression normalized to unstimulated control.

ACKNOWLEDGEMENTS: The author would like to thank the EPSRC Centre for Innovative Manufacturing in Regenerative Medicine (ECP007/1010) for funding and Michael Rotherham for technical advice on the qPCR.

Osteosarcoma cell encapsulation for biomedical applications

R Ribeiro^{1,2}, AM Ferreira^{1,2,3}, K Dalgarno¹

¹ *School of Mechanical and Systems Engineering, Newcastle University, UK.* ² *Institute Of Cellular Medicine, Newcastle University, UK.* ³ *Arthritis Research UK Tissue Engineering Centre, UK*

INTRODUCTION: Single cell encapsulation with semi-permeable biodegradable shell is an attractive procedure for different biomedical applications¹, such as bioprinting and regenerative medicine. The work reported in this paper explored the use of PLL to encapsulate single osteosarcoma cells (U-2 OS), evaluating the effect of different PLL concentrations on the viability and morphology of the cells.

METHODS: Single osteosarcoma cells (U-2 OS cells) were encapsulated into poly-L-lysine (PLL, MW 15,000-30,000, Sigma Aldrich UK) shells. For encapsulation, PLL was dissolved into Hank's Balanced Salt Solution (HBSS) without phenol red at four different concentrations: 400 µg/mL, 200 µg/mL, 100 µg/mL, 50 µg/ml. A cell suspension of 4×10^6 cells per count was prepared for each polymer concentration, and then incubated for 15 minutes at 37°C in 5% CO₂ for polymer coating. Afterwards, encapsulated cells were washed twice with HBSS, using centrifugation at 250g for 5 min to remove any polyelectrolyte excess. Cell viability was evaluated by MTT (3-(4,5-dimethylthiazol-2-yl)-2,5-diphenyltetrazolium bromide) and Live-Dead assays after 4 hours, and 1, 3, and 7 days. The mechanism of capsule release was studied using Transmission Electron Microscopy (TEM) and cell morphology by fluorescence and confocal microscopy. For fluorescence and confocal imaging, the PLL was labelled with fluorescein isothiocyanate (PLL-FTIC, MW 15,000-30,000, Sigma Aldrich).

RESULTS: Osteosarcoma cells were successfully encapsulated using PLL as a polycation. MTT and live dead assays showed a viability increase with polymer concentration decrease, obtaining about 70% viable cells 7 days after encapsulation at lowest concentration (50 µg/ml). However, fluorescence and confocal microscopy demonstrated that cells were not fully encapsulated at this low concentration (Fig. 1b)). For higher concentrations (200 and 400 µg/ml) cells were still encapsulated after 24 hours and undergoing apoptosis. The cytotoxic effect of the higher polymer concentrations was confirmed by TEM, where highly vacuolated cells and high polymer uptake was observed.

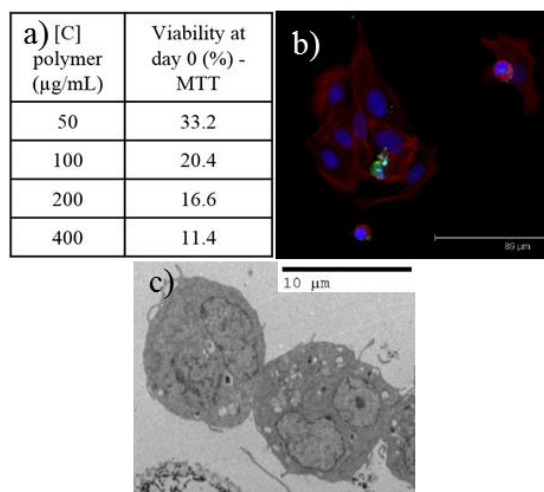


Fig. 1: a) Cell viability 4 hours after encapsulation; b) Confocal microscopy image of U-2 OS cells 4 hours after encapsulation (50 µg/mL); c) TEM image 4 hours after encapsulation (50 µg/mL).

DISCUSSION & CONCLUSIONS: The best cell survival was obtained for the two lower concentrations. Encapsulated cells with these two polymer concentrations were able to recover and self-renew within three days post-encapsulation, achieving after one week 71% and 45% of cell viability in contrast to <10% survivability level achieved for the highest PLL concentration. For the lowest concentration it is likely that unencapsulated cells contributed to the higher viability, as their proliferation would not be inhibited by the coating. By confocal and TEM, the formation of the initial PLL capsule was confirmed as well as the polymer incorporation. Polymer endocytosis was seen after 4 hours and for up to three days of encapsulation. Engineering a protective cell surface coating without causing damage to the cell membrane or cell death is possible by controlling the polyelectrolyte concentration, but could be enhanced through choice of an alternative encapsulant.

ACKNOWLEDGEMENTS: R Ribeiro would like to thank Newcastle University for funding his studentship.

Regulation of Wnt signalling and promotion of bone mineralisation using peptide-conjugated magnetic nanoparticles

M Rotherham¹, JR Henstock¹, O Qutachi², KM Shakesheff², AJ El Haj¹

¹*Institute for Science and Technology in Medicine, Keele University, Stoke-on-Trent, UK.* ²*School of Pharmacy, University of Nottingham, Nottingham, UK.*

INTRODUCTION: Wnt signalling is involved in the regulation of a number of cellular processes, and is an essential regulator of the differentiation of human mesenchymal stem cells (hMSC). Recombinant Wnt proteins may therefore have considerable therapeutic value, however they are both expensive and difficult to produce in sufficient quantities with efficacious bioactivity. The synthetic peptide UM206 is a ligand for the Wnt receptor Frizzled. By attaching UM206 peptide to magnetic nanoparticles (MNP), the synthetic ligand complex can be remotely manipulated using a magnetic field, allowing external control of the binding affinity between the peptide and Frizzled. Remote manipulation of Wnt signalling using magnetic nanoparticles has been shown previously¹. Wnt signalling synergistically interacts with other signalling pathways which transduce growth factor signals such as bone morphogenic proteins (BMPs) in order to modulate bone development². The use of Wnt activating MNP and BMP2 in bone development is investigated using *in vitro* and an *ex vivo* chick femur model.

METHODS: hMSC (P3-5) were isolated from fresh bone marrow (Lonza). UM206 peptide was covalently conjugated to MNP (Micromod) by carbodiimide activation. 2×10^5 cells were labelled with 25 $\mu\text{g}/\text{mL}$ of UM206-MNP. Chick Femur's were isolated from E11 Dekalb chicks. Magnetic stimulation (1hr sessions, 1Hz) was provided by an oscillating magnetic force bioreactor (MICA Biosystems).

RESULTS: Stimulation of hMSC with UM206-MNP resulted in nuclear translocalisation of β -catenin and activation of a Wnt TCF/LEF luciferase reporter, both hallmarks of Wnt pathway activation. Pathway activation in this manner was also unaffected by the addition of the Wnt inhibitor Dkk1. Treatment of hMSC with UM206-MNP in osteogenic media resulted in increased matrix production and organisation after 21 days as shown by Alizarin red, Sirius red and Osteocalcin staining. In the chick femur bone formation model, injection of UM206-MNP labelled cells into the epiphyseal region resulted in an increase in mineralisation over unlabelled

control cells as shown by μCT and Histology. The addition of BMP2 to the injection site resulted in a synergistic increase in bone mineral density over UM206-MNP or BMP treatment alone groups.



Fig. 1: Bone formation in chick foetal femur. Whole mount image showing calcium deposition (Alizarin red staining) in the bone collar and secondary mineralisation sites at the epiphyseal regions injected with hMSC labelled with UM206-MNP.

DISCUSSION & CONCLUSIONS:

Remote Wnt pathway activation in hMSC using peptide functionalised MNP has been demonstrated. UM206-MNP mediated Wnt pathway activation has been shown to support bone formation *in vitro* and in an *ex vivo* chick femur model. Enhanced bone formation when UM206-MNP were delivered with BMP2 releasing microparticles was also shown and demonstrates the synergistic interaction between certain growth factors and signalling pathways can be important for bone tissue formation. This work shows that Bio-ligand functionalised MNP technology is capable of facilitating external control over signal transduction and has applications both as a research tool and for regulating tissue formation in clinical cell therapies.

ACKNOWLEDGEMENTS: Dr's Bin Hu and Neil Farrow are acknowledged for providing the Wnt reporter. We acknowledge the BBSRC (grant number BB/G010560/1) for funding this work.

Label-free monitoring of cell-seeded collagen type I hydrogels reveals marked changes in extracellular architecture over time

[K Sanen](#)¹, [R Paesen](#)¹, [W Martens](#)¹, [S Luyck](#)¹, [JB Phillips](#)², [I Lambrichts](#)¹, [M Ameloot](#)¹

¹ [Biomedical Research Institute, Hasselt University, Diepenbeek, Belgium.](#) ² [Biomaterials & Tissue Engineering, Eastman Dental Institute, University College London, UK](#)

INTRODUCTION: The field of neural tissue engineering has provided a range of artificial nerve conduits to guide axonal growth. For optimal regeneration, the scaffold needs to mimic key features of the native environment: Schwann cells that secrete neurotrophic factors and align to direct neurite outgrowth and an organized extracellular matrix (ECM). Recently, glial differentiated human dental pulp stem cells (d-hDPSCs) were shown to self-align within a tethered collagen type I hydrogel system [1]. However, changes in hydrogel architecture remain to be elucidated. Although many optical microscopy techniques can visualize individual cells in their ECM, most of them require exogenous dyes which could have phototoxic effects and perturb native cellular behaviour [2]. In order to truly understand ECM remodelling by embedded cells, it is essential to monitor the interaction of these cells with the 3D construct continuously in a label-free manner.

METHODS: d-hDPSCs were seeded in a tethered collagen type I hydrogel [1]. These 3D constructs were monitored in real-time by two-photon excitation (TPE) autofluorescence and second harmonic generation (SHG) imaging microscopy to visualize hDPSCs and collagen type I fibres respectively. To capture possible effects of local hydrogel remodelling by the cells, different zones near cellular processes were taken into account. The resulting images with high contrast and submicron resolution were further analysed by our new and flexible image correlation spectroscopy (ICS) based model [3] to characterize and quantify the spatial organization and structural characteristics of collagen type I fibres over time.

RESULTS: Shortly after casting ($t = 0\text{h}$), cells appeared round and collagen type I fibres seemed to be randomly oriented (Fig. 1, left). After contraction ($t = 32\text{h}$), alignment of both cells and collagen fibres was observed (Fig.1, right). ICS analysis revealed a time-dependent increase in collagen density, which was similar for all the zones near cellular processes. In addition, a more preferential orientation of the collagen type I fibres parallel to the longitudinal axis of the construct (same direction as cell alignment) was observed. Zones in line with cellular processes were

remodelled significantly faster with regard to direction of fibre orientation compared to zones not in line with cellular processes.

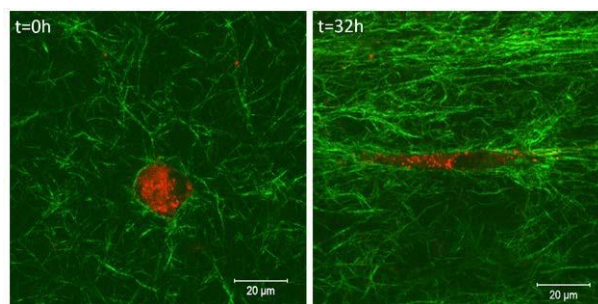


Fig. 1: Label-free and real-time monitoring of hDPSCs contracting a tethered collagen type I hydrogel. Red = TPE cellular autofluorescence; Green = SHG signals from collagen type I fibres.

DISCUSSION & CONCLUSIONS: For the first time, the process of cellular self-alignment in a collagen type I hydrogel has been monitored label-free and in real-time. Furthermore, a good estimate on the average collagen density and the preferential orientation of fibres could be obtained by ICS analysis. The detailed quantification of hydrogel architecture in different zones over time made possible by these techniques will contribute to successful future development, screening and selection of scaffolds for a broad range of tissue engineering applications.

ACKNOWLEDGEMENTS: This research is part of the Interreg EMR IV-A project BioMIMedics (www.biomimedics.org) and is co-financed by SMEs, the European Union, local governments, Research Foundation Flanders (grant 11N0914N) and research institutes. The authors are grateful to L. Michiels¹, N. Smisdom¹ and K. Notelaers (M4I Division of Nanoscopy, Maastricht University, Maastricht, The Netherlands) for their input.

Polymeric-nanoparticles for the delivery of small molecules during bone fracture repair

E Scarpa¹, AA Janeczek¹, ROC Oreffo¹, TA Newman² and ND Evans¹

¹ Bone and Joint Research Group, Centre for Human Development, Stem Cells and Regeneration, Southampton General Hospital, Tremona Road, Southampton, SO16 6YD, UK. ² Clinical Neurosciences, Building 85, Highfield Campus, University of Southampton, Southampton, SO17 1BJ, UK.

INTRODUCTION: In the UK approximately 2.3 million people experience a bone fracture every year. 10% of these fractures results in a ‘non-union’. Skeletal stem cells (SSC) hold significant therapeutic potential for application in bone reparation and fracture healing.

The activation of the Wnt signaling pathway is pivotal in determining SSC proliferation and osteoblastic differentiation¹. This can be achieved by the use of small molecules including 6-bromoindirubin-3’oxime (BIO). However, targeted delivery of BIO to the injury site is crucial in order to avoid off-target detrimental effects.

Polymersomes (PMs) are polymeric nanoparticles that can be loaded with small therapeutic molecules enabling spatio-temporal controlled delivery². The aim of this study was to demonstrate PMs internalization into SSC and the efficient loading of PMs with BIO.

METHODS: PMs were produced by nanoprecipitation of the block-copolymer polyethylene glycol-b-polycaprolactone (5k-b-18k). The hydrodynamic size of the PMs was measured using dynamic light scattering (DLS). PMs were loaded with 100 mM sodium fluorescein and cellular uptake and induced cytotoxicity were assessed on freshly isolated human SSCs using cytofluorimetry. In addition, PMs were loaded with 200 mM BIO and tested on a reporter cell line for their ability to activate the Wnt pathway.

RESULTS: The average size of PMs was measured by DLS of 61.85 nm ± 24.22 nm. PM size was unaffected by incorporation of a payload. After three hours incubation 99.70% ± 0.29% of the SSCs had internalised the fluorescein-loaded PMs, without any cytotoxicity (n=4) (Figure1). BIO-loaded PMs were able to induce the activation of the Wnt signalling pathway in a dose-dependent manner. We observed a slow release of BIO over time; while 100% ± 5.6% of BIO was retained within the PMs after 36 hours, 70% ± 1.2% had been released after 4 weeks (Figure2).

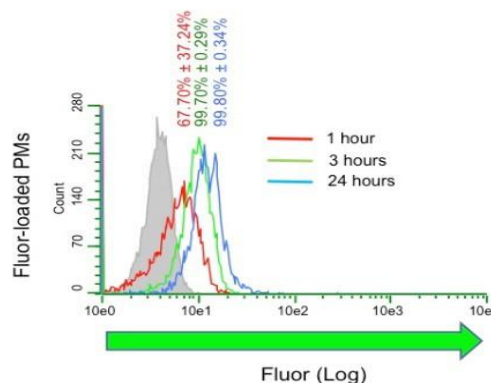


Fig. 1 Cytofluorimetric analysis showing the percentage of uptake of fluorescein-loaded PMs in SSCs after incubation for 1, 3 or 24 hours.

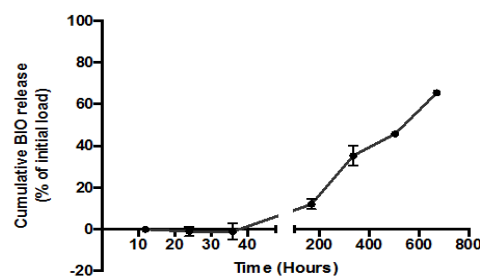


Figure 2: Cumulative release of BIO from loaded PMs over 4 weeks.

DISCUSSION & CONCLUSIONS: The high internalisation rate measured within SSCs confirms that PMs are a suitable delivery system for the targeting of skeletal stem cells. BIO-loaded PMs were demonstrated to activate the Wnt signalling pathway and showed a slow release rate of the payload over time. These results demonstrate the ability to deliver small molecules with polymersomes and the subsequent control of the Wnt signalling pathway. This strategy could be employed as a novel, and directed targeted therapy for bone regeneration.

ACKNOWLEDGEMENTS: The authors wish to thank the Institute for Life Sciences (IFLS) Southampton and the Wessex Medical Research charity for funding.

Mathematical models as a tool to direct the spatial distribution of cells and materials in tissue-engineering conduits for peripheral nerve repair

RJ Shipley¹, RH Coy², T Evans², OR Evans², G Kennedy³, D Hodgson², JB Phillips⁴

¹ UCL Mechanical Engineering, University College London, UK. ² CoMPLEX, University College London, UK. ³ UCL Engineering, University College London, UK ⁴ Biomaterials & Tissue Engineering, UCL Eastman Dental Institute, University College London, UK

INTRODUCTION: Current approaches for tissue engineering conduits for peripheral nerve repair use experiments to inform ‘best guess’ designs of structure/ composition, by incorporating materials and cells in a suite of spatial arrangements (e.g. fibres, channels). These solutions fall short of the gold-standard autograft, partly as the impact and interplay of spatial distribution of materials, cells and cell-secreted factors are not well understood. We present a mathematical modelling approach to direct the choice of these parameters, whilst minimising the number of animal experiments.

METHODS: Two case studies are presented, on the spatial distribution of seeded cells and material components, respectively. Throughout, coupled systems of partial differentiation equations describe how key variables (e.g. oxygen and factor concentrations, cell density) vary in both space and time; seeding distributions are captured through initial conditions, and material boundaries through no entry conditions. A random walk model describes the evolution of neurites generated at the proximal stump [1]. Parameter values are informed by reported experimental data where available [2].

Case Study 1 explores the interplay between hypoxia, angiogenesis and cell survival. Independent of the seeding strategy, hypoxia can induce cell death in vivo, wasting valuable cells and producing an uncharacteristic biological environment. However, local oxygenation must be sufficiently low to induce cells to produce angiogenic molecules and stimulate vascularization of the conduit to promote long-term function. The model explores how controlling the spatial distribution of cell seeding impacts cell survival and angiogenic growth factor production.

Case Study 2 explores the impact of material topology and density on neurite elongation through a repair construct. Neurites respond to the material through the underlying chemical and mechanical imparted to the growing cells.

RESULTS: Case study 1: The spatial and temporal distributions of oxygen, angiogenic growth factors and cell viability are intimately linked. The model predicts the balance between

cell density and induced gradients in angiogenic growth factors for defined cell seeding densities and distributions (see example in Fig 1).

Case study 2: The model predicts an optimum material density that provides sufficient physical stimulation to support neurite elongation, and also sufficient capacity to enable growth.

Seeded Cell Density:
1.15 mill cells/ml

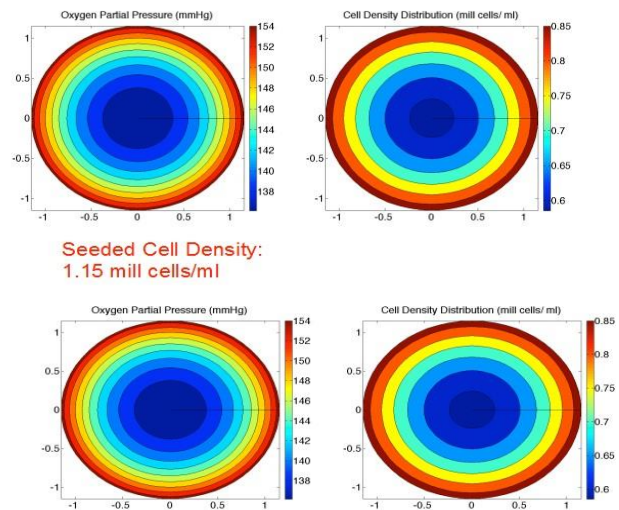


Fig. 1: Spatial distribution of both oxygen and cell density, resulting from an initially uniform cell seeding density of 1.15 mill cells/ml (top). Predicted link between minimum oxygen and maximum growth factor concentrations, and initial cell seeding density (bottom).

DISCUSSION & CONCLUSIONS: To match or surpass the efficacy of autografts it is essential to understand how to organise therapeutic cells and materials within conduits to support regeneration. Mathematical modelling has potential to direct this design process, streamlining a field that currently relies on costly experimentation.

Amniotic membrane as a tissue engineering substrate for corneal-derived mesenchymal stem cells

LE Sidney*, MJ Branch*, OD McIntosh, K Selwyn, CY Lee, A Hopkinson

Academic Ophthalmology, Division of Clinical Neuroscience, University of Nottingham, UK,

*equal contributors

INTRODUCTION: Amniotic membrane (AM) is commonly used clinically for ocular surface reconstruction and as a substrate for limbal epithelial stem cell culture and transfer¹. With mesenchymal stem cell (MSC) therapies for corneal regeneration being increasingly investigated, AM is also being considered as a substrate. We have previously developed a highly effective thermolysin-based denuding technique that removes the epithelium, but preserves the basement membrane integrity of AM². This study aims to characterise the relationship between corneal-derived MSC (cMSC) and AM, with a comparison between non-denuded (intact) AM and denuded AM.

METHODS: cMSC were extracted from corneoscleral rims and cultured in M199 containing 20% FBS until passage 3. Human AM was obtained with consent, and processed to remove the spongy layer. Denuding was achieved using thermolysin. cMSC were seeded on intact AM (iAM), and on the basement membrane and stromal side of denuded AM. Cells were characterised by proliferation, viability and immunofluorescence studies.

RESULTS: cMSC adhered to and proliferated on all preparations of AM. However, proliferation rates were significantly higher on denuded AM than on iAM (fig. 1A). Live/Dead™ staining showed initial adherence of live cells was highest on basement membrane. However, by day 7, cMSC on basement membrane and stroma were confluent and there were few dead cells compared to non-seeded controls. cMSC on iAM did not form a confluent monolayer but appeared to form channels amongst the non-viable AM epithelial cells (fig 1B). cMSC maintained an MSC phenotype on AM, shown by immunocytochemistry. Sectioning of the AM-cMSC constructs revealed that cells did not penetrate or remodel the basement membrane. cMSC seeded on the stromal side began to penetrate the extracellular matrix, creating a more three-dimensional substrate, but did not infiltrate the full thickness of the AM in the 14 day culture time.

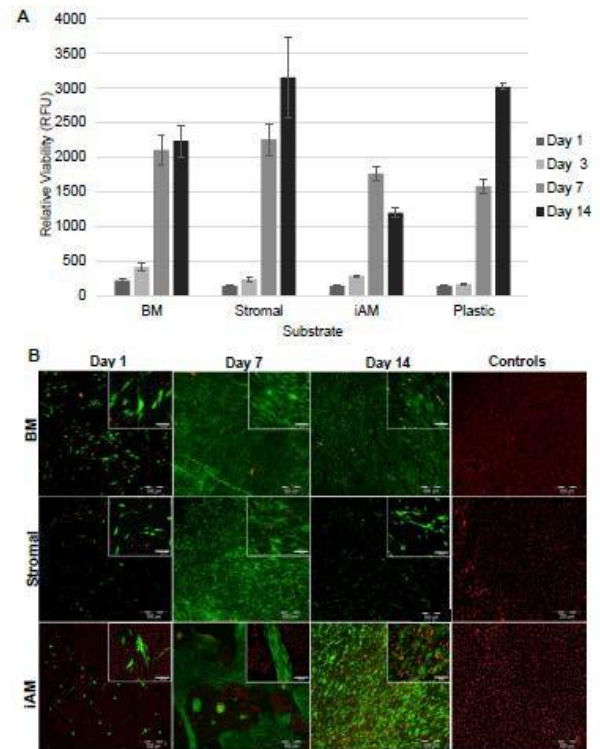


Fig. 1: Proliferation and viability of cMSC on AM over 14 days. (A) Presto blue fluorescence proliferation assay. (B) Live/Dead™ viability assay. Controls are AM without cMSC seeding. BM, Basement membrane; iAM, intact AM.

DISCUSSION & CONCLUSIONS: AM shows potential as a tissue engineering substrate for cMSC, but only in the denuded form, where cells can freely proliferate. AM has promise due to its availability, biological properties and the ability to store as a dry matrix, to be used off-the-shelf.

ACKNOWLEDGEMENTS: This work was funded by a project grant from Fight for Sight.

Investigation into the importance of maintaining CD34 expression in corneal stroma-derived stem cells

LE Sidney, HS Dua, A Hopkinson

Academic Ophthalmology, Division of Clinical Neuroscience, University of Nottingham, UK

INTRODUCTION: Keratocytes are specialised mesenchymal fibroblasts populating the corneal stroma, which can be characterised by expression of the progenitor marker CD34. We have previously demonstrated that CD34⁺ limbal keratocytes become multipotent progenitor cells *in vitro*, known as corneal stroma-derived stem cells (CSSC). CSSC potentially play a regenerative role *in vivo*, and therefore have considerable potential as a stem cell therapy for ocular surface regeneration. However, expansion in conventional foetal bovine serum (FBS)-containing medium leads to loss of CD34 and associated progenitor activity. We investigated methods of optimising *in vitro* culture for maintenance of CD34, with subsequent assessment of the importance of CD34 expression in CSSC.

METHODS: CSSC were extracted from human corneoscleral rims and phenotype assessed at early (P1) and late (P4) passage, when cultured in either: M199 with 20% FBS; DMEM-F12 with 20% KSR, 4 ng/mL bFGF and 5 ng/mL LIF (SCM); endothelial growth medium (EGM); or MethoCult™ (MC). Gene expression of isolated CD34⁺ CSSC and effect of CD34 siRNA knockdown were then evaluated by RT-qPCR.

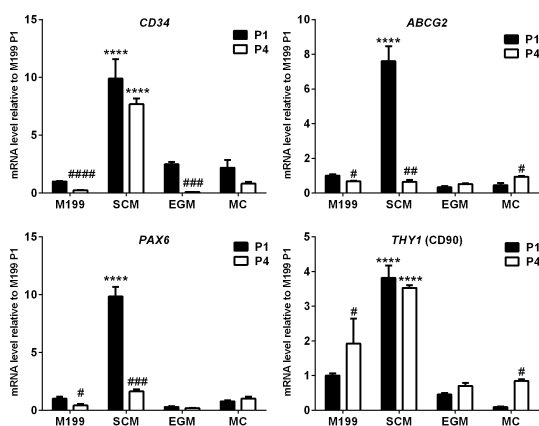


Fig. 1: Comparative effect of media on gene expression of CSSC. Relative levels of mRNA were determined by RT-qPCR for the following genes CD34, ABCG2, PAX6, THY1 (CD90). *Statistical significance vs. M199 P1. # Statistical significance of P1 vs. P4, same media.

RESULTS: SCM was the only medium to maintain CD34 gene expression from P1 to P4 (fig. 1), and exhibited upregulation of progenitor cell markers ABCG2, PAX6 and THY1. Immunocytochemistry demonstrated increased expression of CD34, CD90, ABCG2 and SSEA4 in SCM compared to other media (fig. 2). CD34⁺ CSSC had significantly increased expression of pluripotency markers compared to CD34⁻ cells. Knockdown of CD34 had significant effects on the regulation of pluripotency genes.

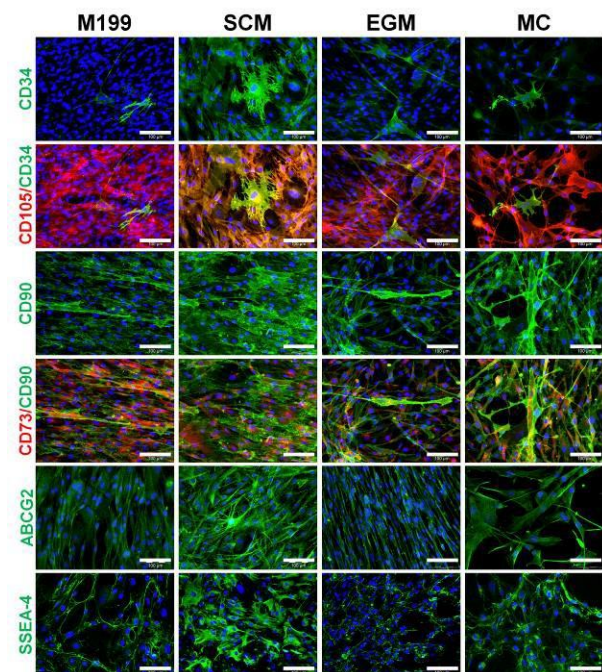


Fig. 2: Comparative effect of media on protein expression of CSSC at P1. Immunocytochemistry was performed at P1. All images shown with DAPI counterstain (blue), scale bar=100 μm.

DISCUSSION & CONCLUSIONS: Results demonstrate that maintenance of an optimal progenitor phenotype is medium-dependent, and CD34 expression is linked to CSSC stem cell properties. Once standardised and bankable, a CSSC therapy could lead to the next generation of ocular regeneration strategies.

ACKNOWLEDGEMENTS: Funding provided by Royal College of Surgeons of Edinburgh and Fight for Sight.

Evaluation of human skeletal progenitor cell function modulated by laser titanium surface modification

KE Sisti,^{1,2,3}; MC de Andrés¹, DA Johnston⁴; AC Guastaldi,³ ROC Oreffo¹

¹*Bone and Joint Research Group, Centre for Human Development, Stem Cells and Regeneration, Institute of Developmental Sciences, University of Southampton, Southampton, UK.* ²*CeTroGen Laboratory UFMS, Campo Grande - Brazil.* ³*Biomaterial Research Group, Institute of Chemistry - UNESP, Araraquara - Brazil.* ⁴*Biomedical Imaging Unit, Faculty of Medicine, University of Southampton, Southampton, UK.*

INTRODUCTION: A number of approaches have been advocated to improve the Titanium (Ti) surface to enhance cell function. Light Amplification by Stimulated Emission of Radiation (LASER) treatment is an innovative method that results in increased surface area, enhanced wettability and, in preclinical bone models, results in high removal torques.² Understanding how to control, manipulate, and enhance the intrinsic healing events modulated through osteogenic differentiation of human skeletal stem cell (hSSCs) through application of modified surfaces offers significant potential for the orthopaedic field. Based on the hypothesis that modified surfaces can modulate the initial osteoinductive responses of cells, this study set out to examine the osteo-regenerative potential of Ti modified by LASER beam on hSSCs compatibility and subsequent cell function.

METHODS: hSSCs populations were isolated from the bone marrow of haematologically normal patients following appropriate consent. STRO-1+ hSSC function was examined for 10 days across four groups using Ti discs: i) machined Ti surface group in basal media (Mb), ii) machined Ti surface group in osteogenic media (Mo), iii) LASER modified Ti group in basal media (Lb) and, iv) LASER modified Ti group in osteogenic media (Lo). Molecular analysis and qRT-PCR as well as functional analysis including biochemistry (DNA, alkaline phosphatase (ALP) specific activity), live/dead immunostaining (cell tracker green/Ethidium Homodimer-1), and fluorescence staining (for vinculin and phalloidin) were undertaken. Inverted, confocal and scanning electron microscopies were used to characterise cell adherence, proliferation, and phenotype.

RESULTS: Enhanced cell spreading and morphological rearrangement, including focal adhesions were observed following culture of hSSCs on Laser surfaces in basal & osteogenic conditions. Molecular Analysis demonstrated enhanced alkaline phosphatase and collagen Type I

expression on Titanium laser treated surfaces in osteogenic conditions.

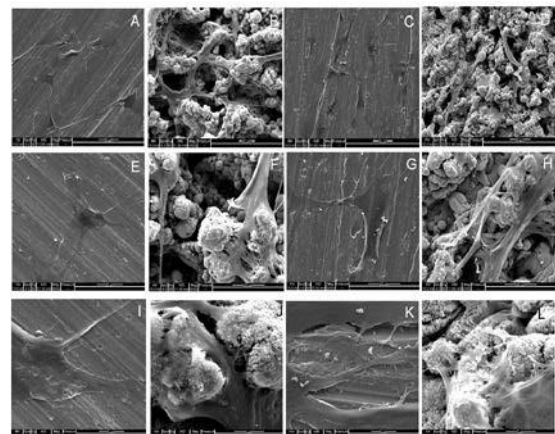


Fig. 1: SEM micrographs of hSSCs cultured for 10 days on Mb (A,E and I), Lb (B,F and J), Mo (C,G and K) and Lo (D, H and L) showing cell adherence in all groups.

DISCUSSION & CONCLUSIONS:

Biocompatibility was closely related to cell viability and proliferation (attachment, adhesion, spreading) in the early phase of the cell/material interaction. The current studies demonstrate that LASER modified Ti surfaces altered the behaviour of hSSCs with altered adhesion, osteogenic gene expression, cell morphology and cytoskeletal structure. Ti LASER modification appears to have the potential to enhance osseointegration between Ti-bone cells, with important implications for surgical application.

ACKNOWLEDGEMENTS: The orthopaedic team at Southampton GH for samples, Science without Borders and BBSRC for financial support.

Epigenetic regulation of interleukin-8, an inflammatory chemokine, in osteoarthritis – a potential therapeutic target

A Takahashi^{1,2}, MC de Andrés¹, K Hashimoto², E Itoi², ROC Oreffo¹

¹*Bone and Joint Research Group, Centre for Human Development, Stem Cells and Regeneration, Institute of Developmental Sciences, Southampton, UK.* ²*Department of Orthopaedic Surgery, Tohoku University School of Medicine, Sendai, Japan*

INTRODUCTION: Inflammation has been implicated in the development and progression of OA¹. Interleukin 8 (IL-8) is an inflammatory chemokine, involved in the inflammatory process and the pathophysiology of OA. Importantly, within *IL8*, the 1000-bp of the proximal promoter region contains only three CpG sites all located close to transcriptional binding sites for NF-κB, AP-1 and C/EBP². However, the methylation status of these CpG sites and subsequent involvement in the regulation of *IL8* regulation, especially in OA, remains, to date, unknown.

METHODS: Human articular cartilage samples were obtained from 15 patients following hemiarthroplasty as a consequence of femoral neck fracture (NOF) and from 15 OA patients who underwent total hip arthroplasty. *IL8* expression levels and the percentage CpG methylation were quantified using qRT-PCR and pyrosequencing to compare OA patients with non-OA controls. Isolated primary human chondrocyte samples (n = 7) were cultured for 5 weeks in 2 groups: (i) cultured without treatment (control culture) and (ii) cultured using 2 μM 5-azadeoxycytidine (5-aza-dC). The effect of CpG methylation on *IL8* promoter activity was determined using a CpG-free vector; co-transfections with expression vectors encoding NF-κB, AP-1 and C/EBP were subsequently undertaken to analyse for *IL8* promoter activity in response to changes in methylation status. Furthermore, to determine the CpG sites critical for *IL8* promoter activity, we compared *IL8* wild type promoter construct activity against 6 vectors containing mutations at different CpG sites.

RESULTS: *IL8* expression was observed to be 37-fold higher in OA patients compared to NOF patients (Figure 1). OA chondrocytes displayed a 22%, 26% and 15% statistically significant (P<0.01) reduction in methylation status at the -116, -106 and -31 CpG sites respectively (Figure 2). Multiple regression analysis revealed that the degree of methylation of the CpG site located at -116-bp was the strongest predictor of *IL8* expression.

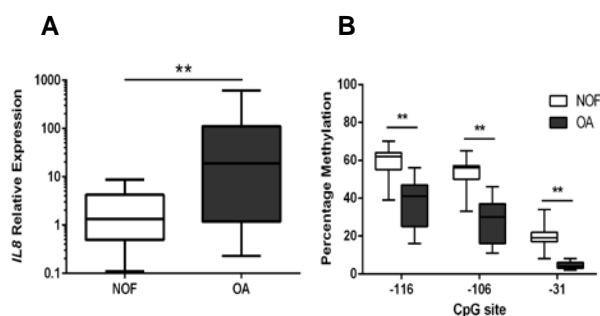


Fig. 1: A. Relative mRNA expression of *IL8* in non-cultured primary human chondrocytes obtained from patients with femoral neck fracture (NOF) and OA patients. mRNA expression was analysed by qPCR and normalised against GAPDH. B. Percentage of methylation of the indicated CpG sites in the *IL8* proximal promoter in the same samples analysed by bisulfite pyrosequencing. N = 15, **P<0.01.

DISCUSSION & CONCLUSIONS: The current study shows that the increased expression of *IL8* in human osteoarthritic chondrocytes is regulated by DNA demethylation in cooperation with transcription factors. We demonstrate for the first time that the percentage methylation of specific CpG sites correlates with *IL8* gene expression level in clinical OA samples. Furthermore, DNA methylation of specific CpG sites appears to be a basal repression mechanism of *IL8* expression. These findings offer a potential predictive marker for OA and, importantly, a putative target, in this inflammatory chemokine, for pharmacological intervention in the treatment of OA as well as, potentially, other arthritic diseases.

ACKNOWLEDGEMENTS: The authors acknowledge the orthopaedic surgeons at Southampton General Hospital for provision of the femoral heads and BBSRC for funding.

3D Collagen model using static compressive loading for assessing cell-mediated mineralization

D Thomas¹, C Matthews², RA Brown³

¹ [Eastman Dental Institute](#), University College London, UK

² [Locate Therapeutics Limited](#), Nottingham UK. ³ [Institute of Orthopaedics & Musculoskeletal Science](#),

Division of Surgery, University College London, UK

INTRODUCTION: There is a need for 3D *in vitro* test (i.e. specifically not *in vivo*) to provide a method of screening materials destined for tissue replacements or implantation. Ideally these tests would be used as models to screen potentially harmful materials before animal testing stages. Implementing this further stage of testing would aim to screen out materials that pass 2D testing in standard well plate type assays, but may not be suitable in 3D environments. The method of plastic compressed collagen (Brown et al) has been successfully used with a range of cell types, maintaining cell viability in engineered 3D tissue-like mimics. This study introduces the use of 3D plastic compressed collagen models [1] with the bone cell line MG63 to investigate their response to PLGA particles under commercial development (Locate plc., Nottingham), in particular its effects on functional mineral deposition using static compression analysis to assess changes in construct stiffness, correlated with mineral production.

METHODS: *Cell culture:* MG63 Cells were cultured in DMEM 10% FBS 5% Penicillin/streptomycin and incubate at 37C 5% CO₂. Models consisted of a single plastic compressed type I rat tail collagen. Where samples differ from collagen only samples the addition of either PLGA (1mg/ml), MG63 cells at 300,000 cells per sample or both were dispersed into the neutralized collagen before compression. Samples were left to culture for 7, 11, 14, 20, 32 & 40 days. Compressive mechanical properties (modulus) of samples was analysed by DMA mechanical testing at 1.0mN to 8000mN at 400mN/min for 20 minutes, correlated with microCT analysis and routine histology.

RESULTS: The key finding of the study was the increase in modulus of cellular constructs with PLGA between 32 and 40 days corresponding to cellular mineralization of the collagen matrix. The increase in modulus of cell constructs +PLGA was almost 7 fold over the period from day 11 to 40 and far in excess of that seen with cells only (Fig.1)

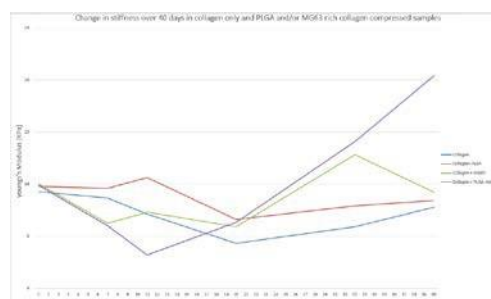


Figure 1. Compression tests of 3D collagen constructs. Constructs were made for (i) collagen only (ii) collagen + PLGA, (iii) Collagen + MG63 cells only, (iv) collagen + PLGA + MG63 cells and incubated for 40 days.

Micro CT images (fig.2) showed much greater focal deposits of mineral within the Collagen + MG63 + PLGA samples compared to that of the Collagen +MG63 only.

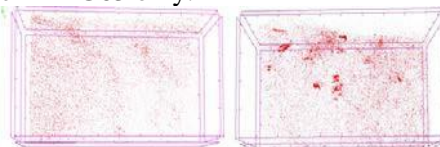


Fig.2 Micro CT image of the collagen + MG63 sample after 40 days in culture (left). Collagen + MG63 + PLGA (right). Mineral deposits are highlighted with a red scatter.

DISCUSSION & CONCLUSIONS: This study has tested a compressed collagen 3D model tissue as a potential biomaterials test using PLGA particles as an exemplar material critically assessing new mineral formation in terms of their functional mechanical behaviour in compression. The addition of PLGA particles produced an increase in mineral deposition, correlating between the increased modulus and Micro CT, indicating that this may represent an excellent 3D *in vitro* assay to predict biomaterial performance

ACKNOWLEDGMENTS: Research funded by EU Fr7, 'BioDesign' programme. We are grateful for the expert technical assistance of George Georgiou (UCL) with the mechanical analysis.

Endocannabinoids can prevent interleukin-1 β -induced cartilage degradation while enhancing mesenchymal stem cell chondrogenesis

SD Thorpe¹, A Gowran², JH Kim¹, DA Lee¹

¹

Institute of Bioengineering, School of Engineering and Materials Science, Queen Mary University of London, London, UK. ²Laboratory of Vascular Biology and Regenerative Medicine, Centro Cardiologico Monzino-IRCCS, Milan, Italy

INTRODUCTION: Cannabinoids have anti-inflammatory effects and reduce joint damage in animal models of arthritis [1]. Both synthetic cannabinoids and the endocannabinoid anandamide (AEA) have been shown to inhibit cytokine-induced nitric oxide (NO) production [2] and prevent interleukin-1 β (IL-1 β) induced proteoglycan and collagen degradation in articular cartilage [3]. While there is increasing evidence endorsing the chondroprotective effects of cannabinoids, their use in tissue engineering strategies for cartilage repair has not yet been investigated. Mesenchymal stem cells (MSCs) are extensively used in cartilage repair strategies, however little is known about the influence of cannabinoids on MSC chondrogenesis [4]. The objective of this work was to investigate the hypothesis that indirect modulation of AEA through inhibition of its degradation by the integral membrane enzyme fatty acid amide hydrolase (FAAH), would both enhance MSC chondrogenesis and prevent IL-1 β induced cartilage degradation.

METHODS: Firstly, full depth bovine cartilage explants (\varnothing 5mm) were cultured with AEA (10 or 50 μ M), FAAH inhibitor URB597 (1 or 5 μ M), or DMSO in the presence or absence of IL-1 β (5 ng/mL) for 15 days. Secondly, human bone marrow-derived MSCs were encapsulated in agarose hydrogels and cultured in chondrogenic differentiation media with the addition of URB597 (1 or 5 μ M), AEA (1, 10 or 50 μ M) or DMSO for 21 days. Explants and agarose constructs were analysed for DNA, sulphated glycosaminoglycan (sGAG), collagen content and nitric oxide (NO) release. Statistical significance was confirmed using ANOVA with Tukey's test.

RESULTS: Treatment of explants with IL-1 β significantly increased catabolic sGAG release (Fig. 1A), and nitric oxide production (Fig. 1B). When URB597 was combined with AEA treatment, sGAG release was reduced toward control levels (Fig. 1A). While treatment with URB597 or AEA alone did not affect NO production in the absence of IL-1 β , NO production was significantly down-regulated with IL-1 β treatment in the presence of 50 μ M AEA (Fig 1B). Treatment of explants with both URB and AEA also reduced NO production (Fig 1B).

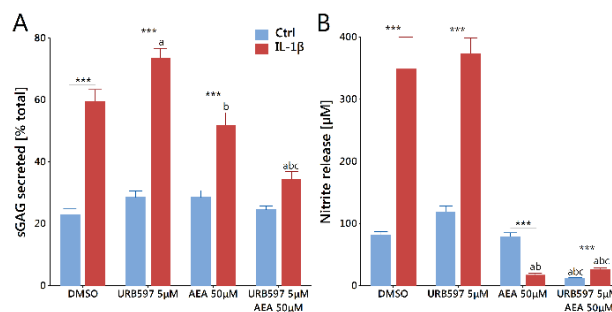


Fig. 1: sGAG (A) and NO (B) secretion from cartilage explants. Mean \pm SEM.

Cell viability, DNA content and collagen accumulation within MSC seeded agarose constructs was not affected by FAAH inhibition in the presence or absence of AEA (not shown). However, FAAH inhibition with 1 μ M URB597 did significantly increase sGAG accumulation in these constructs (Fig. 2).

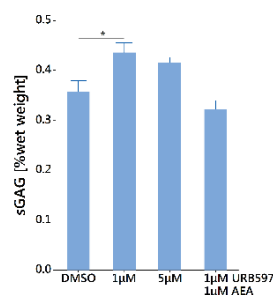


Fig. 2: sGAG accumulation in MSC seeded agarose constructs. Mean \pm SEM.

DISCUSSION & CONCLUSIONS: The endocannabinoid AEA in conjunction with the FAAH inhibitor URB597 can almost entirely abrogate IL-1 β induced cartilage degradation while demonstrating the potential to enhance MSC based cartilage repair.

ACKNOWLEDGEMENTS: Funding provided by Marie Curie Actions FP7 Intra European Fellowship (GENOMICDIFF 301509) and Queen Mary University of London.

A technique to enhance the desiccation tolerance of mammalian cells: exploitation of novel proteins from *Deinococcus radiodurans*

I Tundidor-Peréz^{1,2,3}, P Patel², DYS Chau¹

¹The Research Centre in Topical Drug Delivery and Toxicology, Department of Pharmacy, University of Hertfordshire, Hatfield, UK. ²Department of Human and Environmental Sciences, University of Hertfordshire, Hatfield, UK. ³Department of Biomedicine and Biotechnology, University of Alcalá, Madrid, Spain.

INTRODUCTION: One of the greatest hurdles associated with the use of human cells is the logistics associated with their transport and long-term storage. Current protocols require the use of undesirable supplements (i.e. animal sera and/or DMSO), liquid nitrogen and/or reliance of expensive infrastructure. However, evidence suggests that the preparation of these cells in a desiccated state may be a feasible alternative. *Deinococcus radiodurans* is a bacterium that is highly resistant to a range of environmental hazards including survival at low water levels [Slade and Radman, 2011]. As such, we propose the use of the *D. radiodurans* survival mechanisms (i.e. protein expression) in order to enhance the desiccation tolerance of mammalian cells and/or their recovery from a low water content environment.

METHODS: *Deinococcus radiodurans* (BA816, ATCC) was cultured in Optimized medium, at 35°C, and the cell lysate obtained via sonication in PBS before being confirmed by SDS-PAGE. Human keratinocyte cells (HaCaT, CLS) were cultured in DMEM in a humidified-incubator at 37°C and 5% CO₂ until needed. 200,000 cells were seeded within a 12-well plate and *D. radiodurans* extract was added in a 1:10 ratio. Following 24h, the media was removed and the cells were allowed to dry for 2, 4, 6, 24 and 48 hours under four differing conditions (i.e. at 4°C, 37°C, room temperature (~19 °C) and in the laminar flow cabinet at maximum air flow). Rehydration was achieved using DMEM for 10 minutes prior each time point and following this, cells were assessed for cellular activity and viability using the CellTiter AQ Proliferation/MTS assay (Promega).

RESULTS: A purified *D. radiodurans* lysate was achieved using a reproducible protocol. Viability of the HaCaT cells was significantly higher when supplemented with the bacterial lysate following desiccation than their respective negative control after 2, 4, and 6 hours.

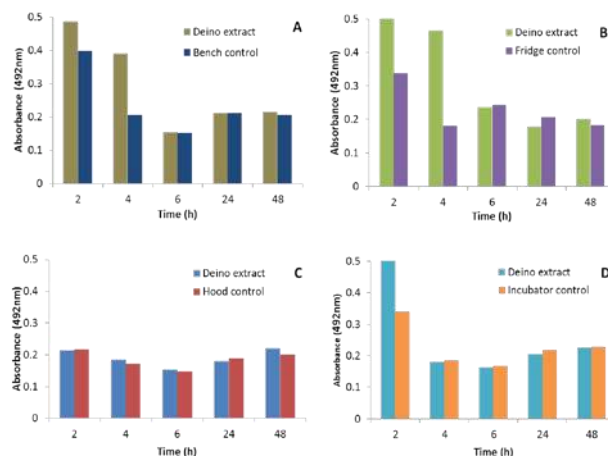


Fig. 1: Comparison between samples treated with *Deinococcus radiodurans* extract and respective controls in terms of cell viability under (A) bench (B) fridge (C) hood (D) incubator

DISCUSSION & CONCLUSIONS: The trend reflected by the current data suggests that *D. radiodurans* extract can enhance and/or extend cell viability over a number of desiccated environments. Increasing the amount of bacterial lysate and/or the use of permeability reagents to facilitate internalisation of these proteins is also being considered in follow-on experiments. The need for characterisation and identification of the novel proteins is also ongoing. These results suggest that *D. radiodurans* may offer the opportunity to be exploited as a novel technique to enhance desiccation-tolerance and/or enhance survivability of mammalian cells within a low water environment.

ACKNOWLEDGEMENTS: ITP would like to thank the University of Hertfordshire for hosting and providing funding as part of the ERASMUS-EU Exchange programme.

The effects of insulin upon skeletal muscle tissue engineered collagen constructs.

MC Turner, DJ Player, NRW Martin, MP Lewis¹

¹*School of Sport, Exercise and Health Sciences, Loughborough University, Loughborough, UK*
M.C.Turner@lboro.ac.uk

INTRODUCTION: The development of skeletal muscle tissue engineered constructs has primarily been used to investigate skeletal muscle development and mechanical properties¹. However, despite skeletal muscle being a major site for insulin stimulated glucose disposal², little research has investigated the response of skeletal muscle tissue engineered constructs to this hormone. Therefore, these experiments aimed to elucidate the effects of insulin upon collagen gel-based skeletal muscle tissue engineered constructs.

METHODS: The development of collagen gel skeletal muscle constructs has been outlined previously¹. In brief, a mix of type I rat tail collagen and minimal essential medium was neutralised in a drop wise manner with sodium hydroxide. C2C12 skeletal muscle precursor cells were seeded at a density of 4×10^6 per ml and mixed with neutralised collagen solution, before being set in pre-sterilised chambers between two A-frames (See Figure 1A).

Constructs were grown in standard growth medium (GM) (DMEM, 20% Foetal Bovine Serum, 1% Penicillin/streptomycin) for four days before being changed to differentiation media (DM) (DMEM, 2% Horse Serum, 1% Penicillin/streptomycin), supplemented with/without 100nM insulin. During differentiation, media was changed daily for ten days, before constructs were acutely stimulated with insulin for 30 minutes (See Figure 2).

The effect of insulin on activation of downstream signalling pathways in these models was analysed by measurement of the expression of phosphorylated (Ser⁴⁷³) and total Akt protein (western blotting). Gene expression of glucose transporter 4 (GLUT4), Hexokinase II (HKII) and, Peroxisome Proliferator-Activated coactivator (PGC1- α) mRNA was investigated by qPCR.

RESULTS: Chronic insulin exposure significantly reduced collagen gel width ($p < 0.05$) (See Figure 1B). Furthermore, insulin exposure increased HKII expression compared to control constructs ($p < 0.05$), whilst significantly reducing GLUT4 mRNA expression ($p < 0.05$). There was no effect of insulin exposure upon PGC1- α mRNA expression ($p > 0.05$).

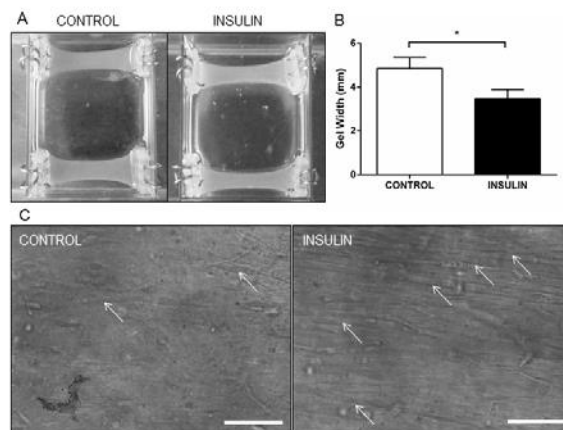


Figure 1: Collagen gel skeletal muscle tissue engineered constructs grown in the absence or presence of insulin. A; Macroscopic images, B; Gel width following insulin exposure, C; Microscopic images of skeletal muscle myotubes in culture. Arrows denote formation of myotubes. Scale bar is 100 μ m. Data is mean \pm SD. *significantly different between conditions ($p < 0.05$).

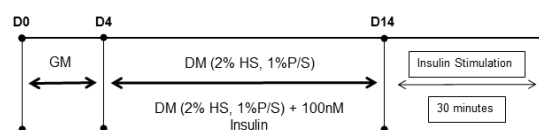


Figure 2: Protocol schematic of collagen gel skeletal muscle constructs differentiated in the absence or presence of insulin.

DISCUSSION & CONCLUSIONS: The experiments conducted present initial data on the effect of insulin exposure upon collagen gel-based skeletal muscle tissue engineered constructs. It shows that these constructs are responsive to insulin, as shown by morphological and molecular changes. The effects of insulin exposure upon these constructs are similar to those observed *in vivo*. Therefore, these models have the potential to be used to investigate insulin stimulation and glucose uptake and the implications of metabolic diseases, such as insulin resistance, upon skeletal muscle.

Dextran use in corneal decellularisation: how, where, and if?

SL Wilson¹, AP Lynch², M Ahearn^{2,3}

¹*Academic Ophthalmology, University of Nottingham, UK.* ²*Trinity Centre for Bioengineering, Trinity College Dublin, Ireland,* ³*Department of Mechanical and Manufacturing Engineering, Trinity College Dublin, Ireland.*

INTRODUCTION: Dextran is routinely used as a de-swelling agent during organ culture and for preservation of corneal tissue. To date, no detailed study has investigated dextran use in corneal decellularisation procedures. Since small changes to procedures may have large impacts on decellularisation efficacy and the structure of the resulting scaffold, the aim of this study was to systematically investigate dextran use in the decellularisation of adult porcine corneas.

METHODS: Six groups of 8 mm adult porcine corneal buttons were investigated: i) Freshly dissected; (ii) native cornea; (iii) freeze-thaw; (iv) detergent using 0.5% (w/v) sodium dodecyl sulphate (SDS) and 1% (w/v) Triton X-100; (v) detergent/dextran, as detergent treatment, with the addition of 5% dextran used *throughout* the procedure; (vi) detergent/dextran-wash; as detergent treatment, followed by an additional washing step in 5% dextran *at the end* of the procedure. Tissue transparency, thickness and mass pre/post decellularisation was measured. Removal of detectable cellular and immune reactive material was evidenced by histological and quantitative assays. Retention of corneal architecture and intrinsic biological cues (glycosaminoglycans and collagen-I) were assessed *via* histological, immunofluorescence, electron microscopy and biochemical analysis.

RESULTS: All decellularised tissues experienced a significant reduction in transparency (*Fig 1A*), mass, and residual DNA (*Fig 1B*) compared to native tissue, with dextran having no apparent effect on mass and residual DNA. Dextran use did preserve/restore normal tissue thickness whilst maintaining higher levels of glycosaminoglycans (*Fig 1C*). Dextran had a positive effect with regards to maintaining/restoring the collagen tissue microstructure. Electron microscopy studies (*Fig 1D*) revealed that the use of dextran *throughout* the whole decellularisation protocol was vital for maintenance of the nanoscale ultrastructural organisation, and that use of dextran *at the end* of the decellularisation protocol did not sufficiently preserve/restore the nanoscale ultrastructure of the corneal tissue.

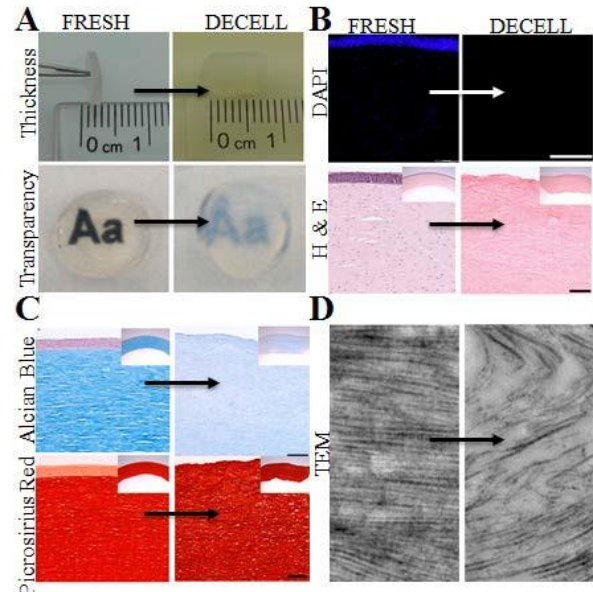


Fig. 1: Comparison of freshly dissected corneal tissue to decellularised tissue: A thickness and transparency; B Residual nuclear material; C Glycosaminoglycan and collagen preservation; D Collagen fibril ultrastructure.

DISCUSSION & CONCLUSIONS: This study highlights the importance of performing systematic, in-depth studies with extensive characterisation when devising appropriate decellularisation procedures for clinical translation. Seemingly small changes to procedures can have huge impacts on the resulting acellular scaffold which will ultimately affect the efficacy, biocompatibility and regenerative capacity of the tissue upon recellularization either *in vivo* or *in vitro*.

ACKNOWLEDGEMENTS: This was a collaborative project between Trinity College and the University of Nottingham. Invaluable technical assistance and expertise from Denise Mclean, in the Advanced Microscopy Unit (School of Life Sciences, University of Nottingham), is very much appreciated. Funding from E-COST Action BM-1302; EPSRC Engineering, Tissue Engineering and Regenerative Medicine (E-TERM, EP/I017801/1; Science Foundation Ireland; and Marie Marie-Curie Action COFUND (11/SIRG/B2104) are all gratefully acknowledged.

Preclinical musculoskeletal junction testbed: co-culture of 3D tissue engineered skeletal muscle and bone constructs

NM Wragg¹, DJ Player¹, NRW Martin¹, Y Liu², MP Lewis¹

¹School of Sport, Exercise and Health Sciences, Loughborough University

²Wolfson School of Mechanical and Manufacturing Engineering, Loughborough University

INTRODUCTION: Current preclinical tests utilize a combination of monolayer cultures and animal models to assess biocompatibility¹. This is despite ethical considerations, a lack of cross-species translation, cost and non-relevant structural and biochemical pathways. Therefore, a relevant tissue engineered (TE) model of the musculoskeletal system is proposed (MSk). In order to create a relevant 3D TE preclinical MSk testbed, each component (skeletal muscle and bone constructs) must first be capable of simultaneous culture in a single contiguous system. This work presents conditions for the successful co-culture of 3D tissue engineered skeletal muscle and bone models.

METHODS: C2C12 murine muscle precursor cells (MPC) and TE85 human osteosarcoma cells were seeded within type-1 rat-tail collagen (2.20mg/mL) and collagen/nano-hydroxyapatite constructs respectively. Nano-hydroxyapatite (nHA) was precipitated through the reaction of calcium acetate and ammonium phosphate tribasic solutions. After removal of unbound water, the nHA was mixed with the collagen prior to cell seeding. Skeletal muscle (C2C12) constructs (SkM) were tethered at either end by bespoke polythene mesh floatation bars to facilitate alignment of MPC's and subsequent differentiation into myotubes. Bone (TE85) constructs (B) were set within a bespoke circular mould and restrained by a centrally located pin and bead. Both constructs were placed in 20% FBS high glucose DMEM for 4 days and then cultured in 2% horse serum high glucose DMEM for a further 10 days; these being the standard conditions to induce MPC differentiation.

RESULTS: Both SkM and B constructs reduced in width and diameter over the 14 day time-course, indicating successful cell attachment and remodelling. Immunohistochemical analysis showed successful myotube formation within the skeletal muscle construct and a randomly orientated, osteocyte-like morphology with clear cell protuberances within the bone model.

DISCUSSION & CONCLUSIONS: This work demonstrates the successful simultaneous co-culture of tissue engineered skeletal muscle and bone within a single system. This data shows conservation of previously reported morphological observations of a collagen-based skeletal muscle construct^{2,3} without obvious negative effects from the adjacent bone culture. The bone construct similarly showed no deviation from expected observations and therefore shows potential for muscle and bone co-culture within a contiguous construct.

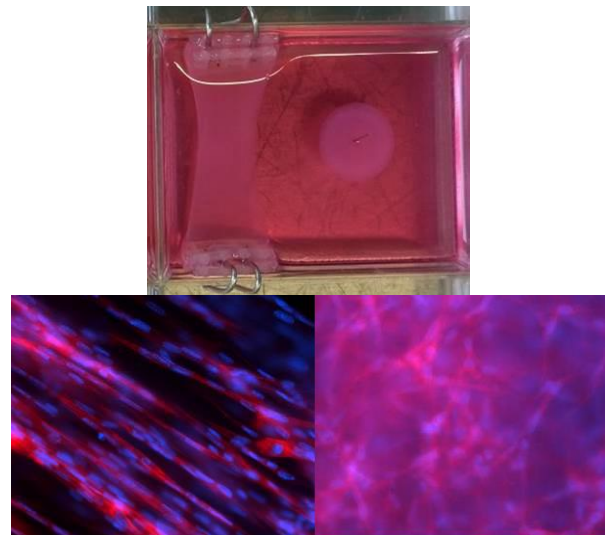


Fig. 1: (Top) Collagen based skeletal muscle and bone constructs cultured in a single well for 14 days. (Bottom Left) 40x mag. Parallel alignment of C2C12 myotube structures within skeletal muscle construct. (Bottom Right) 40x mag. Randomly aligned osteocyte-like morphology of TE85s within collagen scaffold. Immunohistochemistry: Phalloidin (actin) - Red; DAPI (nuclei) - Blue.

ACKNOWLEDGEMENTS: With thanks to the EPSRC as the funding body. This work was carried out in affiliation with ARUK.

Skeletal stem cell sorting: characterisation of physical properties for microfluidic separation applications

[JM Xavier](#)^{1,2}, [P Rosendahl](#)³, [D Spencer](#)¹, [O Otto](#)³, [J Guck](#)³, [ROC Oreffo](#)², [H Morgan](#)¹

¹*School of Electronics and Computer Science and Institute for Life Science, University of Southampton, Southampton, UK.* ²*Institute of Developmental Sciences, University of Southampton, Southampton, UK.* ³*Biotechnology Center, Technische Universität Dresden, Dresden, Germany.*

INTRODUCTION: Skeletal stem cells (SSC) represent a sub-population of mesenchymal stem cells, which can be found in the bone marrow with osteogenic, chondrogenic and adipogenic differentiation potential. However, a challenge remains to obtain, *in vitro*, a population of cells with homogeneous regeneration and differentiation capacities¹. Challenges include a) the rarity of SSC in bone marrow aspirates, estimated at between 1 in 10-100 thousand mononuclear cells²; b) the ambiguity of SSCs and thus the lack of a specific SSC marker³ and c) the complexity of bone marrow tissue.

Microfluidics provides novel solutions to cell separation based on bio-physical features of single cells¹. We have examined the bio-physical properties, including size, dielectric properties and deformability, of MG-63 and human SSCs with the aim of designing a device for sorting SSCs with enriched purity and cell yield.

METHODS: Primary human bone marrow stromal cells (hBMSCs) were harvested from marrow samples and enriched for SSC populations using MACS separation with Stro-1, followed by plastic culture adherence. Stro-1 hBMSCs and MG-63 were harvested and re-suspended in 1mM EDTA, 0.25% BSA in PBS for microfluidic impedance cytometry (MIC) or 0.5% methylcellulose in PBS for real time deformability cytometry (RT-DC) measurements, respectively. Impedance measurements were made using microfluidics chips with sinusoidal voltages applied at fixed frequencies to electrodes. The differential current was measured using a trans-impedance amplifier and a digital impedance analyser. RT-DC was assessed by image analysis of high-speed videos of the cells when pushed through a constriction in a PDMS micro-channel⁴.

RESULTS: MG-63 deformability was compared to HL-60 cells, a promyeloblast cell line from human peripheral blood. The two cell populations were clearly identified as shown in Figure 1 (a). MG-63 cells displayed a higher stiffness, deforming less than HL-60, despite their larger size.

Analysis of MG-63 mixed with human PBMCs using impedance spectroscopy (Figure 1b) demonstrated clear separation of the MG-63 and the three populations of leukocytes. Table 1 summarises the dielectric properties of MG-63 and Stro-1⁺ hBMSCs determined by MIC and fitting to a double shell model.

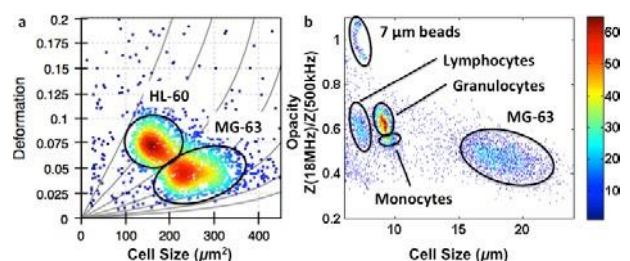


Fig. 1: (a) Deformability and (b) opacity (Z at 18 MHz / Z at 0.5 MHz) vs cell size scatter plots of MG-63 and HL-60 cells (RT-DC) and MG-63 and PBMCs (MIC).

Table 1. Biophysical parameters of MG-63 and Stro-1⁺ hBMSCs as determined by MIC. Values represent the Mean \pm SD ($N=3$).

	MG-63	Stro-1 ⁺ hBMSCs	P-Value
Cell radius (μm)	9.25 \pm 0.25	9.33 \pm 0.29	0.736
Nuclear radius (μm)	7.00 \pm 0.75	5.50 \pm 0.43	0.039
Nucleus/Cytoplasm ratio	0.758 \pm 0.094	0.589 \pm 0.029	0.041
Mem. capacitance (mF/m^2)	13.6 \pm 1.0	12.4 \pm 3.1	0.558
Cytop. conductivity (S/m)	0.57 \pm 0.25	0.9 \pm 0.0	0.085
N. env. Capacitance (mF/m^2)	36.0 \pm 8.4	31.9 \pm 9.9	0.613
Nuc. env. conductivity (S/m)	0.0037 \pm 0.0018	0.0013 \pm 0.0003	0.084
N.plasm conductivity (S/m)	2.3 \pm 0.42	2.2 \pm 0.47	0.797

DISCUSSION & CONCLUSIONS: Impedance and deformability cytometry demonstrate clear differences between MG-63 and normal leukocytes. Future analysis of Stro-1⁺ SSCs should identify biophysical features that will allow label-free separation of SSCs from bone marrow with significant physiological and therapeutic implications.

ACKNOWLEDGEMENTS: The authors would like to acknowledge Sarah Helps for fabricating the MIC chips.

Characterisation of human cardiovascular tissue in calcific disease using Raman spectroscopy

[AYF You](#)^{1,2,3}, S Bertazzo¹, JP St-Pierre^{1,2,3}, JAM Steele^{1,2,3}, AH Chester⁴, MH Yacoub⁴, [MM Stevens](#)^{1,2,3}

¹ *Department of Materials, Imperial College London, London SW7 2AZ, UK.* ² *Department of Bioengineering, Imperial College London, London SW7 2AZ, UK.* ³ *Institute of Biomedical Engineering, Imperial College London, London SW7 2AZ, UK.* ⁴ *National Heart & Lung Institute, Harefield Heart Science Centre, Imperial College London, Harefield, Middlesex UB9 6JH, UK.*

INTRODUCTION: Calcification of human tissues occurs naturally in bone, deep zone of the cartilage and teeth. However, certain pathological processes can result in ectopic soft tissue calcification. Using scanning electron microscopy with energy-dispersive X-ray spectroscopy (SEM-EDS), our group previously identified spherical calcium phosphate deposits within aortic tissues of diseased and even healthy donors [1,2]. These spherical deposits consist of a highly crystalline form of calcium phosphate, which differs from bone mineral in both its crystallinity and structure. Previously to that report, calcification of blood vessels has been observed in diseased tissues. Thus far their composition and relation to the organic component of the tissue have not been evaluated. In this work, aorta samples from healthy human donors and patients were analysed using numerous cutting edge spectroscopic techniques including Bio-Raman spectroscopy characterisation in tandem.

METHODS: Raman mapping of aorta explants was carried out with a 785 nm diode spot laser at 80 mW power (at objective). Measurements were collected using a Renishaw InVia dispersive spectrometer system.

Preprocessing of Raman spectra consisted of Savitsky-Golay smoothing (3 points), Weighted Least Squares Polynomial Baseline Correction (3rd order) and Multiplicative Scatter Correction (MSC), which were applied to the mapped spectra prior to data analysis.

RESULTS: Correlative analysis of Bio-Raman spectroscopy, electron microscopy and inductively coupled plasma mass spectrometry, shows that the calcified material are primarily found deep within the aortic tissue, not only on the surface and are made up of magnesium substituted calcium phosphate with high crystallinity. This is in stark contrast to calcifications of atherosclerotic plaques and bone mineral, which comprise apatite showing low levels of crystallinity and not significant magnesium substitution. Analysis of the Bio-

Raman spectroscopic maps showed a difference in the phosphate ν_1 Raman band and an increased presence of β -carotene and cholesterol with increased amounts of mineral particles. Differences in the co-localisation profiles associated to different levels of calcification, indicates a trend from non-cell towards cell-mediated calcification.

DISCUSSION & CONCLUSIONS: The results of this study suggest that calcification processes and pathways in vascular tissues are different from those of bone and that there is interplay between mineral content and changes in smooth muscle cell and foam cell behaviour.

Differences in the cells and matrix composition adjacent to the calcification suggest either a change in the gene expression phenotype of the smooth muscle cells linked to cholesterol uptake or migration of foam cells from the intima into the media.

The characterisation and study of these tissues can thus contribute to a better understanding of pathophysiological tissue calcification processes.

ACKNOWLEDGEMENTS: This template was modified with kind permission from eCM Journal.

Design of scaffold morphology for optical cell differentiation using novel polymerisation techniques

T Zhou¹, ED McCarthy¹, C Soutis¹, SH Cartmell¹

¹ [School of Materials](#), The University of Manchester, UK

INTRODUCTION: The physical and chemical properties of a scaffold influence a cell's bio-activity once the latter is seeded by cells. By engineering the materials of the scaffold, it can exhibit the best imitation of the natural extracellular environment to provide optimum conditions for cell adhesion and differentiation. In this study, we employ in-situ polymerisation to produce a specialized 3D polylactic acid cell-scaffold structure using Mg/Al layered-double-hydroxide (CO_3^{2-}) as the initiator without using potentially toxic industrial catalysts.

METHODS: The initial hybrid product is prepared by the reaction of 95% L,D-Lactide by mass and 5% LDH by mass heating in the oven at 150 °C for 24 hours. The ring structure of the L,D-lactide is opened by the carbonate-intercalated LDH initiator to form a poly(lactide) / Mg lactate ionomer complex. Then methylene chloride (CH_2Cl_2) is used to extract soluble poly(lactide) from the polymer product by centrifugation at 8000 rpm for 10 minutes leaving the insoluble scaffold phase. Finally, the insoluble component is vaporized in air for 12 h to fully remove the solvent.

RESULTS: A selection of SEM images (Fig. 1) was taken to examine the microstructure and morphology of the porous-structured scaffold material, which remained after extraction from the hybrid polymerization products. A porous structure is visible, indicating that polymerising L,D-Lactide with a carbonate-intercalated hydrotalcite as an initiator can synthesis a porous structure. By inspection, the structure is quite heterogeneous in terms of having a wide pore size distribution. As a consequence, the mean pore size was difficult to calculate properly. However, with the help of micro CT (X-ray Micro Computed Tomography), we can learn more about the whole structure about the scaffold in future, e.g., porosity, pore size, interconnectivity.

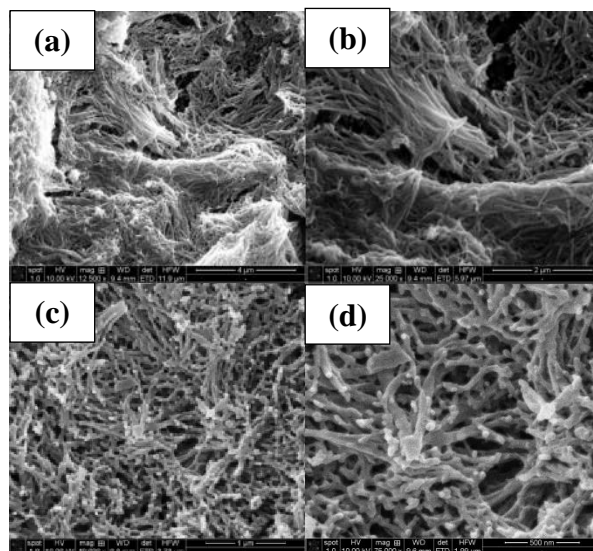


Fig. 1: SEM micrographs of magnesium lactate scaffold with 5% LDH (CO_3^{2-}) concentration at the magnifications of (a) $\times 12.5K$ (b) $\times 25K$ (c) $\times 40K$ (d) $\times 75K$.

DISCUSSION & CONCLUSIONS: This study has confirmed the formation of a porous structure suitable for a potential cell-growth scaffold. It was chemically identified as a poly(L,D-lactide) / magnesium lactate complex [1] using XRD. For future work, other lactone monomers can be applied for the copolymerization (e.g. caprolactone and valerolactone). And further material characterization will include NMR (Nuclear Magnetic Resonance Spectroscopy) and AFM (Atomic Force Microscopy) Based on the scaffold morphology, it is expected that osteoblast (bone) cells could be seeded on the scaffold during in-vitro experiments in tissue engineering. Then, PicoGreen and Alamar Blue Assay can be used to test the biocompatibility of the scaffold, by indicating the distribution of live cells across the material.

Development of an *in vitro* peripheral nerve model using xenogeneic nerve tissue

L Zilic¹, JW Haycock¹, S-P Wilshaw²

¹*Department of Materials Science & Engineering, University of Sheffield, Sheffield.* ²*Institute of Medical and Biological Engineering, Faculty of Biological Sciences, University of Leeds, Leeds*

INTRODUCTION: Peripheral nerve injuries affect 1 in 1000 of the population [1]. Injuries greater than 1 – 2 cm are normally bridged using autografts, which direct regenerating axons, by topographic guidance [2]. Commercially available products such as nerve guide conduits are not particularly suitable as they lack architecture similar to that of the native ECM of the nerve. It is hypothesized that an acellular nerve would facilitate regeneration of axons at the cellular level, encouraging regeneration within a native microenvironment. The present aim is therefore to develop compatible, non-immunogenic, nerve grafts to restore sensory and motor function using a novel technique to decellularise porcine nerve. The acellular nerve will then be used as a basis for the study of perfused flow within the tissue for the introduction of Schwann cells - as the delivery of such cell types is reported to improve nerve cell development.

METHODS: Porcine peripheral nerves were decellularised using low concentration (0.1 %; w/w) sodium dodecyl sulphate and nuclease enzymes. The structure and ECM components of the acellular nerves were characterised using histological, immunohistochemical staining as well as biochemical assays and biomechanical testing. The acellular nerves were repopulated initially with RN22 Schwann cells labelled with CellTracker red and incubated under perfused flow using a bioreactor.

RESULTS: Decellularisation of nerves resulted in a 95 % (w/w) DNA reduction with the preservation and retention of the native nerve architecture and important ECM components collagen, laminin and fibronectin. Biomechanical testing indicated that the decellularisation process had minimal effect on the mechanical properties. Characterisation of the repopulated nerve showed Schwann cells distributed throughout the tissue.

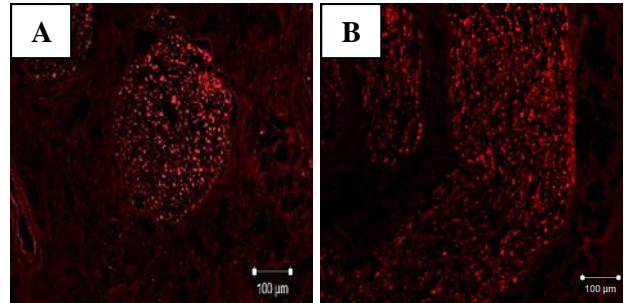


Fig. 1: Repopulation of acellular peripheral nerve with Schwann cells. A&B shows cells fluorescently labelled with CellTracker[®] red in transverse and longitudinal nerve sections, respectively.

DISCUSSION & CONCLUSIONS: The acellular nerves can be used as a model to study perfused flow within the tissue for the introduction of Schwann cells. Key questions can additionally be asked using this as a model, including the influence of a native 3D environment on cell migration and development.

ACKNOWLEDGEMENTS: This work is funded by the EPSRC (U.K.)